UNIVERSITY OF BIRMINGHAM

IN VITRO CHARACTERISATION OF HUMAN CLEFT FIBROBLASTS ISOLATED FROM PATIENTS WITH DIFFERING CLEFT MANIFESTATIONS

By

NAVEED SAEED

A thesis submitted to the University of Birmingham for the degree of

DOCTOR OF PHILOSOPHY

School of Dentistry

College of Medical and Dental Sciences

The University of Birmingham

January 2019

ABSTRACT

Following surgical correction of cleft lip and palate a number of patients develop post-operative complications including oronasal-fistulae (ONF) and hypertrophic scarring (HTS). As these conditions can form due to pathological wound healing, this study aimed to characterise fibroblast behaviour, derived from patients with differing cleft phenotypes, to identify potential contributing factors. Fibroblasts were isolated from oral mucosal tissues derived from 29 cleft patients and were subsequently characterised and compared in terms proliferation, migration, ECM deposition and gene expression. Cleft fibroblasts were clustered into two statistically distinct migratory groups: fast and slow, with fast migrating fibroblasts secreting greater amounts of collagen. Although these groups did not correlate with cleft phenotype, CL fibroblasts all presented increased motility coupled with increased collagen deposition and upregulation of *COL1A1*. As both elevated motility and collagen secretion are hallmarks of HTS, it is possible that patients with faster migrating fibroblasts, including those derived from CL, may be at greater risk of pathological wound healing. Further, as fast migrating fibroblasts contained greater quantities of F-actin and upregulated ARP2, a major component of the ARP2/3 complex which acts as an actin filament nucleator, the observed increase in motility may be a result of altered cytoskeletal dynamics.

ACKNOWLEDGEMENTS

Firstly, I would like to extend my sincere gratitude and appreciation to my supervisors, Dr Richard Shelton, Professor Gabriel Landini and Professor Paul Cooper. They were a constant source of guidance and encouragement throughout my years at the school of Dentistry and helped mould me into a more competent researcher. It was always a great comfort knowing that your doors were open to provide me with advice, constructive criticism and support.

I would also like to extend special thanks to Dr Joseph Hardwicke who was the lead supervisor during the first year of my PhD. You were a great help during my transition into postgraduate research and you taught me many of the skills that I used throughout my PhD. Despite moving on it was always encouraging to know that you kept up to date with the project and my progress.

I am also very grateful to Mr Bruce Richard who always took the time to make me feel welcome at the BCH. I am appreciative for all that you have done for the project including helping me with sample collection and liaising with the HBRC.

The laboratory staff at the BDH have all been a great help throughout my PhD, I would especially like to thank Gay Smith, Michelle Holder, Jianguo Liu, Helen Wright and Sue Finney. Each of you have my appreciation and thanks for helping me within the laboratory, training me to use equipment and conduct specialist techniques.

I wish to thank all of the postgraduate students, both past and present, at the School of Dentistry. Many of you supported me and offered encouragement or guidance during my PhD, I would like you to know that I greatly valued both the casual conversations and in-depth discussions.

Most of all I would like to thank my family, especially my mother, who has always encouraged me to study and become the best I can be both personally and academically. My wife has been an endless ocean of support throughout the entirety of my PhD. She has been with me through the good times and the bad, offered me emotional support and put up with me spending most of my time at the university. I have no doubt that without you this thesis would not have reached completion.

TABLE OF CONTENTS

CHAPTER ONE: INTRODUCTION

CHAPTER TWO: MATERIALS AND METHODS

CHAPTER THREE: CHARACTERISATION OF HUMAN CLEFT FIBROBLASTS

CHAPTER FOUR: ANALYSIS OF CLEFT FIBROBLAST MIGRATION

CHAPTER FIVE: THE INFLUENCE OF FOLIC ACID ON CLEFT FIBROBLAST BEHAVIOUR

CHAPTER SIX: GENERAL DISCUSSION AND CONCLUDING REMARKS

LIST OF FIGURES

LIST OF TABLES

LIST OF EQUATIONS

LIST OF ABBREVIATIONS

ANOVA	Analysis of variance
BCA	Bicinchoninic acid
BCH	Birmingham children's hospital
BDH	Birmingham dental hospital
BLCLP	Bilateral Cleft lip and Palate
BSA	Bovine serum albumin
cDNA	Complimentary Deoxyribonucleic acid
CL	Cleft lip only
CLP	Cleft lip and palate
CLP(L)	Lip tissue derived from patients with cleft lip and palate
CLP(P)	Palatal tissue derived from patients with cleft lip and palate
CMFDA	5-chloromethylfluorescein diacetate
CNCC	Cranial neural crest cells
CP	Cleft palate only
CS	Chondroitin sulphate
Ct	cycle threshold
DAPI	4′,6-diamidino-2-phenylindole
DMEM	Dulbecco's modified eagle's medium
DMSO	Dimethyl sulfoxide
DNA	Deoxyribonucleic acid
DNase I	Deoxyribonuclease I
DS	Dermatan sulphate
DT	Doubling time
ECM	Extracellular matrix
EDTA	Ethylenediaminetetraacetic acid
EGF	Epidermal growth factor
EMT	Epithelial mesenchymal transition

FA	Folic acid
FBS	Fetal bovine serum
FGF	Fibroblast growth factor
FITC	Fluorescein isothiocyanate
GAG	Glycosaminoglycans
GCP	Good clinical practice
GWAS	Genome wide association studies
HBRC	Human biomaterials resource centre
HCL	Hydrochloric acid
HEPES	4-(2-hydroxyethyl)-1-piperazineethanesulfonic acid
HGF	Human gingival fibroblasts
HKG	Housekeeping gene
HS	Heparan sulphate
HTA	Human tissue authority
HTS	Hypertrophic scarring
IHC	Immunohistochemistry
IMS	Industrialized methylated spirit
IRAS	Integrated research application system
LUCLP	Left unilateral cleft lip and palate
ML	Millilitre
MMP	Matrix metalloproteinase
MTT	3-(4,5-dimethylthiazol-2-yl)-2,5-diphenyltetrazolium bromide
NADH	Nicotinamide adenine dinucleotide
NADPH	Nicotinamide adenine dinucleotide phosphate
NHDFF	Neonatal human dermal foreskin fibroblasts
NIHR CRN	National institute of health research clinical research network
nsCLP	Non-syndromic cleft lip and palate
NTD	Neural tube defects
OD	Optical density

OFC	Orofacial clefts
ONF	Oronasal fistulae
PBS	Phosphate buffered saline
PCR	Polymerase chain reaction
PDGF	Platelet-derived growth factor
PI	Propidium iodide
PRS	Pierre robin syndrome
qPCR	Real time polymerase chain reaction
RA	Retinoic acid
RDA	Recommended daily allowance
RGB	Red green blue
RNA	Ribonucleic acid
ROCK	Rho-associated coiled-coil-containing protein kinase
RUCLP	Right Unilateral cleft lip and palate
RWA	Remaining wound area
sCLP	Syndromic cleft lip and palate
SD	Standard deviation
sDMEM	Supplemented Dulbecco’s modified eagle's medium
SEM	Scanning electron microscope
TGFα	Transforming growth factor alpha
TGFβ	Transforming growth factor beta
uCLP	Unilateral cleft lip and palate
VEGF	Vascular endothelial growth factor
VWS	Van der woude syndrome
WASP	Wiskott–Aldrich syndrome protein
WAVE	WASP-family verprolin homologue
WHO	World health organisation

CHAPTER ONE:

INTRODUCTION

1.1 General introduction

Cleft lip, with or without cleft palate, is the most common craniofacial abnormality in humans (Dixon et al, 2011). Clefts not only affect facial aesthetics but also disrupt speech development, nutrition and development of the normal dentition. The defects encompass wide phenotypic variation with occurrence varying according to both ethnicity and gender (Dixon et al, 2011) although the precise aetiology remains controversial. However, there is significant evidence which suggests that the occurrence of clefts is due to both genetic and environmental cues (Mossey and Modell, 2012). Cleft repair is accomplished surgically and there are a number of treatment protocols available, each with associated merits and drawbacks. Following surgical repair there are a number of post-operative complications that can occur, most commonly, hypertrophic scarring and oronasal fistulae (Soltani et al, 2012; Hardwicke et al, 2014).

1.2 Cleft anatomy

Orofacial clefts (OFC) are a group of craniofacial abnormalities with differing degrees of severity and associated patient morbidity. Common manifestations of OFC include: cleft lip and palate (CLP), cleft palate only (CP), cleft lip only (CL), these conditions can occur both unilaterally and bilaterally.

1.2.1 Cleft lip

Cleft lip, in isolation, accounts for approximately 20% of all cases of orofacial clefts (Hoffman, 2011). Cleft lip ranges from incomplete unilateral cleft lip to complete bilateral cleft lip involving the majority of the upper lip. The mildest form of cleft lip, termed microform cleft lip, is characterised as a small notch on the vermillion border combined with the presence of fibrous tissue at the peripheral regions of the defect (Kim et al, 2010). A more extensive incomplete cleft lip extends beyond the vermillion border, the marked border of the upper lip, into the cutaneous regions of the upper lip combined with varying degrees of separation of the

orbicularis oris muscle and overlying skin, this separated muscle partially reattaches close to the alar base of the nose. Conversely, in cases of complete cleft lip the orbicularis oris muscle fails to fuse and remains separated, extending to, and inserting into the columella, the tissue between the nostrils that links the tip of the nose with nasal base, medially and the alar base, the tissue at the side of the nose, laterally (Laberge et al, 2007). This leads to the characteristic nasal deformity associated with cleft lip. It is important to note that each of the aforementioned conditions can be unilateral or bilateral in nature.

1.2.2 Cleft palate

Clefting of the primary and secondary palate, as with cleft lip, manifests with varying degrees of severity. Combined CLP accounts for approximately 50% of all cases of OFC, with cleft palate in isolation comprising the remaining 30% (Hoffman, 2011). Primary palatal clefts occur anterior to the incisive foramen of the hard palate and extend into the alveolus and maxilla (Goodacre et al, 2008). Failure of the palatal shelves to fuse leads to the incidence of secondary palatal clefts that occur posterior to the incisive foramen, extending to this point from the soft palate. Submucosal cleft palate (SMCP) is a comparatively rare form of cleft palate where there is muscular separation of the soft palate whilst mucosal surface integrity is maintained. It is commonly associated with a bifid uvula, a notch to the posterior hard palate, a zona pellucida (Calnan's triad) and malorientation of the palatal rugae (Ojia et al, 2013; Richard et al, 2000). Though cleft lip and cleft palate often occur simultaneously, the high frequency of each condition occurring in isolation, coupled with the development of the lip and palate being due to distinct embryological events, has led to speculation that cleft lip and cleft palate may be disparate clinical entities, of differing causation. However, some have concluded that further investigation of cleft lip and cleft palate is required to identify the contributory factors that lead to clinical appearance of one phenotype over the other (Harville et al, 2005).

1.3 Embryological development of the lip and palate

Human facial development begins approximately 4 weeks after conception and continues into the 12th week of development, at which point many of the key facial structures including can be observed. Embryological development of the facial structures involves a complex interplay between various cell populations coupled with multiple signalling pathways to coordinate tightly controlled cellular behaviours including: growth, proliferation, differentiation, migration and apoptosis (Hu et al, 2013); the general process of facial development is outlined below.

1.3.1 Neuralation and the origins of the neural crest

During neuralation bilateral regions of the ectoderm become elevated to form the neural folds which form around a central neural groove; this developing structure termed the neural plate. Central reorientation of the neural plate leads to proximity and convergence of the opposing neural folds to form the neural tube; this will eventually differentiate into the central nervous system (CNS) (Bronner-Fraser, 1994). The principal pluripotent cell type in facial development are the neural crest cells which are able to differentiate into diverse cell lineages, including fibroblasts (Bronner-Fraser, 1994; Huang and Saint-Jeannet, 2004). These cells are derived from the boundaries of the neural folds during neuralation. This is achieved when the neural crest cells undergo a process of epithelial to mesenchymal transition (EMT) which permits delamination from the ectoderm (Strobl-Mazulla and Bronner, 2013), thereby enabling widespread migration across the developing embryo; the neural crest population that contribute to development of the facial mesenchyme are called the craniofacial neural crest cells (CNCC).

1.3.2 Formation of the nose and lip

Following delamination from the neural folds CNCCs undergo extensive migration along highly preserved migratory pathways; this includes migration to the site ventral to the forebrain, which will become the frontonasal prominence, and into the pharyngeal arches. The first

pharyngeal arch is pertinent to facial development as it separates to form the paired maxillary processes, which will develop into the maxilla, and the paired mandibular processes, which will form the mandible. The development of the external facial structures is principally a result of the expansion, migration, differentiation and fusion of these facial processes (Schoenwolf et al, 2015). During the process of continued growth of the frontonasal prominence, two ectodermal thickenings emerge on its surface; these are the nasal placodes. Lateral and medial swellings develop and surround each nasal placode and grow outwards, whereas the nasal placodes remain stationary to form the nasal pits and develop to form components of the olfactory system (Senders et al, 2003). Whilst this process is taking place there is concurrent medial growth of the paired maxillary and mandibular prominences, the two mandibular prominences meet and fuse at the midline thereby forming the structures of the lower jaw. Following this, the maxillary prominences grow towards the midline and fuse with the lateral nasal prominences to form the nasal alae and lateral regions of the nose, the maxillary processes then fuse with medial nasal process to form the intermaxillary segment. The intermaxillary segment, also called the globular process, is comprised externally of the philtrum of the upper lip but also leads to formation of internal structures including the primary palate (Senders et al, 2003; Lan et al, 2015). Further, the fusion of the maxillary and mandibular prominences leads to the formation of the cheeks whilst the maxillary process leads to the formation of the peripheral regions of the upper lip.

1.3.3 Formation of the hard and soft palate

Once the formation of the primary palate is complete by the end of the seventh week, the secondary palate, which will comprise the posterior two thirds of the hard palate and the soft palate, begins to develop in a process that takes up until week 12th of development to fully mature. Vertical bilateral outgrowths from the maxillary processes, termed the palatal shelves, emerge in the same plane as the tongue. The palatal shelves undergo a period of rapid growth

and expansion with eventual elevation above the tongue. Continued medial growth and orientation into the correct plane leads to shelf proximity at the midline. Opposing palatal shelves, which are covered in epithelium, commence fusion with the primary palate and each other by interaction with filopodia on opposing borders and merge thereby forming the temporary midline epithelial seam (Diewert et al, 1992); this is subsequently replaced with mesenchyme to produce a continuous palate (figure 1). The palatal mesenchyme then differentiates forming both regions of bone, by replacing existing cartilaginous support and muscle corresponding with the hard and soft palate respectively. Disruption at any embryological stage, for example, by delays in cell migration, malposition, fusion deficiencies or obstruction has the potential to result in pathological development. Subsequently this may lead to clefts of the lip or palate, or a combination of cleft lip and palate (Yu et al, 2009).

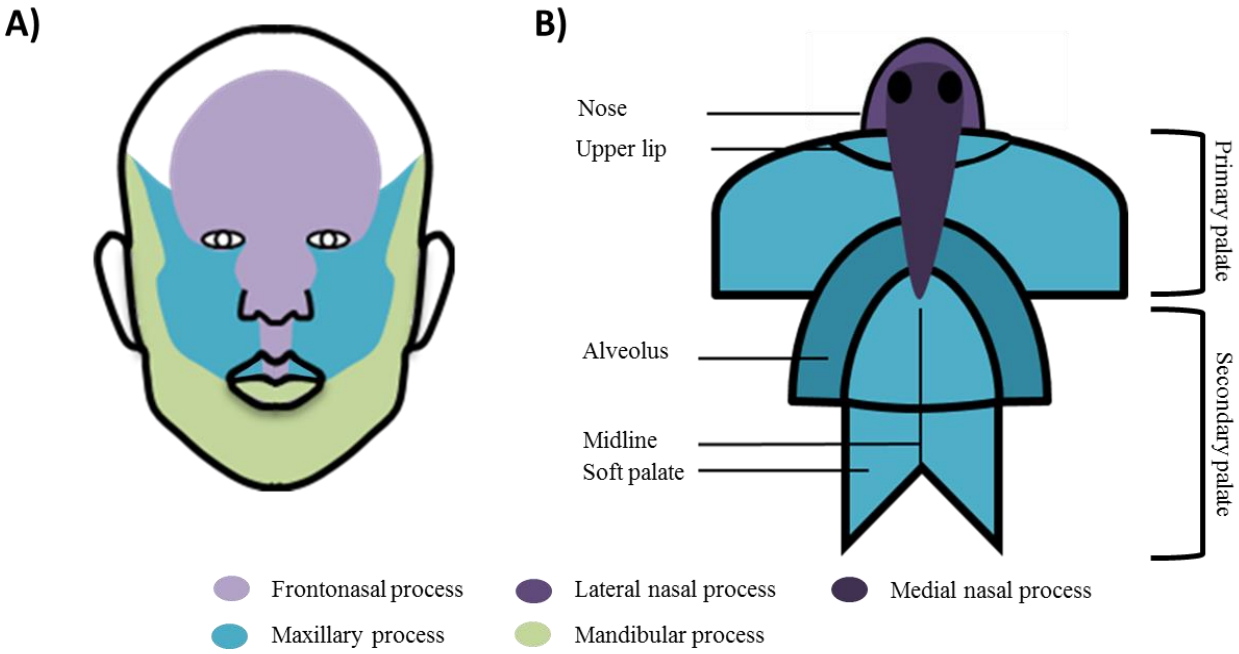

Figure 1: Schematic of embryological origins of the face and palate. A) The frontonasal prominence, paired maxillary processes and paired mandibular processes merge at precise loci to form normal facial morphology. B) The frontonasal derived lateral nasal processes form the outer regions of the nose whereas the medial nasal process merges with maxillary process to form the intermaxillary segment comprising the philtrum and the primary palate. Images recreated based on: (A) Dixon et al, 2011; (B) Cobourne, 2004.

1.4 Classification of clefts

Currently, there are a number of accepted cleft classification systems, though there is no single globally recognised standard (Smith et al, 1998). In 1989, Otto Kriens introduced the LAHSHAL diagrammatical classification system (Kriens, 1989) whereby letters were used to indicate the location in which clefting was present; thus when a patients' cleft was diagnosed they would be assigned letters based on the area affected. In brief: L = Lip (right) A = Alveolus (right) H = Hard Palate (right) S = Soft Palate H = Hard Palate (left) A = Alveolus (left) L = Lip (left). Upper case letters denoted a complete cleft whilst lower case letters denoted an incomplete cleft. This system was subsequently modified, by omitting an 'H', forming the LAHSAL system (Figure 2) and was adopted by the Royal College of Surgeons of England to standardise record keeping in the Craniofacial Anomalies Register (Hodgkinson et al, 2005).

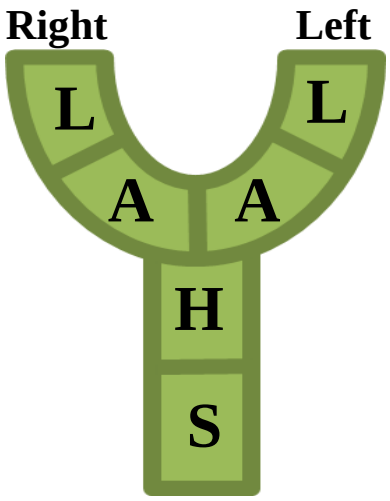

Figure 2: Schematic of the LAHSAL classification system for OFCs. LAHSAL is used in the United Kingdom. The system split the defect into right and left portions as if looking directly at the patient. Each region is denoted a letter and clefts are classified based on the region affected. Upper case letters denote complete clefts whilst lower case represents incomplete clefts, '.' are also incorporated into the system which represents an unaffected region. For example: complete bilateral cleft lip and palate would be 'LAHSAL', left unilateral cleft lip and palate would be '..HSAL' and left unilateral incomplete cleft lip would be '…..l'. L/l = lip; A/a = alveolus; H/h = hard palate; S/s = soft palate.

1.5 Genetic aetiology of cleft lip and palate

The precise aetiology of OFC in humans remains inconclusive at present but there is significant evidence to support a genetic basis to cleft development (Dixon et al, 2011). For example, genetic proximity between individuals with CLP, who have an approximate occurrence rate of 0.15% in the general population, and their relatives has been shown to be a major determinant in occurrence rates, as siblings of patients with CLP have an increased 3.5% chance of cleft development, whilst this decreases to 0.6% for first cousins (Grosen et al, 2010). Further, concordance rates between monozygotic twins has been estimated to be 36% and a significantly lower 4.7% between dizygotic twin pairs (Wyszynski et al, 1996). However, the absence complete concordance between monozygotes suggests that whilst genetic proximity may be a significant contributory factor, there are likely a number of underlying environmental factors that also play a causal role in terms of OFC development.

1.5.1 Syndromic and non-syndromic cleft lip and palate

Cleft lip and cleft palate may manifest in conjunction with a number of other physical anomalies, in such cases the condition is referred to as syndromic CLP (sCLP) as opposed to non-syndromic CLP (nsCLP) in which the congenital defect occurs in isolation. Syndromic forms of clefting are usually associated with Mendelian modes of inheritance and tend to be a result of single gene mutations that can be either autosomal dominant or recessive in nature (Rimoin et al, 2006). In syndromic cases, clefting can either be the primary malady, that occurs in conjunction with other minor defects, or clefts can be a secondary condition that occur in conjunction with one, or multiple, detrimental congenital malformations.

Van der Woude syndrome (VWS) is an autosomal dominant condition that is phenotypically very similar to nsCLP, with only lower lip pits and hypodontia manifesting as additional features. The syndrome is caused due to a nonsense mutation on the *IRF6* gene; this was

identified when studying the genome of monozygotic twins that were discordant for VWS (Kondo et al, 2002). Popliteal pterygium syndrome (PPS) is closely related VWS as its shares all of its clinical features with the addition of popliteal webbing, syndactyly and genital malformations; although other clinical features may also be represented (Lees et al, 1999). VWS and PPS are clinically related due to both syndromes developing as result of differing mutations of *IRF6*, this suggests the importance of the *IRF6* transcription factor to normal embryological development. Genetic clues provided from sCLP forms provide indications as to possible causal candidate loci in non-syndromic forms of clefting. As such, genetic markers involved in VWS/PPS may also be related in nsCLP predisposition; this suggestion has led to identification of *IRF6* variants that may also be associated with nsCLP (Zucchero et al, 2004). To date, several other candidate loci have been identified to have potential causal links to cleft palate development. However, as nsCLP susceptibility arises through a myriad of genetic and environmental factors, coupled with largely sporadic rather than Mendelian inheritance (Jugessur et al, 2009), identification of contributory genetic factors has proven difficult.

There are a number of methodologies employed to aid in gene discovery of markers associated with development of nsCLP. Candidate gene approaches are the most widely used technique, they make use of prior knowledge with regards to gene function and its potential influence on the development of disease. In terms of nsCLP, many candidate genes have been selected based on their expression within the developing facial mesenchyme in animal models. For example, the elevated expression of transforming growth factors (TGFs), in particular the TGF beta 3 (*TGFB3*) isoform, within the developing palatal epithelium during palate morphogenesis (Fitzpatrick et al, 1990) coupled with the finding that murine models lacking *TGFB3* display clefts of the secondary palate with complete penetrance (Proetzel et al, 1995) due to a failure

of palatal shelf fusion (Kaartinen et al, 1997), established TGF isoforms as potential candidate genes in the development of nsCLP (Lidral et al, 1997).

Linkage analysis is a statistical methodology that makes use of the linkage phenomenon whereby alleles in close chromosomal proximity tend to be inherited together more frequently than expected by chance. This analysis is generally conducted on large multiplex families, or smaller consanguineous families, which have multiple members with CLP; this enables the identification chromosomal loci that have greater statistical likelihood to contain genetic markers that are associated with clefting. This technique has implicated sequence variations in the proximity of *SOX9* as being associated with the sCLP Pierre Robin Sequence (PRS) (Benko et al, 2009). PRS can be associated with cleft palate and is characterised by micrognathia, underdevelopment of the lower jaw, glossoptosis, downward displacement of the tongue coupled with the resultant airway obstruction and a wide U-shaped cleft palate (Figueroa et al, 1991). The condition is termed a sequence, as opposed to a syndrome, due to having multiple conditions that manifest due to a single anomaly (Shprintzen et al, 1992). In the case of PRS the primary anomaly is micrognathia, which leads to a group of clinical manifestations that arise from the abnormal posterior displacement of the tongue. Abnormal mandibular growth leads to malpositioning of the tongue which physically obstructs the palatal shelves from fusing, giving rise to the characteristic wide U-shaped palatal cleft (Breugem et al, 2009).

A major advancement in identification of genes contributing to nsCLP was established due to the use of genome wide association studies (GWAS). This technique involves large scale examination and comparisons between the entire genome of cleft patients and unaffected controls to determine whether genetic variants, and previously identified candidate genes, are associated with OFC. For example, GWAS was used in order to investigate the potential role of *IRF6* variants, which have consistently been associated with both syndromic and non-

syndromic forms of cleft, across 460 nsCLP patients relative to 952 control patients; it was concluded that the *IRF6* variant, rs642961, was involved in the development of nsCLP within the selected sample population (Birnbaum et al, 2009). Further, utilisation of GWAS data to study genetic susceptibility to nsCLP has resulted in the identification of many other genetic markers that have potential causal roles (Setó-Salvia et al, 2014). However, the development of nsCLP is unlikely to be the result of a single genetic anomaly, rather it is likely that the cause is multifactorial with several converging genetic and environmental factors that each play a contributory role (Dixon et al, 2011).

1.6 Influence of the environment

Normal foetal development is not just a product of the genetic blueprint as it is also significantly influenced by external environmental factors. A prerequisite of healthy foetal development is adequate maternal nutrition; thus maternal dietary deficiencies may have significant adverse effects. The dietary deficiencies coupled with other environmental factors that can increase the risk of OFC development are discussed below.

1.6.1 Folic acid

Folate is an essential vitamin that is present in leafy green vegetables, legumes and some fruits. Folic acid (FA) is a stable synthetic form of folate that has a 70% higher bioavailability than naturally occurring folates, as a result it is often used to fortify foods and in vitamin supplementation products (McNulty et al, 2004). Folic acid has a number of essential biological roles including acting as a carrier for one-carbon methylation reactions and in production of thymine and purine bases during nucleic acid synthesis; thus it is required for optimal DNA synthesis and cell division (Figueiredo et al, 2009). The developing embryo is completely reliant on maternal dietary intake (Pisano et al, 2010); therefore, adequate maternal folate levels are essential.

1.6.2 Folic acid deficiency associated congenital abnormalities

Development of the lip and palate occurs as a result of the growth, migration and convergence of several facial prominences in response to the precise interplay between intracellular and external stimuli, such as folic acid (Wahl et al, 2015); therefore, maternal deficiency of folic acid can have significant adverse effects during development. FA deficiency has been identified to play a causal role in a number of craniofacial developmental disorders including neural tube defects (NTD) such as anencephaly and encephalocele (Wald et al, 1991). Folate deficiency has also been demonstrated to increase the risk of CLP (Wilcox et al, 2007). A number of studies have found significant reductions in OFC incidence in offspring with mothers who take folic acid supplements or multivitamins containing folic acid (Shaw et al, 1995). In addition, a reduction in the prevalence of OFCs in children born between 1990 and 1996 was observed immediately following introduction of folic acid fortification of US national grain supplies thereby suggesting its protective role against OFC (Yazdy et al, 2007). The offspring of animal models that have been subjected to low folate and folate deficient diets were shown to be at significantly greater risk of cleft development when compared with the offspring of mothers with normal folate intake (Domoslawska et al, 2013; Elwood et al, 1997). Furthermore, drugs that have been shown to block normal FA activity induced cleft palate in 39% of murine offspring and this was coupled with other craniofacial deformities (Azarbayjani et al, 2001).

1.6.3 Other environmental factors associated with cleft formation

Maternal zinc deficiency has been highlighted as having a possible causal link to orofacial clefts (Munger et al, 2009) and as zinc has been shown to be involved in a wide variety of metabolic processes (Vallee et al, 1993) it may be involved in craniofacial development. However, the precise role of zinc in palatal development remains unclear. Cholesterol deficiency may also be a contributing factor to OFC (Murray et al, 2004). This may be due to

the involvement of cholesterol in the maturation and post-translational modifications of the protein sonic hedgehog (shh) (Porter, 2006; Lewis et al, 2001). Hence it is suggested that cholesterol deficiency may perturb the shh signalling pathway which may lead to cleft development (Porter, 2006). Both deficiency and excess vitamin A, specifically its derivative retinoic acid (RA), have roles in OFC development (Lammar et al, 1985; Nugent et al, 1999). It has been shown that RA is involved in palatogenesis through interaction with its receptors *RAR* (retinoic acid receptor) and *RXR* (retinoid X receptor). When activated, these receptors stimulate the retinoic acid response element (*RARE*), initiating transcription of targets that play roles in palatal shelf outgrowth, elevation and fusion (Nugent et al, 1995; Ackermans et al, 2011). Thus dietary excess of Vitamin A can lead to overexpression of these targets by *RARE* whilst deficiency may lead to under-expression of these targets. Conversely however, levels marginally above the recommended daily allowance (RDA) have been shown to protect against CLP (Mitchell et al, 2003).

Maternal tobacco smoking during pregnancy has been linked to CLP development, this increase in risk has been quoted as being greater than 20% in susceptible individuals (Little et al, 2004). Similarly, excess alcohol consumption has been reported to increase susceptibility to OFC (Lorente et al, 2000), though data is somewhat inconsistent (Meyer et al, 2003). Adverse effects from prescription medicine have also been associated with cleft development. Statins are commonly used to lower levels of cholesterol, however their inhibitory effect may be passed on to the developing foetus, through placental transmission and subsequently they may exert an inhibitory effect on shh and other associated morphogens (Edison et al, 2004). Other medications that may be implicated in CLP development include corticosteroids (Pradat et al, 2003) and anticonvulsants (Abrishamchian et al, 1994). Maternal use of recreational drugs, such as cocaine, have also been implicated in development of CLP. A study of infants with mothers that used cocaine during pregnancy found that 14% developed cleft lip whilst 21% developed

cleft palate (Fries et al, 1993). It was proposed that cocaine exposure could cause vasoconstriction of uterine blood vessels which increased intrauterine hypoxia leading to perturbed development (Webster et al, 2007). This hypoxic effect may also occur during heavy maternal smoking (Webster et al, 2007) and high altitude living as increased risk of craniofacial defects has been observed at higher altitudes (Castilla et al, 1999). Planned pregnancy has recently been shown to reduce the risk of CL/P (Mossey et al, 2007) likely due to lifestyle changes that occur prior to the critical period of facial development in the first trimester.

1.7 Epidemiology of cleft lip and palate

A relatively large number of studies have aimed to identify the international incidence of CLP although the precise indication of incidence rates has been hindered by the different experimental techniques and data collection mechanisms utilised between research groups. This issue has been exacerbated by institutional differences in classification systems, variance in sample sizes, low population generalisation and the lack of randomized sampling (Mossey et al, 2002). Furthermore, data collected from many developing countries lack national registries of congenital malformations. Due to this, cleft prevalence is largely taken from treatment centres in more developed areas thus outcomes are potentially inaccurate as data from more rural regions that lack adequate surveillance systems is limited (Mossey et al, 2009; Acuña-González et al, 2011).

Despite the aforementioned difficulties epidemiological studies of OFC have been conducted and the commonly quoted global incidence rate is reported to be 1 in 700 live births (WHO, 2002). According to data derived from the cleft registry and audit network (CRANE), an annual report is published with regards to the number of children born with clefts in the United Kingdom. The total number of children born with OFC between 1st January 2017 and 31st December 2017 was 1068, this equated to a national incidence rate of 1 in 657 live births

(CRANE, 2018). Further, the majority of children born with clefts displayed cleft palate in isolation (45%) whilst significantly fewer displayed cleft lip in isolation (22%). When clefts of the lip and palate occurred in conjunction (CLP), it was found that 22% patients had unilateral CLP whilst the remaining 11% displayed bilateral CLP (CRANE, 2018). In terms of global incidence rates, a large-scale study was undertaken that comprised data collection over a five-year period which included 34 US states and 30 countries (Tanaka et al, 2013). The data was normalised such that the incidence rate was estimated per 10,000 live births. The study found that the majority of US states had prevalence rates between 7 and 13 per 10,000 live births, with outliers in West Virginia (2.59) and Maryland at (21.46) but an overall national average of 7.75 (per 10,000 live births respectively). The US national average was comparable with that of another large-scale study which concluded the US incidence rate as 10.2 per 10,000 live births (International Perinatal Database of Typical Oral Clefts working group, 2011). Internationally, there are large variations between reported incidences thus suggesting ethnicity as a potential contributory factor for OFC. Countries with the highest reported rates are Japan (19.05), Mexico (13.69), and Norway (12.73) whilst the countries with the lowest rates were Cuba (3.81), Spain (3.79) and South Africa (3.13), although the causal factor which results in individuals to be at greater or lower risk based on country of origin has not yet been identified (Tanaka et al, 2012). Notably however, these rates were extracted from birth defect surveillance systems, some of which were solely hospital based and therefore only represented a portion of the population that accessed these facilities. Despite this, the general trend mirrored those of other studies which found Asian populations had the highest prevalence rates (Habib, 1978) whilst African populations had the lowest (Vanderas, 1987).

A retrospective European multicentre study of the incidence of cleft palate found that out of 3852 cases 54.8% were isolated CP, 18% were associated with other malformations such as cleft lip and 27.2% were related to recognised syndromes (Calzolari et al, 2004). Cleft lip is

approximately twice as common in males whereas cleft palate is twice as common in females (Martelli et al, 2012). This gender bias extends to cleft laterality, with an approximate 2:1 ratio of left unilateral clefts in males compared with females (Dixon et al, 2011). The occurrence of OFC among 54,000 relatives of cleft sufferers was documented in a landmark Danish study which found an occurrence rate of 3.5% amongst first degree relatives (parents; siblings), 0.8% amongst second degree relatives (half siblings, nieces/nephews, aunts/uncles and grandparents) and 0.6% between third degree relatives (first cousins) (Grosen et al, 2010). It is important to note that whilst comprehensive, this study only recorded occurrence rates amongst a large Danish experimental group and as ethnicity was likely to have an influence on incidence of OFC these values may not be globally representative.

1.8 Clinical management

Treatment of CLP occurs immediately after birth as mothers are referred to specialist nurses in order to receive advice on caring for cleft patient and in some cases pre-surgical intervention may be required prior to definitive repair (Pool, 1995). Repair of the cleft lip typically occurs at approximately 3 months of age whereas repair of the cleft palate occurs at 6 months of age. When cleft lip and palate occur in combination patients are subject to two operations, the first to repair the cleft lip and the second to repair the cleft palate (Sitzman et al, 2017).

1.8.1 Pre-surgical intervention

Large cleft defects or those with a severe protruding pre-maxilla often merit early intervention in order to improve prognosis (Figure 3). Markedly wide clefts of the lip may require initial treatment via lip taping; this procedure follows similar principles to the orthodontic brace in that there is gradual tissue remodelling under tension via regular tightening. The procedure involves placing surgical tape on either cheek attached to a skin adhesive; the length of the tape is then progressively decreased as either end of the alveolar defect increases in proximity. There are varying reports of success using this technique and one study reported that routine use of

this technique, yielded an average decrease in the alveolar gap from 12.4mm to 5.8mm (Pool, 1995). The use of infant orthopaedics, such as Latham palatal devices which are screwed onto the palate and gradually tightened to reduce cleft width, remain highly controversial. The procedure involves surgically pinning the device onto the palate coupled with a screw that is tightened daily which gradually moves to draw each palatal segment closer. In the case of patients with severe protrusive pre-maxilla this device may also be connected to the nasal septum in order to align it correctly for future definitive surgery (Nahai et al, 2005). However, a Dutch cleft study group concluded such orthopaedic devices have no effect on facial appearance (Prahl et al, 2006), thus the technique is not used in the UK (though popular elsewhere worldwide). A surgical technique that may be utilised in cases of bilateral CLP, or very wide unilateral CLP, is the lip adhesion technique. The basic principle of this technique involves changing the class of the defect from complete to incomplete to aid in definitive repair and reduce deformity (Nagy et al, 2009).

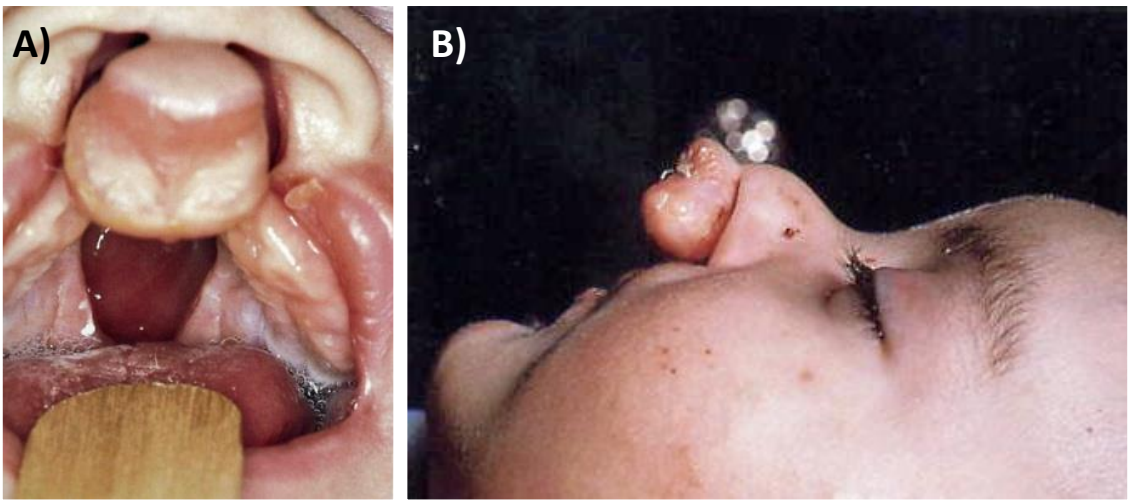

Figure 3: Photographs of orofacial clefts from two patients. A) Frontal view, B) lateral view. Both patients may benefit from pre-surgical intervention such as lip taping or lip adhesion in order to reduce the severity of the deformity prior to surgery.

1.8.2 Definitive surgery and post-operative complications

Both globally and regionally there is considerable difference in the surgical protocols used to treat CLP. This was recently highlighted by the Eurocleft study which found that for treatment of just one cleft phenotype (unilateral complete cleft lip affecting the hard and soft palate) there were 194 variations in cleft closure protocols between 201 cleft teams throughout Europe (Shaw et al, 2001). The time points for cleft lip and cleft palate repair are also subject to wide variation, some surgical protocols include neonatal repair (Desai et al, 1990). However, neonatal repair is controversial due to the possibility of the patient suffering from undiagnosed syndromic OFC, including congenital heart disease (Shafi et al, 2003) or respiratory issues, which may lead to anaesthetic complication (Kulkarni et al, 2013). In the UK, lip closure routinely occurs approximately three months after birth (Somerville et al, 2005), thus providing adequate time to detect other genetic anomalies. Further, surgical repair is not generally conducted until the criteria for the rule of 10's has been fulfilled in order to mitigate the risk of post-operative complications. This criterion suggests that surgical repair is not conducted until the patient is at least 10 weeks of age, weighs more than 10 lb (4.5kg) and has a haemoglobin count greater than 10g/dl (Chow et al, 2016). Palatal closure occurs around six months of age as up until this time infants are obligate nasal breathers thus closure may lead to respiratory distress (Smith et al, 2013). This early palatal closure aids in speech development but may impede facial growth, whilst late (adult) palatal closure increases the likelihood of normal facial aesthetics but also irreversible damage to speech (Richard et al, 2006). Though the surgical procedures may vary the fundamental goals of cleft surgery remain the same.

The functional aim of cleft lip surgery is to re-establish the muscular competence of the orbicularis oris muscle that encircles the mouth although improvement in aesthetic quality is important. Aesthetic improvements include restoration of Cupid's bow, the double curve of the

upper lip, with clear demarcation of the vermillion border as well as restoration of the vertically grooved philtrum to establish typical facial features. In the case of complete cleft lip, rhinoplasty may also be necessary to correct the cleft nose deformity at the end point of facial growth (Singh et al, 2009). The main complication of cleft lip surgery is the failure to re-establish the muscular integrity of the orbicularis oris muscle, possibly leading to a secondary deformity due to the manifestation of a visible muscular lateral bulge (Matic et al, 2011). Hypertrophic scarring is a further post-operative complication resulting from pathogenic wound healing and is characterised by visible lip regression, leading to asymmetry and potential nasal stenosis (Soltani et al, 2012), possibly necessitating revision surgery.

The main surgical outcome of palatoplasty is to reshape the palatal defect such that it mimics typical anatomical form and function. Further, surgical repair should aim to reinstate the ability to completely close the velopharyngeal sphincter thus permitting velopharyngeal competence. Various complications can arise post-operatively, the most important of which is palatal dehiscence, which gives rise to varying degrees of oronasal fistula (ONF). Development of an ONF reinstates the link between the oral and nasal cavities following primary palatal surgery, thus necessitating secondary surgery (Anani et al, 2012). This defect is often recurrent (Diah et al, 2007) and leads to nasal regurgitation of food, hyper-nasal speech and increased nasal air flow (Sadhu et al, 2009). This abnormal association linking the oral and nasal cavities tends to develop on the secondary palate. The regions of the secondary palate mostly affected are hard palate (54%) and the hard-soft palatal junction (36%) (Diah et al, 2007). The diameter of fistulae can also vary with larger fistulae presenting more serious symptoms. According to Diah et al, (2007), ~10% of fistulae were relatively small (1-2mm), 36% were medium size (2-5mm) and 54% were greater than 5mm. Post-operative ONF formation may be due to a number of factors including surgical technique (Amaratunga, 1988), type of cleft (Murthy et al, 2011), width of

cleft (Parwaz et al, 2009) and age of palatal closure (Emory et al, 1997). However, a recent comprehensive systematic review, pertaining to the incidence of ONF following primary palatal repair, concluded the global incidence of ONF to be 8.6% with surgical technique and continent of origin having no significant effect on ONF development. It was however found that ONF had a greater statistical likelihood in cases of CLP compared with clefts in isolation (Hardwicke et al, 2014). The Pittsburgh fistula classification system was developed in order to standardise types of fistula and replace ambiguous descriptive classifications. The system addresses 7 types of fistula with each type relating to the region of the palate affected (Smith et al, 2007).
Velopharyngeal insufficiency can result from inadequate extension of the soft palate either due to limited soft tissue availability or surgical technique, leading to hypernasality. Speech therapy may be sufficient to correct minor cases of hypernasality; however, patients with an anatomical defect may require prostheses (pharyngeal obturators) or, most often, surgery (posterior pharyngeal wall augmentation or pharyngoplasty) to restore normal speech (Fisher et al, 2009).

Hypertrophic scarring (HTS) is a post-operative complication that generally occurs 3-6 months following cleft repair. The reported incidence of HTS following cleft repair varies widely however a recent comprehensive retrospective study found that the incidence of HTS following cleft repair was 25% (Soltani et al, 2012). The condition is characterised by deposition of large amounts of collagen during the wound healing process often leading to potentially painful thick red scarring at the site of repair. Following formation of a hypertrophic scar its size may remain stable or begin to regress (Muir et al, 1990). Regression of the scar can lead to shortening of one side of the repair leading to lack of healing uniformity across the wound area (Rabello et al, 2014); this may necessitate revision surgery in order to restore aesthetics and symmetry.

Another major complication of palate repair, albeit delayed, is the possibility of maxillary hypoplasia (Moreira, 2014; Shetye, 2004). The manifestation of this mid-facial deficiency leads

to a concave facial profile, often accompanied by a crossbite, which, in severe cases, may require orthognathic surgery to restore facial aesthetics (Sakaguchi et al, 2008). The development of this condition cannot solely be attributed to the width of cleft, the surgical protocol applied or individual differences in wound healing (Farranto et al, 2014; Weinzweig et al, 2006). Rather, excessive hypertrophic scarring following primary palatoplasty has been cited as the cause (Fudalej et al, 2012), this may be due to excessive palatal wound contracture by myofibroblasts during the proliferative phase of wound healing leading to the generation of rigid collagen-rich tissues (Beyeler et al, 2014). Whilst there is little research into the potential physiological deficiencies of cleft fibroblasts, it is possible that due to a number of genetic factors that contribute to cleft formation, fibroblasts in affected individuals may be behave abnormally thereby giving rise to pathological wound healing due to abnormalities in migration or proliferation which are fundamental processes to normal wound healing.

1.9 Histological structure of clefts

The oral mucosa, which is the tissue type present in the lip and palate, comprises three distinct layers: the oral epithelium, lamina propria and underlying submucosa. The oral epithelium is characterised by five epithelial layers, the most superficial layer is the stratum corneum, which is a layer of approximately 15-20 flattened dead cells, with both nuclei and organelles absent which plays a protective role. The stratum granulosum is a transitional layer that comprises migrating keratinocytes from the significantly thicker stratum spinosum that lies beneath. The deepest layer of the stratified squamous epithelium is the stratum basale, a single layer of highly proliferative cuboidal epithelial cells that migrate more superficially to form and maintain the other epithelial layers (Squier et al, 2001). The lamina propria is the connective tissue layer of the oral mucosa and is composed largely of fibrous collagen type I and III as well as elastin which is secreted by the population of fibroblasts that are present throughout the lamina propria. These fibroblast populations are critical to normal wound healing following cleft repair as they

secrete essential growth factors that attract other fibroblasts and rapidly proliferate following the creation of wounds such as those caused by surgical incisions. Due to the fundamental roles that these cleft fibroblasts play, this cell type was selected to characterise in the present study.

1.10 Fibroblast use in biological research

Fibroblasts are stromal cells of mesenchymal origin with many functions that are pivotal to both human development and maintenance. Fibroblasts are generally abundant but are often found *in vivo* as single cells embedded within the fibrillar extracellular matrix (Eckes et al, 1993). Dormant fibroblasts *in vivo* are often described as being in a quiescent state prior to activation from an external stimulus, such as due to exposure to cytokines and growth factors, which initiate their functional response (Chen et al, 2012). Fibroblasts are one of the most widely used cell types in biological research due to their abundance and amenability to culture *in vitro*, despite this, molecular characterisation of fibroblasts remains poorly defined. Fibroblasts have been shown to express a number of molecular markers, including vimentin, although other cells of mesenchymal origin also express this molecule (Camelliti et al, 2005). However, fibroblastic lineage is often assessed by the absence of other distinct genetic markers characteristic of other cell types (Chang et al, 2002). Fibroblast morphology is often described as spindle shaped, however *in vitro*, specific morphology may be influenced based on the level of confluence, cell cycle, supplementation conditions and differentiation state. Fibroblasts often display cytoplasmic extensions with lamellipodia and filopodia branched towards the direction of migration demonstrating cellular polarity (Bliokh et al, 1980).

1.10.1 Physiological function of fibroblasts

Fibroblasts are primarily secretory cells that provide mechanical integrity to tissues through continuous production of ECM molecules such as collagens and glycosaminoglycans. Fibroblasts deposit crucial components of the ECM, including ground substance and a number of fibres, into the local milieu to provide tissue integrity by increasing its mechanical strength.

Fibroblasts also play a key role in tissue homeostasis, this is achieved through continued ECM remodelling via secretion of both ECM precursors and enzymes involved in the breakdown of matrix macromolecules; this balance of ECM production and degradation is conducted in regulated manner to ensure tissue homeostasis. Further, fibroblasts also secrete a large cohort growth factors and cytokines that act in both an autocrine and paracrine manner leading to recruitment and activation of other local cell types thereby playing a critical role in both the early inflammatory phases and the later tissue remodelling stages of wound healing.

1.10.1.1 The role of the ECM

The extracellular matrix is a complex biological, physical and physiological support network that has many functions. Its primary function is as a natural scaffold that provides mechanical integrity to tissues, this is achieved primarily through fibrillar collagen proteins which are embedded into heterogeneous support network which contain an abundance of cell types and macromolecules. Many cell types use ECM components, including glycoproteins such as fibronectin, to permit integrin regulated cell-ECM adhesion to enable the cell to undertake their specific function. This adhesion can occur through cellular focal adhesions, which connect cellular actin to the ECM, or through hemi-desmosomes, which connect the ECM to intermediate filaments such as vimentin (Alberts et al, 2015). The ECM also behaves as a physical barrier between tissues and acts as an intermediary for intercellular communication. In addition, the ECM acts as physical storage unit for a host of growth factors which can be mobilised following physiological change thus permitting swift local growth factor induced responses without the immediate need for cellular secretions (Taipale et al, 1997).

During craniofacial development, the facial prominences expand as a result of cell proliferation and ECM deposition by new and existing cells in the surrounding tissues (Schoenwolf et al, 2015). The increase in volume of craniofacial tissues prior to fusion is understood to be contributed to equally by both proliferation and ECM accumulation thus precise production of

ECM is pivotal to normal facial development as perturbations may lead to disrupted facial development and potentially the formation of clefts (Meng et al, 2009). Due to this, cleft fibroblast production of ECM components may be a contributing factor for different clinical manifestations of clefts. In addition, controlled secretion of ECM by fibroblasts is key to normal wound healing following cleft repair with overproduction leading to increased risk of HTS and ONF. Differences in ECM production may also contribute to patients, with phenotypically comparable clefts, displaying distinct clinical outcomes following cleft repair.

1.10.1.1.1 Collagen synthesis and function

Collagen fibre production is achieved due to the synthesis of intracellular precursors which are secreted into the extracellular space in order to undergo maturation into collagen fibres. Initially, fibroblasts transcribe and translate alpha chain peptide precursors with the amino acid glycine comprising approximately one third of the peptide sequence; this is referred to as pre-pro-polypeptide. The elevated glycine content is important in the eventual formation and stabilisation of collagens. As glycine is the smallest amino acid, its high content permits close peptide association thereby facilitating the formation of hydrogen bonds and intermolecular crosslinking (Shoulders and Raines, 2009). Following this, the pre-pro-polypeptide chain undergoes a series of post translational modifications. First the signal peptide sequence at the beginning of the chain, which was involved in the initiation of protein synthesis, is removed thereby converting pre-pro-polypeptide into pro-polypeptide. This then undergoes hydroxylation and glycosylation of amino acids along the peptide chain, these modifications enable three modified pro-polypeptide chains to fold into a triple helix structure to form pro-collagen (Kielty and Grant, 2002). Pro-collagen is then processed into secretory vesicles and exocytosed into the extracellular space. When in the ECM, collagen peptidases cleave the ends of the pro-collagen chains to form tropocollagen, tropo-collagens then undergo assembly into collagen fibrils via the action of lysyl oxidases which covalently bond lysine residues between

opposing tropocollagen molecules to form collagen fibrils (Kielty and Grant, 2002). Collagen is a key structural protein in the ECM which owes its ubiquity and efficacy to both the tensile strength and compressibility of its fibres. Currently there are 28 types of collagen identified (Richard-Blum, 2011), each with differing tissue abundances relating to their local function. Collagen type I and type III are understood to make up approximately 80% and 20% of the total dermal and mucosal collagen, respectively (Tracy et al, 2016), with other collagen types, such as collagen type V, being produced in smaller amounts (2-4%) (Smith et al, 1986). Collagens can be broadly categorised into two distinct types: fibrillar and non-fibrillar collagens. Fibrillar collagens include types I, II, III and V which due to their interconnected fibrils allow the ECM to act as a biological scaffold.

1.10.1.1.2 The function of Glycosaminoglycans

Glycosaminoglycans (GAG) are linear polysaccharide components of the ECM that exist both independently and bound to larger proteoglycan sugars. GAGs are hydrophilic in nature therefore have an important function in the maintenance of osmotic balance between the ECM and neighbouring tissues in order to provide adequate local hydration (Couchman et al, 2012). This is achieved by means of the negative charges along their chains attracting positive sodium ions (Na^+) which, via osmosis, attract water molecules. Chondroitin sulphate (CS) and dermatan sulphate (DS) are the most abundantly produced GAGs in dermal and mucosal ECM (Tracy et al, 2016). CS and DS are very similar in structure however the presence of iduronic acid along the chain of DS makes it a distinct GAG. CS and DS can exist both bound to proteoglycans or as unbound GAGs, the latter has been shown to act as a preliminary substrate for fibroblast migration in the ECM. It has also been suggested that CS and DS may be associated with improved wound healing as scarless foetal wounds contain much greater amounts of CS and DS when compared with adult skin (Carrino et al, 2000). Heparin sulphate (HS) is another type of GAG that is secreted and binds to cell surfaces in the ECM, this protein has an array of

functions but one of its major roles is acting as regulator to aid in cell response to particular growth factors such as fibroblast growth factor (FGF) and epithelial growth factor (EGF) as a result modulating proliferation and other cell behaviours (Rabenstein, 2001).

1.10.1.1.3 Overview of related ECM molecules

Fibronectin is secreted by fibroblasts into the ECM milieu as soluble glycoprotein dimers, these bind to integrin receptors on surrounding cell surfaces leading to clustering of integrins and increased local fibronectin concentrations. Integrin bound fibronectin molecules interact with each other to form associations with the local ECM neighbouring cell populations, thus are involved in key cell behaviours (Wierzbicka-Patynowski et al, 2003). Fibronectin molecules also offer additional structural support to surrounding tissues and also play a role in cell-ECM adhesion and cell proliferation. Furthermore, these molecules aid in cellular migration they increase tension within the ECM. This tension plays a role in fibroblast to myofibroblast transition which is essential for both normal ECM regulation and ECM deposition in acute wounds (Pankov et al, 2002). Fibronectin is also essential during embryogenesis as it has been shown to act as scaffold for cell attachment and as a guidance system for migrating embryonic cells and structures (Sakai et al, 2003). Elastin is secreted from fibroblasts as its precursor tropoelastin; following formation of elastic fibres it functions to provide a degree of elasticity to the ECM and surrounding tissues and offers some resistance against mechanical stresses and strain (Kristensen et al, 2016).

1.10.2 Fibroblasts in disease

As previously outlined, fibroblasts exhibit an array of functions that are critical to health and normal homeostatic conditions and perturbations to normal fibroblast behaviours can lead to a number of adverse physiological effects. The major function of fibroblasts continued ECM remodelling, excessive or diminished production of ECM, due to abnormal fibroblast behaviour, can have significant adverse effects. Following surgical repair of clefts there are a

number of post-operative complications that can occur, including hypertrophic scarring and formation of oronasal fistulae. Whilst these complications are likely the result of many contributory factors, pathological cleft fibroblast ECM deposition may potentially play a significant role in their formation.

Hypertrophic scarring is a cutaneous condition that can occur following traumatic injury or surgery. The condition is characterised by excessive unaesthetic scarring and is believed to be a result of disproportionate collagen deposition by fibroblasts following injury (Soltani et al, 2012). In the maturation phase of normal wound healing collagen production and collagen breakdown by matrix metalloproteinases are in equilibrium; however, in hypertrophic scars this does not occur. Increased quantities of collagen fibres at the wound site leads to increased mechanical tension across the wound that causes greater fibroblast-to-myofibroblast differentiation which in turn secrete greater amounts of collagen thereby exacerbating the condition (Schmieder et al, 2017). Keloid scarring is similar to hypertrophic scarring however the former is characterised by excessive scar tissue formation beyond the boundaries of the original wound. Keloid scarring is also caused by excessive fibroblast deposition of ECM and despite the clear clinical distinction, may be caused by the same pathophysiological process (Schmieder et al, 2017). Chronic wounds are injured tissues that have a significantly delayed wound healing process often with prolonged inflammatory phases leading to greater incidence of bacterial invasion thus patient morbidity (Levinson, 2013). Fibroblasts at the site of chronic wounds have been shown to have an abnormal morphology and significantly decreased proliferation thus hindering the phase of healing in which expansion of local fibroblast populations leads to greater total ECM deposition at the site (Agren et al, 1999). Fibroblasts in chronic wounds have been shown to have a perturbed response to *TGFβ1*, which would normally induce myofibroblast differentiation and lead to wound contraction, due to down

regulation of TGβR2 (Kim et al, 2003; Cha et al, 2008). Due to these fibroblast abnormalities, chronic wounds might result in delayed healing and significant patient distress.

1.10.3 Fibroblast motility

Cell motility is central to normal fibroblast activity in a range of biological processes including embryonic development, wound healing and maintenance of regular homeostasis (Alberts et al, 2015). For example, during normal dermal wound healing a cascade of events are initiated following coagulation, this includes an inflammatory response as a result of chemical stimuli released via platelet degradation and locally recruited leukocytes. The resulting increase in cytokine concentration at the wound site leads to a chemotactic response whereby fibroblast migrate to the site of injury from adjacent tissues in response to chemical signals leading to the secretion of essential biomolecules, including collagens and glycosaminoglycans, to construct a provisional extracellular matrix (McDougall et al, 2006; Acharya et al, 2008); adequate fibroblast motility into the wound site is therefore critical to wound site matrix remodelling. The speed of fibroblast migration is critical in normal wound healing and can be a significant contributory factor in fibrosis, which is characterised by the accumulation of fibrous connective tissues resulting in the formation of excessive scarring across the wound site (Darby et al, 2007). This is due to the exertion of a tractional force onto the underlying matrix by fibroblasts when migrating, this increased mechanical stress across the matrix stimulates myofibroblast differentiation via mechanotransduction (Huang et al, 2012). Myofibroblasts synthesise abundant ECM and cause wound contracture resulting in further increases in wound site tension thereby promoting additional fibroblast differentiation via positive feedback (Tomasek et al, 2002). As the initial rate of fibroblast migration is related to the amount of ECM deposition and wound contracture, fibroblast migration rates into the wound following cleft repair are related to fibrosis (Beyeler et al, 2014). Thus it is possible that cleft patients with disrupted fibroblast migration rates may be at increased risk of pathological wound healing and development of

post-operative complications. Due to this, it is important to understand the mechanisms and underlying the regulatory processes of fibroblast migration which would aid in understanding the pathological wound healing observed in some patients following cleft repair.

1.10.3.1 Model of cellular locomotion

The coordinated activity of many intercellular proteins regulates the processes that drive cell migration. External stimuli such as growth factors, cytokines and physical stresses are detected by membrane bound receptor molecules inducing a signalling cascade that promote cell migration toward or away from the stimuli (Alberts et al, 2015). In response to external stimuli the initial locomotory response is the protrusion of cytoskeletal projections called lamellipodia and filopodia. These cellular projections are thought to form due to polymerisation forces. Cytoskeletal actin filaments at the periphery of the cell membrane undergo repeated small scale polymerization with actin monomers, due to the elasticity of actin fibres each additional monomer exerts a force on the dynamic cell membrane, this elastic force propels the membrane forward leading to the formation of cellular protrusions (Mogilner et al, 1996; Caballero et al, 2015). These protrusions are thought to act as the cell's mechanoreceptors which assess the feasibility of migration in a particular direction (Riveline et al, 2001) and form the cells leading edge. This leading edge forms in the region closest to the stimuli in the case of a chemo-attractive response or will form in the opposite direction due to a chemo-repellent response. Following establishment of migration directionality, nascent adhesion complexes form between the base of the leading edge and the underlying substrate. This adhesion stabilises the site of membrane protrusion and firmly attach the cell extensions to the ECM. The cell-ECM adhesion sites produced can vary widely, nascent adhesions usually form first as they are small simple complexes that can be produced rapidly in the immediate region behind the leading edge. As migration continues nascent adhesions mature into focal complexes and are normally situated further back from the leading edge at the lamellipodium-lamellum border; these complexes can

mature into complete focal adhesions and are situated at sites of parallel to large actin bundles or stress points at the centre of the cell body (Zimerman et al, 2004). These anchorage points are central to normal cell migration and limit retrograde flow which are inward pulling forces, usually responsible for cell spreading, produced by excess tension from actin polymerization at the cell border (Mayor et al, 2016; Anderson et al, 2008). Adhesion sites limit inward pulling forces by acting as traction points that are able to resist these regressive forces by allowing effective transfer of kinetic energy onto the migrating surface. The next step in cell locomotion is the translocation of the cell body. The mechanical forces required to translocate the cell are produced by interactions of non-muscle myosin II with bundles of actin through formation of actomyosin complexes. Myosin II contraction leads to rearrangement of the network of actin filaments eventually forming parallel bundles of actin fibres, which have lower resistance to the contractile force produced by myosin II, leading to greater mechanical force generation. Contractile myosin II is primarily located at the rear of the cell leading to inward cytoskeletal pressure creating forward dynamic flow of cellular components (De Pascalis et al, 2017). Following myosin II and actin contraction large amounts of energy is generated which enables the cell to propel itself forward through use of the tractional force produced between the cell body and the ECM via adhesion sites (Ananthakrishnan et al, 2007). The cycle of cell migration is completed by retraction of the cells trailing edge. Detachment of the trailing edge can only be achieved by disassembly of the adhesive anchorage sites that form in the early stages of cell motility. The detachment of adhesive complexes occurs by the interaction of microtubules with focal adhesions. Microtubules bind to adhesion complexes and induce release of cytoskeletal stress fibres that were responsible for the mechanotransduction of cellular contraction force leading to detachment of cell-ECM adhesive contacts (Broussard et al, 2008; Kaverina et al, 1999; Raab et al, 2017). It is important to note that migration is a highly dynamic process and many of the aforementioned functions often occur concurrently in different regions of the cell.

1.10.3.2 Molecular regulation of cell motility

The individual processes in cell migration are regulated by interaction of intercellular regulatory molecules which influence cell mechanics. The Rho family of GTPases are small guanine nucleotide-binding proteins that, coupled with downstream effectors, act as molecular switches within the cell and can stimulate cytoskeletal conformational change and the formation of adhesive complexes. Though there are over 20 members of the Rho family, Rac1, RhoA and CDC42 are thought to be the most significant in relation to cell motility (Lawson et al, 2017). Intercellular Rac1 and CDC42 proteins are activated in response to external stimuli. Through interaction with the downstream effectors Wiskott–Aldrich syndrome protein (*WASP*) and WASP-family verprolin homologue (*WAVE*), which in turn activate the Arp2/3 complex, *RAC1* and *CDC42* regulate lamellipodial actin dynamics through repeated actin polymerisation. This leads to cellular polarity due to the initial formation of cellular protrusions and the leading edge (Tapon et al, 1997); however, in general the formation of broad lamellipodial pods are thought to be due to the action of *RAC1* whereas formation of filopodia is due to the action of *CDC42* with actin at the peripheral regions of the leading edge (Hernández-Vásquez et al, 2017). RhoA proteins are primarily located towards the rear and the trailing edge of the migrating cell (Kurokawa et al, 2005). Following activation, RhoA stimulates its downstream serine/threonine kinase effector rho-associated coiled-coil-containing protein kinase (*ROCK1* and *ROCK2*). Myosin phosphatases bind to myosin II and prevent its phosphorylation hence interaction with actin filaments due to relaxed state of myosin. ROCK proteins inactivate myosin phosphatase subunits thus allowing continued myosin II phosphorylation (Foxall et al, 2016). Activated myosin II promotes the maturation of nascent adhesion molecules in focal adhesion complexes thus permitting mechanotransduction of force from actomyosin contraction and the generation of tractional forces which propel the cell forward (Machacek et al, 2009; Parsons et al, 2010).

1.10.4 Myofibroblasts

Myofibroblasts are terminally differentiated fibroblasts that are distinguished by responses to specific stimuli (Schmitt-Gräff et al, 1994). Myofibroblasts are characterised by incorporation of smooth muscle actin into their cytoskeletons, this actin isoform is not found in undifferentiated fibroblasts and is generally only present in smooth muscle cells (Gabbiani, 2003; Tomasek et al, 2002). Fibroblast to myofibroblast differentiation occurs in response to a number of interlinked factors and only following a normal wound healing response. During the proliferative phase of wound healing local fibroblast proliferation increases significantly. Each new fibroblast recruited to the site generates new cell-ECM contacts through secretion of collagens and fibronectin; this secretion generally occurs along lines of tension increasing mechanical stress at the site (Hinz et al, 2001). Migrating fibroblasts, within the dynamic ECM complex, exert tractional forces between their cell body and the ECM molecules to which they are attached, this leads to increased rigidity between fibroblast-ECM contacts and increased intercellular stress resulting in a myofibroblast differentiation response (Hinz et al, 2003). Coupled with mechanical stress the presence of elevated levels of transforming growth factor 1 (TGFβ1) at the wound site is also understood to play a causal role in fibroblast to myofibroblast differentiation (Marinković et al, 2012). TGFβ1 is present in the ECM milieu in its latent form and is activated in response to environmental changes such as imbalances in pH, oxidative stress or due to proteolytic cleavage that would likely occur during a wound healing response. Activated TGβ1 has been shown to stimulate fibroblast to myofibroblast differentiation as treated cells subsequently express smooth muscle actin (Vaughan et al, 2000); furthermore, this has been shown to occur both *in vitro* and *in vivo* (Desmoulière et al, 1992). In addition, inhibition of TGFβ1 during the wound healing process has been shown to significantly decrease smooth muscle actin levels in local fibroblast populations indicating decreased overall differentiation (Hinz et al, 2001). Although the precise involvement of

TGFβ1 in myofibroblast differentiation remains unclear it has been speculated that due to the physiological effects of TGFβ1 on cell migration, proliferation and adhesion, TGFβ1 may induce mechanosensitivity in the local fibroblast populations leading to an exaggerated response to mechanical stresses and thus myofibroblast differentiation (Hinz et al, 2003). An important distinction to make is that in healthy tissues this fibroblast to myofibroblast differentiation does not occur. This is due to latency of TGFβ1 and the relative elasticity of the ECM as a result of a mature network collagen fibres, elastin fibres and glycosaminoglycans. Due to the ability of these ECM fibres to deform, less mechanical stresses are transferred to the largely quiescent ECM embedded fibroblasts. These fibroblasts also have fewer cell-ECM contacts which further decreases cell stress and prevents differentiation (Hinz et al, 2003.

Myofibroblasts are highly responsive to the effect of secreted cytokines at the site of injury, as a result these cells are involved in the secretion of large amounts of ECM related molecules, particularly during the proliferative phase of healing when collagen production is significantly greater than collagen degradation by MMPs (Bagalad et al, 2017). In addition to producing significant amounts of ECM myofibroblasts are also pivotal to wound contracture. Myofibroblast contraction is associated with its characteristic smooth muscle actins interaction with non-muscle myosin; this generates the contractile forces responsible for wound contraction (Powell et al, 1999). Mechanotransduction of contractile forces generated by myofibroblasts during this process are transferred from intercellular actin stress fibres to the ECM through use of specialised transmembrane molecules which connect cytoskeletal components to integrin associated fibronectin (Powell et al, 1999; Tomasek et al, 2002); this contractile force reduces the space between ECM components leading to gradual wound contraction. Following wound contraction, local myofibroblasts undergo apoptosis in order to prevent an exaggerated wound healing response (Desmoulière et al, 1995); however, in some cases myofibroblasts may persist

in the wound site, in such cases pathological healing can occur leading to incidence of hypertrophic scarring and fibrosis (Tomasek et al, 2002; Van De Water et al, 2013).

1.11 Wound healing

A wound is characterised by damage or disruption to the normal anatomical form and function of biological tissues. This damage can range from superficial injury due to breakdown of epithelial integrity to damage of multiple tissue types extending into subcutaneous matter causing perturbations to nerves, blood vessels and organs as well other tissue types (Robson et al, 2001). In the case of primary cleft repair, surgical incisions are required to re-orientate tissues into the correct plane restoring the aesthetic and functional roles of the lip and palate. This process results in formation of wounds along lines of incision which are sutured together to enable primary intention wound healing. However, if the normal wound healing process is disturbed by overproduction of ECM by local fibroblasts, HTS can occur and the precise tissue orientation can become disrupted leading to tissue regression and failed repairs.

1.11.1 Normal wound healing

The role of wound healing is to restore normal tissue integrity and function. This process is governed by complex interplay between an array of immunological, cellular and biochemical components in an organised cascade which work in unison to deliver adequate repair over a predictable period of time. Wound healing occurs in three major overlapping phases: the inflammatory phase, the proliferative phase and the maturational phase. Wound healing can occur by primary intention, where wound boundaries are held adjacent to each other to promote faster healing, or by secondary intention when wound boundaries cannot be placed in proximity.

1.11.1.1 Inflammatory phase

Immediately following the generation of a wound, extravasation of blood into the injured tissue triggers vasoconstriction of local blood vessels with the functional aim of preventing exsanguination. Combined with this vasoconstrictive reflex, both the extrinsic and intrinsic

coagulation cascade are activated (Sinno et al, 2013). This leads to aggregation of platelets at the site which in turn interact with exposed collagen and other extracellular matrix molecules leading to release of clotting factors and the eventual formation of a blood clot comprising principally fibrin and fibronectin (Hawiger, 1987). This fibrin clot acts as a provisional matrix onto which cell migration can occur during the later stages of wound healing. Degranulation of platelets at the site leads to release of stored growth factors and cytokines via the exocytotic function of platelets; this increases local concentration of chemoattractants such as epidermal growth factor (*EGF*), platelet derived growth factor (*PDGF*) and transforming growth factor beta (TGFβ) which leads to the initial migration of neutrophils to the site (Lawrence, 1998). Neutrophils remove foreign particulate matter and scavenge for debris and also phagocytose any bacteria at the site. Monocytes are then attracted to the wound site and alongside removing foreign bodies, secrete increased quantities of *EGF, PDGF* and TGFβ in an autocrine fashion leading to the recruitment of fibroblasts, which deposit provisional ECM, and promotion of angiogenesis (Broughton et al, 2006). This marks the end of the inflammatory phase and the start of the proliferative phase.

1.11.1.2 Proliferative phase

Following attainment of haemostasis and a successful immune response the wound begins to undergo intensive tissue repair through the proliferative phase of wound healing (Young et al, 2011). The proliferative phase is initiated approximately 48 hours post injury and generally overlaps with the inflammatory phase. The proliferative phase is characterised by increased cellular growth and activity due to the functional aim of replacing the fibrin clot, which offers limited protection against further traumatic injury, coupled with revascularisation, wound contraction and epithelisation of the wound site (Gonzalez et al, 2016). The proliferative phase can take up to 3 week following wounding based on the type of tissue effected, severity, age and general health of the patient (Guo et al, 2010)

1.11.1.2.1 The role of fibroblasts in the proliferative phase of wound healing

Fibroblasts from tissues adjacent to the site of injury migrate into the wound in response to chemotactic proteins secreted during the inflammatory response, the secreted chemokines at the wound site are diverse general include members of the epidermal growth factors (*EGF*), fibroblast growth factor (*FGF*) and Transforming growth factor (*TGF*) families (Barrientos et al, 2008) are diverse. Fibroblasts are able to migrate into the fibrin clot and subsequently break down, the fibrin and fibronectin in the provisional matrix by the action of secreted matrix metalloproteases (MMPs). Once at the site of injury fibroblasts are stimulated by local cytokines, including TGFs which have been shown be potent fibroblast mitogens and also act to increase fibroblast collagen deposition and differentiation (Liu et al, 2016), this stimulates fibroblasts to undergo extensive proliferation to generate an increased concentration in the injured area (Stadelmann et al, 1998). Fibroblasts secrete extracellular matrix proteins, namely: hyaluronic acid, fibronectin, and proteoglycans such as heparan sulphate, chondroitin sulphate and dermatan sulphate which are all deposited into the surrounding tissues aiding in the formation of granulation tissue (Bainbridge, 2013). Fibroblasts also synthesise collagens which are essential ECM components that provide mechanical integrity and support to the repair site and replace the fibrin clot foundation which provided little resistance to further traumatic injury. This collagen matrix also provides a surface upon which other cell types can adhere and migrate thereby aiding in eventual angiogenesis and connective tissue formation (Robson et al, 2001). During the proliferative phase, collagen production by fibroblasts is significantly higher than collagen breakdown leading to a net gain of total collagen at the wound site. This collagen contains a higher proportion of unorganised collagen type III (40%) when compared with normal uninjured tissues (20%) (Velnar et al, 2009). During the proliferative phase of wound healing fibroblasts differentiate into myofibroblasts in response to elevated *TGFB1* concentrations (Evans et al, 2003) and increased tractional forces across the ECM produced by

migrating fibroblasts (Li and Wang, 2011). Myofibroblast differentiation at the site leads to wound contracture due the interaction of smooth muscle actin with myosin based complexes which generate contractile force which pull the wound edges into proximity (Shin et al, 2004).

1.11.1.2.2 Revascularisation

Increased cellular activity at the wound site increases local oxygen and nutrient requirements which is provided through angiogenesis initiated in response to secreted growth factors such as vascular endothelial growth factor (*VEGF*) and a decreased local pH. These conditions promote migration of endothelial cells to the wound site which migrate out from damaged or pre-existing capillaries forming capillary sprouts (Greenhalgh, 1998). This vascular sprouting is the foundation of new blood vessels as the sprouts grow due to proliferation and eventually reattaching to neighbouring blood vessels thereby increasing local blood flow and giving granulation tissue its distinctive red colour (Tonnesen et al, 2000).

1.11.1.2.3 Epithelialisation

Epithelialisation begins to occur a few hours following injury when the basal layer around the periphery of the wound begins to increase in size due to increased epithelial proliferation. Epithelial cells then detach from the periphery of the wound and migrate along the deposited collagen fibres across the surface of the wound as epithelial sheets (Baum et al, 2005), continued proliferation leads to multilayers and the eventual epithelisation (Pastar et al, 2014).

1.11.1.3 Maturational phase

The final phase of the healing process commences approximately 8 days after injury and is related to the maturation of the repair in a process that can take many months to reach completion (Broughton et al, 2006) as it is focussed primarily on the development of new epithelium and the formation of scar tissue. The remodelling phase begins when the collagen production and collagen degradation reach equilibrium, following this the disorganised collagen type III fibres, which were produced abundantly by fibroblasts during the proliferative

phase, are gradually replaced by the more organised collagen type I. Due to this, the tensile strength of the scar tissue is increased reaching 50% of the strength of surrounding uninjured tissues after 3 months and eventually 80% strength following completion of the healing process (Morton et al, 2016); despite completion of wound healing scar tissue does not reach the same level of tissue integrity as uninjured tissue.

1.12 Aims of the study

Background: Following cleft repair approximately 10% of patients develop ONF (Hardwicke et al, 2014) and 25% develop HTS (Soltani et al, 2012). To date a number of risk factors have been suggested including width of cleft and surgical protocol, although these are likely contributory factors, it is possible that pathological wound healing, due to fundamental differences in fibroblast behaviour at the wound site, can also contribute to the development of these post-operative complications.

Aim: To investigate the differences in extracellular matrix production and expression between cleft fibroblast to identify markers that may be associated with the pathological wound healing.

Background: Due to the formation of the lip and palate being distinct embryological events coupled with the high incidence of cleft lip and cleft palate occurring in isolation, it has been speculated that CL, CP and CLP may be disparate clinical entities with differing causation. As expansion of the facial growth centres occurs in part due to extracellular matrix accumulation, it is possible that differences in the behaviour of fibroblasts, which are the principle secretors of ECM, may be associated with cleft phenotype.

Aim: To characterise the behaviour of cleft fibroblasts isolated from patients with differing cleft phenotypes to determine whether they are physiologically distinct.

Background: Folate deficiency has been repeatedly associated cleft development (Jahanbin et al, 2019). Despite this, the precise physiological mechanisms and cell behaviours that are contributed to by folic acid in order for it to induce its protective function remains undefined.

Aim: To investigate the behavioural changes induced by the presence of folic acid to cleft fibroblasts *in vitro.*

CHAPTER TWO:

MATERIALS AND METHODS

2.1 Ethical approval for collection of human tissue following cleft repair

All work including sample collection and subsequent tissue processing was fully compliant with the University of Birmingham's ethical code of conduct. Ethical approval for the project entitled "Cellular characterisation of the human cleft palate with clinical correlation" (IRAS project ID: 171283) was obtained prior to sample collection (REC reference: 15/NW/0079). Samples were stored and anonymised by the Human Tissue Authority (HTA) licenced Human Biomaterials Resource Centre (HBRC reference: 13-163) based at the University of Birmingham. In addition, prior to commencement of the project, training for Good Clinical Practice (GCP) was successfully completed and certification was awarded by the National Institute of Health Research Clinical Research Network (NIHR CRN).

2.1.1 Sample collection

Samples were collected from patient's undergoing primary surgery to repair cleft lip only (CL), cleft palate only (CP) or cleft lip and palate (CLP) at the Birmingham Children's Hospital (BCH) irrespective of gender or ethnic background in order to obtain a broad sample cohort. Patients previously diagnosed by BCH clinicians as presenting physical characteristics indicative of syndromic forms of CLP as well as patients undergoing revision surgery were excluded from the study. Consent was obtained from the child's legal guardian by completion of HBRC documentation after the aims of the project were clearly explained and any queries addressed. The samples that were collected are summarised in table 1.

2.1.2 Transportation of samples

During surgical cleft repair, tissue excess to requirement was removed and wrapped in sterile gauze and placed into a sterile universal container, which contained 10ml of Dulbecco's modified eagle medium (DMEM), in theatre. Samples were then immediately transported to

the BCH laboratories where they were logged and the containers packaged ready for transport. Samples were then sent to the HBRC by licensed carriers where the samples were anonymised and any patient related information recorded and stored for the duration of the project. Samples were then transported to the Birmingham Dental Hospital laboratories (BDH) for tissue processing. Transportation of samples was conducted as quickly and efficiently as possible with less than 2 hours from operating theatre to BDH laboratories (Figure 4).

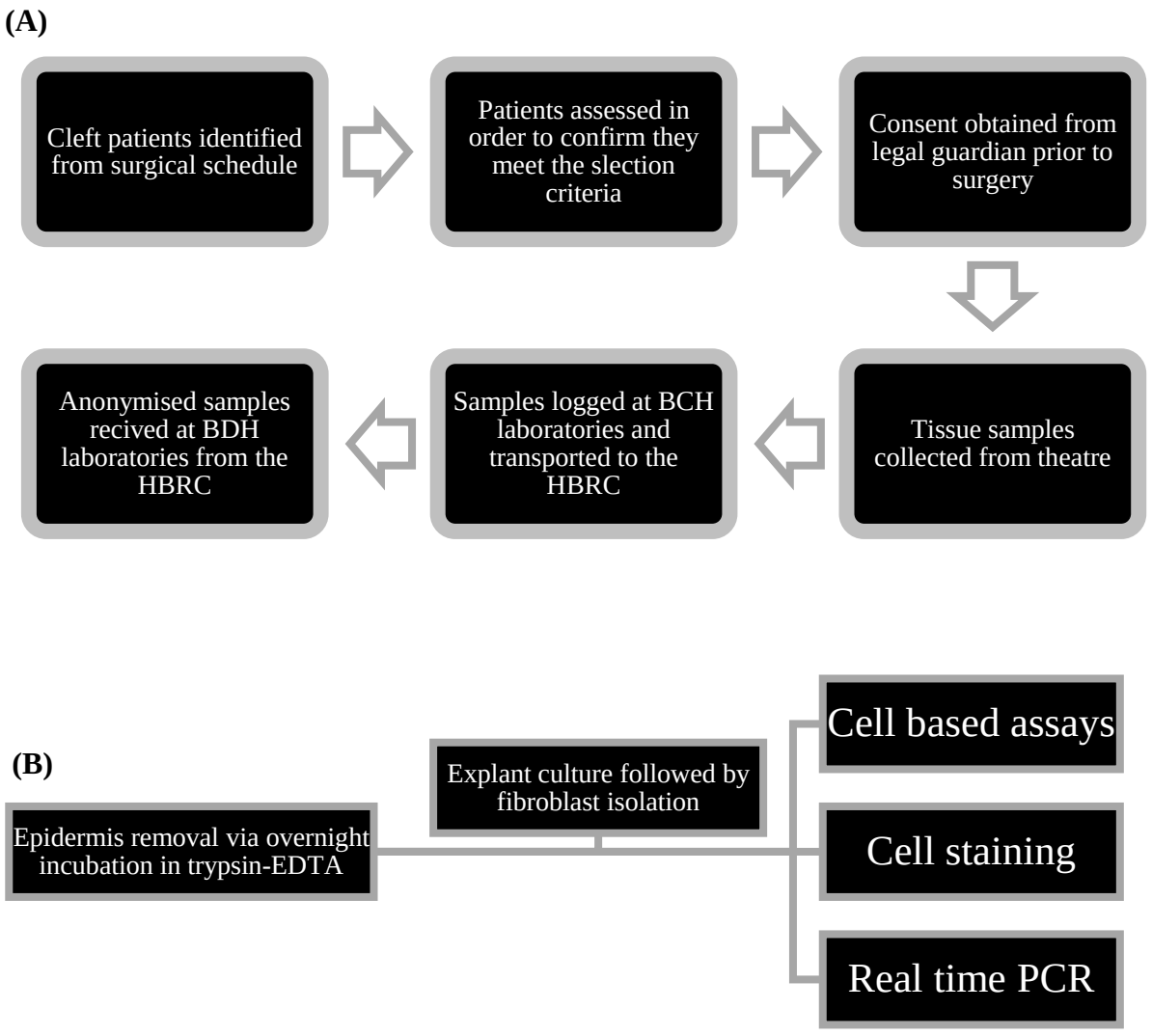

Figure 4: (A) Summary of sample collection protocol. (B) general fibroblast characterisation protocol following arrival of cleft tissue samples

CLEFT SAMPLES FOR CELL CULTURE															
Patient ID	ID number	Study group	Tissue type	CLP (LIP)	CLP (PALATE)	CL	CP	Lip tissue	Palate tissue	LUCLP	RUCLP	BLCLP	Age (days)	Weight (kg)	Sex
S101590	15	CLP (LIP)	LIP	1	0	0	0	1	0	1	0	0	113	5.8	M
S101593	16	CLP (PALATE)	PALATE	0	1	0	0	0	1	0	0	1	252	13.5	M
S101594	17	CLP (LIP)	LIP	1	0	0	0	1	0	1	0	0	129	7	M
S101637	6	CLP (LIP)	LIP	1	0	0	0	1	0	0	0	1	111	5.7	F
S101633	2	CL	LIP	0	0	1	0	1	0	0	0	0	128	6.2	M
S101636	12	CL	LIP	0	0	1	0	1	0	0	0	0	186	7.5	M
S101597	8	CLP (PALATE)	PALATE	0	1	0	0	0	1	1	0	0	186	8	F
S101596	4	CL	LIP	0	0	1	0	1	0	0	0	0	104	7.2	F
S101600	3	CLP (PALATE)	PALATE	0	1	0	0	0	1	0	1	0	176	6.3	M
S101635	5	CLP (PALATE)	PALATE	0	1	0	0	0	1	0	1	0	227	5.6	F
S101601	9	CLP (LIP)	LIP	1	0	0	0	1	0	0	1	0	227	5.6	F
S101603	10	CLP (LIP)	LIP	1	0	0	0	1	0	1	0	0	132	7.5	M
S101632	1	CLP (LIP)	LIP	1	0	0	0	1	0	0	0	1	130	6.9	M
S101604	14	CLP (LIP)	LIP	1	0	0	0	1	0	1	0	0	109	6.8	M
S101631	11	CLP (PALATE)	PALATE	0	1	0	0	0	1	0	1	0	179	6.9	F
S101634	13	CLP (LIP)	LIP	1	0	0	0	1	0	0	1	0	179	6.9	F
S101605	7	CLP (PALATE)	PALATE	0	1	0	0	0	1	1	0	0	241	8.8	M
S230110	25	CLP (PALATE)	PALATE	0	1	0	0	0	1	0	1	0	254	8.1	F
S245930	27	CLP (PALATE)	PALATE	0	1	0	0	0	1	0	0	1	255	8.9	M
S248308	20	CL	LIP	0	0	1	0	1	0	0	0	0	89	4.3	F
S250290	23	CLP (LIP)	LIP	1	0	0	0	1	0	0	0	1	141	6.28	F
S245348	22	CLP (PALATE)	PALATE	0	1	0	0	0	1	0	1	0	218	9.2	M
S277778	19	CL	LIP	0	0	1	0	1	0	0	0	0	168	-	M
S278580	26	CL	LIP	0	0	1	0	1	0	0	0	0	193	-	F
S281630	24	CP	PALATE	0	0	0	1	0	1	0	0	0	463	-	M
S281750	18	CP	PALATE	0	0	0	1	0	1	0	0	0	220	-	M
S285028	28	CP	PALATE	0	0	0	1	0	1	0	0	0	372	-	M
S286370	21	CP	PALATE	0	0	0	1	0	1	0	0	0	544	-	F
S287316	29	CP	PALATE	0	0	0	1	0	1	0	0	0	285	8.2	M
Total = 29	Total = 29	Total = 4	Total = 2	Total = 9	Total = 9	Total = 6	Total = 5	Total = 15	Total = 14	Total = 6	Total = 7	Total = 5	Total = 29	Total = 23	Total = 29

Table 1: Summary of details pertaining to cleft tissue samples collected from the BCH where: 1 = positive and 0 = negative. Patient ID = anonymised patient reference number; ID number = shorthand notation used for laboratory purposes; CLP (LIP) = lip tissues isolated from patients with CLP; CLP (PALATE) = palatal tissues isolated from patient with CLP; CL = cleft lip; CP = cleft palate; LUCLP = left unilateral CLP; RUCLP = right unilateral CLP; BLCLP = bilateral CLP.

2.2 Cell culture

All cell culture and tissue processing was conducted aseptically and, unless otherwise stated, were conducted within a Guardian MSC TI200 class II laminar flow cabinet (Monmouth Scientific, UK). All cultures were maintained at 37°C in an atmosphere of 5% CO_2 in a humidified Heracell™ 150i CO_2 incubator (Thermo Fisher Scientific, UK). Cells were cultured in tissue culture treated T75 Nunc™ EasYFlask flasks (Thermo Fisher Scientific, UK). Unless otherwise stated, cells were cultures in Dulbecco's modified eagles medium (DMEM) (Biosera, UK), which was supplemented with: 10% foetal bovine serum (FBS) (Biosera, UK), 2.5% 4-(2-hydroxyethyl) piperazine-1-ethanesulfonic acid (HEPES) buffer (1M) (Sigma, UK), 1% Penicillin-Streptomycin (10mg/ml) (Sigma, UK), 1% amphotericin B (250 μg/ml) and 1% L-glutamine (200 mM) (Sigma, UK). Cultures were monitored using an inverted light microscope (Primovert, Zeiss, Germany) was used to assess the degree of confluence, monitor for signs of infection and cell counting. Cell counts were conducted using an improved Neubauer haemocytometer (Agar Scientific, UK).

2.2.1 Primary fibroblast isolation and culture

Fresh excess cleft lip and palate tissue was obtained from CLP patients and stored in 5ml trypsin- ethylenediaminetetraacetic acid (EDTA) (0.25%) (Invitrogen, UK) overnight at 4°C in order to facilitate detachment of the epidermis. Following overnight incubation, sterile scalpels were used in order to remove the epidermis from the underlying tissue. This submucosal connective tissue was fragmented into approximately $1mm^2$ fragments, using a sterile scalpel and placed into a T25 flask, with sterile tweezers, to permit adherence. CLP fibroblasts were cultured via explant culture in supplemented DMEM (sDMEM), as per the supplementation protocol described in section 2.2, and were maintained in controlled incubators. Culture

medium was removed and replenished 5 days after initial seeding, so explants were not disrupted, and every 2 days subsequently.

2.2.2 Sub-culturing

When 80% confluent, cell cultures were rinsed with 5ml 37°C phosphate buffered saline (PBS) in order to remove any residual supplemented DMEM that could potentially interfere with cell detachment. Cells were then treated with 4ml trypsin-EDTA (0.25%) and incubated at 37°C for approximately 5 minutes, light microscopy was utilised in order to visually inspect the cells to assess if they had detached from the surface of the flask. When all cells were detached, 4ml sDMEM was added to the flask in order to inactivate the trypsin-EDTA. This solution was then transferred to a universal tube and centrifuged (Jouan, UK) at 900rpm for 5 minutes to create a cell pellet in the base of the universal. The supernatant was then aspirated followed by resuspension of the cell pellet in 5ml sDMEM ready for cell seeding and counting.

2.2.3 Cell counting

Cells were pelleted and re-suspended as described in section 2.2.2. Cells were then counted using a haemocytometer following cleaning of the surface. Coverslips were first placed onto the counting platform of the haemocytometer followed by the addition of ten microliters of cell suspension which was pipetted into the counting chamber and viewed using a light microscope. The counting chamber comprised of four separate grids, each comprising of 16 distinct equally sized squares, the number of cells in each grid was counted and an average was calculated. For consistency the cells touching the upper or left boundaries of the grid were excluded whilst those on the lower and the right of the grid were included. Once the average cell number per gird was obtained, the value was multiplied by $1x10^4$ thereby providing the number of cells/ml and this value was corrected with the corresponding dilution factors in order to obtain the total cell number in the cell suspension.

2.2.4 Cryopreservation and cell retrieval

Following subculture, cells were cryopreserved in order to maintain stocks of cells at low passage for all future experiments. Once pelleted, cells were re-suspended to a concentration of $1x10^6$ cells/ml in cryopreservation media which consisted of: 60% Supplemented DMEM, 30% FBS and 10% dimethyl sulfoxide (DMSO) (Sigma, UK). This cell suspension was then placed into cryogenic vials (Thermo Fisher Scientific, UK) and stored in expanded polystyrene boxes, which permit gradual changes in temperature, overnight in an ultra-low temperature freezer at -80°C (New Brunswick, UK). The cryovials were then transferred to liquid phase nitrogen dewars for long term storage at -196°C. When required, cryopreserved cells were retrieved from storage and rapidly thawed in a water bath (Grant, UK) at 37°C, this was then diluted into 10ml of sDMEM. Following centrifugation (900g for 5 minutes), the supernatant was aspirated and cell pellets were re-suspended in sDMEM and seeded into T75 flasks.

2.3 Supplementation with experimental reagents

A number of dietary factors and cytokines can have a significant effect on cell behaviour. In order to assess the effects of folic acid, transforming growth factor alpha (TGFα) and members of the transforming growth factor beta (TGFβ) superfamily, these were added in a range of physiologically relevant concentrations into cell cultures following cell seeding. See table 2 for details relating to dilution protocols and concentrations used to treat cells. The normal formulation for DMEM contains a basal level of FA therefore for the purposes of FA supplementation studies FA negative sDMEM (Sigma, UK) was used. This media was utilised so that cell behaviour in the absence of FA could be observed whilst permitting controlled and consistent FA concentrations throughout all experiments.

Experimental reagent	Reconstitution protocol	Concentrations used for experiments	Source
Folic acid	1M NaOH for a 50mg/ml stock. Primary stocks were diluted in deionised water to make secondary stocks of 1mg/ml.	20nM, 10μM, 20μM, 30μM	Sigma, UK
Recombinant Human TGF-β1	10mM citric acid for 0.1mg/ml stock	5nM and 20nM	PeproTech UK (100-21)
Recombinant Human TGF-β2	Deionised water for 0.1mg/ml stock	5nM and 20nM	PeproTech UK (100-35B)
Recombinant Human TGF-β3	10mM citric acid for 0.1mg/ml stock	5nM and 20nM	PeproTech UK (100-36E)
Recombinant Human TGF-α	Deionised water for 1mg/ml stock	5nM and 20nM	PeproTech UK (100-16A)

Table 2: Experimental reagents employed to assess how cleft fibroblasts respond following their addition to the supplementation protocol; all reagents were reconstituted according to the manufacturer's recommendation.

2.4 Cell proliferation assays

A number of methodologies were employed in which indicate the total cell number within cultures which, when paired with data relating to the initial seeding densities and culture duration, can be used to infer cell proliferation rates. These included growth curves obtained via manual counts from which population doubling times (DT) were calculated and 3-(4,5-dimethylthiazol-2-yl)-2,5-diphenyltetrazolium bromide (MTT) assays which require spectrophotometric analysis.

2.4.1 Growth curves and doubling times

In order to assess how CLP fibroblasts grew in culture growth curve models were employed. Once cells had reached approximately 80% confluence cells were trypsinised, pelleted and re-suspended as previously described (section 2.2.2). Cells were then seeded into 35mm petri dishes (Corning, UK) at a concentration of $5x10^4$ and incubated at 37°C. Cell growth was then assessed by counting the number of cells in each 35mm petri dish every 48 hours post-seeding,

until confluence was reached, using a haemocytometer as previously described in section 2.2.3. In order to calculate population doubling times the following equation was used:

$$\textbf{Doubling time} = \frac{\text{Duration (hours in culture) x log(2)}}{\log(\text{final concentration}) - \log(\text{initial concentration})}$$

Equation 1: equation used in order to calculate fibroblast doubling times

2.4.2 MTT assay as an indicator of cell proliferation

Cell metabolic activity was assessed through use of the MTT reduction assay (Vybrant® MTT Cell Proliferation Assay Kit, Thermo Fisher scientific UK), from which data pertaining to cell growth was extrapolated. The MTT assay is based on a redox reaction between MTT and the mitochondrial respiration products NADH and NADPH, which results in the yellow MTT solution forming insoluble purple formazan crystals (Koyanagi et al, 2016). This reaction takes place due to the presence of mitochondrial reductase which is present in live cells thus the amount of formazan produced can be related to the number of viable respiring cells. This reaction can also act as an indication of cell proliferation as generally the higher the number of active cells the greater the concentration of formazan crystals that form, though increased cellular respiration due to external factors may also have an effect. Cells were seeded into 96 well plates (Thermo Fisher Scientific, UK) at a concentration of $2.5x10^3$ followed by the addition of 200µl of supplemented DMEM in each well. This assay involved the addition of 10µl MTT (5mg/ml in PBS) per 100µl of media in each well followed by incubation at 37°C for 4 hours, the media was then removed and 50µl DMSO was added to each well which acts as a solubilising agent to dissolve the formazan crystals. The 96 well plate was then placed onto a plate rocker for 5 minutes, to aid in crystal dissolution, followed by insertion into a universal microplate spectrophotometer (ELx 800, Bio-TEK instruments) and the absorbance of each

well was measured at 540nm and were conducted daily. Blank cell negative wells were used as controls and were treated as previously described, when cells were treated with experimental reagents, see table 2, negative controls were also implemented within which samples were subject to the same methodology as above but in the absence of the experimental variable.

2.5 Cell viability assays

2.5.1 Trypan blue dye exclusion assay

The Trypan blue dye exclusion assay is commonly to stain non-viable cells. Trypan blue is negatively charged and does not interact with viable cells, however cells with damaged membranes readily absorb the dye causing them to be stained blue and observable under light microscopy. Cleft fibroblasts were pelleted and re-suspended, 100µl of this cell suspension was then placed in an Eppendorf tube containing an equal of Trypan blue dye (0.4%) (Sigma, UK). Damage to the integrity of cell membranes leads to uptake the dye, causing them to be labelled blue, and regarded as non-viable; cells that do not uptake the dye remain unstained and are considered viable. The number of viable and non-viable cells are counted as in section 2.2.2. Percentage cell viability is then calculated using the following equation:

$$\textbf{Viable cells}\ (\%) = [1.00 - (Number\ of\ stained\ cells \div Total\ number of\ cells)] \times 100$$

Equation 2: equation used in order to calculate cell viability

2.5.2 Live/dead viability assay

Live/dead assays are common dye-based cell viability assays whereby live cells are stained with calcein AM (Ebioscience, UK) and generally fluoresce green while non-viable cells are stained with propidium iodide (Sigma, UK) and fluoresce red however fluorescence can be varied due to differing dye illuminating wavelengths. Calcein AM is cell permeable, when it passes through the cell membrane of a viable cells the presence of active intracellular esterases

cleave ester groups thereby converting the structure of dye so that it fluoresces green, this reaction does not occur in non-viable cells. Propidium iodide penetrates damaged cell membranes where the dye interacts with negatively charged nucleic acids producing red fluorescence in non-viable cells. In order to conduct live/dead staining 20µl 2mM propidium iodide stock solution was added to 10ml of sterile serum free DMEM containing 5µl 4mM calcein AM stock solution; this working reagent (2µM calcein AM and 4µM propidium iodide) was made fresh for each assay. Two types of live/dead staining were employed: the adherent cell imaging and the microplate method, which was used when cell numbers were low.

2.5.2.1 Imaging and counting labelled adherent cells

Cells were seeded onto 35mm petri dishes at a concentration of $1x10^4$ and cultured for 24 hours. Following this, cultures were incubated with 1ml live/dead working reagent for 45 minutes at 37°C. Cells were then washed with once with PBS followed by the addition of 1ml of DMEM to each culture and imaged immediately using a fluorescent microscope (Nikon TE300 Inverted microscope, UK). If quantification was required, cells were detached from dishes by incubation with 2ml trypsin for 5 minutes followed by centrifugation at 900g for 5 minutes and re-suspended in 1ml PBS, the number of green and red fluorescing cells were then counted using a haemocytometer.

2.5.2.2 Microplate method

Cells were seeded in 96-well plates at a concentration of $1x10^3$ and cultured for 24 hours. Following this, 100µl live/dead working reagent was added to each well and incubated for 45 minutes at 37°C/5% CO_2 and each well was then washed with PBS followed. The fluorescence intensity of each well was then measured using a fluorescent microplate reader (Twinkle CB970, Berthold technologies, UK) at 490nm (for Calcein AM) and 530nm (Propidium iodide).

2.6 Selection of a suitable cell migration assay

There are a number of cell migration assays that are used to assess migration rates in adherent cells. Here, three assays were assessed in order to determine the most suitable for determination of migration rates of cleft fibroblasts *in vitro*. The parameters assessed included: uniformity of wound area and assay reproducibility (based on the initial width of the wound and differences in wound area between replicates), alterations to surface topography and cell viability.

2.6.1 Scratch wound assay

Scratch wound assays were conducted as previously described (Liang et al, 2007). CLP fibroblasts grown in T75 flasks were re-suspended into sDMEM and subsequently seeded into six well plates at concentration of $5x10^5$ and grown to confluence. Once cells reached the suitable level of confluence was determined via microscopy, a 200µl pipette tip was used to scratch the monolayer through the centre of the well in one precise movement, and this approach introduced a linear wound with a defined margin. Each well was then washed twice with phosphate buffered saline (PBS) in order to remove the cellular debris created by scratching the monolayer leaving a cell free region.

Following comparative analysis, the scratch wound assay was deemed unsuitable for the analysis of cleft fibroblast migration due its lack of reproducibility as a result of its tendency to produced wounds with irregular margins and varying wound widths across the length of the scratch. Further, it was shown that the mechanical disruption of the monolayer led to significant topographical damage to the tissue culture polystyrene which manifested as linear abrasions across the surface; this also resulted in significant cell death along the wound margins which persisted despite washing with PBS.

2.6.2 Parafilm assay

Parafilm (Pechiney Plastic, USA) was cut into 1mm x 20mm strips using a scalpel, and was subsequently disinfected by immersion in hydrogen peroxide for 30 minutes and air dried. Using sterile tweezers, the strips were placed across the centre of a six well plate and adhered to the tissue culture polystyrene by application of gentle pressure with the tweezers. Once the Parafilm was in place cells were seeded into the well at a concentration of $5x10^5$ and were grown to confluence. Once this level of confluence was confirmed through microscopy, sterile tweezers were employed to gently detach the Parafilm from one side in order to permit removal of the strip in one precise movement. The well was then washed twice with PBS leaving a cell free region in place of the Parafilm strip.

The Parafilm assay was also deemed to be unsuitable for the comparison of cleft fibroblast migration derived from different patients. This was due to the deposition of hydrophobic paraffin residues on the surface of the cell free region following removal of the Parafilm strip, which could potentially disrupt normal fibroblast motility. Further, there was considerable fibroblast migration beneath Parafilm prior to its removal which led to irregular initial cell boundaries at the periphery of the wound.

2.6.3 Ibidi cell migration assays

Ibidi culture inserts (Thistle Scientific, UK) are commercially available cell culture inserts that enable the production of defined linear 500μm cell free region. This is achieved due to separation of two small silicone wells by 500μm thick wall. The Ibidi culture insert was used according to the manufacturer's recommendation and placed into a 35mm petri dish, the presence of an inert degradable surface coating at the bottom of the insert permits firm adherence to tissue culture polystyrene. Cells were then seeded into each well at a concentration of $5x10^4$ and grown to confluence at which point the insert was removed using sterile tweezers

and the petri dish was washed twice in PBS, leaving a linear cell free region with reproducible dimensions (Figure 5). The Ibidi cell migration assay was deemed most suitable assay for the comparative assessment of cleft fibroblast migration *in vitro*. This was due to its generation of a defined cell free region with well-defined borders within a confluent monolayer. Further, there was no cell migration beneath the insert prior it its removal indicating the insert was tightly adhered to the well. There was a slight residual material following removal of the insert but this was shown to dissipate following washing with PBS.

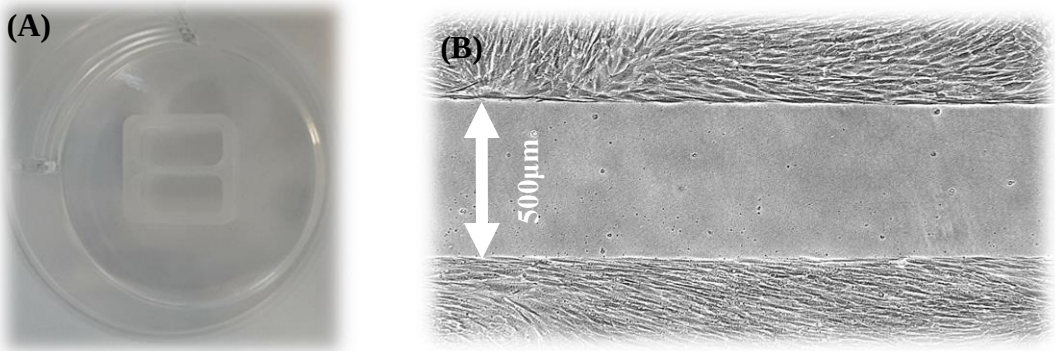

Figure 5: Ibidi *in vitro* migration assay. (A) Photograph of Ibidi tissue culture insert adhered to the base of a multiwall (B) Cell free region produced following removal of the insert.

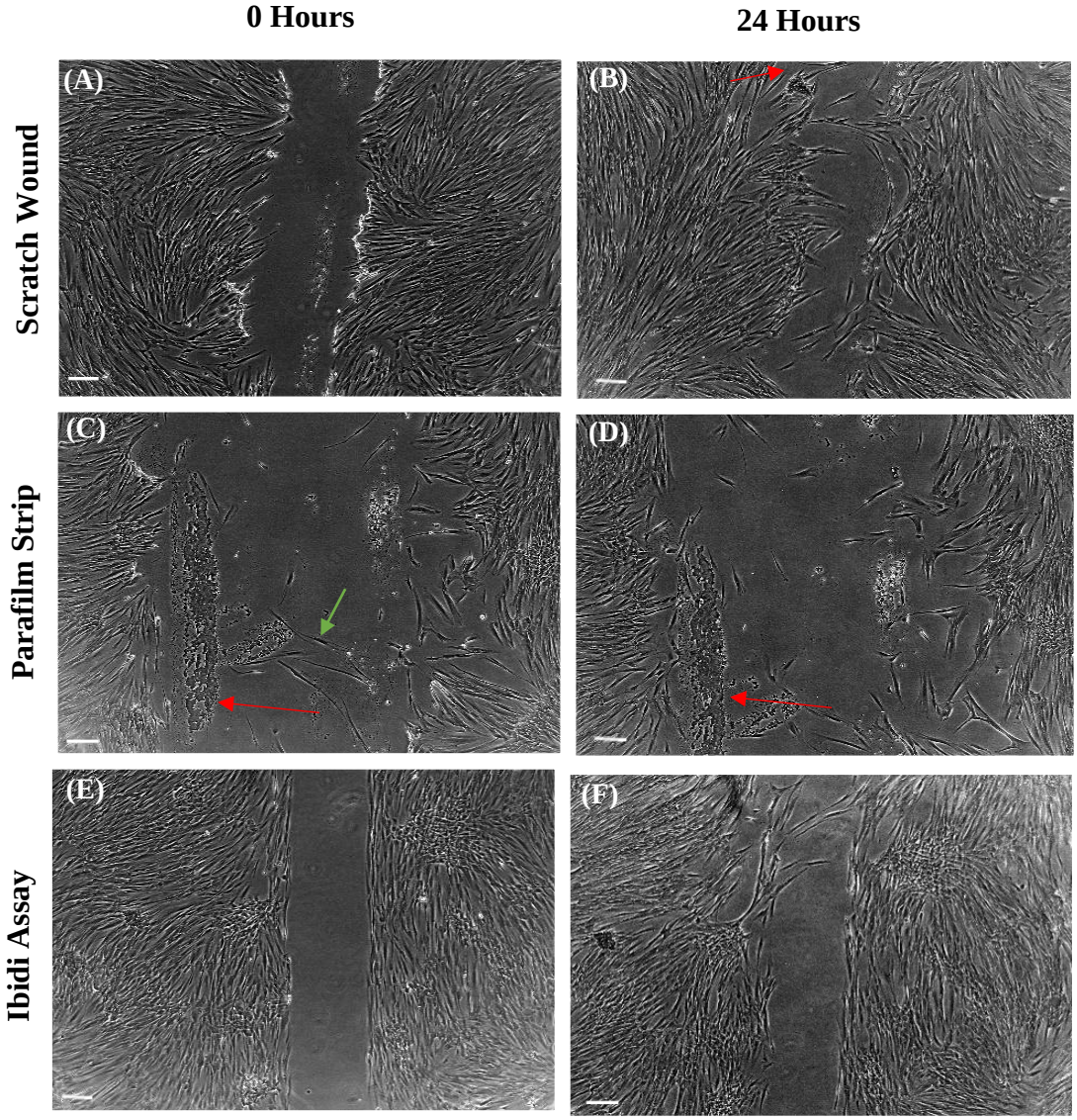

Figure 6: Imaging of cell wound closure using three different wound healing assay at 0 hours and 24 hours. (A) At 0 hours the initial cell free region formed via scratching the surface of the monolayer was irregular along the wound edge there also seemed to be a build-up of cells along the periphery of the wound despite washing. (B) At 24 hours cells had begun to migrate into the wound but there was also a cluster of dead cells visible (arrowed) which may have been cells wounded by scratching the monolayer. (C) The Parafilm strip assay produced the largest cell free region at 0 hours however there were a number of cells that migrated underneath the Parafilm where the strip was attached (green arrow). Additionally, there was a visible deposition of material onto the surface of the cell culture dish (red arrow). (D) At 24 hours cells had begun to migrate into the wound and the deposited surface residue was still present after 24 hours (arrowed). (E) The Ibidi insert produced a well-defined wound edge with cells growing at either side. (F) After 24 hours cell had begun to migrate into the wound (n=9) error bars = 200μm.

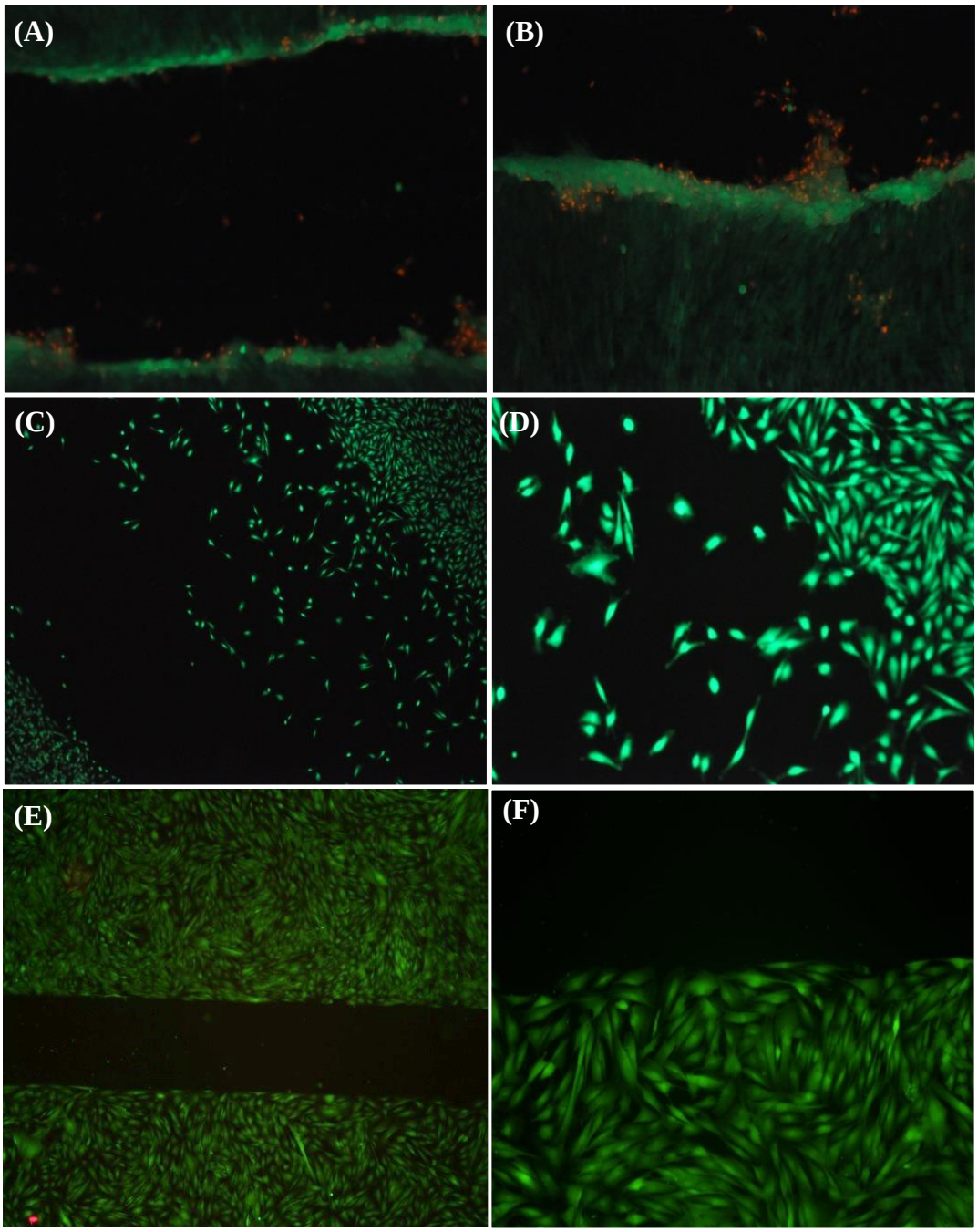

Figure 7: Live/dead staining for scratch, Parafilm and Ibidi wound healing assays. The scratch wound assay (A-B) caused clumping of cells along the wound edge with a number of dead cells (stained in red) being released from the base of the aggregation and floating into the culture. The Parafilm strip assay (C-D) did not lead to clearly defined borders at the wound edge as there was cell migration into the wound site; most cells that had migrated into the wound remained viable and of a regular morphology. The Ibidi wound healing assay (E-F) produced well defined wound edges with cells at the periphery appearing viable. Error bars = 200μm.

2.6.4 Proliferation inhibited cell migration assays

In order to assess the potential influence of cell proliferation on the rate of cell migration, into a cell free area, Ibidi cell migration assays were repeated with growth inhibited cells and compared with their non-inhibited counterparts. Cells were treated with 4μg/ml mitomycin C (Sigma, UK) for 3 hours and seeded into each well of an Ibidi insert at a concentration of $5x10^4$. When confluent, inserts were removed and images of cell migration into the cell free region were captured at multiple time points following removal.

2.6.5 Culture substitution migration assays

Due to the differences in cell migration rates observed between cells derived from different patients a culture substitution assay was developed in order to assess the effects of secreted cytokines and cell migratory behaviours. Two groups of cells (one fast migrating and one slow migrating) were seeded into separate Ibidi cell culture inserts, at a concentration of $5x10^4$ per well, alongside 3ml of sDMEM, after 24 hours the culture media from both was removed and placed into separate vials. Ibidi inserts were them removed and cultures were washed. Next, the stored cell culture medium from each culture was placed into the well of the opposing cell type such that fast cells were supplemented with conditioned media from slow migrating cells and slow migrating cells were supplemented with conditioned media form fast migrating cells. Phase contrast images were then captured at multiple time points for later analysis wound closure.

2.6.6 Image capture, processing and analysis

Phase contrast images were obtained using a Nikon TE300 Inverted microscope (Nikon, UK) and captured using MicroManager (V14.1.4) at 0 hours, 12 hours, 24 hours, 48 hours after removal of the culture insert, or initiation of a wound. This permitted digital images of cell migration into the wound area to be observed at various time points and comparisons between

patients and experimental conditions to be made. For each replicate a total of 3 images were taken in order to image the whole length of the wound, surface markers were used to ensure that the same region was not imaged twice and all assays were conducted in triplicate providing a total of 9 images per patient for each time point. Images were imported into the open source software imageJ (version 1.51) (Schindelin et al, 2012) and a stage micrometre was used in order determine and set the scale. Using the free form drawing tool the boundaries of the wound were measured by carefully drawing around the leading edges of each opposing cell boundary in order to obtain the area of the wound that remained cell free. The area of any cells that had migrated into the wound, and were not a part of the leading edges of the wound, was measured and subtracted from the initial measurement in order obtain an absolute area. Cell migration rates were presented in terms of remaining wound area (RWA%) which was obtained using the following equation:

$$\textbf{Remaining wound area } (\%) = \frac{\text{Area (24 hours post wounding)}}{\text{Area (0 hours post wounding)}} \text{x}100$$

Equation 3: equation pertaining to the calculation of RWA(%) based on initial wound area and remaining wound area after 24 hours.

2.6.7 Ibidi assays following supplementation with experimental reagents

In order to assess the effect of FA, differing TGFβs and TGFα on wound closure, cells were treated with each reagent using the treatment protocol defined in table 2. Ibidi inserts were then utilised in order to assess cell migration as described in section 2.6.3.

2.7 Real time polymerase chain reaction

A quantitative real time polymerase reaction (qPCR) methodology was utilised in order to compare differences in the basal gene expression profiles between cleft patients. This technique was also employed to assess any variance in gene transcripts in response to external stimuli including folic acid and transforming growth factors.

2.7.1 Cell lysis

When cleft fibroblasts were 80% confluent, media was aspirated from T75 flasks and washed with PBS in order to completely remove any remnants of supplemented DMEM, as it could have interfered with cell lysis, and were then pelleted as in section 2.2.2. Total ribonucleic acid (RNA) was then extracted from cell pellets using an RNeasy mini kit (Qiagen, UK) according to the manufacturer's instructions. Following centrifugation 350µl of lysis buffer (buffer RLT) including mercaptoethanol (Sigma, UK) was added to the cell pellet to lyse the cells, this solution was then transferred to an Eppendorf followed by the addition of 350µl 70% ethanol.

2.7.2 RNA extraction

The cell lysates were then processed further to produce the pure RNA required for cDNA synthesis. Following cell lysis, each 700µl sample was placed into an RNeasy spin column which was mounted on a collection tube which acted to collect any flow through following centrifugation steps. Samples were then centrifuged (Centrifuge 5415D, Eppendorf UK) at 10,000rpm for 30 seconds to remove excess buffer whilst retaining the RNA on the spin column membrane. This was then washed with 350µl of buffer RW1, which was used to clean the sample to remove any impurities from lysed cells including remnants of carbohydrates, proteins and fatty acids whilst retaining the RNA. Deoxyribonuclease I (DnaseI) (Qiagen, UK) was then added to the RNeasy membrane and incubated at room temperature for 15 minutes to eliminate

any potential DNA contamination, followed by a second wash with buffer RW1. The samples were then washed twice with buffer RPE so that any remaining salts would be removed. The RNeasy spin column was then transferred to a 1.5ml collection tube followed by the addition of 30µl RNase free water (Sigma, UK) to the membrane. The samples were then centrifuged at 10,000rpm for 1 minute to elute the RNA which was stored at -80°C until required.

2.7.3 RNA quantification

The purity and concentration of the cleft fibroblast RNA was determined by the measurement of the optical density (OD) of the sample using a spectrophotometer (Biophotomerter plus, Eppendorf UK). This analysis also assessed the absorbance ratio between 260/280nm ($OD_{260/280nm}$), pure RNA has a ratio of 2.0 however ratios between 1.8 and 2.1 are generally deemed an acceptable level of purity for qPCR applications (Gallagher, 2001). To quantify and assess the purity of the RNA 2µl of the RNA sample was placed into a plastic cuvette containing 68µl of diluent (RNase free water) and placed into a spectrophotometer which had already been normalised against the background OD of 70µl of RNase free water and the optical density was measured, only samples within the acceptable range were processed further.

2.7.4 cDNA synthesis

RNA samples were reverse transcribed to form complimentary DNA (cDNA) from each patient using a cDNA synthesis kit (Tetro™ Reverse Transcriptase kit, Bioline UK). Samples were thawed and diluted to a concentration of 2µg/ml, 12µl RNA was then placed into a 100µl tube containing 8µl of mastermix. The samples were incubated, using a thermal cycling block (Veriti, Applied Biosystems UK), at an annealing temperature of 45°C for 30 minutes to activate reverse transcriptase and generate DNA from an RNA template; this was followed by a 5-minute incubation at 85°C to deactivate enzymatic activity.

2.7.4.1 Concentrating cDNA

Complimentary DNA was then diluted with RNase free water to a final volume of 500µl and placed into labelled micron filters (Millipore, UK). Samples were centrifuged twice at 10,000rpm and 8,000 rpm respectively until 50µl of cDNA was achieved. The filters were then inverted and spun at 800rpm for 1 minute in order to elute the concentrated cDNA sample.

2.7.5 Primer design

Genes of interest were selected following a review of the literature and their primers were designed using the following online open source software. Gene ascension numbers were obtained by searching the Genbank nucleotide database, once the ascension number was identified it was input into the primer identification tool Primer-BLAST. Where possible, the parameters for the real time primers were set to obtain a product length between 200 base pairs with a guanine and cytosine content between 20-80% and melting temperatures between 57-60°C. Details relating to primers are shown in table 3.

2.7.5.1 Validation of real time PCR primers

Prior to real time PCR, preliminary experiments were conducted on each primer designed to determine the amplification efficiency of the primers following a DNA amplification cycle. A primer efficiency of 2.0 denoted a 100% efficiency, meaning that the concentration of amplicon doubled following each PCR cycle. Although an efficiency of 2.0 is considered optimal, in practice primer efficiencies of 1.7–2.2 are considered acceptable for qPCR according to the manufacturer, as the data analysis software takes into account each primer when calculating the amount of amplicon (Dietrich et al, 2011). This efficiency was assessed via serial dilutions of test cDNA, derived from pooled cleft fibroblast RNA, in RNase free water (100%, 50%, 10%, 1%, 0.1% and 0%) followed by efficiency analysis using a light cycler 480 (Roche, UK) (Figure

10). Melt curve genotyping was conducted to confirm that only one target was being amplified as the presence of primer dimers could interfere with amplicon quantification (figure 11).

2.7.6 Housekeeping genes

Housekeeping genes (HKG) are essential for accurate qPCR analysis as HKGs offer a baseline point of reference, relating to the amount of amplicon, from which a ratio of gene expression between gene targets and HKG can be calculated and presented as fold changes. A total of 4HKG were selected from the literature (table 3), the most suitable was determined based on the expression of HKG with the lowest geometric mean between all of the cleft patient cDNA. This was determined using the Microsoft Excel based statistical analysis program entitled 'Bestkeeper' (Pfaffl et al, 2004). Based on this analysis actin beta (*ACTB*) was deemed the most suitable HKG due to the low standard deviation (SD) across the patient cohort (Figure 8).

(A)

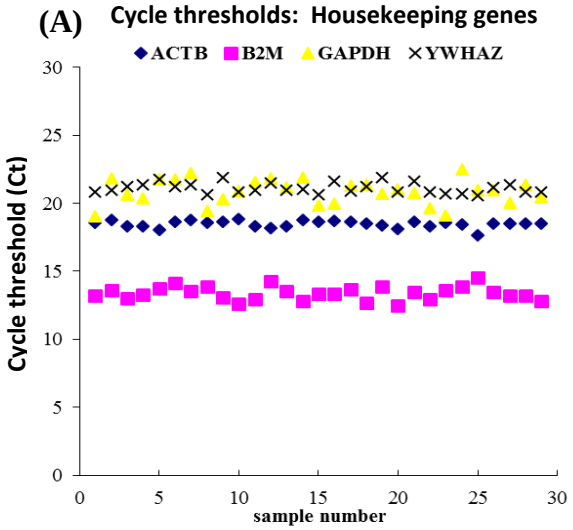

	ACTB	B2M	GAPDH	YWHAZ
geo Mean [CP]	18.47	13.37	20.83	21.12
ar Mean [CP]	18.48	13.38	20.85	21.12
min [CP]	17.62	12.47	19.06	20.54
max [CP]	18.84	14.52	22.47	21.9
std dev [± CP]	0.19	0.4	0.74	0.32
CV [% CP]	1.05	3	3.54	1.53
min [x-fold]	-1.82	-1.73	-3.46	-1.49
max [x-fold]	1.3	2	3.14	1.72
std dev [± x-fold	1.15	1.33	1.68	1.25

Figure 8: Overview of housekeeping genes. (A) Cycle thresholds of 4 HKG assessed in this study. (B) Outline of data pertaining cleft patients CP's, *ACTB* demonstrated the lowest overall standard deviation therefore was selected as the reference HKG.

Gene symbol	Gene name	Accession number	Primer sequence (5' – 3')	Amplicon size (bp)	Efficiency
Housekeeping Genes					
ACTB	Actin Beta	NM_001101	F-CATCGAGCACGGCATCGTCA R-TAGCACAGCCTGGATAGCAAC	211	2.021
B2M	Beta-2-Microglobulin	NM_004048	F-ACCCCCACTGAAAAAGATGA R-ATCTTCAAACCTCCATGATG	114	1.834
GAPDH	Glyceraldehyde-3-Phosphate Dehydrogenase	NM_002046	F-CTCCTGTTCGACAGTCAG R-GCCCAATACGACCAAATC	111	2.017
YWHAZ	Tyrosine 3-Monooxygenase/ Tryptophan 5-Monooxygenase Activation Protein Zeta	NM_003406	F-ACTTTTGGTACATTGTGGCTTCAA R-CCGCCAGGACAAACCAGTAT	94	1.988
Target Genes					
ACTA1	Actin, Alpha 1	NM_001100.3	F- AGCTACCCGCCCAGAAACTA R- GTCGCCCACGTAGGAATCTT	200	1.739
ACTA2	Actin, Alpha 2	NM_001613.2	F- GCCAAGCACTGTCAGGAATC R-GTCACCCACGTAGCTGTCTT	213	2.126
BMP7	Bone Morphogenetic Protein 7	NM_001719.2	F- CAGGTCATTGGCTGGGAAGT R- GGCTGGTAGGCGCTCATAAT	72	1.954
CDC42	Cell Division Cycle 42	NM_001791.3	F- GGTGGAGAAGCTGAGGTCAT R- CATCGCCCACAACAACACAC	99	1.937
CK5	Keratin 5	NM_000424.2	F-CCAAGCCAATTGCAGAAC CA R-AAATTTGGGATTGGGGTGGG	198	1.931
COL1A1	Collagen Type I Alpha 1 Chain	NM_000088.3	F- GGTCAAGATGGTCGCCCC R- GGAACACCTCGCTCTCCAG	262	1.911
COL2A1	Collagen Type II Alpha 1 Chain	NM_001844.4	F- CTTGGCCCAAAGAAAACCCG R- GTAGGTGACGTTCTGGTGGG	186	1.820

COL3A1	Collagen Type III Alpha 1 Chain	NM_000090	F- TGGAGGATGGTTGCACGAAA R- ACAGCCTTGCGTGTTCGATA	73	2.150
COL4A1	Collagen Type IV Alpha 1 Chain	NM_001845	F- GGCAGATTCGGACCACTAGG R- GCGTCTGTGGCAATACTAGC	186	1.878
COL5A1	Collagen Type V Alpha 1 Chain	NM_000093.4	F- CTTGGCCCAAAGAAAACCCG R- GTAGGTGACGTTCTGGTGGG	152	1.816
CSPG4	Chondroitin Sulfate Proteoglycan 4	NM_001897.4	F- GTCACAGCTGGCCCTCG R-TCCTGGGCTGCCTCCAG	299	1.761
DSE	Dermatan Sulfate Epimerase	NM_013352.3	F- GGCTGGGAGCGGATCTTTC R-TGGCTGTCGTAGTTGGCATT	192	1.919
EGF	Epidermal Growth Factor	NM_001963	F- CTTGGGAGCCTGAGCAGAAA R- GCACAAGTGTGACTGGAGGT	89	1.839
EGFR	Epidermal Growth Factor Receptor	NM_201283	F- GGTGGCATTTAGGGGTGACT R- CAAGGGAACAGGAAATATGTCGAA	173	1.794
ELN	Elastin	NM_001081754.2	F- CTTAAGCCAGTTCCCGGAGG R-GGGCTGCAGACACTCCTAAG	193	1.779
FGF12	Fibroblast Growth Factor 12	NM_004113.5	F- TGGTGAAGGCTATCTCTACAGT R- CTGATTCTTGCTGGCGGTAC	119	2.143
FN1	Fibronectin 1	NM_212478.2	F- CCGCCGAATGTAGGACAAGA R- GACAGAGTTGCCCACGGTAA	261	2.047
FOLH1	Folate Hydrolase 1	NM_004476.1	F- CAGTAGAGCAGCAGCACAGG R- AAACCACCCGAAGAGGAAGC	182	1.887
HSPG2	Heparan Sulfate Proteoglycan 2	NM_005529.6	F- TACACACGCCACCTGATCTC R-GCAGCTGCCAGTAGAAGGAC	184	1.791
ICAM1	Intercellular Adhesion Molecule 1	NM_000201.2	F- TCTTCCTCGGCCTTCCCATA R- AGGTACCATGGCCCCAAATG	152	1.935
IRF6	Interferon Regulatory Factor 6	NM_001206696	F- CTAAGACGTCGAGGAGCGTG R- CCCAGGCCTTTGCTCAATCT	100	1.747

LAMA1	Laminin Subunit Alpha 1	NM_005559.3	F- GTCCAATCTGTACGTCGGGG R- CACTGTTCTGGAAAAGCCCG	243	1.993
MCM2	Minichromosome Maintenance Complex Component 2	NM_004526.3	F- CACCTCCGAGTGCTTTGTCT R- ATACGCAACTCACGCCAAGA	137	1.922
MK167	Marker Of Proliferation Ki-67	NM_002417.4	F- CGTCCCAGTGGAAGAGTTGT R- CGACCCCGCTCCTTTTGATA	143	1.862
MMP2	Matrix Metallopeptidase 2	NM_174745.2	F- TGCTCCACCACCTACAACTT R- CCTGGAAGCGGAATGGAAAC	121	1.706
MMP9	Matrix Metallopeptidase 9	NM_031055.1	F- TCTTCCCTGGAGACCTGAGA R- TTTCGACTCTCCACGCATCT	107	1.974
MTHFR	Methylenetetrahydrofolate Reductase	NM_001330358.1	F- GAAGGTGCCTCTGTTCCCTC R- GGCTGGGTTCCTACTGATGG	173	1.854
PCNA	Proliferating Cell Nuclear Antigen	NM_002592.2	F- CGGTTACTGAGGGCGAGAAG R- GCTGAGACTTGCGTAAGGGA	95	1.808
PXN	Paxillin	NM_002859.3	F- GGAAAAGTTGCGGGGCATAG R- CAAGAACACAGGCCGTTTGG	239	2.029
RAC1	Rac Family Small GTPase 1	NM_018890.3	F- TACGCCCCCTATCCTATCCG R- AACACATCGGCAATCGGCTT	91	1.905
RHOA	Ras Homolog Family Member A	NM_001313941.1	F- AGCCAAGATGAAGCAGGAGC R- TTCCCACGTCTAGCTTGCAG	162	1.944
SOX9	SRY-Box 9	NM_000346.3	F- AGGAAGTCGGTGAAGAACGG R- CGCCTTGAAGATGGCGTTG	84	1.969
TGFA	Transforming Growth Factor Alpha	NM_001308158.1	F- CTTGGAGAACAGCACGTCCC R- CCAGAATGGCAGACACATGC	162	1.764
TGFB1	Transforming Growth Factor Beta 1	NM_000660.6	F- ATGGAGAGAGGACTGCGGAT R- TAGTGTTCCCCACTGGTCCC	167	1.747
TGFB2	Transforming Growth Factor Beta 2	NM_001135599.3	F- CCCCGGAGGTGATTTCCATC R- CAACTGGGCAGACAGTTTCG	171	1.979
TGFB3	Transforming Growth Factor Beta 3	NM_003239.4	F- GTGCCGTGAACTGGCTTCT R- CTTGGCGATGGGGAGAAAGT	207	2.006

TGFBR1	Transforming Growth Factor Beta Receptor 1	NM_004612.3	F- GTGACAGATGGGCTCTGCTT R- AGGTGATGACTTTACAGTAGTTGGA	213	1.918
TGFBR2	Transforming Growth Factor Beta Receptor 2	NM_001024847.2	F- GTTGGCGAGGAGTTTCCTGTT R- GTCCTATTACAGCTGGGGCA	487	1.924
TUBA1	Tubulin Alpha 1	NM_006009.3	F- AAGCAGCAACCATGCGTGA R-CCGTCTCACTGAAGAAGGTGT	282	1.991
VCAM1	Vascular Cell Adhesion Molecule 1	NM_001078.3	F- GGACCACATCTACGCTGACA R- TTGACTGTGATCGGCTTCCC	184	1.951
VIM	Vimentin	NM_003380.4	F-CGGCTGCGAGAGAAATTGC R-CCACTTTCCGTTCAAGGTCAAG	124	1.845

Table 3: Table outlining all the names of all the primers, sequences and ascension numbers used in this study. Primer efficiency relates to how well each primer amplifies its target each PCR cycle, an efficiency of 2.0 denotes 100% efficiency.

2.7.7 Analysis of gene expression levels

In order to assess expression levels of target genes white 96 well plates (LightCycler 480 multi well plates, Roche UK) were prepared via the addition of 10µl of SYBR green (LightCycler® 480 SYBR Green I Master, Roche UK), 0.1µl of forward and reverse primer, 1µl of test cDNA and the addition of RNase free water (to bring the mix to a total volume of 20µl) into each well of the multiplate. Once the plate had been prepared, it was covered with a plastic sealing foil in order to prevent evaporation and centrifuged at 1500rpm for 3 minutes (Hettich Universal 320R, DJB Labcare UK). The plate was then placed onto the 96 well block of the light cycler and the amplification cycles were initiated (table 4). Gene expression was quantified by measuring the gradually accumulating fluorescent signal in each well (Figure 9). The cycle at which the fluorescent signal exceeded the background fluorescence was measured and called cycle threshold (Ct). Ct was inversely proportional to the amount of target present in each sample so the quicker Ct was achieved the greater the amount of target gene present in the sample. This Ct value was then compared with the Ct value of HKG in order to obtain the delta cycle threshold (ΔCt) from which fold changes were calculated allowing comparisons to be made between samples. The Pfaffl methodology was utilised in order to calculate the relative expression of each sample as it makes use of individual primer efficiencies leading to a more accurate value (Pfaffl, 2001). The Pfaffl method was used by means of the following equation:

$$\boldsymbol{Fold\ change} = \frac{\left(\mathbf{E}_{\mathbf{target}}\right)^{\Delta \mathbf{CP}_{\mathbf{target}}(\mathbf{control-sample})}}{\left(\mathbf{E}_{\mathbf{reference}}\right)^{\Delta \mathbf{CP}_{\mathbf{reference}}(\mathbf{control-sample})}}$$

Equation 4: Calculation of fold changes based on the Pfaffl method. E_{target} = efficiency of target gene; $E_{reference}$ = efficiency of HKG; ΔCP_{target} = Ct target control minus Ct of target sample; $\Delta Ct_{reference}$ = Ct of reference control minus Ct of reference sample.

	Treatment temperature	Duration	Number of cycles
Pre incubation	95 °C	5 minutes	1
Denaturation	95 °C	20 seconds	60
Annealing	60 °C	20 seconds	
Extension	72 °C	30 seconds	
Melt curve	95 °C	Until complete	1
Cooling	4 °C	Hold	1

Table 4: Outline of the relative temperatures and durations used during each cycle in order to amplify DNA and conduct real time PCR.

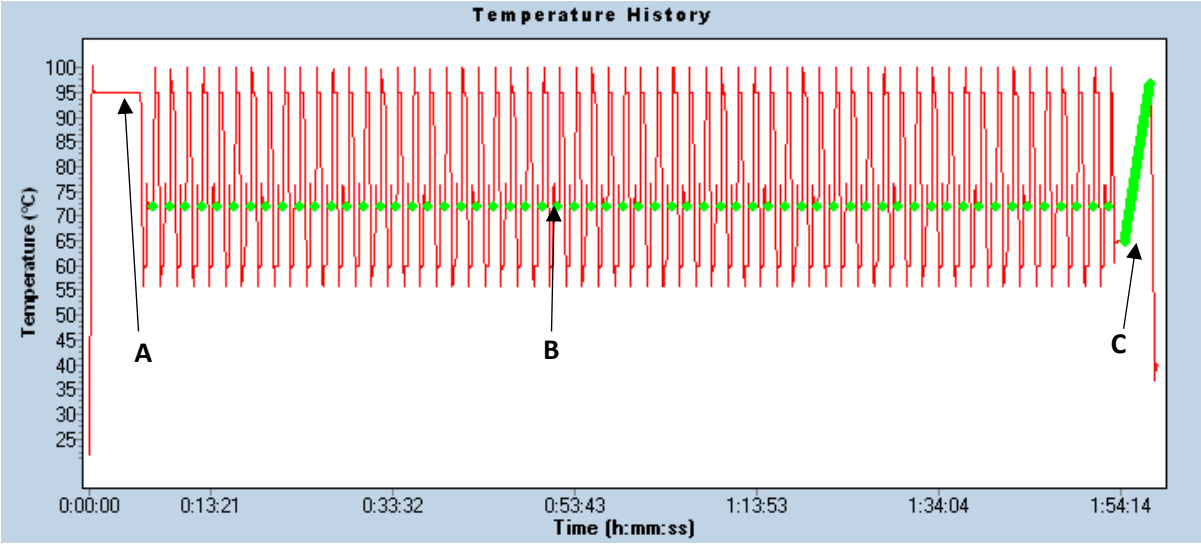

Figure 9: The cyclic temperature changes for the HKG used for gene analysis (ACTB). Pre-incubation followed by denaturation of DNA occurs at 95°C (A), the green spot indicates the point at which the target was quantified (B) and the green line indicates the point at which melt curve analysis took place (C).

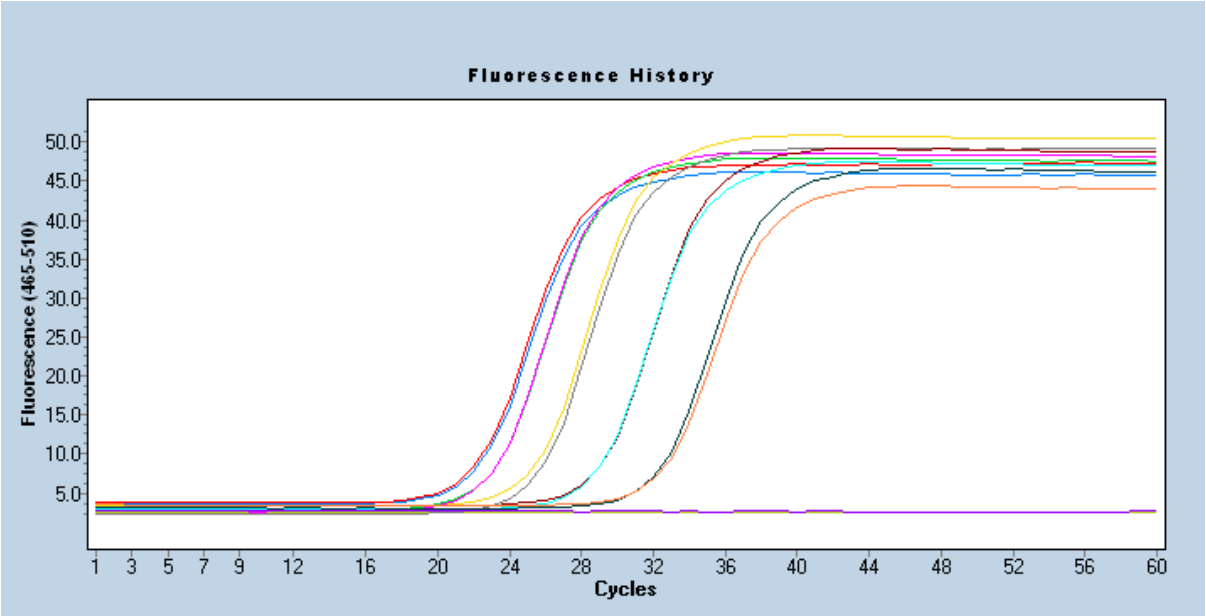

Figure 10: Amplification curve for ACTB. The HKG was serially diluted to 100%, 50%, 10%, 1%, 0.1% and a no template control. This was followed by qPCR in order to assess the amplification efficiency for each primer, a perfect amplification efficiency is 2.0 however ranges between 1.7 and 2.2 are acceptable (see table 3 for all efficiency values).

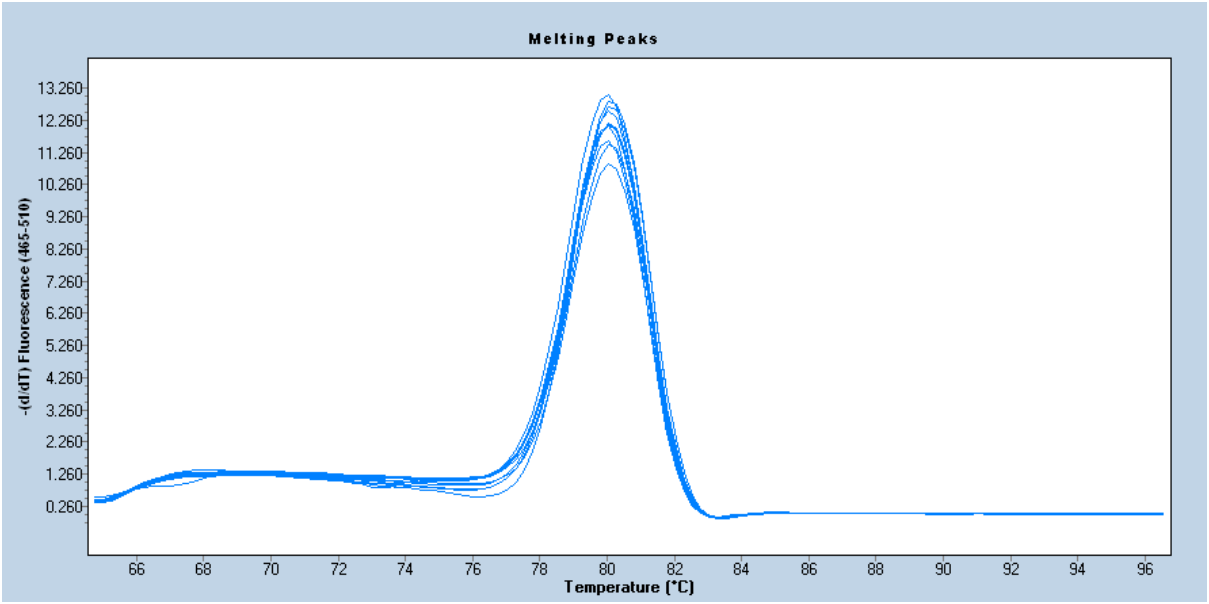

Figure 11: Melting curve for ACTB. Melt curve analysis was conducted in order to confirm that only a single amplicon was being amplified by the primer. The presence of a single peak demonstrates that only one product (the target) was being amplified. This analysis was conducted for all HKG and target genes and if multiple peaks were present primers were redesigned.

2.7.8 PCR following supplementation with experimental reagents

In order to assess the effect of FA, differing TGFβs and TGFα supplementation on cleft fibroblast gene expression, fibroblasts were grown to confluence in T75 flasks and incubated in DMEM for 24 hours under the experimental conditions defined in table 2. RNA was then isolated followed by cDNA synthesis so that qPCR could be conducted on various genes of interest, see section 2.7.1 to section 2.7.7.

2.7.9 Human cell motility PCR array

A PCR array (RT² Profiler™ PCR Array Human Cell Motility, Qiagen UK) was utilised in order to assess the differences in gene expression between six samples for 84 different markers; each related to cell motility. The protocol was similar to that in section 2.7.7 however primers were already lyophilised to each well and the temperatures and number of cycles varied (see table 5).

	Treatment temperature	Duration	Number of cycles
Pre incubation	95 °C	10 minutes	1
Denaturation	95 °C	15 seconds	45
Annealing and extension	60 °C	1 minutes	45
Cooling	4 °C	Hold	1

Table 5: Treatment protocol for PCR array. In accordance with the manufacturers recommendation the temperatures and durations of each PCR cycle was changed to obtain optimal measurement of gene targets for the Human cell motility PCR array.

2.8 Immunostaining

Immunostaining is a biochemical technique whereby specific biomarkers are visually identified. This is achieved by selectively targeting specific antigens within a sample through the use of primary antibodies, that have complimentary epitopes against the target of interest, which can either be detected directly or indirectly, through the use of secondary antibodies which bind to the primary antibody and permit signal amplification (Duraiyan et al, 2001). To detect antigen-antibody complexes, either chromogenic detection, which involves enzymatic conversion of a substrate into a chromogenic product with detectable pigmentation, or immunofluorescence (IF) detection, which makes use of conjugated fluorophores which emit light when excited and permit fluorescent detection at specific wavelengths, can be utilised; IF of specific antigens within biological samples was employed here. Immunohistochemistry (IHC) refers to the use imaging antigen-antibody complexes within tissue sections whereas immunocytochemistry (ICC) refers to imaging cell preparations; IHC and ICC were used here.

2.8.1 Tissue preparation

Cleft samples were immediately washed in PBS for 5 minutes, samples were then placed into labelled histology cassettes and put into pots containing 20ml of 10% neutral buffered formalin (Sigma, UK) and incubated for 24 hours at in a fume hood (Permier laboratory system, UK) at room temperature. The tissue was then placed into sample pots containing a graded series of industrial methylated spirit (IMS) (VWR chemicals, UK) with serially increasing concentration starting from 35% IMS with a gradual increase to 100% IMS, this was followed by three incubations in xylene (Genta medical, UK) in order to thoroughly dehydrate the samples. Following xylene treatment sample cassettes were immersed in liquid paraffin wax (Histoplast, Thermo Fisher Scientific, UK) and incubated overnight at 60°C to allow the wax to penetrate

the sample. Following overnight wax incubation, the samples were subject to two further 1-hour wax incubations to remove any xylene residue.

2.8.2 Wax embedding

Wax embedding was conducted using a tissue processing station (Tissue TEK, Sakura, UK). Following tissue preparation samples were placed into a heated liquid paraffin wax holding bath and the samples cassettes were removed using heated forceps. Tissue samples were then placed into a heated stainless steel base mould and orientated into the correct position, liquid paraffin was then poured into the mould whilst ensuring the sample stayed in the correct position and placed onto a cooling plate (-20°C) until the paraffin wax solidified. The wax block was then removed from the moulds and any excess wax was removed from the sample block.

2.8.3 Microtomy and section mounting

Wax embedded tissues were sectioned using a rotary microtome (Leica RM2035, Leica UK). Wax blocks were cooled and mounted onto the specimen holder and clamped into position. The paraffin block was then orientated into the correct plane in relation to the microtome blade. Any excess wax at the base of the block was trimmed, using the rotary action of the hand wheel, until the sample was at the base of the block. Samples were then cut at a uniform speed to form 5μm thick sections. Once cut, forceps were used to carefully remove sections from the knife holder and were placed into a warm water bath (20°C) to remove any surface wrinkles, leaving uniform sections. Sections were then placed onto separate glass microscope slides (Surgipath, UK) and incubated at 45°C for 2 hours to permit adequate section adhesion onto the glass slide.

2.8.4 Immunofluorescent staining protocol

Tissue sections adhered to glass slides were first deparaffinised by two 5 minute washes in xylene. Samples were then rehydrated via washing for 5 minutes each in serially decreasing

concentrations of ethanol starting at 100% and decreasing to 35%, followed by a final wash in deionised water. Glass slides were then inserted into a slide holder and placed into a plastic container containing 500ml of antigen retrieval buffer (1mM sodium citrate; 0.05% Tween 20). Anti-bumping granules were then placed into the container and it was covered in Clingfilm, this was followed by microwaving the slides for 20 minutes or until boiling. Samples were allowed to cool before washing twice in distilled water. Slides were then incubated at 37°C in permeabilisation buffer (0.2% Triton X-100 in PBS) for 45 minutes followed by two washes in PBS. Glass slides were then drained of any excess liquid and a circle was drawn around each sample using an ImmEdge hydrophobic barrier pen (Vector laboratories, UK) followed by the addition of 100µl of blocking buffer (10% bovine serum albumin (BSA) onto each sample for 60 minutes, prior to washing twice in PBS. Primary antibodies were then diluted in blocking buffer using a microliter syringe (Hamilton, UK) and 100µl of this solution was placed onto each sample and incubated overnight in a humidified chamber at 4°C (table 6 for list of antibodies and concentrations used). Glass slides were then washed in PBS followed by the addition of 100µl of secondary antibody and incubated for 60 minutes at room temperature in a dark room. After washing twice in PBS one drop of Vectashield antifade mounting medium with 4′,6-diamidino-2-phenylindole (DAPI) (Vector laboratories, UK) was added on top of each sample followed by mounting glass coverslips which were secured using clear nail varnish.

2.8.5 Immunocytochemistry on fixed cell cultures

In order to conduct immunocytochemistry (ICC) on cell cultures, cells were first grown onto uncoated sterile coverslips until partially confluent, culture medium was then removed followed by 2 washes in PBS. Cells were then fixed by immersing coverslips in 4% buffered paraformaldehyde (Sigma, UK) for 15 minutes, followed by 2 further washes in PBS. Due to most targets being internal, cells were permeablised using permeabilisation buffer (0.2% Triton

X-100 in PBS) for 60 minutes so that the antibodies could pass through the cell membrane and potentially bind to intracellular targets. Cells were then treated with blocking buffer (10% BSA) for 60 minutes in order to block any non-specific binding sites. After washing PBS, the cells were incubated overnight at 4°C with primary antibodies to allow them to bind to the targets of interest. After a further PBS wash, secondary antibodies were incubated with the cells for 60 minutes in a dark room to prevent photodegradation of the secondary antibody bound fluorophores. Vectashield antifade mounting medium with DAPI was then added to the cells and coverslips were mounted onto glass slides and sealed with clear nail varnish.

Antibody	Product ID	Species	Reactivity	Dilution factor	Source
Primary antibodies					
CK5	SC-23877	Mouse	Human	1:100	Santa Cruz
TGFβ1	SC-146	Rabbit	Human	1:200	Santa Cruz
TGFβ2	SC-90	Rabbit	Human	1:200	Santa Cruz
TGFβ3	SC-82	Rabbit	Human	1:200	Santa Cruz
TGFβR1	SC-398	Rabbit	Human	1:200	Santa Cruz
TGFβR2	SC-400	Rabbit	Human	1:200	Santa Cruz
TGFα	SC-36	Mouse	Human	1:100	Santa Cruz
VIM	SC-6260	Mouse	Human	1:100	Santa Cruz
Secondary antibodies					
FITC	SC-2365	Bovine	Anti-Rabbit	1:200	Santa Cruz
FITC	SC-2366	Bovine	Anti-Mouse	1:200	Santa Cruz

Table 6: List of antibodies and the dilution factors used for immunohistochemistry and immunocytochemistry.

2.8.6 Imaging of fluorescent markers

Samples were imaged using an LSM700 confocal microscope (Zeiss, Germany). Green channels were used to image FITC conjugated fluorophores and blue channels were used to image DAPI conjugated fluorophores; all images were taken using the same laser intensity.

2.9 Staining methods

2.9.1 Collagen staining

Sirius red F3B (BDH chemicals) staining is a commonly used technique to visualise and quantify the amount collagen that has been deposited onto a cell culture plate or within a tissue section. Sirius red is highly anionic due to the presence of six sulfonate groups on the dye, these groups strongly interact with cationic collagen fibres leaving red staining across the molecule (Junqueira, et al 1979; Rich, et al 2005). Sirius red staining was conducted using an established protocol (Tullberg-Reinert et al, 1999; Lattouf et al, 2014) to investigate collagen production. Cleft fibroblasts were treated with mitomycin C for 3 hours in order to inhibit proliferation and then seeded into 6 well plates at a concentration of $1x10^6$ and cultured for: 7 days. Culture medium was then removed and each well was washed 3 times with PBS, followed by fixation with 4% buffered paraformaldehyde for 15 minutes. Sirius red was dissolved into distilled water at a concentration of 1mg/ml, this solution was then treated with hydrochloric acid to reach a final pH of 3. Sirius red (1ml) was then added to each well and incubated at room temperature on an orbital shaker overnight. Cultures were then washed 3 times with 5% HCL in order to remove any unbound dye. The bound Sirius red was then dissolved by the addition of 1ml 0.2M sodium hydroxide (NaOH) under constant shaking for 30 minutes in order to elute the dye, this change in pH resulted dissociation of the dye from collagens due to alteration to its ionization state thereby weakening its affinity. This solution (100µl) was then pipetted into a 96 well plate and the absorbance was assessed at 490nm using a spectrophotometer in order to quantify the amount of dye in the sample.

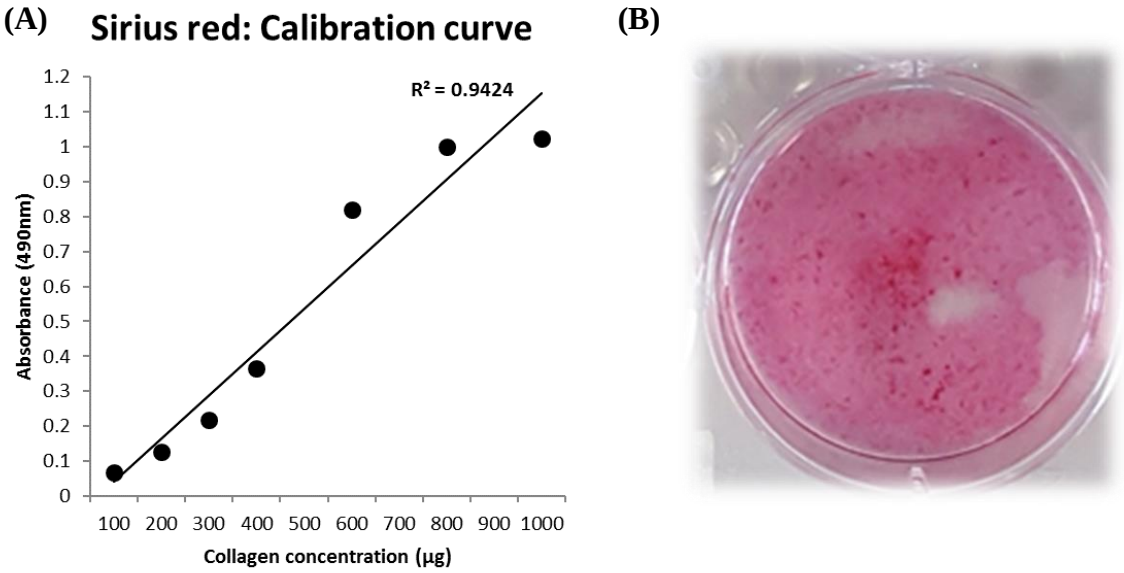

Figure 12: Collagen staining. (A) Calibration curve pertaining to collagen concentration and absorbance. (B) Example of cleft fibroblast secreted collagen staining with Sirius red.

2.9.2 Glycosaminoglycan staining

Alcian blue is a cationic dye which, due to the presence of copper within the dye molecule, stains acidic polysaccharides, such as glycosaminoglycan, blue (Björnsson, 1993). The pH of the dye solution can affect the type of macromolecules that are stained, when at pH 1 only sulphated polysaccharides such as chondroitin sulphate, dermatan sulphate and heparin sulphate are stained. However, increasing the solution to pH 2.5 leads to staining molecules with attached carboxyl groups such as hyaluronic acid (Green et al, 1974). Alcian blue staining and quantitation was conducted based on an established protocol (Fraizer et al, 2010; Björnsson, 1993). Cells were treated with 4µg/ml mitomycin C in culture medium for 3 hours, in order to inhibit proliferation and were then seeded into 6 well plates at a concentration of $1x10^6$ and cultured for7 days. Cell culture medium was then removed and the cells were washed 3 times with PBS, followed by fixation in buffered 4% paraformaldehyde for 20 minutes. Alcian blue

8GX (Sigma, UK) solution was made up by dissolving 1g dye in 100ml OF 18mM H_2SO_4 (Sigma, UK) to achieve a final pH of 1 followed by the addition of 0.25% Triton X-100, this solution was filtered in order to remove any undissolved particulate matter. Alcian blue (1ml) was added to each well and incubated at room temperature overnight on an orbital shaker. Cultures were washed 3 times with 5% HCL to remove any unbound dye, before dissolving the stain in 1ml DMSO and transferring this solution to a 96 well plate for spectrophotometric analysis at an absorbance of 600nm.

2.9.3 Haematoxylin and Eosin (H&E) staining

Paraffin embedded sections on glass slides were de-waxed by immersion in xylene for 5 minutes followed by treatment with 100% and 95% IMS for two washes of 30 seconds each; followed by a further wash in distilled water. Slides were placed in Gills III Haematoxylin (Surgipath, UK) for 2.5 minutes and rinsed in water before differentiation with 0.3% acetic acid (Merck, UK) for 30 seconds followed by treatment with 0.3% HCL for a further 30 seconds. Slides were then immersed in Scott's tap water substitute (Surgipath Europe Ltd), which enhances the stain intensity, for 1 minute followed by treatment with eosin (Surgipath, UK) for 1 minute before rinsing in 100% xylene and 3 further washes in xylene for 1 minute each. Once staining was complete, sections were covered dropwise with DPX mountant (Merck, UK) followed by coverslip placement.

2.9.4 Actin staining and quantitation

Phalloidin staining is a technique used to reveal the presence of actin within a treated sample. Phalloidin binds specifically to F-actin by tightly binding at the sites between actin subunits and interacts stoichiometrically with actin molecules meaning the staining intensity can be correlated with the amount of actin present in the sample and quantified (Wehland et al, 1977).

Phalloidin staining was conducted using ActinGreen™ 488 ReadyProbes™ Reagent (Thermofisher, UK) according to the manufacturer's recommendation. Cleft fibroblasts were grown on sterile glass coverslips until 70% confluent and then fixed with 4% buffered paraformaldehyde for 15 minutes then washed 3 times with PBS. The cultures were then permeablised by treatment with 0.2% Triton x-100 for 60 minutes, following this 1ml of PBS was added to each culture. Two drops of ActinGreen reagent were then added to each ml of PBS and incubated at 37°C for 60 minutes. When stained the coverslips were washed and then counterstained with DAPI and mounted onto glass slides using clear nail varnish. Fluorescently labelled cells were then imaged using an LSM700 confocal microscope (Zeiss, Germany), using the same magnification and laser intensity for all samples, and actin was quantified using imageJ (version 1.51). In order to quantify phalloidin staining, five randomly selected images were captured in red green and blue (RGB) channels so that both total intracellular actin and total cell nuclei, in the same frame of view, would be captured respectively. Image stacks, which had both actin and nuclei stains, were then converted into single images followed by conversion into 8-bit greyscale, thresholding was then applied so that the entirety of the captured image would be converted into binary form with white objects on a black background. The integrated density, which provides you with the sum of the all of the pixels within a frame of view (total pixel value), was calculated for both binary images of actin and total cell nuclei. The integrated density of actin was then divide by the integrated density of the cell nuclei in order to provide a ratio of actin to cell number, this process was repeated for each randomly selected image and an average was calculated (Figure 13).

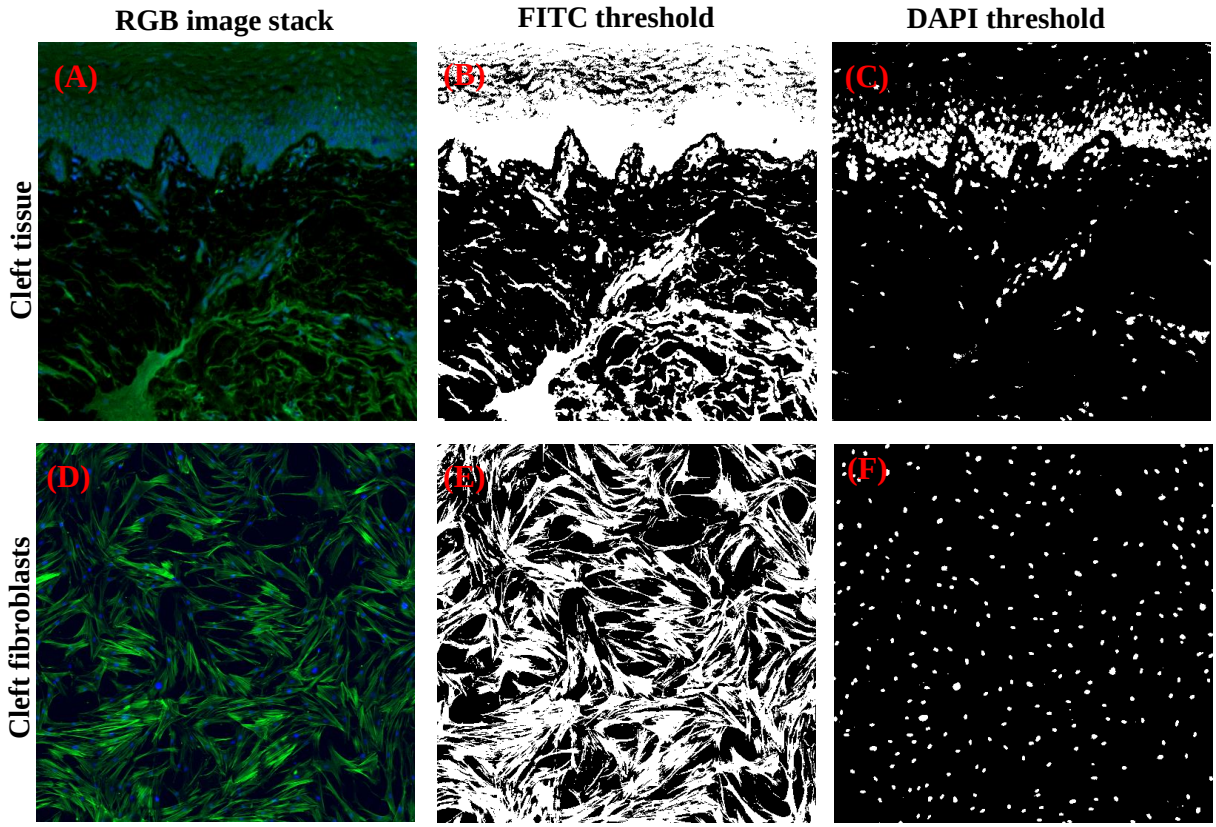

Figure 13: Thresholding method of quantitation based on ratio of phalloidin staining and nuclei staining. Phallodin and nuclei staining for cleft tissue sections (A) and cultured cleft fibroblasts (B), phallodin stains (green) (B and E) were isolated to calculate the integrated density of actin and this was adjusted with respect to total cell numbers based on nuclei staining (blue) (C and F).

2.10 Cell adhesion

2.10.1 Cell to substrate adhesion

Cells were seeded at a concentration of $5x10^4$ into 35mm petri dishes, in the presence or absence of folic acid (see table 2 for details). After 24 hours the supernatant in each well was removed and centrifuged at 900g for 5 minutes, the cells were then re-suspended in 1 ml DMEM and counted using a haemocytometer in order to obtain the number of cells that had not adhered to the petri dish.

2.10.2 Cell to cell adhesion

CellTracker™ Green CMFDA (5-chloromethylfluorescein diacetate) Dye (Thermo Fisher Scientific, UK) is a fluorescent dye commonly used to stain live cells in response to stimuli. The uncharged dye freely diffuses into cells where intracellular esterases cleave lipophilic groups on the compound resulting in a charged compound that bind covalently intracellular components and begins to fluoresce (Lulevich, et al, 2009). The dye remains in the cell for an extended period of time and does not leach to neighbouring cells. CMFDA stock solution was reconstituted in 50µl DMSO to obtain a 10mM stock solution, this was then diluted into pre-warmed 37°C DMEM to obtain a 10µM working concentration. Cells were trypsinised and centrifuged at 900g for 5 minutes followed by resuspension in 5ml CMFDA working solution and incubated at 37°C for 45 minutes. Cells were then centrifuged and resuspended in sDMEM (see table 2 for details) and seeded onto confluent monolayers of unstained cells in 35mm petri dishes under experimental conditions. After 24 hours the supernatant, containing non-adherent cells, was removed, centrifuged and re-suspended in 200µl PBS. This cell suspension was then transferred to a 96 well plate and the fluorescent intensity of the cells was read using a fluorescence plate reader at 490nm in order to quantify number of cells that did not adhere.

2.11 Bicinchoninic acid protein assay

The bicinchoninic acid (BCA) assay (Pierce™ BCA Protein Assay Kit, Thermo Fisher Scientific, UK), was used to determine the total protein concentration within serum free cultures of cleft fibroblasts. This assay is comprised of a two-step reaction, the first step made use of the well-established biuret reaction whereby interaction with protein in the media causes Cu^{2+} to be reduced to Cu^{1+}, this cation then interacts with bicinchoninic acid leading to purple coloured by-product. This purple by-product can be quantified calorimetrically as the intensity of the

colour is directly correlated with the amount of protein within a given sample. Calibration curves using purified bovine serum albumin (BSA) were first created by serially diluting BSA in deionised water in concentrations between 6.25% to 100% and a negative control comprising of just diluent. The BCA reagent was prepared by mixing of reagent A (sodium carbonate, sodium bicarbonate, bicinchoninic acid and sodium tartrate in 0.1M sodium hydroxide) reagent B (4% cupric sulphate) in a 50:1 ratio for a total working volume of 25ml. 200µl of BCA working reagent was then placed into 96 well plates with 25µl of each standard or sample. The microplate was then placed on an orbital shaker for 1 minute followed by incubation at 37°C for 30 minutes then absorbance of each well was measured at 570nm using a spectrophotometer.

2.12 Proteome Profiler Human XL Cytokine Array

Cytokines, chemokines and growth factors are ECM related molecules that mediate specific cell responses. The Proteome Profiler Human XL Cytokine Array Kit (R&D systems, UK) is a membrane based sandwich immunoassay that has 105 soluble antibodies marked on the surface of a nitrocellulose membrane. Proteins within a sample bind directly to their specific antibody on the membrane surface, the quantity of bound protein can then be quantified through us of X-ray analysis and quantification of the pixel density for each region of interest. This assay was used to quantify cytokine secretion by cleft fibroblasts into the culture medium (Figure 14).

2.12.1 Sample preparation of cleft fibroblast Secretome

Cleft fibroblasts were seeded at a concentration of $1x10^6$ into T75 flasks and were incubated for 24 hours to allow cells to adhere to the surface of the flask. After incubation, cultures were washed with PBS followed by the addition of 5ml serum free media into each flask and the cells were incubated for a further 24 hours to allow cytokine release into the medium. Cell culture supernatants were removed and stored in 1ml aliquots at -80°C until needed.

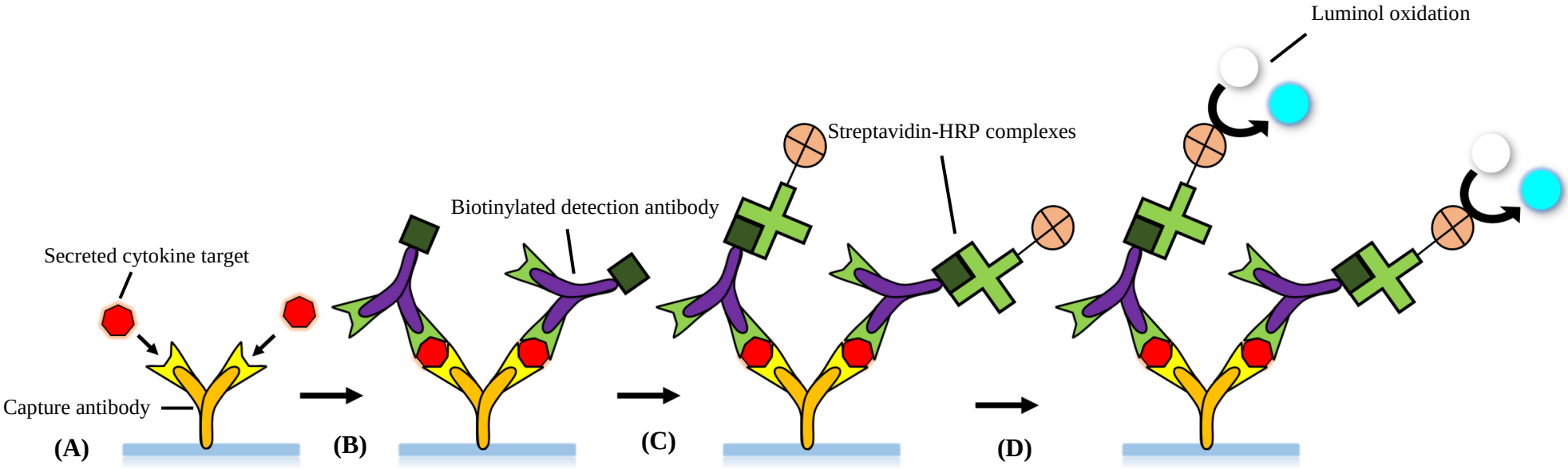

Figure 14: Schematic outlining the general staining principles employed to conduct the cytokine array. (A) Capture antibodies are adhered onto specific locations of the nitrocellulose membrane; these antibodies are complimentary to specific cytokine targets secreted by cleft fibroblasts. (B) Biotinylated detection antibodies are later exposed to the membranes which in turn bind to the capture antibody-cytokine complex. (C) Due to its high affinity streptavidin-horse radish peroxidase (HRP) adhere to detection antibodies. (D) Luminol is oxidised by HRP in the presence of hydrogen peroxide thereby emitting a light signal output that is detectable by x-ray.

2.12.2 Experimental procedure

All reagents, samples and the experimental procedure was prepared and conducted as directed by the manufacturer. Each nitrocellulose membrane was placed into one well of a provided 4 well multi dish using flat bottomed tweezers with the membrane facing upwards. Following this, 2ml blocking buffer was pipetted into each well and the 4 well multi dish was placed on a rocking platform shaker for 1 hour. Samples were then thawed and 300µl of each was diluted into 1200µl of blocking buffer to give a final volume of 1.5ml. After incubation, blocking buffer was removed from each well and 1.5ml of each diluted sample was placed into one of the wells containing the nitrocellulose membrane and incubated overnight at 4°C on a platform shaker. Membranes were then removed and placed into individual plastic containers and washed 3 times for 10 minutes each in 1x wash buffer. The detection antibody cocktail was then prepared by pipetting 30µl of detection antibody into 1.5ml of array buffer for each sample, this was then placed into each well of the multi dish and the membranes were placed back into the wells and incubated at room temperature for 1 hour, followed by a further 3 washes with wash buffer. Next, 2ml of streptavidin-HRP was placed into each well and incubated with the membrane for 30 minutes at room temperature and washed as before. Each membrane was then removed and the excess wash buffer was drained off, the membranes were then placed into a plastic sheet protector and 1ml of chemi-reagent mix (2.5ml stabilized hydrogen peroxide and 2.5ml luminol) was added dropwise to each membrane for 1 minute. The excess reagent was then removed and the samples were prepared for analysis.

2.12.3 Data analysis

Each nitrocellulose membrane was placed into a C-Digit® Blot Scanner (LI-COR, UK) and subjected to a 12-minute scan in order to obtain a digital chemiluminescence reading for each sample spot that was proportional to the amount of protein present in the cell supernatant.

Analysis of the pixel intensity of each spot was conducted using the Li-COR software. Spheres of a standard size were created and allocated to each spot, including reference spots, across the array in order to locate each cytokine (Figure 15). The pixel intensity of each spot was then quantified and the average background pixel intensity was subtracted, leaving a quantitative value for each cytokine from which comparisons between samples were made.

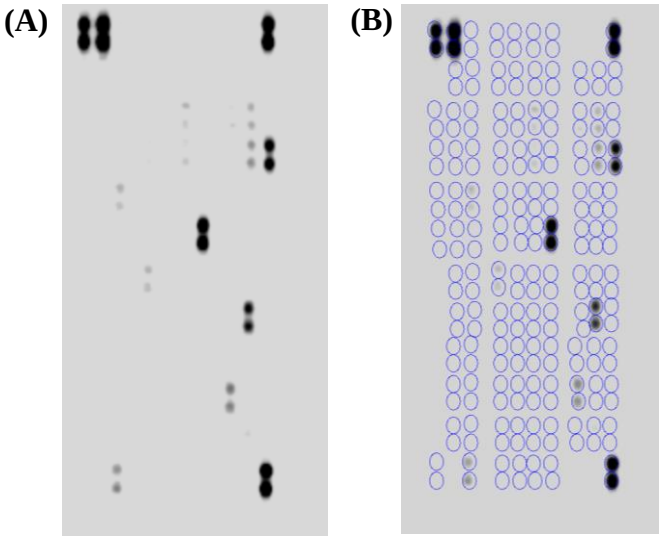

Figure 15: Scans of nitrocellulose membranes used for cytokine array. (A) Digital chemiluminescence readings from nitrocellulose membranes placed into a C-Digit® Blot Scanner. (B) LI-COR software was used to place standard spheres above the location of each sample spot to provide individual cytokine pixel intensity readings.

2.13 Statistical analysis

All statistical analysis was conducted using a statistical analysis package (IBM SPSS Statistics, USA). Data sets were first subject to F-test to assess how the data was distributed, for normally distributed data (parametric) comparisons between data sets were made using a student's t-test or one-way analysis of variance (ANOVA). However, if the data was abnormally distributed (non-parametric) the Mann-Whitney test was conducted; significance was only inferred when $p<0.05$ with a two-tailed distribution. For correlational analyses the distribution of the data was first assessed by conducting a Shapiro-Wilk test of normality. With data sets that were normally parametric, Pearson's correlation was conducted, whereas for data that was non-parametric, Spearman's rho was conducted. Unless expressly stated all data was presented as a mean value with error bars denoting standard deviations between replicate samples. Statistical significance was expressed as follows: *, ** and *** denote $p<0.05$, $p<0.01$ and $p<0.001$ respectively.

CHAPTER THREE:

CHARACTERISATION OF HUMAN CLEFT FIBROBLASTS

3.1 Confirmation of the Fibroblast phenotype

To confirm the cell populations isolated from cleft tissue samples comprised of primary cleft fibroblasts as opposed to a heterogeneous cell population, pooled cleft patient cells were assessed in terms of gene transcript expression for both vimentin (*VIM*), a type of intermediate filament is only found in cells of mesenchymal origin and is commonly used as a fibroblast marker (Change et al,2002) and cytokeratin-5 (*CK5*), a type of intermediate filament specific to epithelial cells (Corr et al, 2015), by real time PCR. It was found that *VIM* was expressed in both pooled cleft fibroblasts and an immortalized H400 keratinocytes (human oral squamous cell carcinoma cell line) control. However, *CK5* was only expressed significantly within H400 cells and was not significantly expressed by pooled cleft fibroblasts. It is important to note that real time PCR cycle threshold (Ct) data with values greater than 40, as with *CK5* expression in pooled cleft fibroblasts, were considered as null expression, as despite potentially being expressed within the cell population the amount was too low to accurately quantify and compare to control samples (McCall et al, 2014).

Immunohistochemical staining for *VIM* in pooled cleft fibroblasts was strongly positive, indicating its presence within the cultured cell population and thereby offering further support towards the confirmation of the fibroblast phenotype.

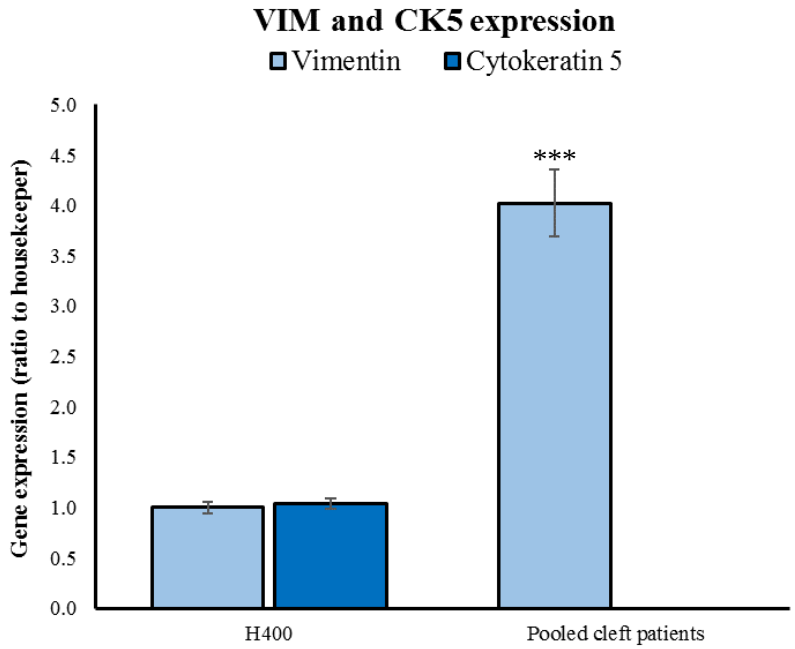

Figure 16: Vimentin and cytokeratin-5 gene expression in H400s and pooled cleft fibroblasts. Vimentin and cytokeratin-5 were expressed in the positive control (H400) against which the expression levels have been normalised. Vimentin (a fibroblast marker) was expressed in a higher ratio in pooled cleft fibroblasts whereas cytokeratin-5 (an epithelial cell marker) had negative expression (where Ct values were >40 or null negative gene expression was inferred). This indicated that there was likely no epithelial cell contamination within cleft cell populations.

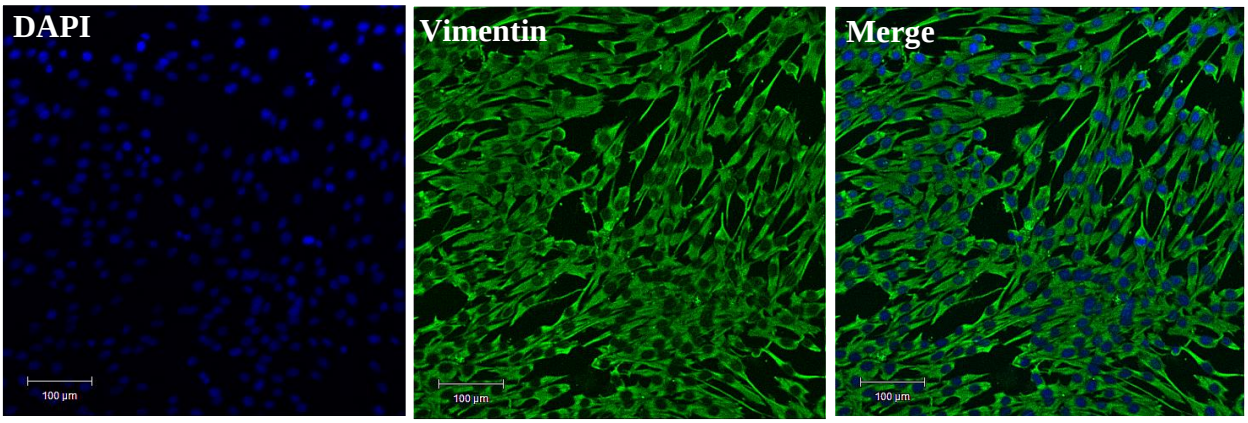

Figure 17: Vimentin staining in cells isolated from cleft tissues. Positive immunocytochemical staining was observed for the fibroblast marker vimentin (green) in cultured cleft fibroblasts (passage one) thereby indicating that the cleft cells isolated from tissue samples were likely fibroblasts.

3.2 Analysis of cleft fibroblast growth with increasing passage

As passaging is a traumatic process that can have a significant effect on normal cell behaviour, including proliferation and gene expression (Hughes et al, 2018), it was necessary to determine the influence of passaging on cleft fibroblast such that the optimal passage number for comparative assessment between patient samples could be selected. To conduct the analysis, cleft fibroblasts derived from the lip of a single cleft patient were assessed, multiple patient samples could not be utilised due low level passages being required to expand stocks of low passage number fibroblast for future analysis. Growth curves were generated from cleft fibroblasts varying between passage zero, which would act as the control due to these cells not yet being subject to passage, and passage five over a 10-day period. Two days after initial seeding cell numbers were comparable for all passages, at day four passages four and five had slight non-significant decreases in cell number when compared with passage zero cell numbers. This disparity increased at days 6 and 8 with cell numbers for passage four and five significantly lower than there passage zero counterparts ($p<0.05$ based on two-tailed distribution t-test). At day 10 all cultures were confluent and cell numbers were comparable across passage zero to five (Figure 18A). Fibroblast doubling times (DT), which were derived from growth curves data, revealed that there were no significant differences between passage zero to three; however, passage 4 and 5 had significantly longer DT when compared with fibroblasts of earlier passages ($p<0.05$) (Figure 18B). Despite this, MTT absorbance values following fibroblast growth for 4 days did not shown any significant differences between passages (Figure 18C). As fibroblast growth was shown to be unaffected at low passages, all subsequent cell based assays were conducted with passage two fibroblasts thus any disruptions in cell behaviour would be consistent across the patient cohort.

3.2.1 Expression of genes associated with cell proliferation with increasing passage

The expression of proliferation associated genes were assessed to determine any changes in expression with increasing passage as increased doubling times had been observed from passage four onwards. *MCM2* expression was stable in fibroblasts that were from passage zero and one; however, *MCM2* expression was significantly upregulated from passage 2 onwards relative to passage zero cells ($p<0.01$) (Figure 19A). *MKI67* expression was similar between passages zero to passage two whereas fibroblasts from passage three to five displayed significantly lower expression than passage zero ($p<0.01$) (Figure 19B). *PCNA* expression was shown to be comparable between passages zero to five with no significant changes in expression (Figure 19C). The data shows that there were changes in the expression of genes associated with cell proliferation as passages increased; however, these changes occurred at an earlier passage than the passage at which changes in cell growth were observed.

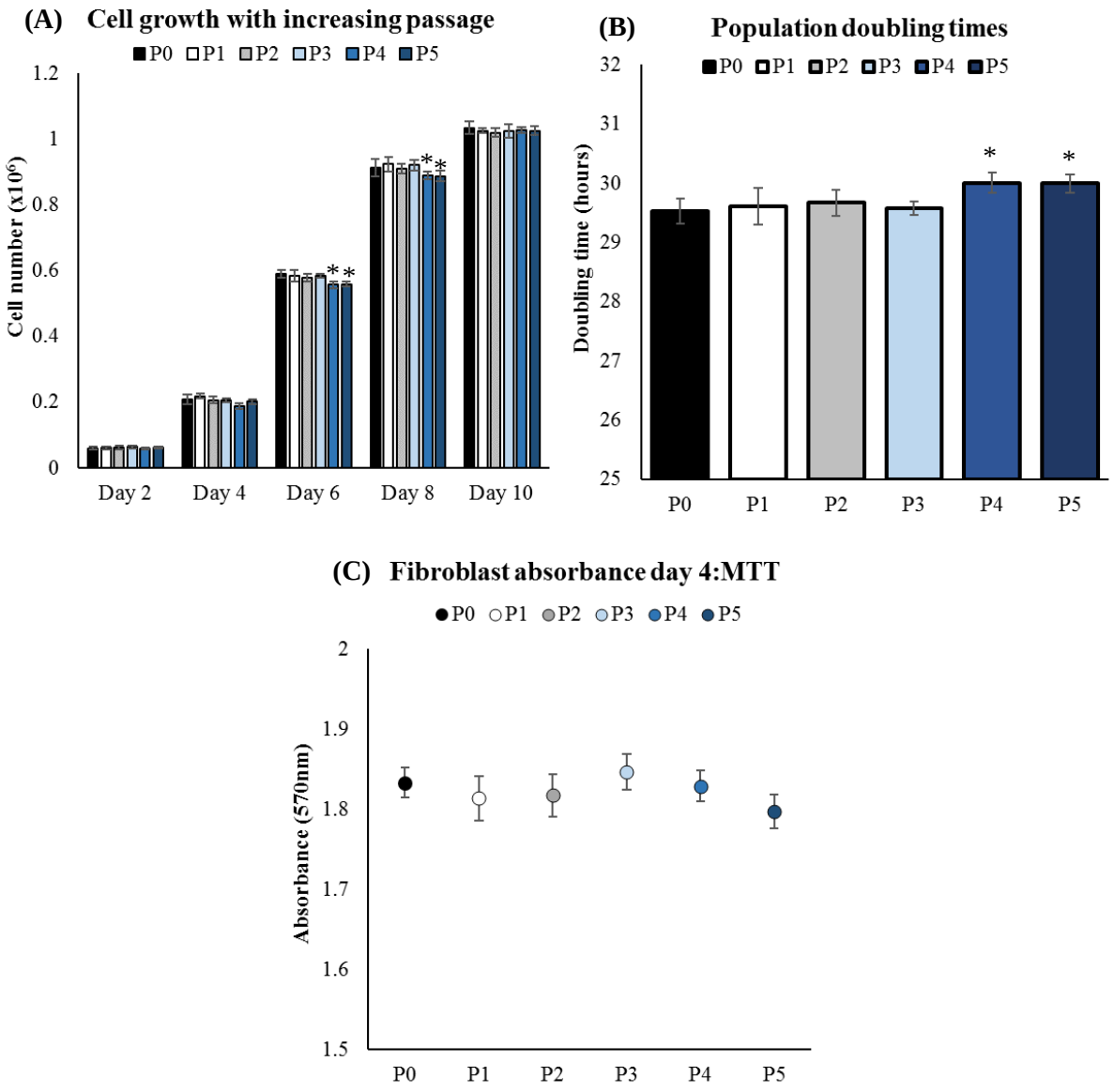

Figure 18: Assessment of cleft fibroblast growth with increasing passage. (A) Growth curve analysis revealed that the rate of cleft lip fibroblast growth, derived from a single patient, was similar between passage zero (control) to three, however from day four onwards cell growth was decreased in passages four, at day 10 all cultures were confluent. (B) There was no significant difference in cell doubling times between passage the passage zero control and three, however passage four and five had significantly higher doubling times when compared with passage zero ($p<0.05$; two tailed t-test) (C) There was no significant difference in the absorbance values of cleft fibroblasts between passage zero and five following four days in culture (n=3).

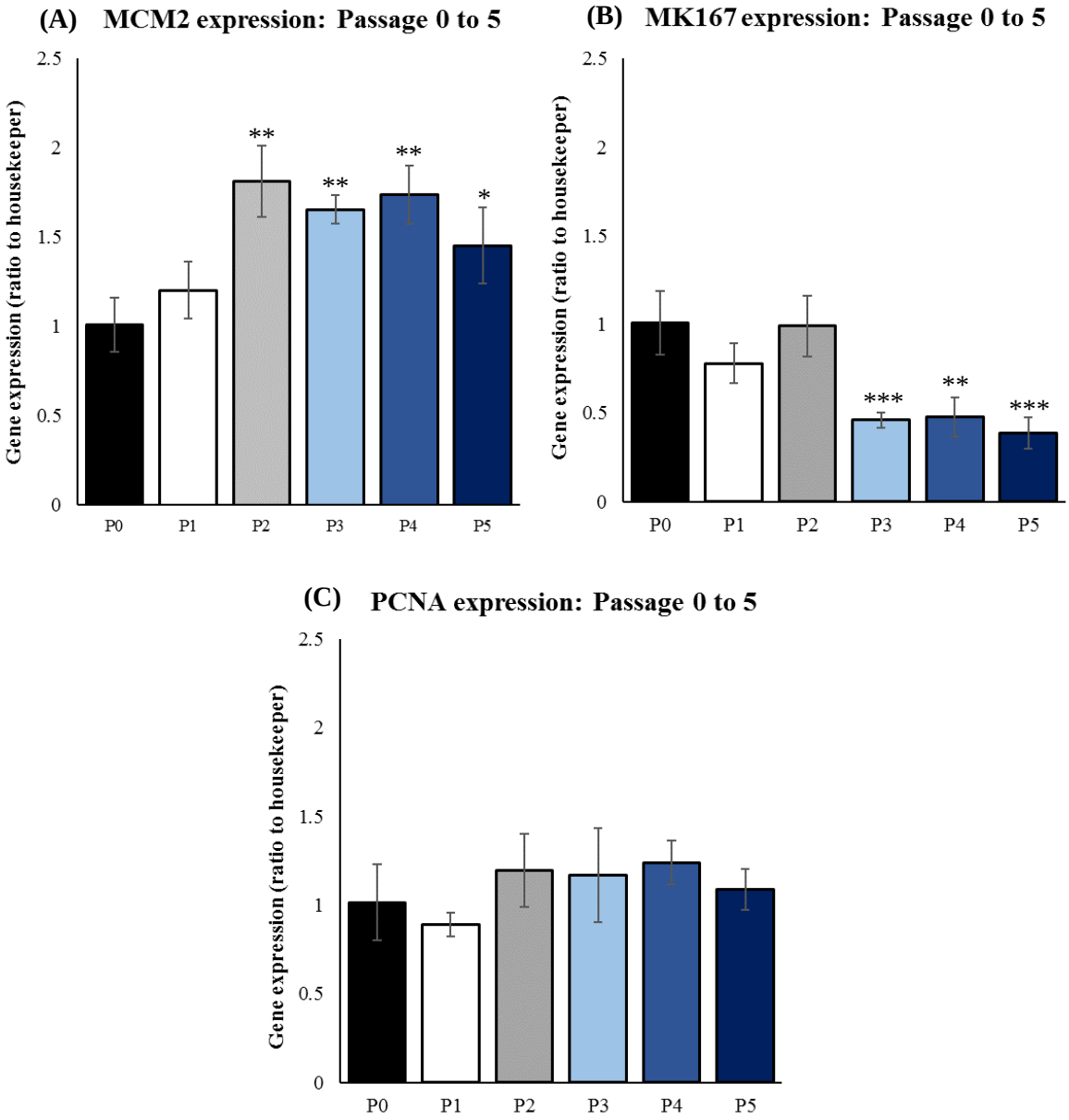

Figure 19: Changes in expression of gene transcripts associated with cell proliferation with increasing passage in cleft lip derived fibroblasts. (A) *MCM2* expression levels were similar in passage zero (control) and one, however from passage two onwards there was an approximate two-fold increase expression when compared with the passage zero control ($p<0.01$); this increased expression remained with all subsequent passages. (B) *MK167* expression was comparable between passage zero, one and two. However, from passage three onwards there was a significant decrease in expression when compared with passage zero control cells ($p<0.01$). (C) There were no significant differences in expression of *PCNA* between passage zero and five (n=3).

3.2.2 Expression of genes associated with cleft development with increasing passage

To determine the most suitable passage number to conduct gene expression analysis on markers that may be involved in the manifestation of different cleft phenotypes, the change in expression of three genes, each of which have been associated with CLP development, were assessed between passage zero (control) to passage five. This data would permit the selection of the most suitable passage number for real time PCR analysis which would be kept consistent for all future analysis. The expression of *IRF6*, a transcription factor that is elevated in the developing palatal shelves and is thought to regulate epithelial to mesenchymal during palatal fusion (Ke et al, 2015), was comparable in fibroblasts from passage zero to two, while from passage three to five there was a 2.5-fold significant increase in expression relative to the passage zero control ($p<0.01$) (Figure 20A); this indicated passaging disrupted expression of a known CLP markers thus fibroblasts with elevated passages should not be used for analysis. *SOX9*, a transcription factor that is elevated in early neural crest progenitor cells (Haldin and LaBonne, 2010) and are involved in the regulation of craniofacial cartilage formation (Lee et al, 2011), displayed significantly reduced expression between the passage zero control and passage one ($p<0.01$), this decreased further at passage four and five (Figure 20B). This significant decrease in *SOX9* expression suggests that the expression of a number of genetic markers may be disrupted after a single passage with further perturbation at elevated passage numbers, thus analysis of gene expression across the patient cohort must be conducted at the same passage so that any perturbation to gene expression caused by passage are consistent for each cleft sample. However, *TGFA*, a potent epithelial mitogen that has been correlated with the development of nsCLP (Lu et al, 2013), displayed stable expression between the passage zero control and each passage number assessed (Figure 20C), this suggests that a number of markers involved in cleft development may be unaffected by the passaging process. All subsequent real time PCR assays were conducted with passage one fibroblasts as this was the lowest possible passage number

that ensured sufficient cell stocks for all future assays. Further, as all samples were assessed at the same passage any genetic dysregulation caused by subculture would be consistent across all the samples assessed.

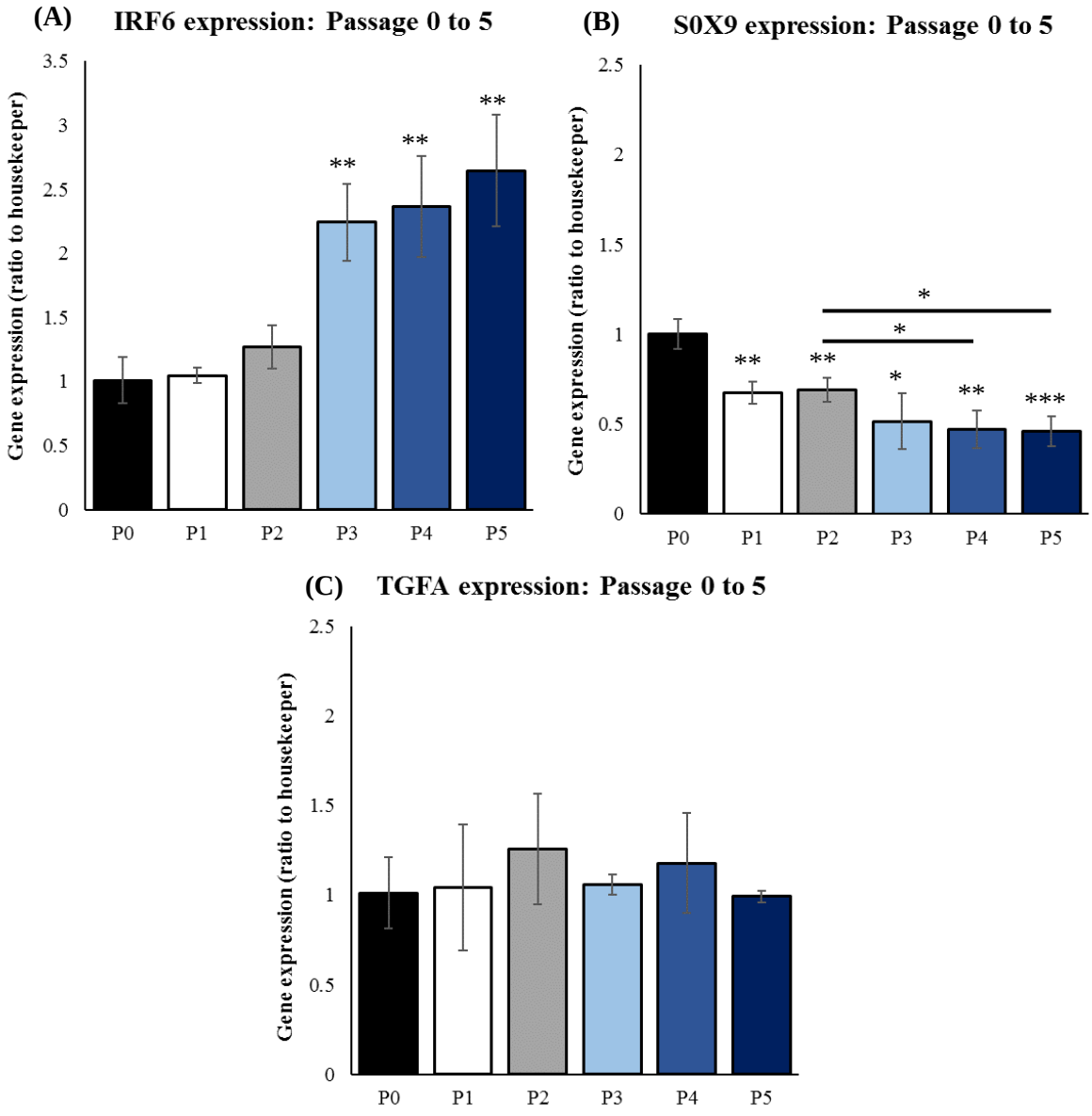

Figure 20: Expression of genetic markers associated with cleft development with increasing passage. (A) *IRF6* expression levels were similar from passage zero to two, however from passage three onwards there is an approximate 2.5-fold increase in expression ($p<0.01$). (B) *SOX9* expression is significantly decreased from passage zero to one ($p<0.01$); this expression decreased further after passage four ($p<0.05$). (C) There were no significant differences in the expression levels of *TGFA* between passage zero and five (n=3).

3.3 Growth curve assays and doubling times for all cleft fibroblast samples

Fibroblast growth is a pivotal behaviour that leads to increased fibroblast concentration thus ECM remodelling within wounded and developing tissues. In order to establish whether fibroblast proliferation was associated with the cleft phenotype manifestation, growth curves were generated to determine the individual growth rates of fibroblasts isolated from each cleft patient. Fibroblasts from patients were seeded at the same concentration and displayed similar cell numbers after 2 days in culture (Figure 21A). However, after 4 days there was some dissimilarities, with the greatest variation observed after 6 days in culture (Figure 21B). At day-8, many of the growth curves were approaching confluence with a marked plateau after 10 days for all patient samples. Population doubling times were calculated from growth curves. The fastest growth was observed for S101603 with a doubling time of 26.11 hours whereas the slowest growth rate was observed in S101634 and had a doubling time of 32.41 hours, interestingly both the fastest and the slowest growth was observed in fibroblasts derived from the same cleft phenotype (CLP(L)). Neonatal human dermal foreskin fibroblasts (NHDFF) were used as non-cleft control cells, it was shown that NHDFF's shared comparably similar DT to a number of cleft fibroblasts although the majority of the patient cohort displayed slightly longer DT due to a comparably reduced growth rate. When comparing cleft types, there were no significant differences in terms of population doubling times between CLP(L), CLP(P), CL and CP (Figure 22). There were no significant differences in DT in terms of cleft laterality between LUCLP, RUCLP and BLCLP. This suggests that fibroblast growth is not influenced by the underlying cleft phenotype.

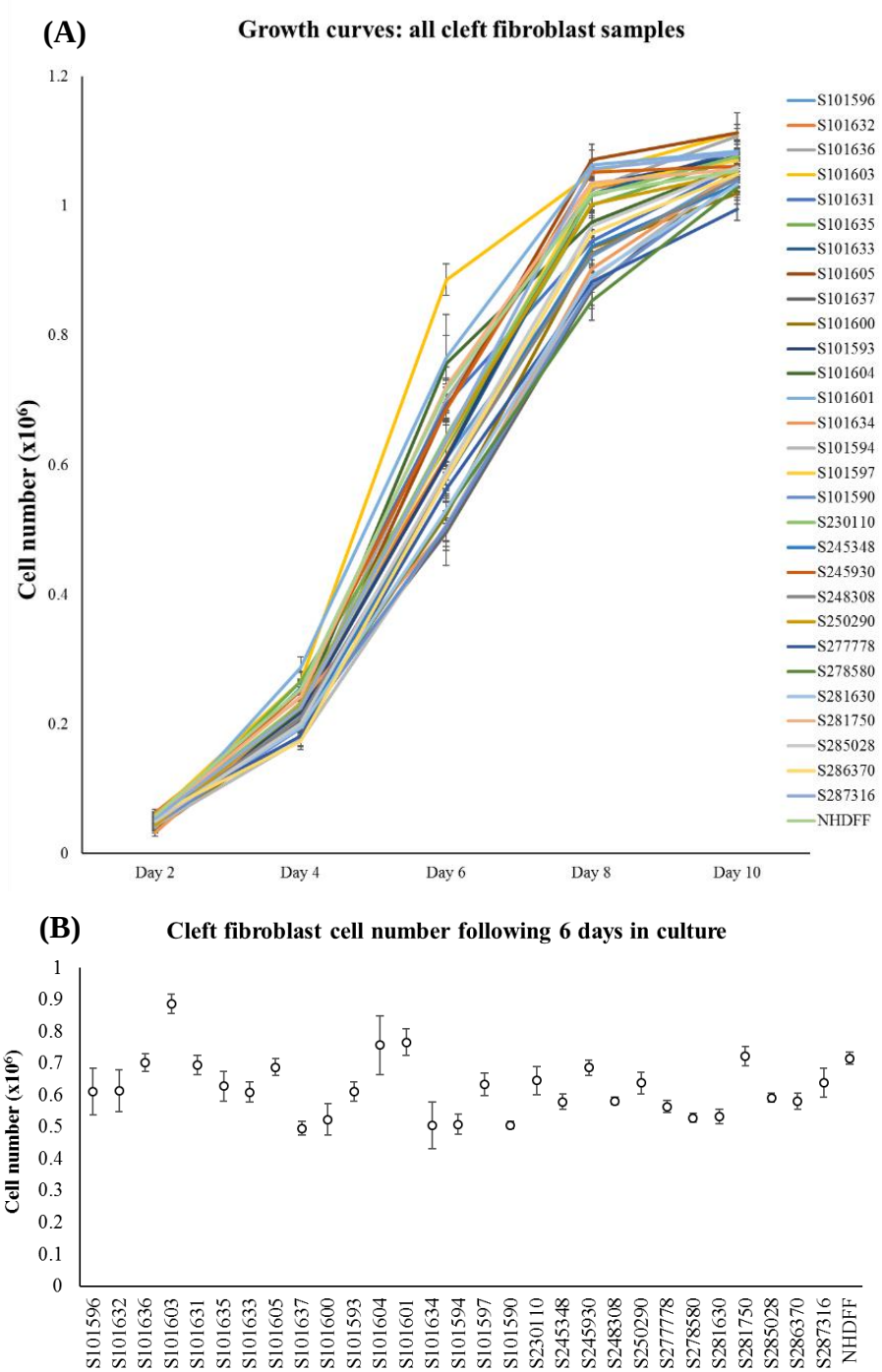

Figure 21: Comparative growth curve assays for each patients fibroblasts to assess changes in cell number with time. (A) Cell growth over a 10-day period after an initial seeding concentration of 0.02 x10^6 with cell counts every 48 hours. (B) The most variation in cell numbers was observed at day 6 with the majority of cell counts between 0.5x10^6 and 0.8x10^6 however there were a number of outliers with values above and below this range. Neonatal human dermal foreskin fibroblast (NHDFF) control cells displayed greater cell numbers at day 6 than the majority of cleft fibroblasts although there were a number of samples with comparable cell numbers at day 6 (n=12).

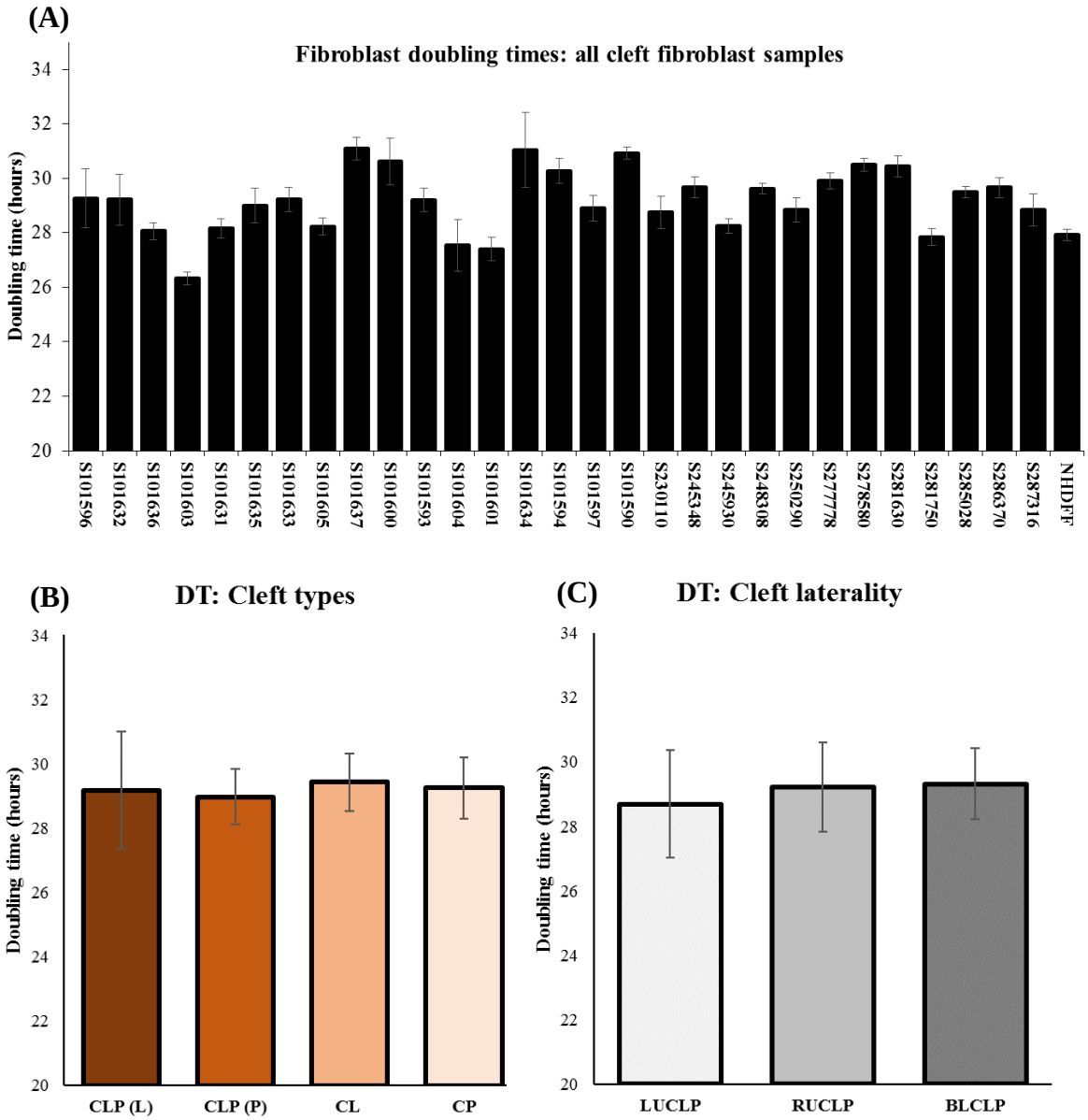

Figure 22: Fibroblast doubling times. (A) Population doubling times (DT) were calculated based on the cell numbers obtained from growth curve models. There were differences between patient fibroblasts with DT varying between 26.11 hours and 32.41 hours; NHDFF DT was faster than the majority of cleft samples although a minority of patients displayed a comparable DT (n=3). (B) Averaged DT was similar between cleft phenotypes with no significant difference. (C) DT did not differ significantly based on cleft lateralitv.

3.3.1 Expression of genes associated with cell proliferation

Expression of gene transcripts associated with cell proliferation were assessed for each cleft patients fibroblasts and correlated with cell doubling times (DT), expression of each gene was also compared between cleft types and cleft laterality.

MCM2 expression varied across samples although most patient-derived fibroblasts demonstrated expression higher than that of that of the non-cleft human gingival fibroblast (HGF) control; HGFs were used as control for real time-PCR assays as they are oral fibroblasts thus are likely to be more comparable to oral cleft fibroblast in terms of gene expression when compared to NHDFF which are dermal fibroblasts (Ebisawa et al, 2011). The highest overall expression was 5.74-fold whilst the lowest was 0.65-fold (Figure 23A). *MCM2* expression was plotted against DT to assess their correlation (Figure 23B) however Spearman's rho revealed that there was no strong significant correlation between *MCM2* and DT. When comparing cleft types, MCM2 expression in fibroblasts from CLP(P) was significantly higher than fibroblasts from CP ($p<0.05$) (Figure 26A). Further, *MCM2* expression differed based on cleft laterality as expression was significantly lower in BLCLP fibroblasts when compared with LUCLP and RUCLP (Figure 26B).

MK167 expression was higher in most samples when compared with the HGF control, however there was large differences between fibroblasts with the highest expression being 5.47-fold and the lowest 0.83-fold (Figure 24A). Spearman's rho analysis showed that there were there were no significant correlations between *MKI67* and DT (Figure 24B). When comparing cleft types, on average CLP(L) fibroblasts had significantly lower expression than all other cleft groups, including: CLP(P) ($p<0.05$), CL ($P<0.05$) and CP ($p<0.05$). In addition, CLP(P) average expression of *MKI67* was significantly lower than that of CP fibroblasts ($p<0.05$) (Figure 26C). Comparing *MK167* expression in CLP patients according to laterality revealed that that

expression was significantly lower in BLCLP fibroblasts than LUCLP and RUCLP (Figure 67D).

PCNA expression varied widely across the cohort with a maximum expression, relative to the HGF control, of 4.51-fold and a low of 0.69-fold. As the data pertaining to *PCNA* expression was deemed to be non-parametric by means of shapiro-Wilk normality test, Spearman's rho test revealed that there was a significant correlation between *PCNA* expression and DT ($p<0.01$) suggesting that patient expression of *PCNA* and the DT, determined from cell growth curves, may be related (Figure 25). Comparing *PCNA* expression between cleft types revealed that expression was significantly lower in CL fibroblasts when compared with both CLP(L) and CLP(P) whereas *PCNA* expression was significantly lower in CP fibroblasts when compared with CLP(P). Fibroblasts from the BLCLP phenotype had significantly lower *PCNA* expression when compared with those with RUCLP (Figure 26E and 26F).

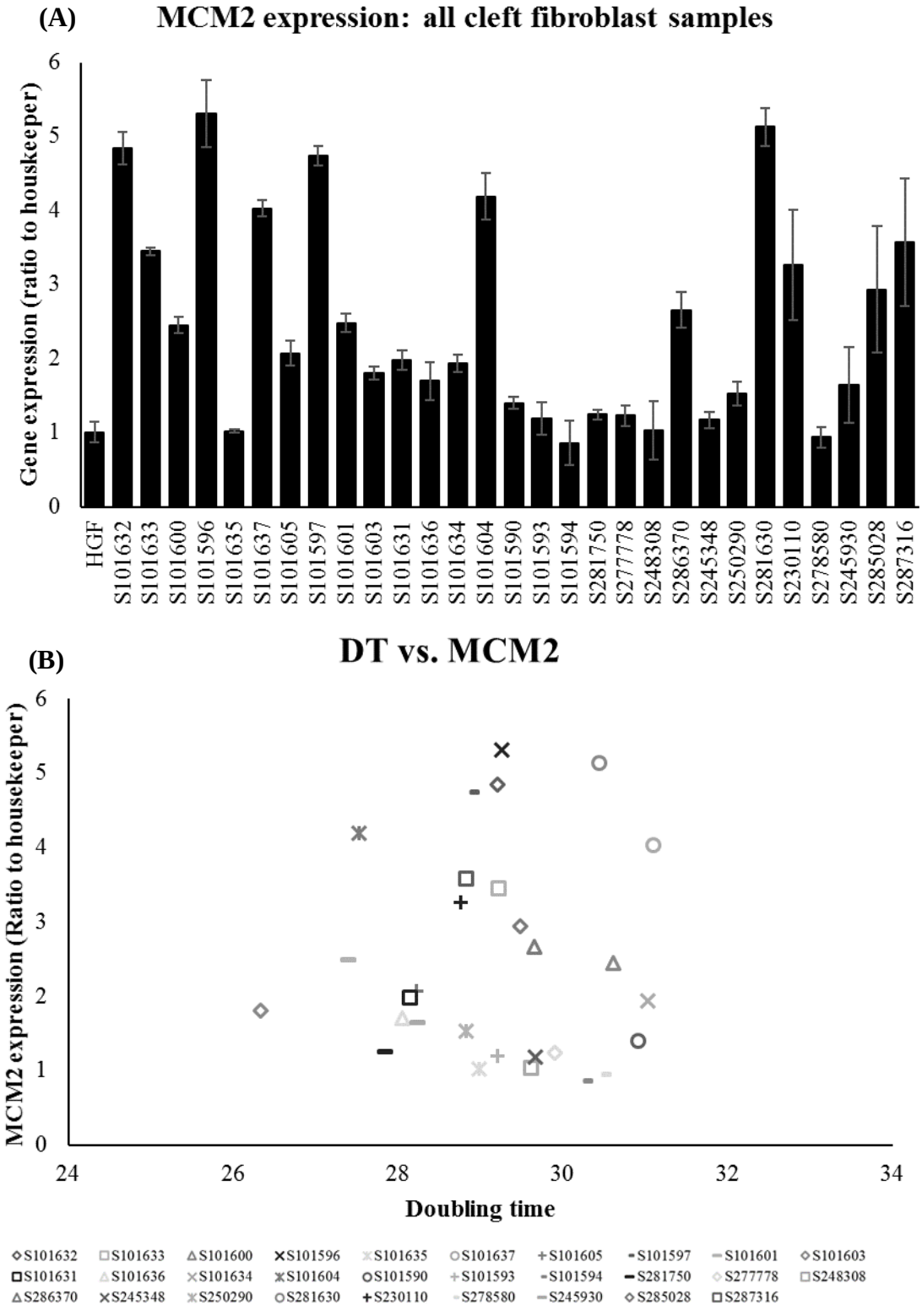

Figure 23: Gene expression for *MCM2*. (A) *MCM2* expression levels varied widely between samples with a maximum fold change of 5.74 and a minimum fold change of 0.65 but in general displayed higher expression than the HGF control. (B) Scatterplot comparing doubling times and *MCM2* expression. Based on Spearman's rho analysis there was no correlation observed between *MCM2* expression and DT (correlation coefficient = 0.093; p=0.39) (n=3).

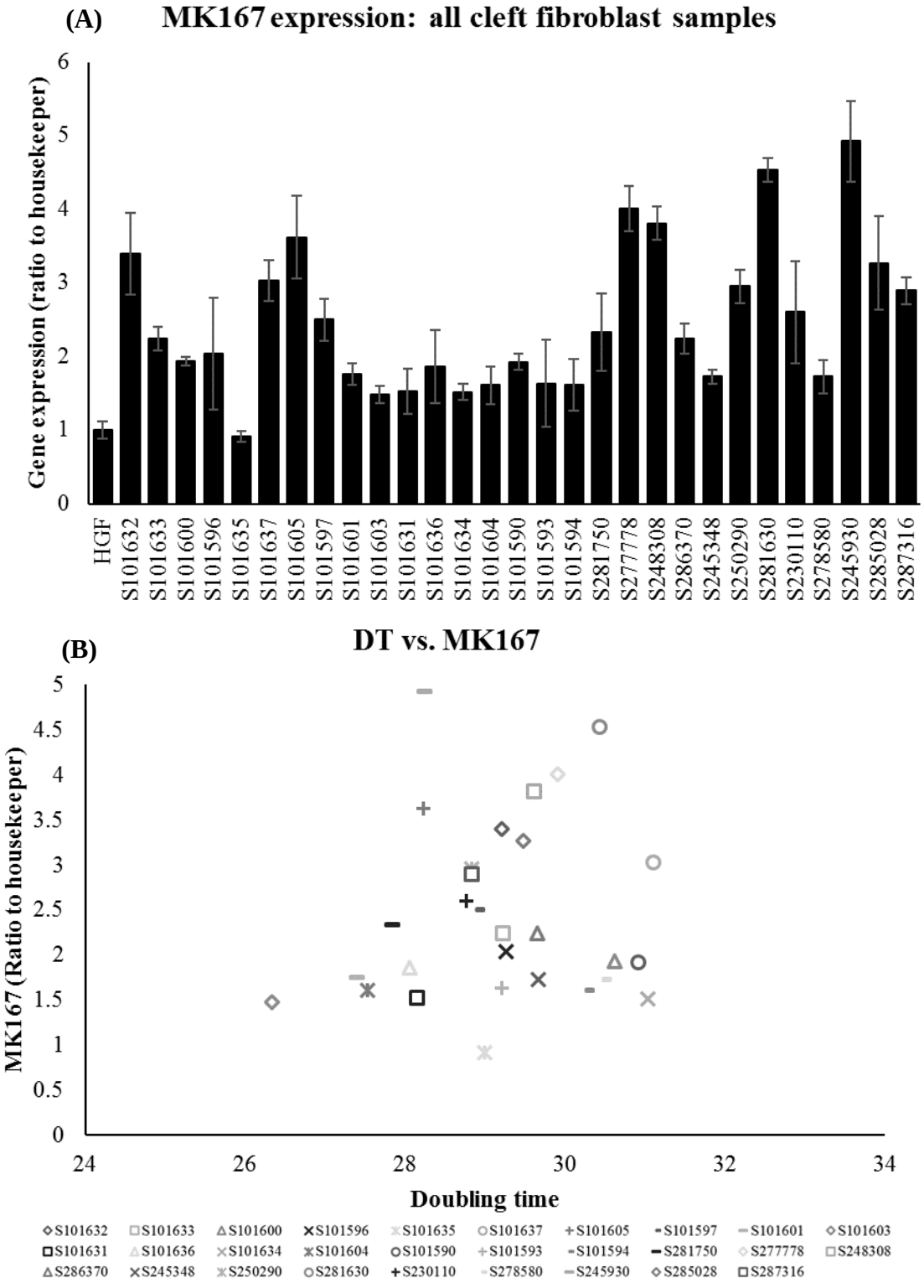

Figure 24: Gene expression for *MK167*. (A) Gene expression levels varied between patient fibroblasts with a maximum fold change of 5.47 and a minimum fold change of 0.83 although the majority of samples expressed *MK167* higher than the HG control. (B) Scatterplot comparing doubling times and *MK167* expression. Based on Spearman's rho analysis there was no correlation observed between *MK167* expression and DT (correlation coefficient = 0.115; p=0.288) (n=3).

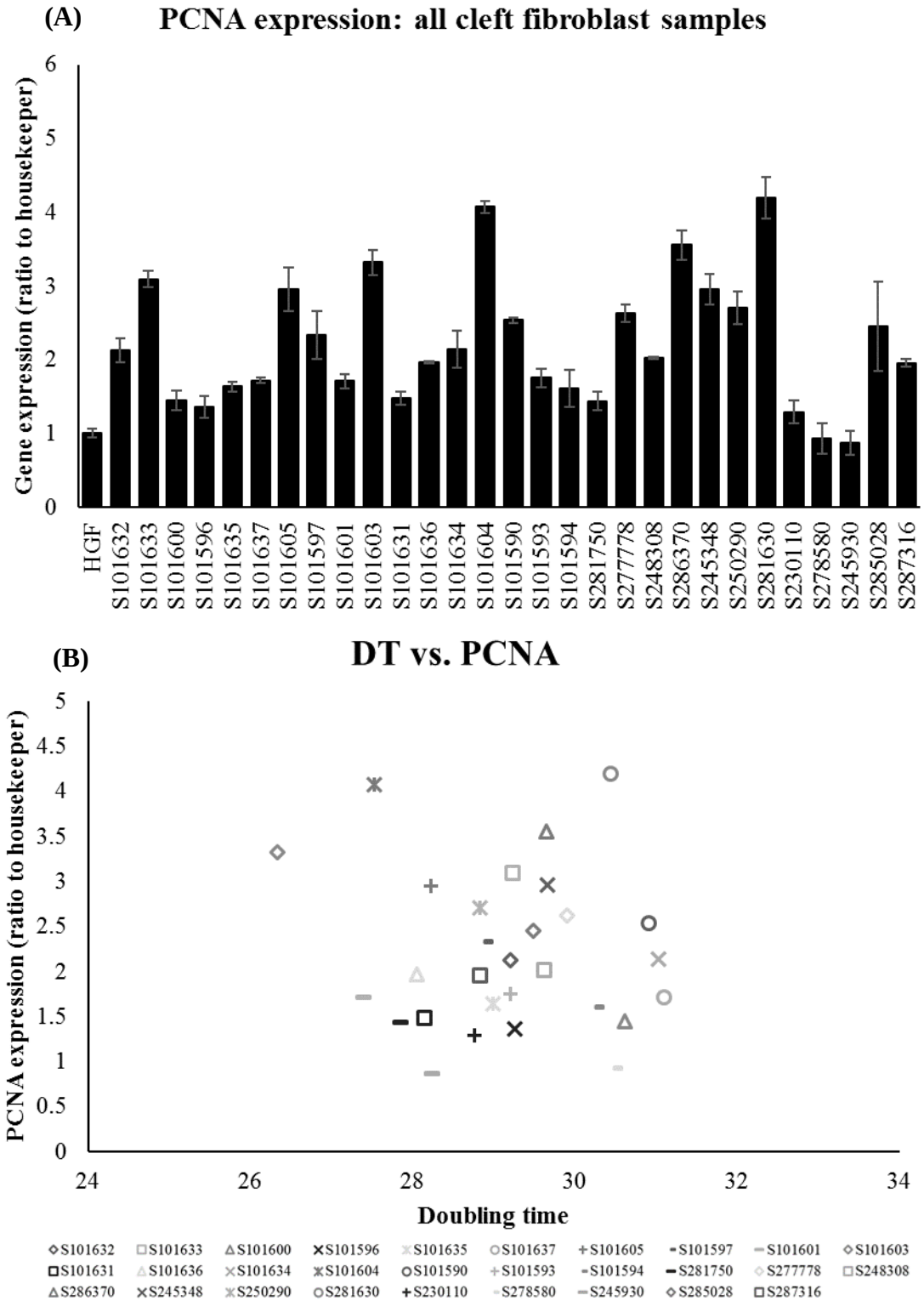

Figure 25: Gene expression for *PCNA*. (A) Gene expression varied between patient fibroblasts with a maximum fold change of 4.51 and a minimum fold change of 0.69 however most samples displayed higher *PCNA* expression relative to the HGF control. (B) Scatterplot comparing doubling times and *PCNA* expression. Spearman's rho analysis revealed there was a significant positive correlation observed between PCNA expression and DT (correlation coefficient = +0.401; $p<0.01$) (n=3).

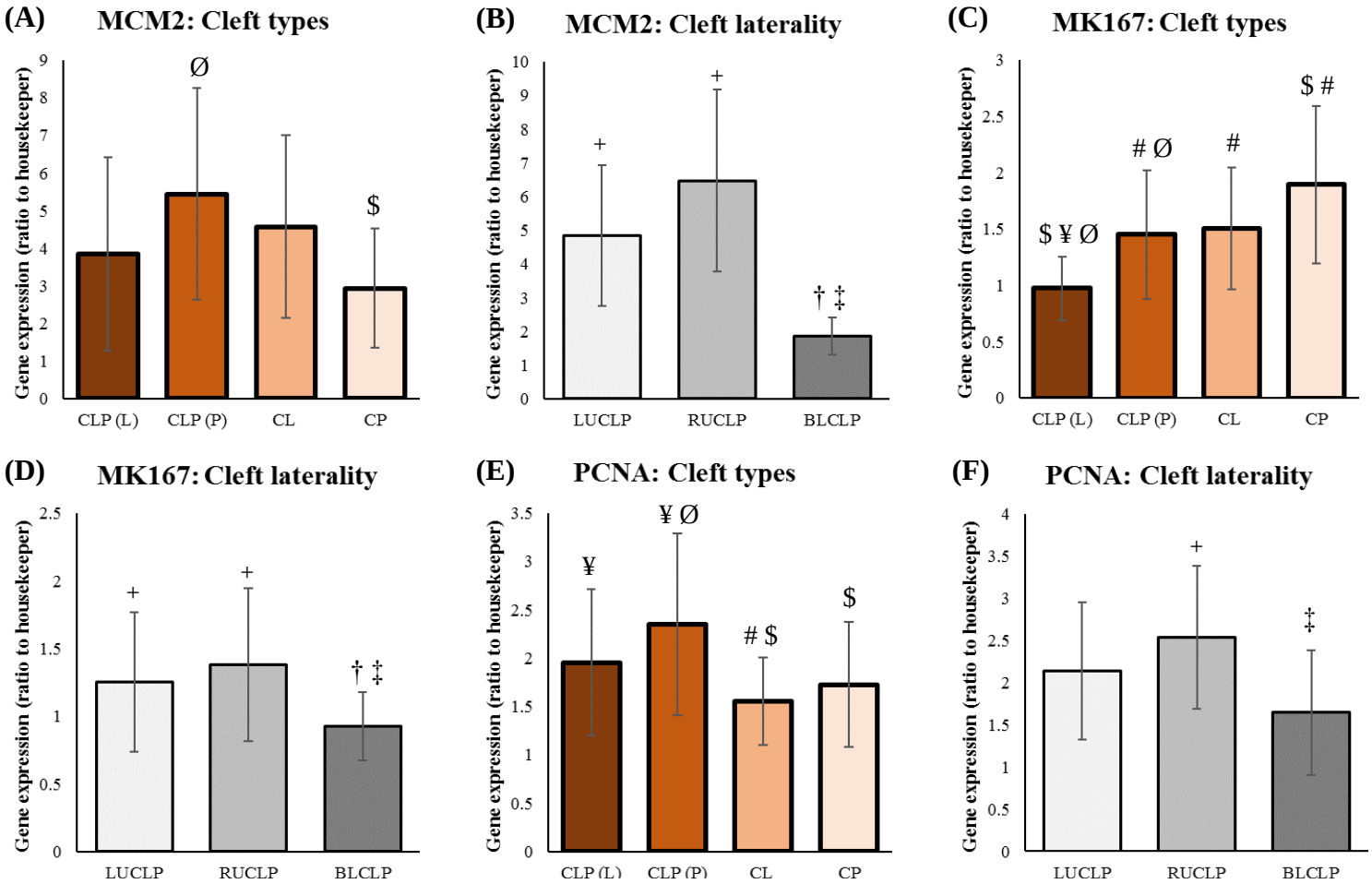

Figure 26: Average expression of proliferation associated genes between cleft types. (A) Average *MCM2* expression was significantly lower in CP fibroblasts when compared with CLP(P) fibroblasts. (B) Both LUCLP and RUCLP expression was significantly higher when compared with BLCLP. (C) Average *MK167* was significantly lower in CLP(L) when compared with CLP(P), CL and CP, CLP(P) patient expression is also significantly lower when compared with to CP. (D) *MK167* expression was also higher in LUCLP and RUCLP when compared with the BLCLP phenotype. (E) Average *PCNA* expression was higher in CLP(L) when compared with CL in isolation, in addition, CLP(P) expression was significantly higher when compared with CL and CP. (F) *MK167* expression was significantly higher in the RUCLP when compared with BLCLP. Data sets comprised of averaged data derived from all samples within the patient cohort that manifested a specific cleft phenotype. Gene expression values are calculated as fold changes in expression ratios relative to the HGF control. On the above graphs, cleft phenotypes were compared to each other individually, as opposed to a control with a single data point, in order to comparatively assess expression between cleft phenotypes. Significant differences were determined by means of student's t-test where: # = $p<0.05$ relative to CLP(L) (n=27); $ = $p<0.05$ relative to CLP(P) (n=27); ¥ =$p<0.05$ relative to CL (n=18); Ø = $p<0.05$ relative to CP (n=15); † = $p<0.05$ relative to LUCLP (n=18); ‡ = $p<0.05$ relative to RUCLP (n=21) and + = $p<0.05$ relative to BLCLP (n=15).

3.3.2 Hierarchical cluster analysis

Hierarchical clustering, which groups data based on statistical similarity, was used to group cleft patient derived fibroblasts based on the data relating to cell growth, namely: growth curve data, DT, MTT absorbance at day four, *MCM2* expression, *MK167* expression and *PCNA* expression. The resulting dendrogram revealed a data outlier, fibroblasts derived from patient S101603, which was significantly different from the rest of the cohort (cluster B) while the remaining samples (cluster A), split into two further clusters at a squared Euclidean distance of 9: groups C with 13 samples and group D with 15 samples. Both groups contain fibroblasts derived from each cleft type; group C contains 13 samples with: 4 CLP(L), 2 CLP(P), 4 CL and 3 CP; group D contains 15 samples with: 5 CLP(L), 6 CLP(P), 2 CL and 2 CP (Figure 27). However, there was a larger proportion of CLP(P) in cluster C (6) when compared with to cluster D (2). This clustering suggests that cleft fibroblasts display a high degree of similarity, in terms of proliferation associated data, and do not differ significantly based on the cleft phenotype of the patients from which they were isolated.

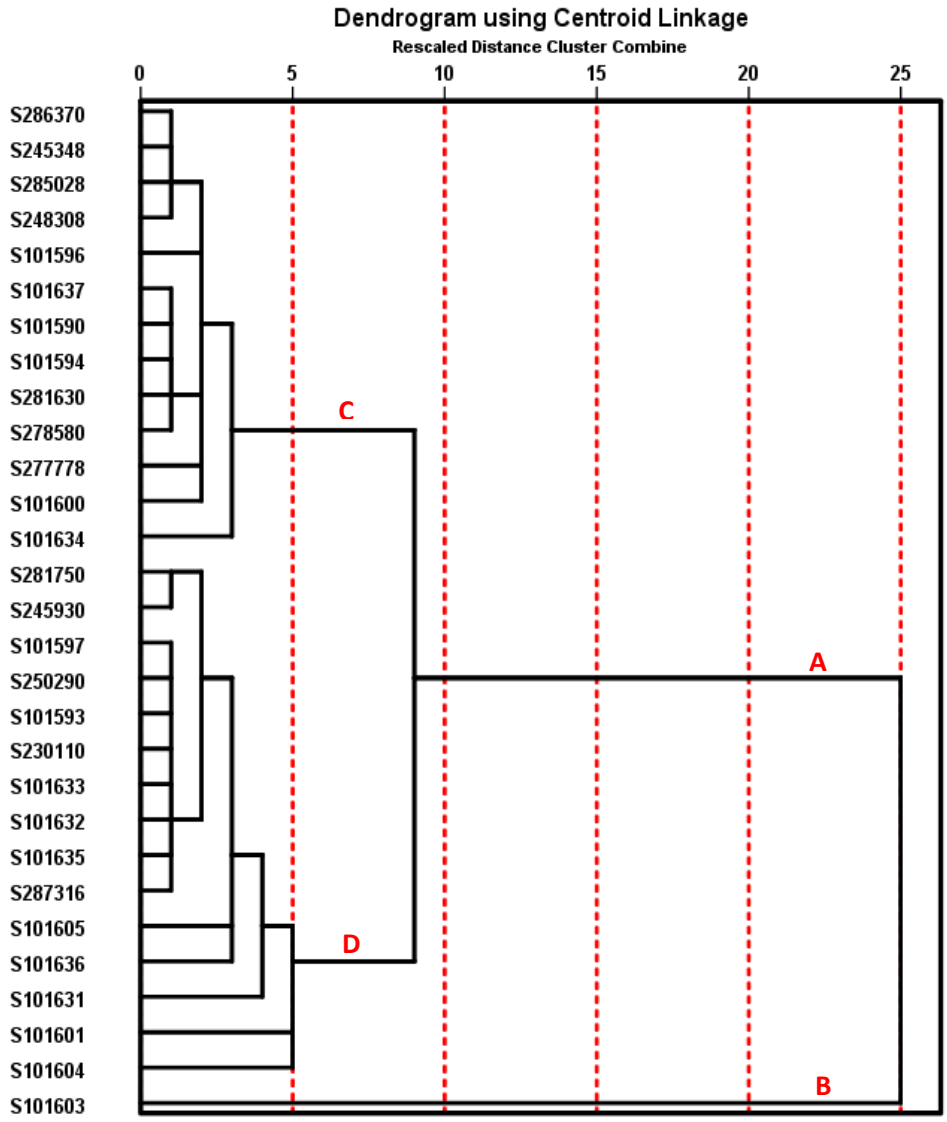

Figure 27: Dendrogram grouping patient fibroblasts following input of all cell growth and gene expression data. Hierarchical cluster analysis was employed to group samples based on growth curve data, DT, MTT absorbance at day four, *MCM2* expression, *MK167* expression and *PCNA* expression. The number of clusters were not predetermined thus cluster membership was based on the data alone. The clustering method employed was the centroid method and the data was measured using the squared Euclidean distance interval. The dendrogram revealed the presence of two statistically distinct clusters; group A comprising of 28 samples and group B comprising of a single outlier. Group A bifurcates further but at a much smaller distance of 9 indicating the two groups share considerable similarity; group C comprises of 13 samples whereas group D comprises of 15 samples.

3.4 Analysis of collagen production for all cleft patients

Collagens are major structural proteins within developing embryological tissues as they permit ECM homeostasis, provide mechanical tissue stability and act as major scaffolds for cell adhesion and motility thereby permitting normal cellular activity. Further, it has been suggested collagen synthesis is critical to normal reorientation of the developing palatal shelves (Ben-Khaial and Shah, 1994), thus collagen production and expression was assessed across the patient cohort in order to determine whether collagen synthesis may be a contributory factor in cleft phenotype manifestation. Sirius red staining was used to quantify the total collagen production for each cleft patients' fibroblasts following 7 days in culture. The mean collagen production across all 29 patients' fibroblasts was 167.98µg however; there was some variation across with the highest total collagen production of 218.82µg and the lowest 136.73µg (Figure 28A). In order to establish whether the differences in collagen production were due to different cleft types, the data from each cleft type was grouped and plotted as an average. CLP(L) and CL fibroblasts produced similar amounts of collagen whilst with CLP(P) and CP derived fibroblasts shared similar levels of collagen production; this suggests collagen production may differ based on the anatomical origin of fibroblasts. CLP(P) and CP cleft phenotypes produced significantly lower amounts of collagen than the CLP(L) fibroblasts and CL fibroblasts respectively ($p<0.05$ and $p<0.05$) (Figure 28B). However, when comparing collagen production in CLP fibroblasts with varying laterality there were no significant differences in collagen production (Figure 28C).

3.4.1 Analysis of collagen expression for all cleft patients

Collagen expression by fibroblasts derived from differing cleft types was assessed. There was some variation in *COL1A1*expression across the sample cohort with a maximum 2.24-fold and a minimum fold change of 0.48-fold (Figure 29A). On average fibroblasts from the CL

phenotype expressed significantly higher levels of *COL1A1* when compared with CLP(P) and CP ($p<0.05$) but not CLP(L). However, CLP(L) fibroblasts displayed significantly higher expression of *COL1A1* when compared with the CP phenotype ($p<0.05$) (Figure 29B). CLP clefts with varying laterality expressed COL1A1 at similar levels with no significant differences between groups (Figure 29C).

COL3A1 expression was variable with a number of fibroblasts expressing *COL3A1* at levels similar to that of the HGF control whilst others displayed expression levels that were significantly higher suggesting patient derived fibroblasts may differ in production of collage type-3. The highest expression was 4.39-fold whereas the lowest was 0.75-fold (Figure 30A). When comparing cleft types, fibroblasts from CL patients expressed significantly lower levels of COL3A1 when compared with fibroblasts from CLP(L) and CLP(P) ($p<0.05$) but not CP (Figure 30B) suggesting when cleft lip and palate manifest together fibroblast expression of *COL3A1* may be upregulated. Further, when comparing cleft laterality, it was found that fibroblasts from patients with the RUCLP phenotype expressed significantly lower amounts of *CLO3A1* when compared with both LUCLP and BLCLP ($p<0.05$) (Figure 30C).

COL5A1 expression varied widely between patient derived fibroblasts but all each sample expressed *COL5A1* in amount greater than the control with a maximum of 12.19-fold and a minimum of 2.84-fold (Figure 31). When comparing cleft types, it was found that CLP(P) fibroblasts expressed significantly lower levels of *COL5A1* when compared with both CLP(L) and C ($P<0.05$). In addition, RUCLP clefts expressed significantly lower levels of *COL5A1* when compared with both LUCLP and BLCLP ($P<0.05$).

3.4.2 Correlations between collagen production and collagen expression

Collagen production, *COL1A1*, and *COL3A1* expression was not normally distributed therefore Spearman's rho test was used to compute the correlation whereas *COL5A1* data was normally

distributed therefore Pearson's correlation was the appropriate correlation test. Spearman's rho analysis revealed that there was a significant negative correlation between collagen production and *COL3A1* expression (correlation coefficient = -0.390; $p<0.01$) and a significant positive correlation between *COL1A1* expression and *COL3A1* expression (correlation coefficient = +0.226; $p<0.05$). Pearson's correlation revealed a significant positive correlation between *COL3A1* and *COL5A1* (correlation coefficient = +0.289; $p<0.05$)

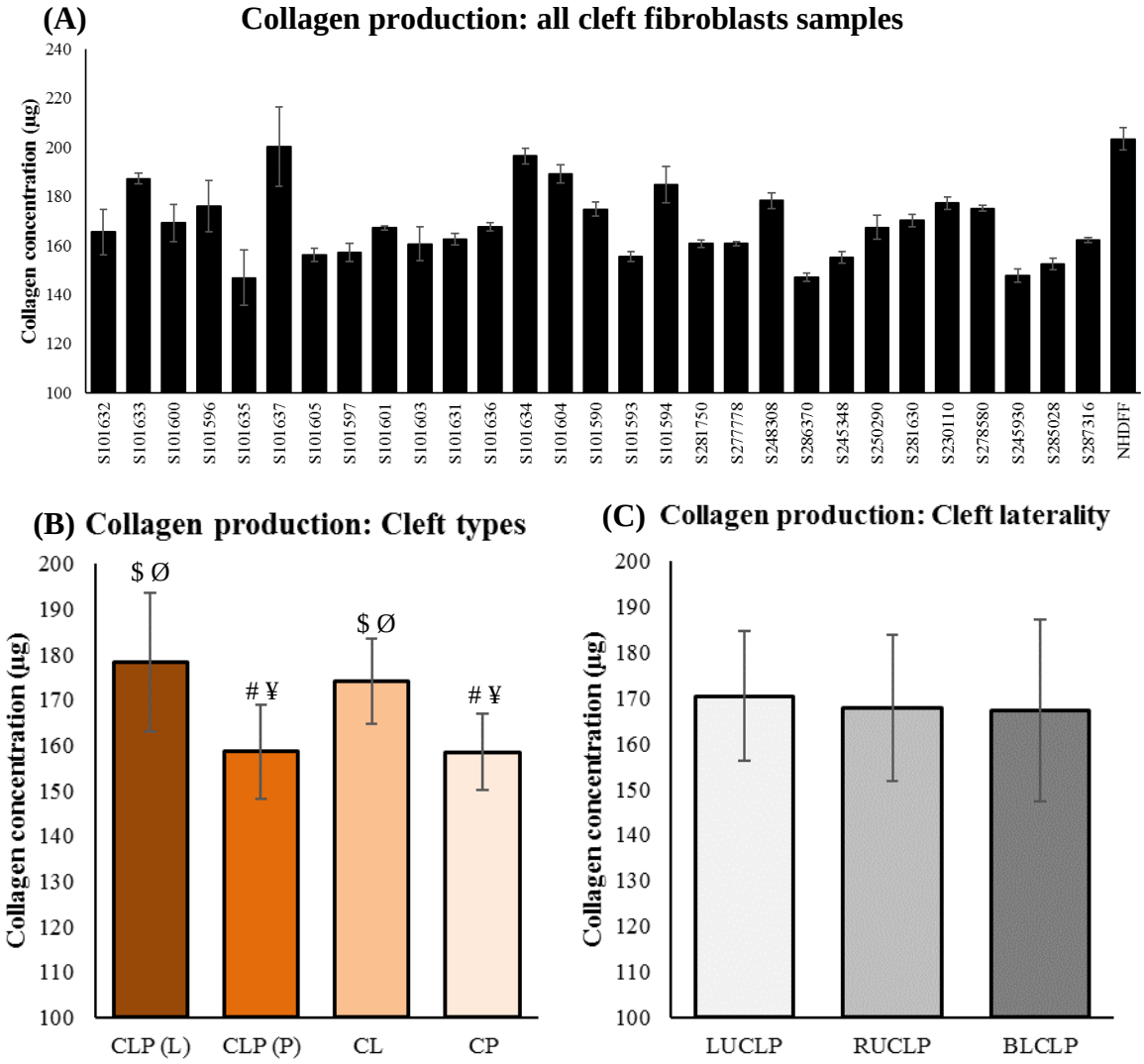

Figure 28: Quantification of collagen production. (A) Collagen production between individual patient fibroblasts was varied with the maximum collagen production was 218.82µg and the minimum was 136.73µg; NHDFF control fibroblasts produced 203.46 µg which significantly greater than the majority of the sample cohort (n=3). (B) Collagen production was significantly higher in CLP(L) and CL when compared with CLP(P) and CP. (C) There was no difference in collagen production between clefts with varying laterality. Significant differences were determined by means of student's t-tests where: # = $p<0.05$ relative to CLP(L) (n=27); $ = $p<0.05$ relative to CLP(P) (n=27); ¥ =$p<0.05$ relative to CL (n=18); Ø = $p<0.05$ relative to CP (n=15).

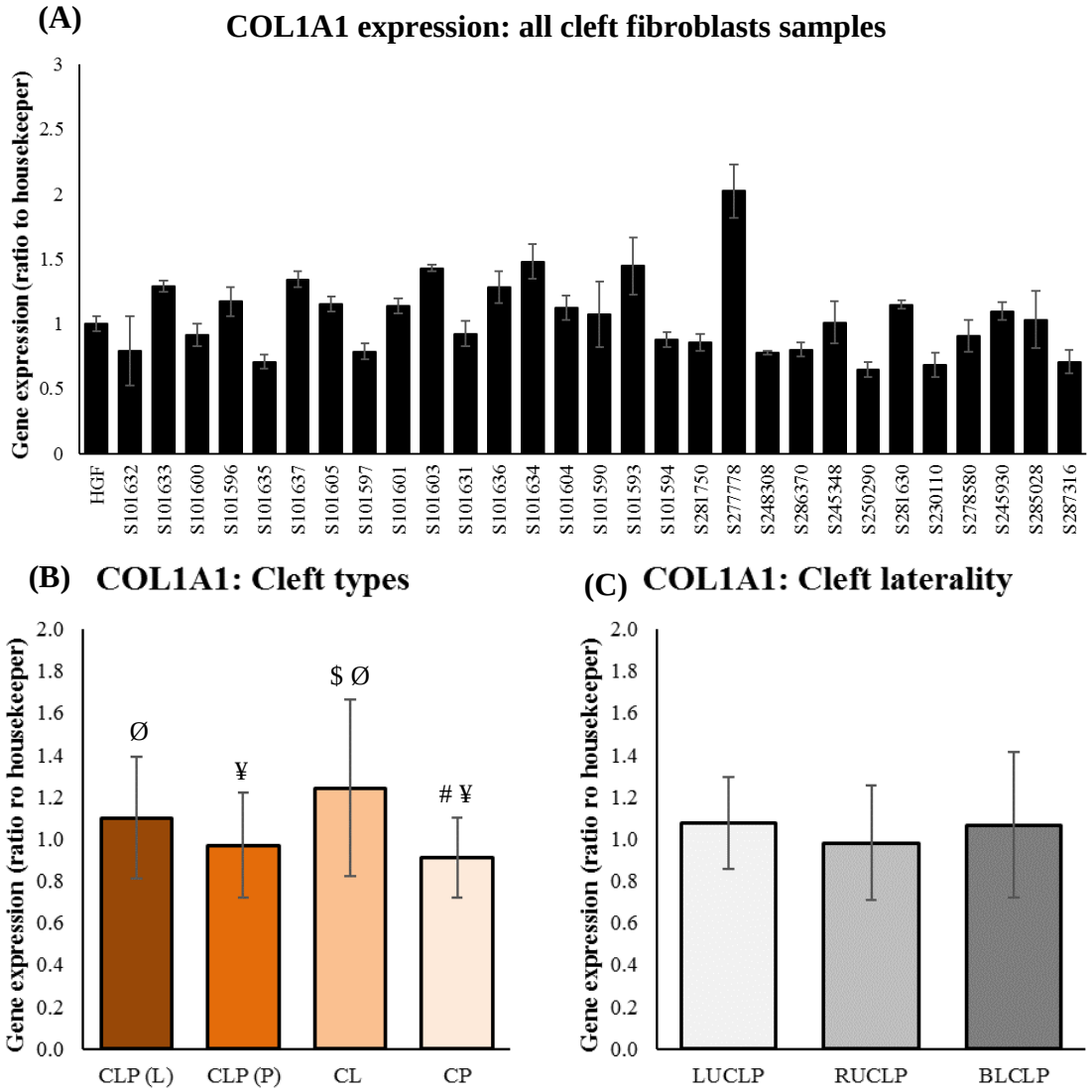

Figure 29: Gene expression of *COL1A1*. (A) Expression of *COL1A1* were similar to the HGF control for the majority of cleft fibroblasts the highest expression was 2.24-fold and lowest was 0.48-fold (n=3). (B) *COL1A1* expression was significantly higher in CL fibroblasts when compared with CLP(P) and CP groups but not CLP(L) however CLP(L) expression was shown to be significantly higher than that of CP. (C) There was no differences in *COL1A1* expression between clefts of differing laterality. Significant differences were determined by means of student's t-tests where: # = $p<0.05$ relative to CLP(L) (n=27); $ = $p<0.05$ relative to CLP(P) (n=27); ¥ =$p<0.05$ relative to CL (n=18); Ø = $p<0.05$ relative to CP (n=15).

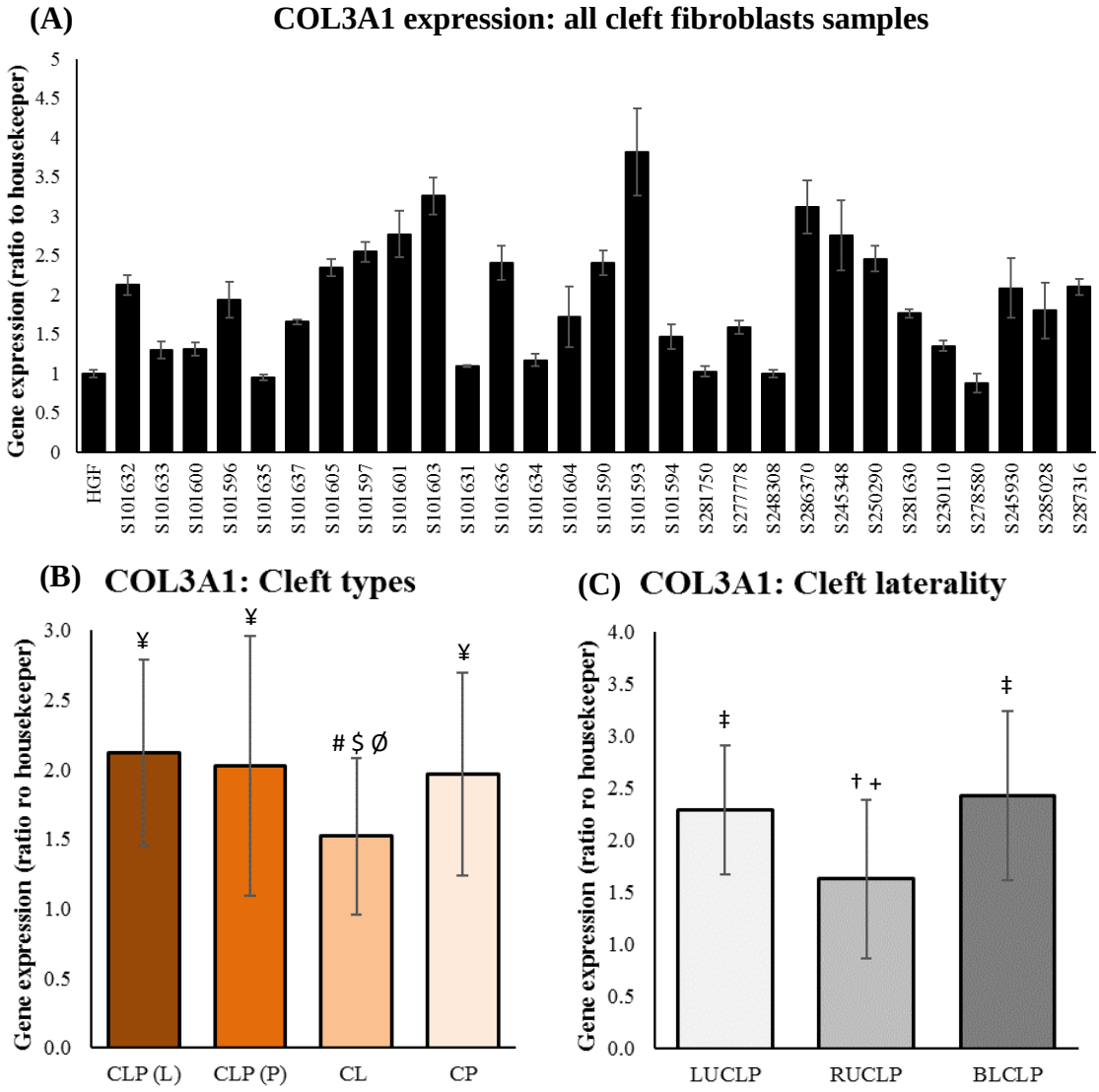

Figure 30: Gene expression of *COL3A1*. (A) A minority of fibroblasts displayed expression levels similar to that of HGF (minimum=0.75-fold) however most expressed *COL3A1* in significantly higher amounts (maximum-3.64-fold) (n=3). (B) Expression of *COL3A1* was significantly higher in both CLP(L) and CLP(P) fibroblasts when compared with CL. (C) *COL3A1* expression was significantly lower in RUCLP cleft types when compared with LUCLP and BLCLP but there was no difference between LUCLP and BLCLP. Significant differences were determined by means of student's t-tests where: # = $p<0.05$ relative to CLP(L) (n=27); $ = $p<0.05$ relative to CLP(P) (n=27); ¥ =$p<0.05$ relative to CL (n=18); Ø = $p<0.05$ relative to CP (n=15); † = $p<0.05$ relative to LUCLP (n=18); ‡ = $p<0.05$ relative to RUCLP (n=21) and + = $p<0.05$ relative to BLCLP (n=15).

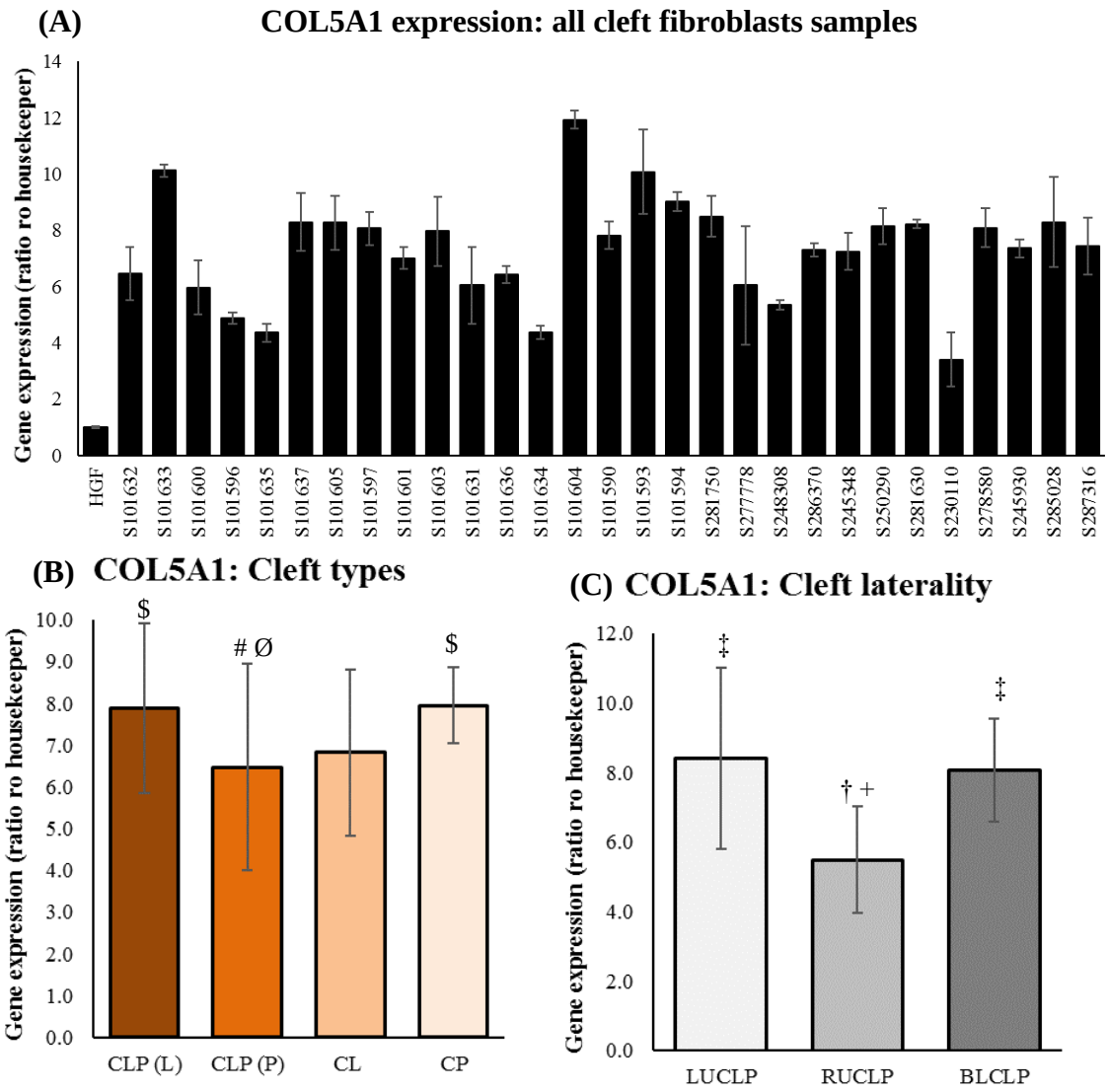

Figure 31: Gene expression of *COL5A1*. (A) Expression of *COL5A1* varied widely but all fibroblasts exhibited expression significantly higher than that of the HGF control as the minimum was 2.84-fold and the maximum was 12.19-fold. (n=3). (B) *COL5A1* expression of CLP(P) was significantly lower than both CP and CLP(L) but not CL. (C) RUCLP expression of *COL5A1* was shown to be significantly lower than both LUCLP and BLCLP. Significant differences were determined by means of student's t-tests where: # = $p<0.05$ relative to CLP(L) (n=27); $ = $p<0.05$ relative to CLP(P) (n=27); ¥ =$p<0.05$ relative to CL (n=18); Ø = $p<0.05$ relative to CP (n=15); † = $p<0.05$ relative to LUCLP (n=18); ‡ = $p<0.05$ relative to RUCLP (n=21) and + = $p<0.05$ relative to BLCLP (n=15).

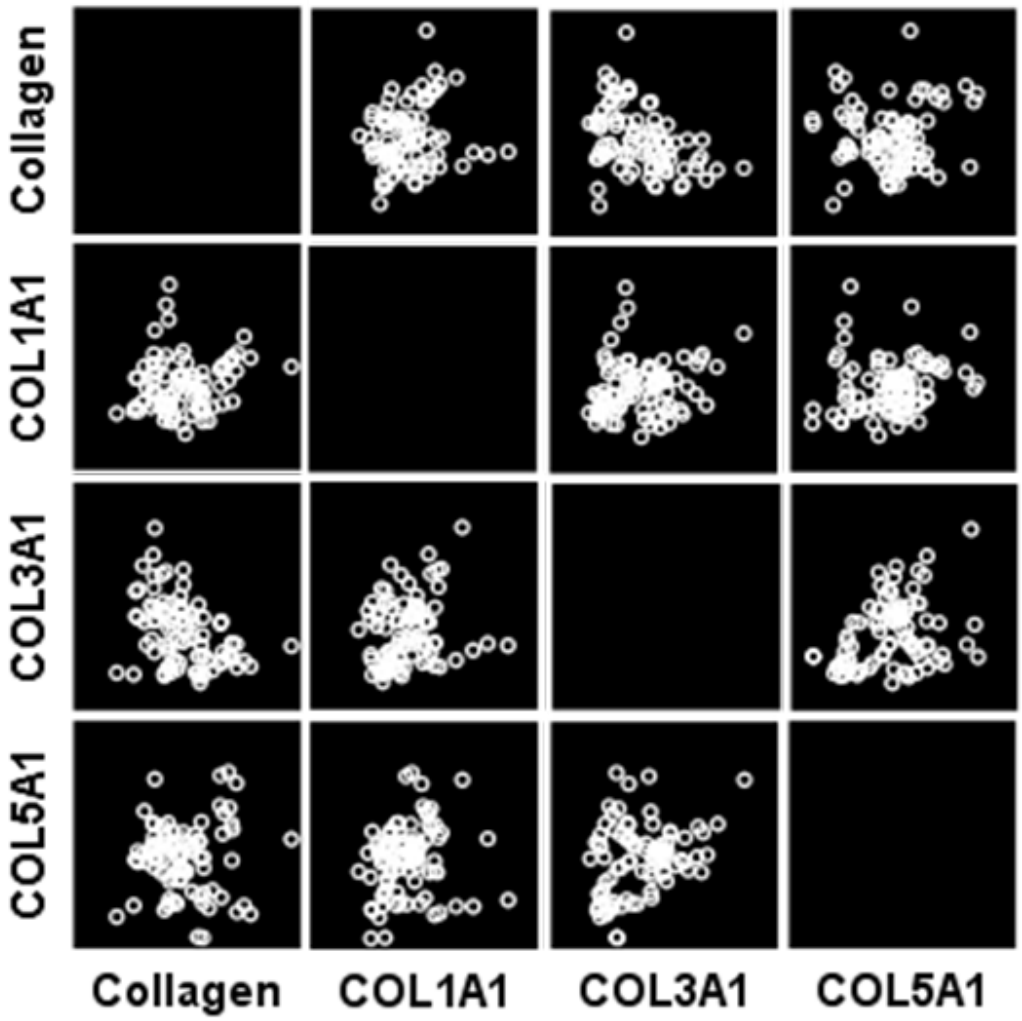

Figure 32: Scatter matrix comparing collagen production and expression of *COL1A1, COL3A1* and *COL5A1*. Shapiro-Wilk test of normality revealed the data relating to collagen production, *COL1A1* and *COL3A1* were non-parametric ($p<0.05$, $p<0.01$ and $p<0.01$ respectively) whereas data relating to *COL5A1* was parametric ($p=0.101$) thus required different tests for correlation analysis. Spearman's rho analysis revealed there was a significant negative correlation between collagen production and *COL3A1* expression (correlation coefficient = -0.390; $p<0.01$), a significant positive correlation between *COL1A1* and *COL3A1* (correlation coefficient = +0.226; $p<0.05$). Pearson correlation revealed a significant positive correlation between *COL3A1* and *COL5A1* (correlation coefficient = +0.289; $p<0.05$).

3.5 Analysis of sulphated glycosaminoglycan production

Glycosaminoglycans (GAG's) are negatively charged hydrophilic polysaccharides that contribute to tissue hydration, water retention caused by GAGs has been proposed to impart intrinsic hydrostatic force that contributes to the expansion, elevation and reorientation of the palatal shelves (Singh et al, 1994; Singh et al, 1997). Due to proposed critical role of GAGs in normal craniofacial development, GAG production and expression was assessed in populations of cleft fibroblasts to assess whether there were differences between cleft phenotypes. Alcian blue staining was utilised in order to quantify sulphated glycosaminoglycan (GAG) produced by cultures after 7 days by means of spectrophotometry. The highest absorbance observed was 0.340 whereas the lowest absorbance value observed was 0.160 (Figure 33A). Across cleft types, absorbance was averaged which revealed that the CLP(L) group produced significantly lower GAG than the CLP(P) group ($p<0.05$) whereas there were no differences with or between CL and CP groups (Figure 33B). When comparing cleft laterality, the RUCLP group had significantly higher absorbance than LUCLP and BLCLP ($p<0.05$) thereby indicating increased GAG production (Figure 33C).

3.5.1 Analysis of sulphated glycosaminoglycan expression

Expression gene transcripts associated with sulphated GAG production were assessed. *CSPG4* expression was similar across the cleft fibroblast cohort however there was some variation as the lowest expression was 0.67-fold and the highest was 2.18-fold (Figure 34A). The CLP(P) fibroblasts had significantly lower *CSPG4* expression when compared the CLP(L) and CP; it was also found that fibroblasts from CL also had significantly lower expression of *CSPG4* than fibroblasts from CP ($p<0.05$) patients (Figure 34B). When grouping fibroblasts based on cleft laterality it was found that those with RUCLP has significantly lower expression of *CSPG4* when compared with those with LUCLP and BLCLP ($p<0.05$) (Figure 34C).

DSE expression was significantly upregulated in some cleft fibroblasts with a maximum expression of 6.36-fold however a number of samples expressed *DSE* in lower amounts but still significantly higher than the control. One sample was an outlier and expressed *DSE* in amounts comparable to the HGF control, as the lowest fold change observed was 1.01-fold (Figure 35A). *DSE* expression was significantly greater in fibroblasts from CP when compared with CLP(P) and CL derived fibroblasts ($p<0.05$) (Figure 35B). *DSE* expression was also shown to be significantly lower RUCLP compared LUCLP and BLCLP ($p<0.05$) (Figure 35C).

HSPG2 was expressed in all cleft fibroblast samples in greater amounts than the HGF control as the lowest expression measured was 1.51-fold and the highest was 3.29-fold (Figure 36A). HSPG2 expression was significantly lower in CLP(P) fibroblasts when compared with both CL and CP ($p<0.05$) (Figure 36B). As seen with both *CSPG4* and *DSE* expression, fibroblasts with RUCLP cleft laterality displayed significantly lower expression of *HSPG2* when compared with both LUCLP and BLCLP (Figure 36C). This suggests that fibroblasts from RUCLP may express and produces different GAG's in higher amounts that there LUCLP and BLCLP counterpart even though Alcian blue staining suggested higher amounts of sulphated GAG were produced by RUCLP fibroblasts.

3.5.2 Correlations between GAG production and GAG expression

Scatter matrix plots and correlation analysis were conducted in order to establish how production of sulphated GAG and expression of sulphated GAG associated genes were related between cleft fibroblast samples (Figure 37). It was found that there was a significant negative correlation between Alcian blue staining and *HSPG2* expression (correlation coefficient = 0.232; $p<0.05$). Likewise, there was a significant negative correlation between Alcian blue and DSE; this suggests that the increased production of GAG in some patient samples was not due to increased expression of *DSE* and *HSPG2* and was potentially the result of *CSPG4* and other

sulphated GAGs. A positive correlation was observed between *CSPG4* and *HSPG2* (Correlation coefficient = +0.376; $p<0.01$) suggesting that it is possible that the genes are upregulated together in some cleft patients fibroblasts.

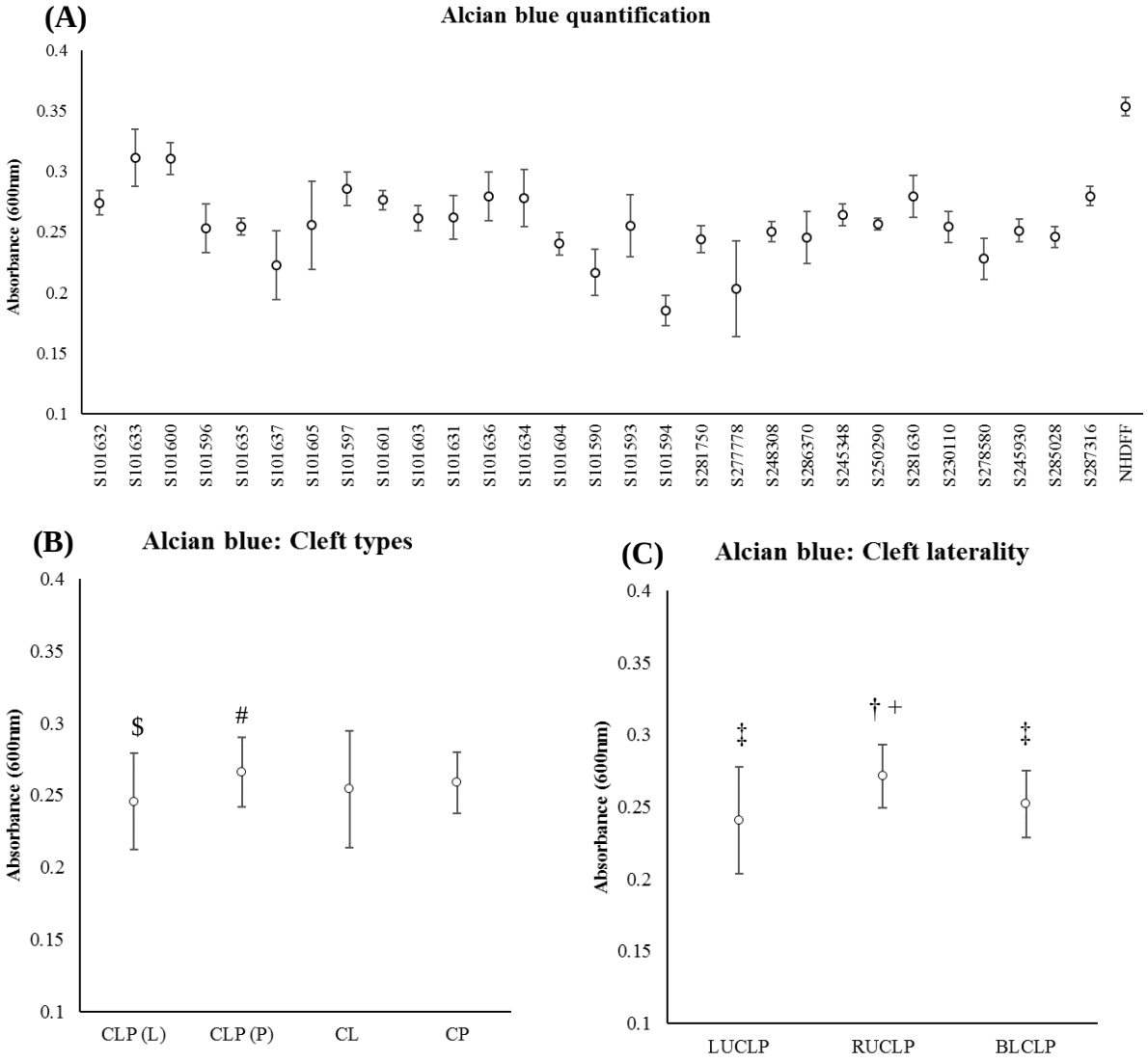

Figure 33: Alcian blue staining for sulphated glycosaminoglycans. (A) Production of glycosaminoglycans was varied with a maximum absorbance was 0.34 and a minimum of 0.16 which indicated there were large differences in GAG production between cleft fibroblasts; the NHDFF control was shown to produce significantly greater amounts of GAG when compared to all the cleft fibroblasts assessed here. (B) Absorbance was significantly higher in CLP(P) when compared with CLP(L) but there were no differences when compared with CL and CP. (C) RUCLP was shown to have significantly higher average absorbance when compared with both LUCLP and BLCLP. Significant differences were determined by means of student's t-tests where: # = $p<0.05$ relative to CLP(L) (n=27); $ = $p<0.05$ relative to CLP(P) (n=27); ¥ =$p<0.05$ relative to CL (n=18); Ø = $p<0.05$ relative to CP (n=15); † = $p<0.05$ relative to LUCLP (n=18); ‡ = $p<0.05$ relative to RUCLP (n=21) and + = $p<0.05$ relative to BLCLP (n=15).

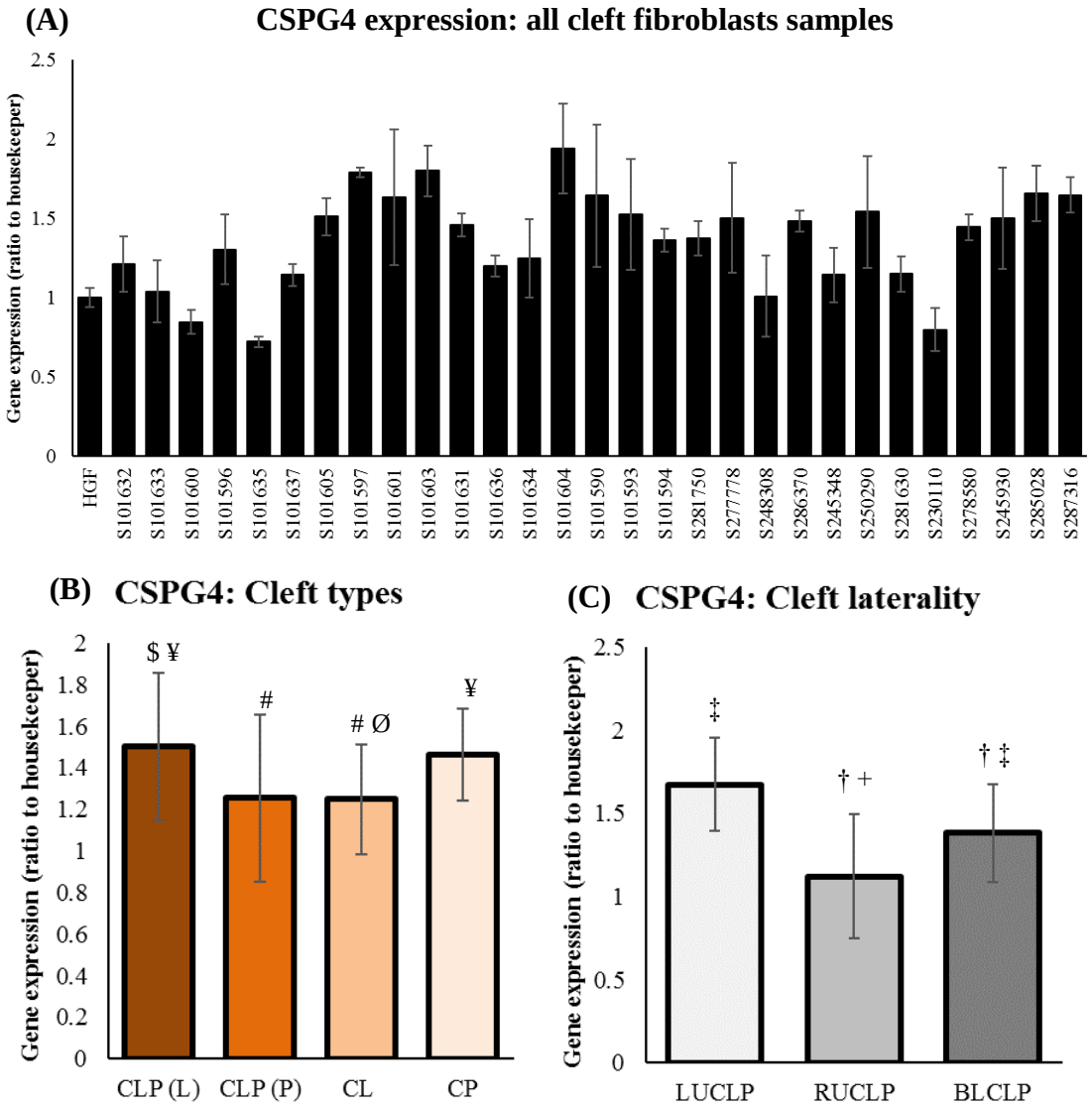

Figure 34: Gene expression of *CSPG4*. (A) Expression of *CSPG4* was similar across all cleft fibroblasts and exhibited amounts similar to that of the HGF control. (n=3). (B) *CSPG4* expression was significantly higher in CLP(L) fibroblasts when compared with both CLP(P) and CL but not CP. Further, CL expression was significantly lower than that of CP fibroblasts. (C) Expression of *CSPG4* in RUCLP fibroblasts was significantly lower than both LUCLP and BLCLP fibroblasts. Significant differences were determined by means of student's t-tests where: # = $p<0.05$ relative to CLP(L) (n=27); $ = $p<0.05$ relative to CLP(P) (n=27); ¥ =$p<0.05$ relative to CL (n=18); Ø = $p<0.05$ relative to CP (n=15); † = $p<0.05$ relative to LUCLP (n=18); ‡ = $p<0.05$ relative to RUCLP (n=21) and + = $p<0.05$ relative to BLCLP (n=15).

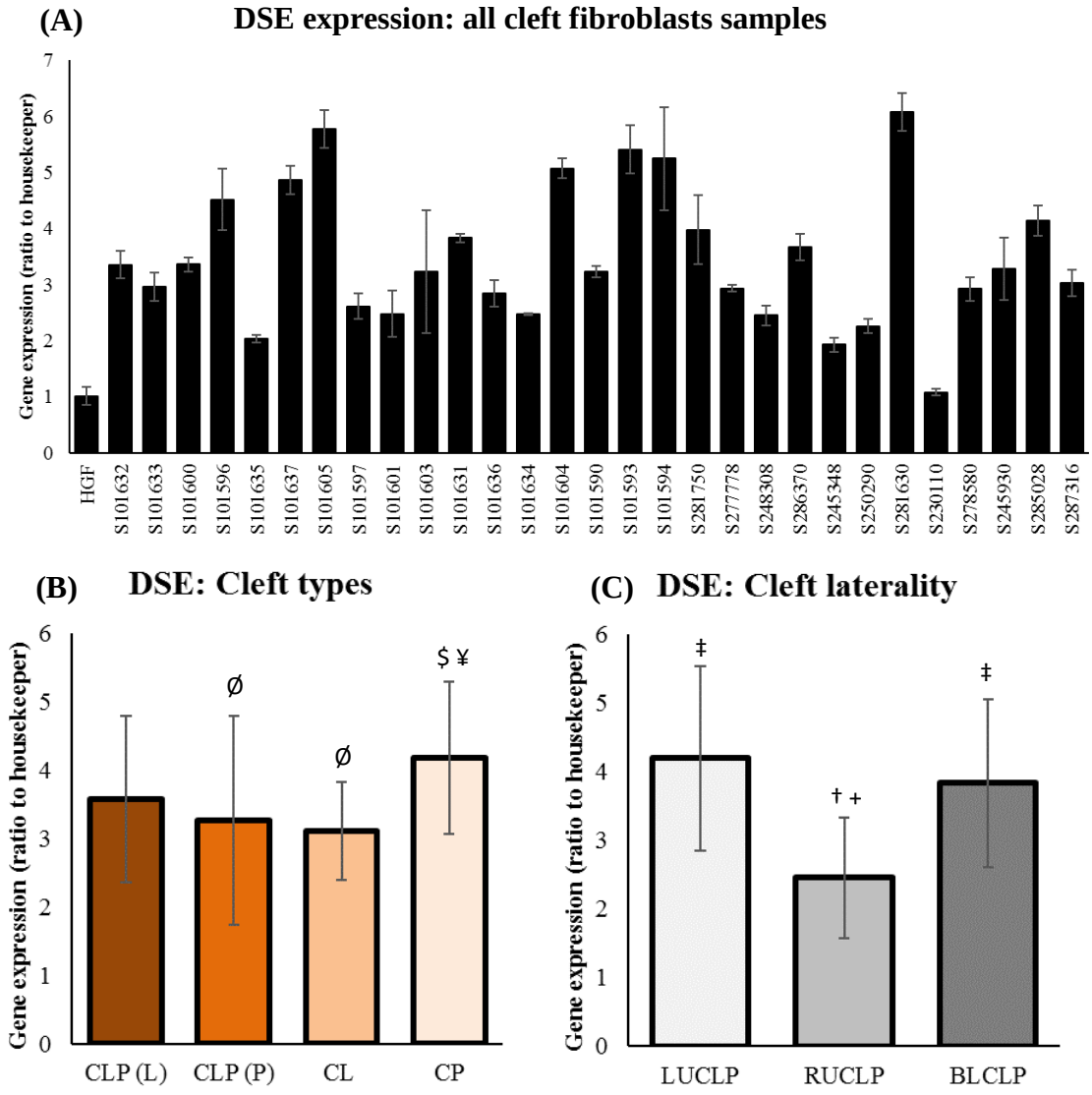

Figure 35: Gene expression of *DSE*. (A) Expression levels of *DSE* was variable across the patient cohort however most fibroblasts exhibited expression levels higher than that of the HGF control (n=3). (B) Fibroblasts from the CP phenotypes displayed significantly higher levels of expression of *DSE* when compared with both CLP(P) and CL but not CLP(L). (C) *DSE* expression was shown to be significantly lower in RUCLP fibroblasts when compared with both BLCLP and LUCLP. Significant differences were determined by means of student's t-tests where: # = $p<0.05$ relative to CLP(L) (n=27); $ = $p<0.05$ relative to CLP(P) (n=27); ¥ =$p<0.05$ relative to CL (n=18); Ø = $p<0.05$ relative to CP (n=15); † = $p<0.05$ relative to LUCLP (n=18); ‡ = $p<0.05$ relative to RUCLP (n=21) and + = $p<0.05$ relative to BLCLP (n=15).

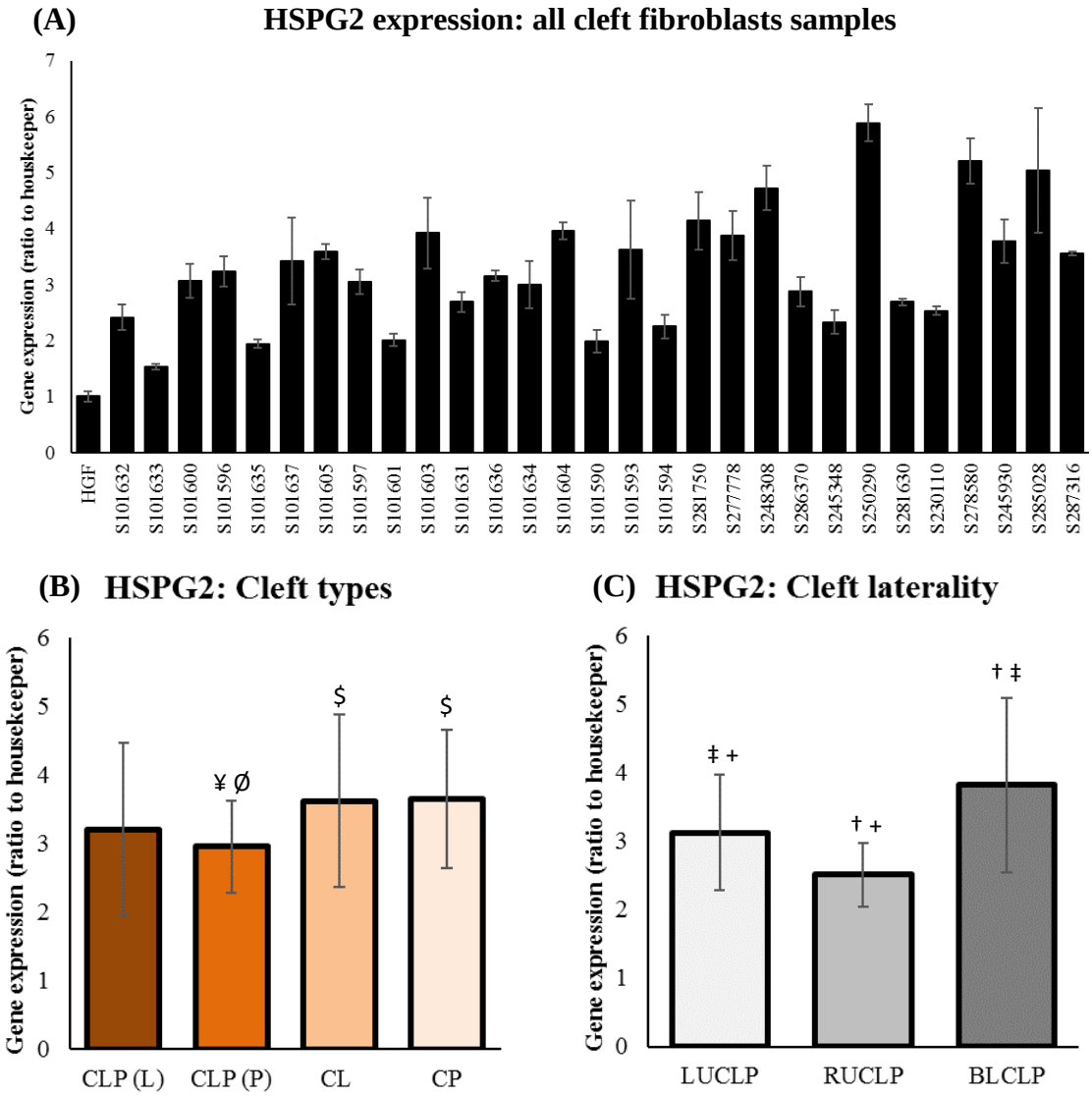

Figure 36: Gene expression of *HSPG2*. (A) Expression levels of *HSPG2* were highly variable across the patient cohort however all samples exhibited expression levels higher than that of the HGF control. (n=3). (B) CLP(P) fibroblasts exhibited significantly lower average expression of *HSPG2* when compared with both CL and CP but not CLP(L). (C) RUCLP fibroblasts had significantly lower average expression of *HSPG2* when compared with both LUCLP and BLCLP. Significant differences were determined by means of student's t-tests where: # = $p<0.05$ relative to CLP(L) (n=27); $ = $p<0.05$ relative to CLP(P) (n=27); ¥ =$p<0.05$ relative to CL (n=18); Ø = $p<0.05$ relative to CP (n=15); † = $p<0.05$ relative to LUCLP (n=18); ‡ = $p<0.05$ relative to RUCLP (n=21) and + = $p<0.05$ relative to BLCLP (n=15).

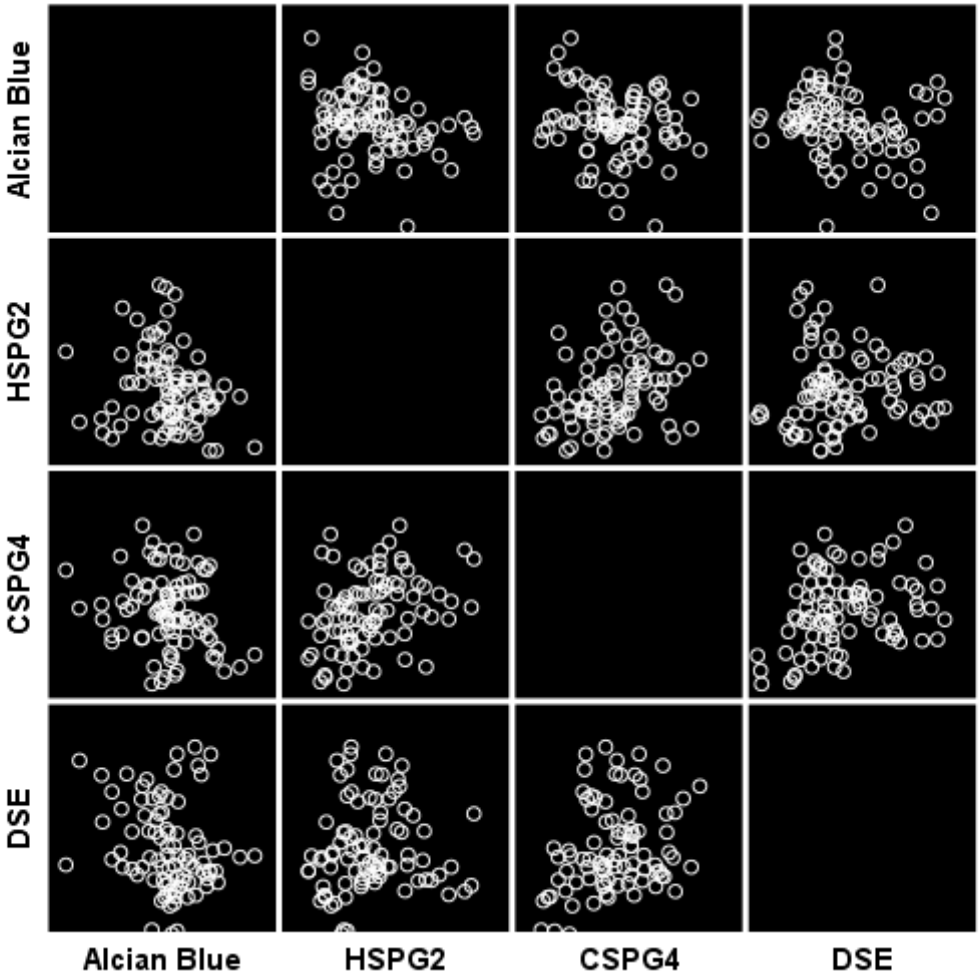

Figure 37: Scatter matrix comparing Alcian blue quantification and expression of *HSPG2, CSPG4* and *DSE*. Shapiro-Wilk test of normality revealed the data relating to Alcian blue quantification and *CSPG4* expression was parametric (p=1.49 and p=0.606 respectively) whereas data relating to *HSPG2* and *DSE* was non parametric ($p<0.01$ and $p<0.01$ respectively) thus required differing test for correlational analysis. Pearson correlation revealed a slight negative correlation between Alcian blue and *CSPG4* though (correlation coefficient= -0.179; p= 0.098). Spearman's rho analysis revealed a significant negative correlation between Alcian blue and *HSPG2* expression (correlation coefficient = 0.232; $p<0.05$) and a significant negative correlation between *DSE* and Alcian blue staining (correlation coefficient = -0.241 ($p<0.05$). Further, a significant positive correlation was observed *HSPG2* and *CSPG4* (Correlation coefficient = +0.376; $p<0.01$).

3.6 Expression of FN1 by cleft fibroblasts

FN1 expression was highly variable as the highest expression observed was 15.49-fold and the lowest was 3.22-fold, this suggested that in general cleft fibroblasts may produce fibronectin in higher amounts than their non-cleft NHDFF counterparts (Figure 38A). When patient expression was grouped based on cleft type it was found that CL fibroblasts expressed significantly lower amounts of *FN1* when compared with CLP(L) and CLP(P) ($p<0.05$) Further, CP fibroblasts expressed significantly lower *FN1* when compared with both CLP(P) and CLP(L); there was no difference between CLP(L) and CLP(P) or CL and CP (Figure 38B). This suggests cleft fibroblast fibronectin production may be significantly higher when cleft lip and palate manifest in conjunction as opposed to their isolated counterparts. When comparing cleft laterality, it was again found that clefts that were RUCLP expressed significantly lower amounts of *FN1* than both LUCLP and BLCLP ($p<0.05$), this suggests that RUCLP derived fibroblasts may produce fibronectin lower amounts than both LUCLP and BLCLP derived fibroblasts (Figure 38C).

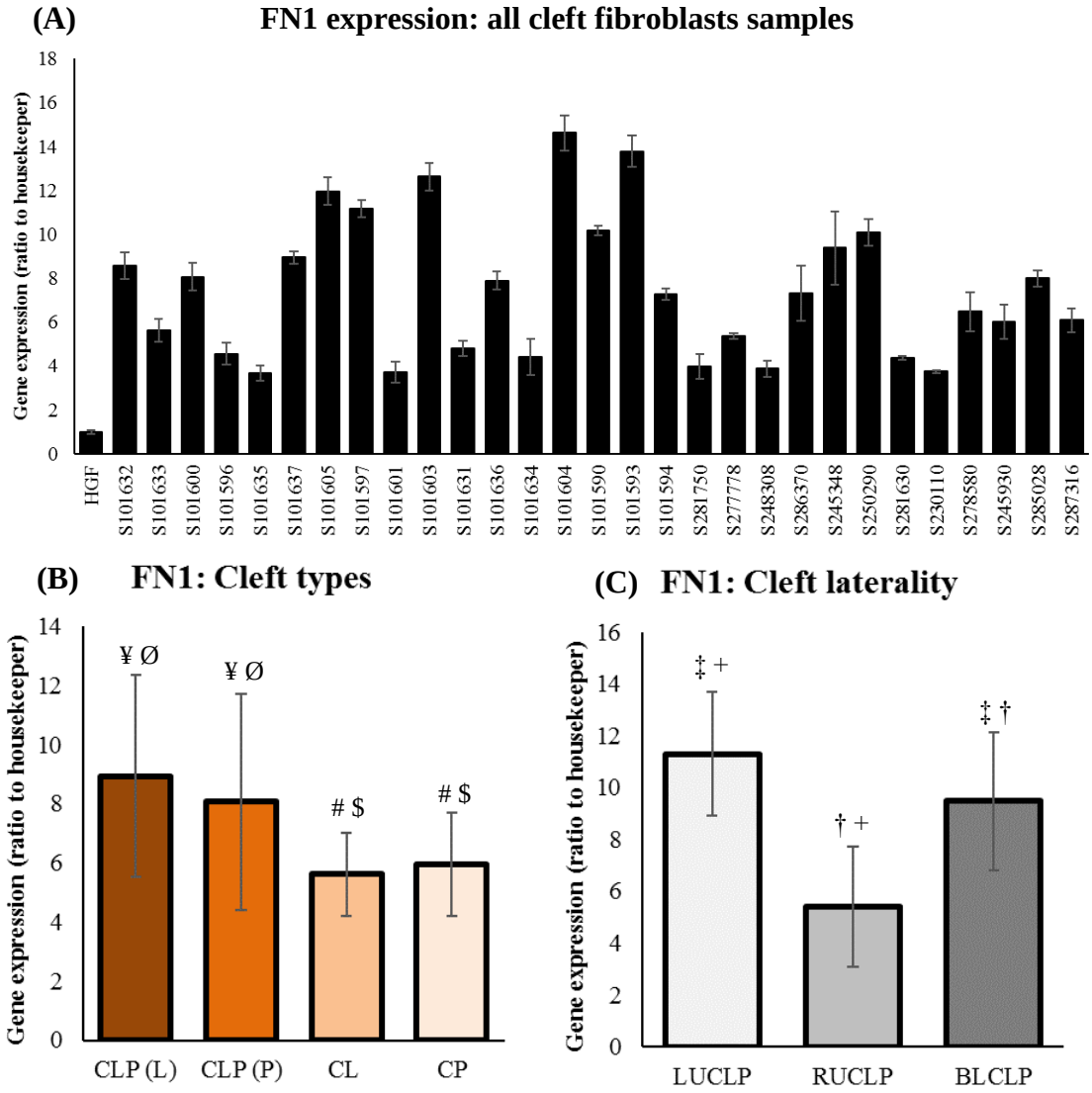

Figure 38: Gene expression of *FN1*. (A) Expression of *FN1* was highly variable across cleft fibroblast samples however samples exhibited expression in greater amounts than that of the HGF control as the maximum fold change was 15.49 and a minimum of 3.22 (n=3). (B) *FN1* expression was significantly higher in CLP(L) fibroblasts when compared with both CL and CP ($p<0.05$). In addition, CLP(P) fibroblasts also exhibited significantly higher expression of *FN1* when compared with CL and CP; there was no differences between CLP(L) and CLP(P). (C) RUCLP fibroblasts exhibited significantly lower average expression of *FN1* when compared with LUCLP and BLCLP. However, LUCLP fibroblasts had significantly higher expression of *FN1* when compared with both RUCLP and BLCLP. Significant differences were determined by means of student's t-tests where: # = $p<0.05$ relative to CLP(L) (n=27); $ = $p<0.05$ relative to CLP(P) (n=27); ¥ =$p<0.05$ relative to CL (n=18); Ø = $p<0.05$ relative to CP (n=15); † = $p<0.05$ relative to LUCLP (n=18); ‡ = $p<0.05$ relative to RUCLP (n=21) and + = $p<0.05$ relative to BLCLP (n=15).

3.7 Expression of Transforming Growth Factor betas

The TGF superfamily are a group of cytokines that can regulate processes such as: cell recruitment, proliferation, ECM deposition, differentiation and apoptosis (Penn et al, 2012), all of which are key to normal craniofacial development. TGFβ1, TGFβ2, and TGFβ3, have all been shown to be expressed either within the epithelium of the palatal shelves or the underlying mesenchyme where they are thought to play critical roles in palatal growth, fusion and epithelial-to-mesenchymal transition (EMT) of the medial edge epithelium (MEE) (Pelton et al, 1990; Kaartinen et al, 1997; Nawshad et al, 2004). Due to the elevation in expression of various TGFβs in key craniofacial structures during development coupled with their potent effects on cell behaviour, the expression of a number TGFβs, and their associated receptors, was assessed to establish potential differences in expression profiles between cleft phenotypes.

Expression of *TGFB1* was highly variable across the sample cohort as a number of samples upregulated *TGFB*1 whilst others were downregulated relative to the control; the maximum expression was 6.60-fold and the minimum was 0.51-fold. This sample variation this did not correlate with cleft type as there were no significant differences in *TGFB1* expression between cleft types. However, there were significant differences between cleft fibroblasts derived from differing cleft literalities as LUCLP fibroblasts had significantly higher average expression when compared with both RUCLP ($0<0.001$) and BLCLP ($p<0.05$) (Figure 39A-C). Expression of *TGFB2* was also highly variable but all samples expressed *TGFB2* in significantly higher amounts than the control. Some samples exhibited *TGFB2* in significantly higher amounts than the overall sample mean as the highest expression observed was 16.34-fold whereas the lowest was 1.92-fold thereby indicating large disparities between cleft fibroblasts. This variability did correlate to some degree with cleft type as *TGFB2* expression was significantly greater in fibroblasts isolated from CLP(L) compared with CLP(P) ($p<0.05$). Further RUCLP fibroblasts

displayed significantly lowered expression when compared with LUCLP ($p<0.05$) and BLCLP ($p<0.001$) (Figure 40A-C). Expression of *TGFB3* was also variable, however a number of samples displayed expression comparable with the control although the maximum expression was 6.48-fold and the minimum was 0.64-fold. These differences in *TGFB3* expression between samples were not based on cleft type or laterality though there was a significant difference in expression between CLP(L) and CP fibroblasts (Figure 41A-C).

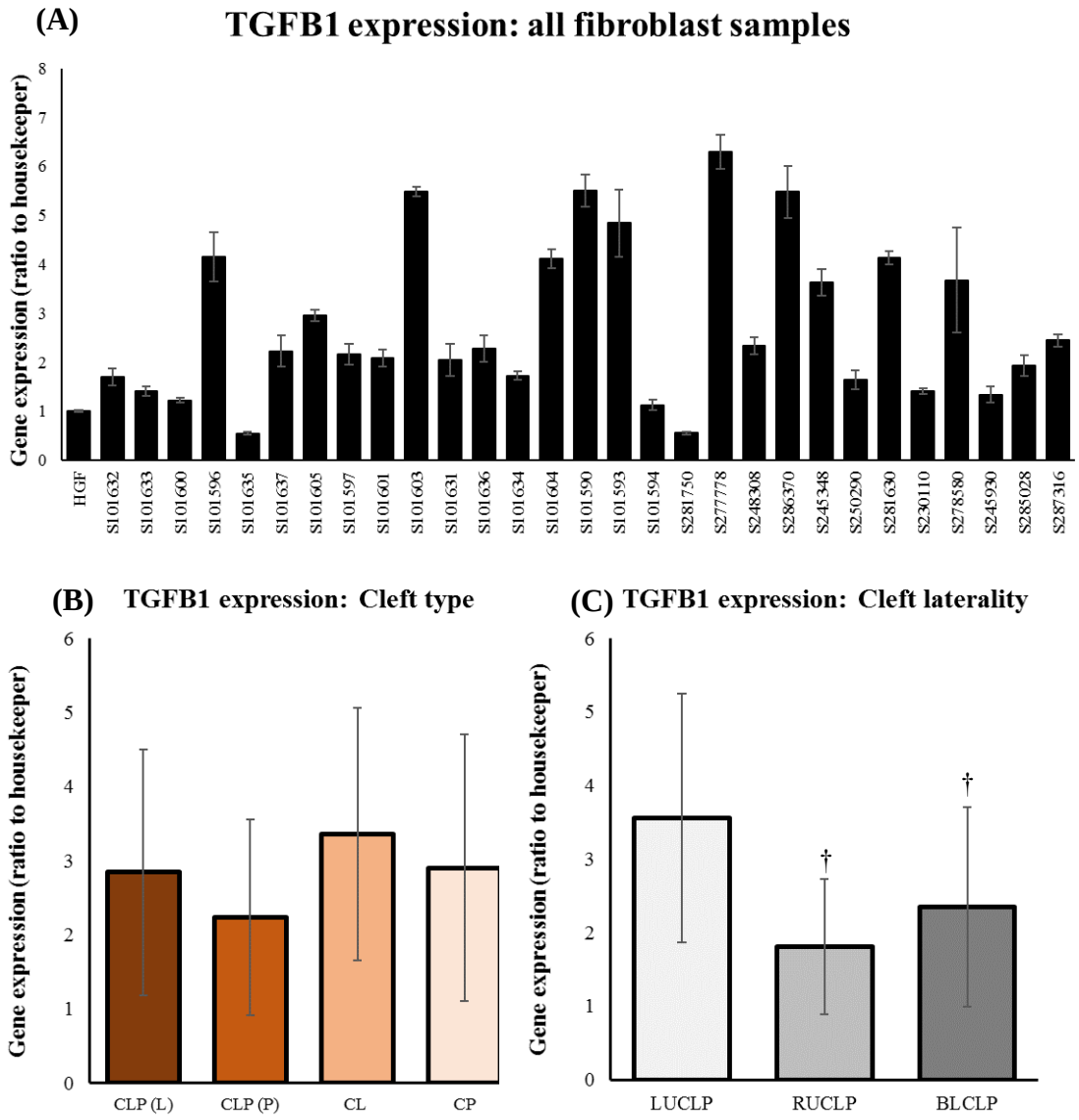

Figure 39: Expression levels of *TGFB1*. (A) Expression levels of *TGFB1* were variable across the sample cohort however most fibroblasts expressed *TGFB1* in significantly higher amounts than the control (n=3). (B) There was no differences in *TGFB1* expression between cleft types. (C) Averages expression of *TGFB1* was significantly in LUCLP relative to RUCLP and BLCLP. Significant differences were determined by means of student's t-test where: † = $p<0.05$ relative to LUCLP (n=18); ‡ = $p<0.05$ relative to RUCLP (n=21) and + = $p<0.05$ relative to BLCLP (n=15).

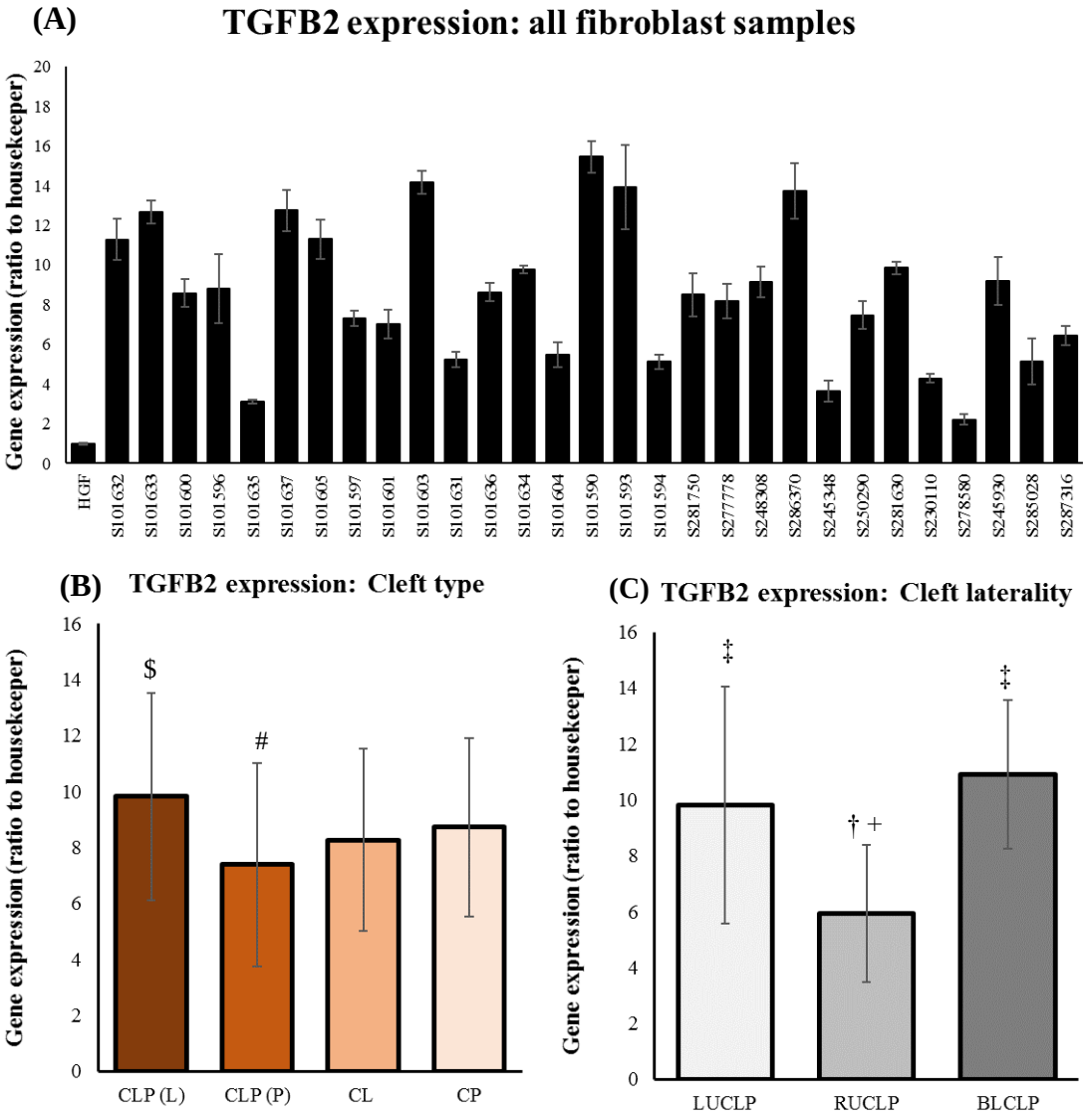

Figure 40: Expression levels of *TGFB2*. (A) Expression of *TGFB2* was highly variable however all samples displayed fold changes significantly greater than the HGF control (n=3). (B) *TGFB2* expression was significantly greater in CLP(L) when compared with CLP(P) but there were fibroblasts with high and low expression in each group. (C) *TGFB2* expression was significantly lower in RUCLP relative to both LUCLP and BLCLP (n=3). Significant differences were determined by means of student's t-test where: # = $p<0.05$ relative to CLP(L) (n=27); $ = $p<0.05$ relative to CLP(P) (n=27); ¥ =$p<0.05$ relative to CL (n=18); Ø = $p<0.05$ relative to CP (n=15); † = $p<0.05$ relative to LUCLP (n=18); ‡ = $p<0.05$ relative to RUCLP (n=21) and + = $p<0.05$ relative to BLCLP (n=15).

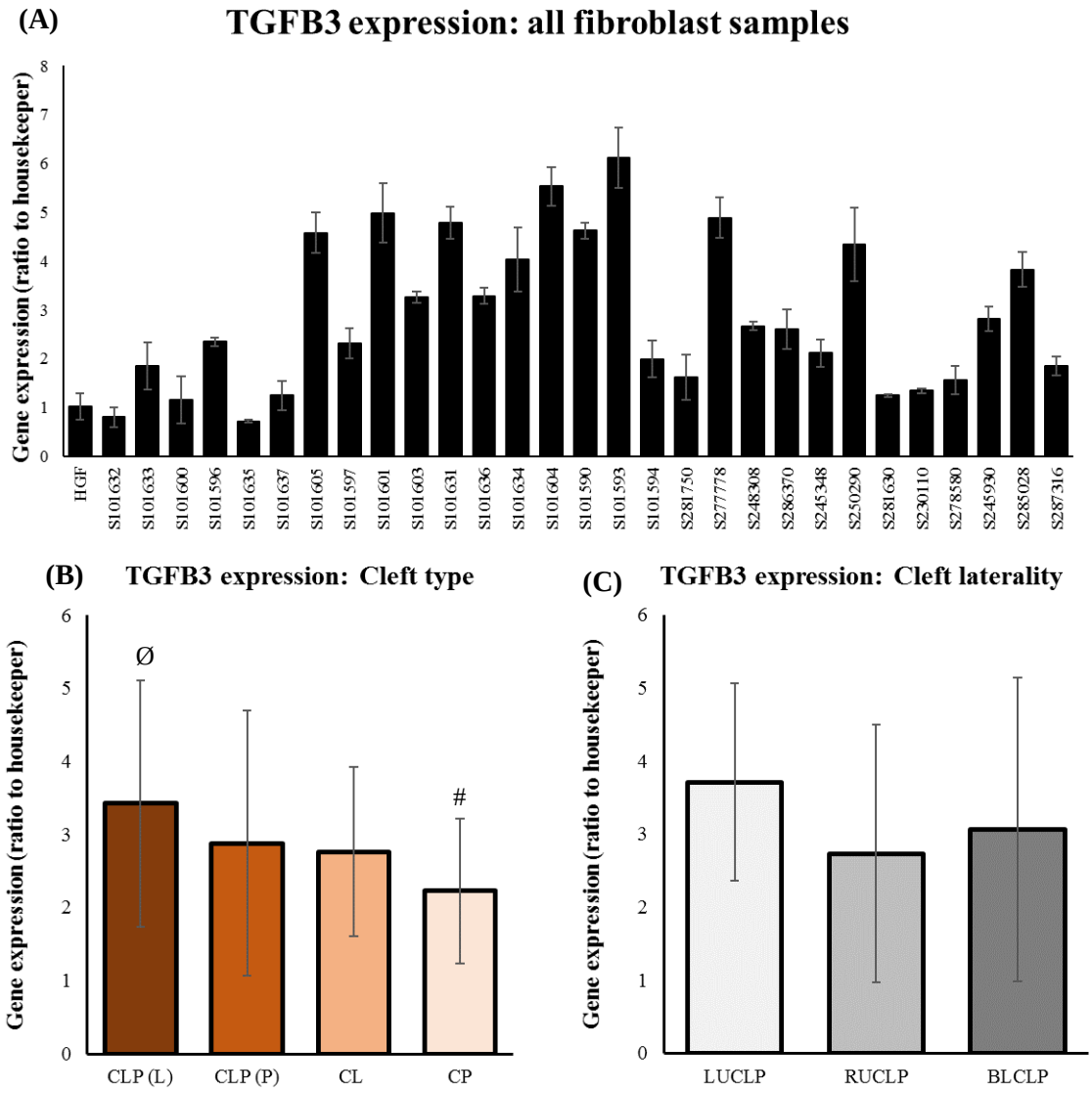

Figure 41: Expression levels of *TGFB3*. (A) Expression of *TGFB3* differed considerably across the sample cohort with some fibroblasts expressing *TGFB3* in amounts comparable with the control and others in significantly greater amounts (n=3). (B) *TGFB3* expression was significantly higher in CLP(L) relative to CP. (C) There were no significant differences in *TGFB3* based on cleft laterality. Significant differences were determined by means of student's t-test where: # = $p<0.05$ relative to CLP(L) (n=27); $ = $p<0.05$ relative to CLP(P) (n=27); ¥ =$p<0.05$ relative to CL (n=18); Ø = $p<0.05$ relative to CP (n=15).

3.7.1 Expression of transforming growth factor beta receptors

The expression of receptors associated with the TGFβ signalling pathway was assessed in order to determine how they differ between fibroblasts derived from different cleft patients. *TGFBR1* expression was comparable with the HGF control for a number of fibroblast samples, however the majority of fibroblast samples expressed *TGFBR1* in significantly amounts as the maximum was 8.20-fold whereas the minimum was 0.63-fold. This difference did not correlate with cleft type as they all shared similar fold changes. However, in terms of cleft laterality it was shown that RUCLP fibroblasts displayed significantly lower expression when compared with LUCLP (Figure 42A-C).

Expression of *TGFBR2* was also varied but the majority of the samples displayed expression in greater amounts than the control as the maximum expression was 6.72-fold. However, a minority of samples shared expression comparable with or lower than the control as the minimum expression observed was 0.59-fold. In terms of cleft type, CLP(L) displayed significantly higher average expression of *TGFBR2* when compared with CP but not other cleft types ($p<0.05$). As with expression of *TGFBR1*, expression of *TGFBR2* was significantly down-regulated in fibroblasts derived from RUCLP when compared with LUCLP derived fibroblasts (Figure 43A-C).

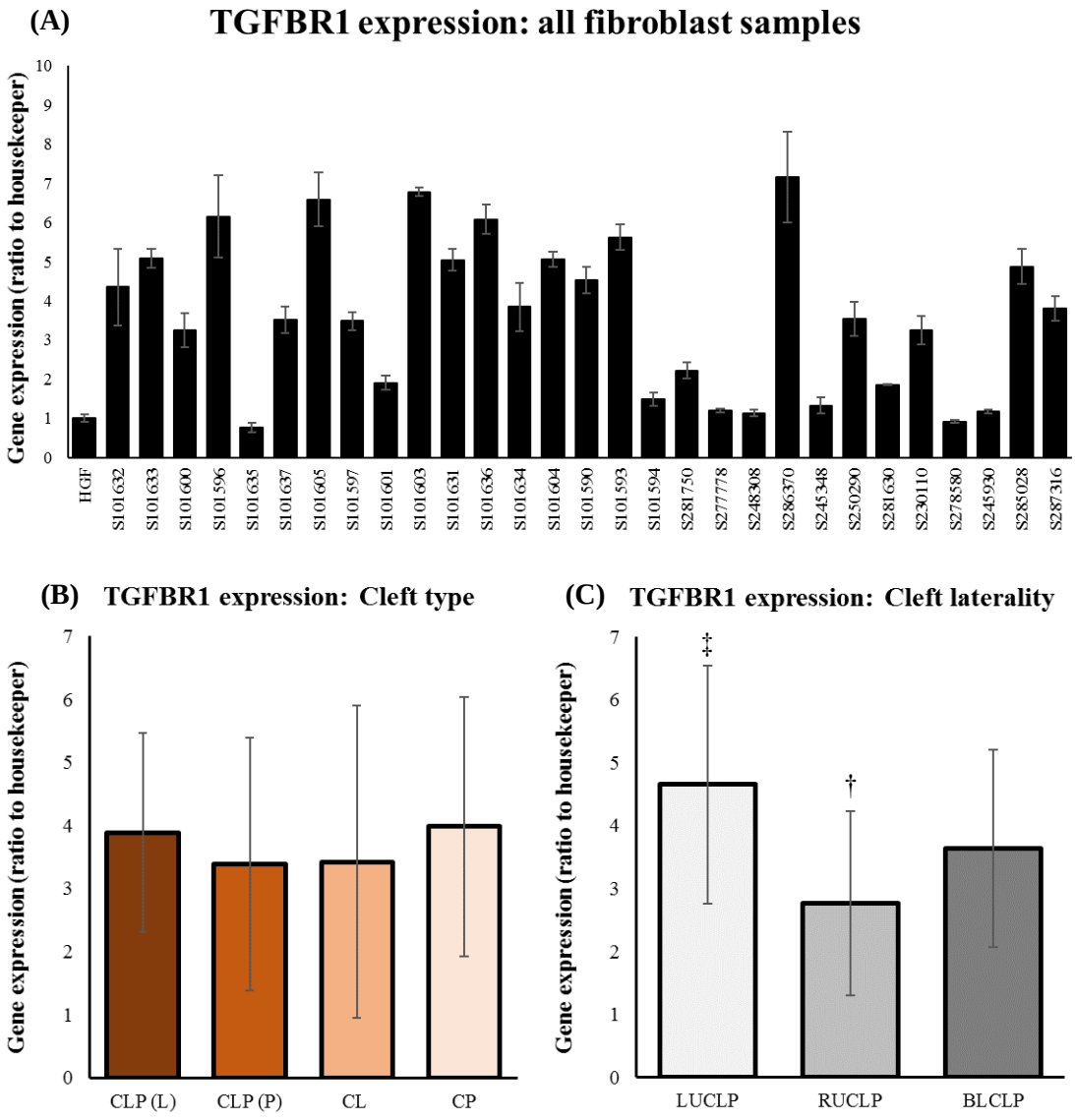

Figure 42: Expression levels of *TGFBR1*. (A) Expression of *TGFBR1* was highly variable across the sample cohort as some fibroblasts exhibited expression levels comparable with the HGF control whereas others were significantly higher. (n=3). (B) There were no differences in *TGFBR1* expression based on cleft phenotype. (C) Average expression of *TGFBR1* was significantly higher in fibroblasts from patients with LUCLP relative to RUCLP. Significant differences were determined by means of student's t-test where: † = $p<0.05$ relative to LUCLP (n=18); ‡ = $p<0.05$ relative to RUCLP (n=21) and + = $p<0.05$ relative to BLCLP (n=15).

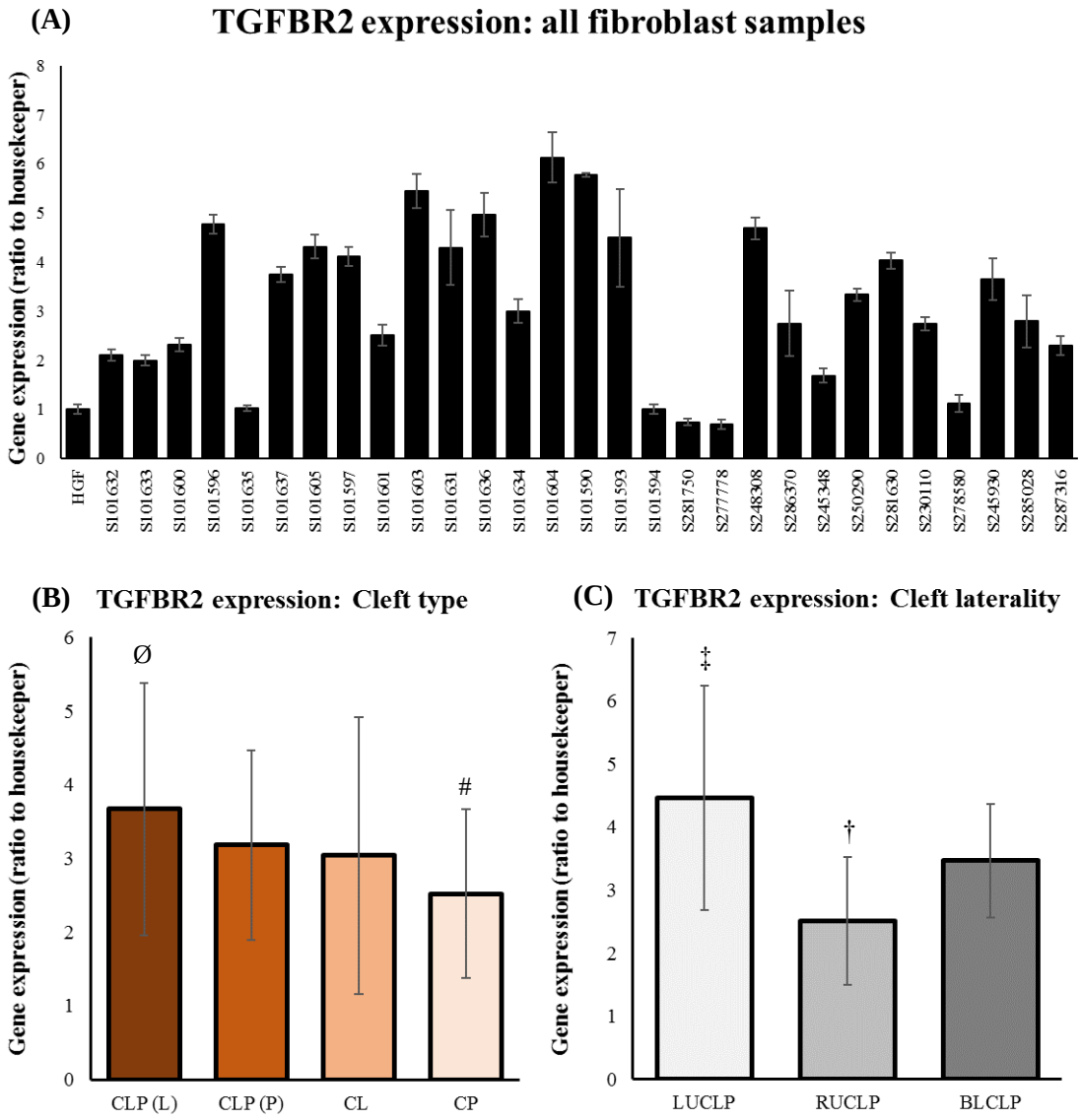

Figure 43: Expression levels of *TGFBR2*. (A) Expression of *TGFBR2* was varied, some samples exhibited expression comparable with the HGF control however the majority of fibroblast samples expressed *TGFBR2* in significantly greater amounts (n=3). (B) Average expression of *TGFBR2* was significantly greater in CLP(L) fibroblasts relative to CP. (C) Average expression was significantly higher in LUCLP fibroblasts relative to RUCLP. Significant differences were determined by means of student's t-test where: # = $p<0.05$ relative to CLP(L) (n=27); $ = $p<0.05$ relative to CLP(P) (n=27); ¥ =$p<0.05$ relative to CL (n=18); Ø = $p<0.05$ relative to CP (n=15); † = $p<0.05$ relative to LUCLP (n=18); ‡ = $p<0.05$ relative to RUCLP (n=21) and + = $p<0.05$ relative to BLCLP (n=15).

3.7.2 Expression of Transforming Growth Factor alpha

Transforming growth factor alpha (TGFα), a potent epithelial mitogen that can also influence fibroblast activity, has been positively identified within the epithelium and the underlying mesenchyme at multiple stages of palatal development (Meng et al, 2009), *TGFA* expression was therefore assessed to determine whether its expression differed between cleft phenotypes. *TGFA* expression was less variable across the sample cohort. There were a number of samples that displayed significant down-regulation of *TGFA* relative to the control although this down-regulation not correlate with cleft type. However, RUCLP fibroblasts displayed significantly lowered average expression of *TGFA* relative to both LUCLP and BLCLP (Figure 44A-C).

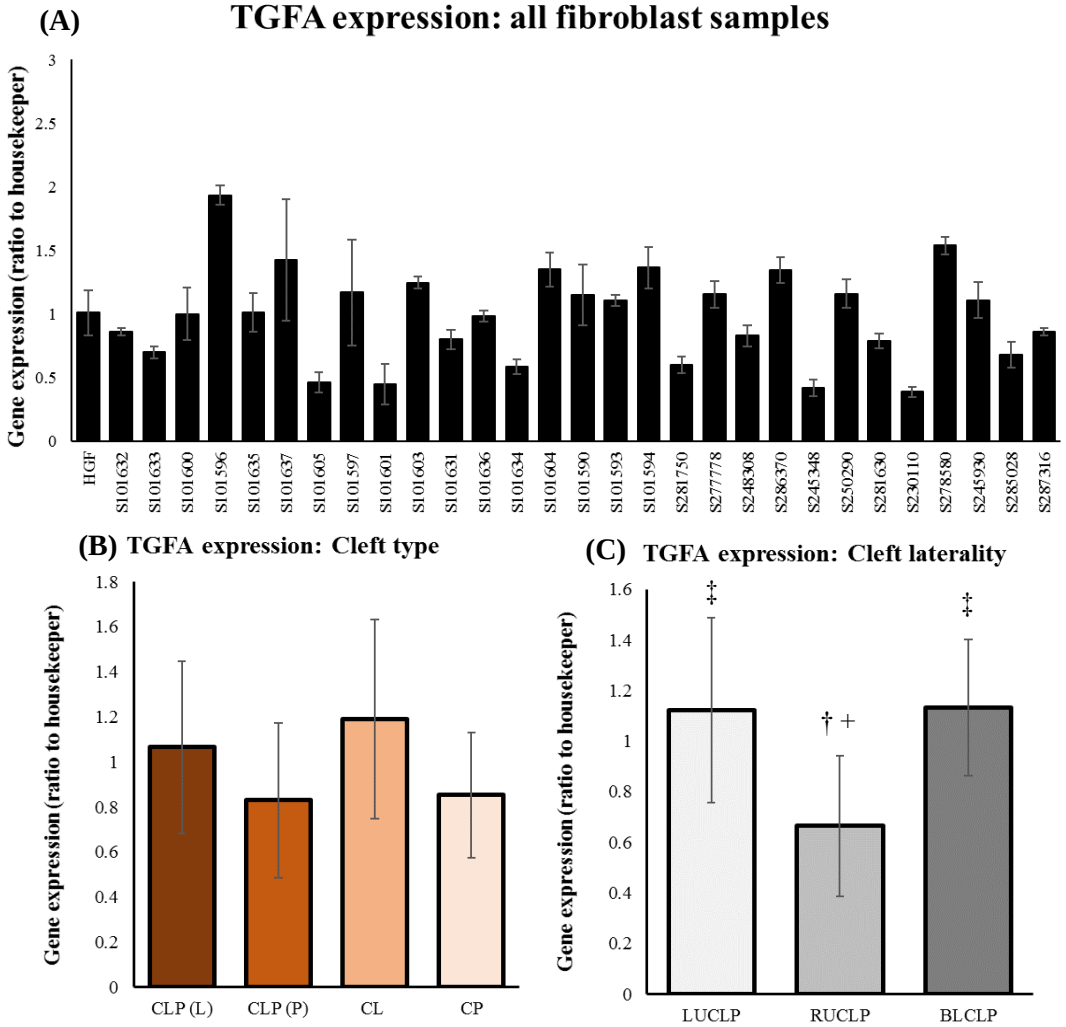

Figure 44: Expression levels of TGFA. (A) A subset of patient samples exhibited expression significantly lower than the control whereas others exhibited expression comparable with the HGF control. (n=3). (B) The expression of TGFA was similar for each cleft type. (C) TGFA expression was significantly lowered in RUCLP fibroblasts relative to LUCLP and BLCLP.

3.8 Discussion

The development of the face, including the lip and palate, is a precise tightly regulated process that encompasses complex interplay between a host of cell types and cell behaviours. The current mechanistic model suggests the morphogenesis of CLP may be due to pathological cell behaviours, including proliferation, adhesion, migration, differentiation and apoptosis, during the critical weeks of early craniofacial development, leading to deviation from the facial blueprint due to obstruction, malposition or failure of fusion facial growth centres as a result of genetic or environmental factors (Mossey et al, 2009). However, the precise mechanisms that give rise to the varying cleft phenotypes is currently poorly understood although it is possible that they may each be a result of differing pathological processes. The cornerstone of the facial developmental process is the rapid migration and proliferation of cranial neural crest cells (CNCCs) following delamination from the neural tube via the process of epithelial-to-mesenchymal transition (EMT) (Strobl-Mazulla and Bronner, 2013). These cells migrate to sites that will become the facial processes and can differentiate into mesenchymal cells with the ability to give rise to diverse cell lineages, including fibroblasts, that contribute to the formation of facial cartilage, bone and connective tissue (Hay, 2005; Huang and Saint-Jeannet, 2004). The formation of the face is a result of the action of these cell types at the five premature facial swellings where there continued proliferation lead to the outgrowth of these facial growth centres (Chai and Maxson, 2006; Jiang et al, 2008). CNCC derived mesenchymal cells, including fibroblasts, are the major secretors of ECM within these facial processes and contribute to their growth through there proliferative activity and continued secretion of ECM prior to fusion of the facial processes (Sun et al, 2000; Jiang et al, 2006). When in proximity, filopodial attachments from cells on the approaching opposing prominence begin to interact, this is followed by the generation and accumulation of larger cellular processes, including adhesion junctions, which lead to precise fusion of the facial processes (Sun et al, 2000).

Fibroblasts are key to these processes as reduced proliferation can lead to reduced cell packing within the facial processes, this could lead to a decrease in overall fibroblast ECM deposition thereby reducing the overall volume of the tissue. Further, due to acting as the biological scaffold, diminished ECM deposition can lead to a reduction in adhesion sites, which are required for cellular motility (Rozario and DeSimone, 2010). Controlled and tightly regulated fibroblast behaviour is therefore essential to normal facial development therefore perturbations in their activity may lead to CLP morphogenesis due to tissue malposition resulting in partial fusion of the facial prominences at various degrees of severity. Due to this, cleft fibroblast behaviour was assessed and compared between cleft patients as it is possible that differences in fibroblast activity may influence the type of cleft that manifests.

3.8.1 Confirmation of the Fibroblast lineage

To reliably compare fibroblasts derived from differing cleft phenotypes it was first necessary to confirm that samples comprised of homogenous fibroblast populations, this was achieved by both real time PCR and immunostaining methodologies. Vimentin (*VIM*) is an intermediate filament that is only found in cells of mesenchymal origin, such as fibroblasts, and has been successfully used as a fibroblast marker in a number of different studies (Ivey et al, 2017; Negmadjanov et al, 2015). It was found that all of the cells stained positive for *VIM* and displayed fibroblastic morphology thereby suggesting there was no epithelial contamination. Further, fibroblasts expressed four-fold increase in *VIM* relative to H400 squamous carcinoma epithelial cell line. Epithelial cells are of ectodermal origin and as result under normal circumstances do not express *VIM* unless undergoing epithelial-mesenchymal transition (EMT) (Abdulkareem et al, 2018) which is not be expected under normal cell culture conditions. It would be expected that homogenous populations of fibroblasts would express *VIM* whereas epithelial cells would exhibit null expression; however, it was shown here that H400 cells did

express *VIM* and this is likely due to being a transformed cancer cell line and not a true primary epithelial cell type. Further, the fibroblast phenotype is often confirmed by the absence of specific markers for other cell lineages (Chang et al, 2002), as epithelial cells had the highest potential to contaminate pure fibroblast cultures, pooled cleft fibroblasts were assessed for the expression of cytokeratin 5 (*CK5*) which is an epithelial marker (Corr et al, 2015). H400 cells were positive for *CK5* whereas pooled cleft fibroblasts were negative. This data suggests cultures were homogenous fibroblast populations therefore any comparisons made between cleft types in subsequent assays would be with cells from the same lineage.

3.8.2 The effect of increasing passage number on cleft fibroblast behaviour

Two-dimensional cell culture involves growing cells onto a substrate with a finite surface area. As cells approach confluence, cell-substrate adhesion molecules are dissociated through use of chemical stimuli such as trypsin-EDTA. Following this, a sub-population of the dissociated cells are reseeded into a separate tissue culture vessel, this process is termed subculture, or passaging, every time this process is conducted the cell passage number is increased by one. Subculture is a traumatic process and can have a significant effect on normal cell behaviours (Hughes et al, 2018), thereby causing cells to behave differently at different passage numbers making comparisons between passages difficult and effecting results and data interpretation. To undertake valid comparative assessments between fibroblasts isolated from different cleft patients it was necessary to determine the effect of varying passage numbers on cell behaviour.

It was found that passaging cells had a significant effect on the growth of cleft fibroblasts as after passage four as fibroblasts were shown to have a significant increase in DT ($p<0.05$). Others have found comparable results with primary human nasal epithelial stem progenitor cells (hNESPCs) which showed a marked increase in DT between passage one and three (Yu et al, 2014). *MCM2*, a component of the mini chromosome maintenance (MCM) complex which acts

a replicative helicase for DNA replication, was significantly upregulated after passage two. *MCM* proteins are thought to be key regulators of cell proliferation during times of replicative stress (Quan Ge et al, 2007), which may occur as a result of repeated DNA replication at elevated cell passages. Abundant MCM proteins are required for cells to survive replicative stress and proliferate normally (Ge et al, 2007) therefore their upregulation in cleft fibroblasts after passage two may be a response to the cell stresses caused by passaging and an attempt to maintain normal proliferative behaviour. Expression of *MK167*, a proliferative marker that is present in all of the active stages of the cell cycle including mitosis, was reduced after passage three, whilst *PCNA* expression, a cofactor to DNA polymerase, remained stable between passages zero to five. A study on human temporo-mandibular joint fibro-chondrocytes (TMJF) demonstrated that both *MK167* and *PCNA* expression was similar between passage one and passage eight but there was a decrease in expression of both genes at passage nine which was suggested to result in reduced proliferation (Garzon et al, 2012). Downregulation of *MK167* after passage three and upregulation of *MCM2* after passage two suggests this variance in expression may account for the significant increase in cleft fibroblast DT after passage three as it has been demonstrated that stable expression of proliferative markers is correlated with stable proliferation (Garzon et al, 2012). As fibroblast growth was shown to be unaffected at low passages, subsequent cell based assays were conducted with passage two fibroblasts thus any disruptions in cell behaviour would be consistent across the patient cohort.

To determine the most appropriate passage number for PCR analysis it was necessary to establish the effect passaging on the expression of genes that are thought to be involved in cleft formation. Polymorphisms of interferon regulatory factor 6 (*IRF6*), a transcription factor that is elevated in the palatal shelves and is thought to regulate epithelial-to-mesenchymal transition during palatal fusion (Ke et al, 2015), are associated with CLP formation (Rahimov et al, 2008; Park et al, 2010). Cleft fibroblasts displayed stable expression of *IRF6* between passage zero

and three followed by upregulation thereafter. Similarly, *SOX9*, a transcriptional regulator involved in craniofacial development (Lee et al, 2011), was downregulated after passage one; whereas *TGFA*, which influences the risk of cleft formation (Sull et al, 2009) displayed stable expression. Variability in expression of cleft associated markers at different passages may lead to false comparisons between samples that are no longer comparable leading to skewed results and to inaccurate conclusions (Hughes et al, 2018). Due to this, only passage one fibroblasts were utilised for PCR analysis; passage zero fibroblasts were required for cell stock expansion.

3.8.3 Growth of cleft fibroblasts

Despite DT varying between 26.11 and 32.41 hours, when grouping data there was no significant differences between fibroblasts derived from different cleft phenotypes. Further, the majority of samples displayed comparable DT to the NHDFF control. Conversely, others have shown NSCLP fibroblasts exhibited significantly higher thymidine incorporation (+151%) compared control fibroblasts isolated from patients with palatal trauma (Marinucci et al, 2009), this suggests that cleft fibroblasts may proliferate faster than their non-cleft counterparts. Gene expression of proliferation associated genes did vary significantly between cleft types therefore it is possible that *in vivo* cleft fibroblasts would proliferate differentially as opposed to their growth on an artificial two-dimensional surface. CLP(P) fibroblasts upregulated *MCM2* relative to CP despite being derived from the same anatomical site. *MCM2* proteins are a pre-requisite for DNA replication and commencement of the cell cycle (Kearsey and Labib, 1998). Elevated MCM expression has been identified in highly proliferative cells (Shetty et al, 2005; Torres-Rendon et al, 2009) whereas quiescent cells display diminished MCM2 expression (Madine et al, 2000). Therefore, it is possible that CLP(P) fibroblast would proliferate faster *in vivo* compared to CP fibroblasts. Further, both types of CLP fibroblasts, CLP(L) and CLP(P), significantly upregulated of *PCNA* when compared with those with CL in isolation. *PCNA* is

also a key coordinator of DNA synthesis as it acts as a platform for recruitment of proteins associated with regulation of the cell cycle and repair of damaged DNA (Zhao et al, 2012). Taken together, this data suggests that fibroblasts from patients that have CLP in combination may proliferate significantly faster *in vivo* relative to their isolated counterparts, this may be a contributory factor in CLP as increased fibroblast proliferation would lead to increased cell packing within developing tissues coupled with the associated increase in ECM deposition both of which are factors that may lead to clefting (Sasaki et al, 2004; Moxham, 2003).

BLCLP is more severe than unilateral CLP (UCLP), which has either left or right laterality, as clefts manifest on both sides of the lip often resulting in patients with a greater likelihood of developmental issues (Annigeri et al, 2012). The prevalence of BLCLP is significantly lower than that of UCLP, a study which assessed 583 cleft patients undergoing surgical repair found BLCLP was the most uncommon cleft type with a 3.8% prevalence rate whereas UCLP was far more common with a 42% prevalence rate (Jagomagi et al, 2010). Although it is possible that BLCLP is just a comparatively rare form of UCLP with the same causation it is also possible that BLCLP is a distinct cleft phenotype with distinct aetiological origins. However, despite this being speculated upon in the literature, there is currently little published evidence to support this suggestion although some have identified potentially distinct genetic origins for BLCLP (Ibitoye et al, 2015; Liu et al, 2005) and have shown variable gene expression between BLCLP and other cleft types (Francois et al, 2017). Here BLCLP fibroblasts presented statistically decreased expression profiles of the proliferative genes *MCM2*, *MKI67* and *PCNA* compared with both RUCLP and LUCLP, suggesting the BLCLP cleft phenotype may be distinct and that the condition may be contributed to by decreased cell growth leading to malposition of the facial growth centres (Chai and Maxson, 2006; Jiang et al, 2008).

3.8.4 Cleft fibroblast production of extracellular matrix

The extracellular matrix (ECM) is a complex meshwork of molecules that are secreted by mesenchymal cells, though fibroblasts are usually the principal secretors of ECM. During craniofacial development, the palatal mesenchyme expands due to the fundamental processes of proliferation and matrix deposition. It is currently thought proliferation and accumulation of ECM contribute equally to the increase in volume of craniofacial tissues prior to shelf adhesion (Ferguson 1998; Nik et al, 2016). Due to this, the accurate manufacture and erection of the facial processes, which lead to development of the lip and palate, are reliant on precise ECM production. Significant perturbations may lead shelf malposition and development of OFC as cleft formation is fundamentally a result of impediments to the processes of palatal shelf elevation, attachment to opposing shelves or failure of shelf fusion (Meng et al, 2009); it is the underlying cause of these pathological processes that are currently being explored.

3.8.4.1 Collagen production

Collagens are major constituents of the ECM, during craniofacial development many different types of collagens are expressed throughout the palatal mesenchyme. During shelf elevation the fibrillary collagen types I, III, and V have been shown to be upregulated throughout the developing palate (Kurisu et al, 1987; Morris-Wiman and Brinkley, 1992) and are critical in providing mechanical integrity throughout the developing shelves whilst influencing cell attachment and migration (Bode, 2000). Further, collagens which are distributed across the entirety of the palatal mesenchyme are thought to contribute to the force that results in both shelf elevation (Bodo et al, 1999) and reorientation (Ben-Khaial and Shah,1994) potentially by increasing tissue rigidity and contributing to the critical volume required before morphogenesis can occur (Ben-Khaial and Shah,1994); however, despite its elevated presence during these critical phases the precise role of collagen in craniofacial development is not fully understood.

The present study found that cleft fibroblast collagen production varied between 167.98µg and 218.82µg. This variability seemed largely due to the anatomical origin of the fibroblasts as when grouped CLP(P) and CP patients, both of which were palatal fibroblasts, had significantly lower total collagen production when compared with both CLP(L) and CL which were lip derived fibroblasts. The behaviour of fibroblasts isolated from different regions can differ significantly (Chiquet et al, 2015). For example, when comparing oral fibroblasts, isolated from tonsil tissue, and dermal fibroblasts, isolated from foreskin, it was found that oral fibroblasts displayed marked differences in proliferation (Lee and Eun, 1999). In addition, fibroblasts isolated from different regions of the oral cavity can also differ in behaviour, it was found that gingival fibroblasts secreted significantly lower total ECM when compared with periodontal ligament fibroblasts (Hou et al, 1995); this suggests differences observed between cleft phenotypes may be due to anatomical origin. However, it is also possible decreased collagen production may be a contributing factor in clefts of the palate as both CLP(P) and CP derived fibroblasts had decreased production potentially leading to malposition of the palatal shelves during fusion, though there is not currently any other published evidence to support this. *COL1A1* expression was also found to be significantly lowered in fibroblasts from CLP(P) and CP when compared with CL whereas *COL3A1* expression was significantly higher in CLP(P) fibroblasts compared with CL. This is significant as during craniofacial embryogenesis the palatal mesenchyme has been shown to decrease production collagen type III and increase production of collagen type I (Morris-Wiman and Brinkley, 1993). Here the opposite pattern of expression was demonstrated by CLP(P) and CP. The ratio of collagen I and III within tissues can significantly impact tissue integrity, when compared with normal skin, hypertrophic scars comprise of significantly greater amounts of collagen III (Oliveira et al, 2009) leading to decreases in mechanical properties, including extensibility and toughness (Corr et al, 2009). Providing CLP(P) and CP elevated expression of *COL3A1* translates to increased collagen III

within the palatal mesenchyme, palatal shelf tissues may exhibit reduced mechanical strength which could potentially interrupt the process of shelf elevation and reorientation which are processes that mediated by force distribution through collagen networks (Bodo et al, 1999; Ben-Khaial and Shah,1994), thereby contributing to clefts of the palate.

3.8.4.2 Glycosaminoglycan production

Glycosaminoglycans (GAG's) are major components of the ECM and, due to the presence of sulphate and uronic acid groups along the GAG chains, that are negatively charged. This makes GAGs hydrophilic and as a result interact with water molecules contributing to tissue hydration (Singh et al, 1994). During craniofacial development many have proposed a contributor to shelf elevation is the swelling of the palatal shelves, due the accumulation of water by GAGs within the mesenchyme, producing an intrinsic hydrostatic force that increases tissue volume leading to elevation (Ferguson, 1978; Brinkley and Moris-Wiman, 1987; Singh et al, 1997). Quantities of GAG are elevated during shelf elevation and prior shelf fusion, when the orientation of palatal shelves is altered, followed by decreased total GAG after successful fusion (Singh et al, 1994; Moxham, 2003). As hydration and subsequent GAG swelling is a major driving force during this process (Brinkley and Moris-Wiman, 1987), appropriate production of GAG's is likely critical to typical craniofacial development. Cleft fibroblast production of GAGs varied considerably across the sample cohort. Despite this, there were samples with high and low production across all cleft types. However, CLP(L) fibroblasts produced significantly reduced GAG compared with CLP(P), it can be stipulated that differing anatomical origins may account for this disparity and not the tissue type as both CLP(P) and CLP(L) are derived from patients with both cleft lip and palate. In the UK, patients with CLP usually undergo lip repair at around 3 months of age coupled with a secondary cleft palate repair in the following months (Sitzman et al, 2017). Thus the patients age at sample isolation may account for the differences in GAG

production observed between CLP(P) and CLP(L). Others have shown that fibroblasts isolated from the cleft lip of neonates, up to 16 days of age, and children, aged between 3 months and 6 years old, displayed differential gene expression profiles, further both populations differed significantly from their adult counterparts (Zivicova et al, 2017); suggesting that the differences observed in GAG production in the present study may potentially be due to patient age.

It is known that GAG's, therefore their expression, is critical to craniofacial development as it has been shown that 5-fluoro-2-deoxyuridine (FUDR), an oncology drug, induces cleft palate by decreasing GAG production in developing embryos by 30% when compared with normal developing palates (Singh et al, 1997). Notably, it is clefts of the palate, not the lip, that FUDR induces (Ferguson, 1978), therefore it can be stipulated that GAG synthesis is more critical in the prevention of cleft palate as opposed to cleft lip. Due to this, it would be expected that there would be downregulation of GAG associated genes in CP patients when compared with those with CL. However, it has been shown here that *CSPG4* and *DSE* are both upregulated in CP derived fibroblasts when compared with CL, it is therefore unlikely that there expression is associated with the cleft phenotype that was manifested. It is possible that expression of the unsulphated GAG Hyaluronic acid, which Alcian blue did not stain at the pH used here, could be downregulated in patients with CP due to its association with palate morphogenesis (Galloway et al, 2013), however this analysis was not conducted. RUCLP fibroblasts produced greater total sulphated GAGs compared to LUCLP and BLCLP; however, RUCLP fibroblasts downregulated *CSPG4*, *HSPG2* and *DSE* thereby suggesting expression may not correlate with GAG production. As sulphated GAG's are key to craniofacial development due to hydration of connective tissues, it is possible that the decreased expression may favour RUCLP manifestation; however, there is currently no other evidence to support this suggestion.

3.8.4.3 Fibronectin expression

Directed CNCC migration is critical to normal development of the craniofacial region as it regulates the location of cell dense regions that that will subsequently differentiate and proliferate to form the facial growth centres. Fibronectin interacts with cellular transmembrane bound integrins and other ECM components including collagens and glycosaminoglycans. Fibronectin is abundant across the CNCC migratory path and is thought to contribute to their migratory directionality (Sternberg and Kimber, 1986). Saturation of CNCC-fibronectin binding domains, with complimentary peptides, leads to stunted migration (Boucaut et al, 1984) whilst presence of fibronectin supports CNCC attachment, spreading and migration (Perris et al, 1996). As CNCCs are the major pluripotent cell type within the craniofacial region it can be inferred that appropriate fibronectin expression is a prerequisite to normal craniofacial development (Snider and Mishina, 2014). Here CLP(L) and CLP(P) fibroblasts significantly upregulated *FN1* when compared with both CL and CP in isolation. It has been shown in CP induced murine models that clefts were caused by perturbed fibronectin arrangements resulting in failure of palatal shelf elevation and midline fusion (Tang et al, 2015; Tang et al, 2016). Additionally, decreasing the efficacy of fibronectin through use of anti-fibronectin to adhere to binding domains also resulted in the formation of clefts (Sakai et al, 2003). This demonstrates that the presence of fibronectin is fundamental to normal craniofacial development; therefore, it is possible the downregulation observed in CP and CL fibroblasts, could be a contributing factor to the development of clefts in those patients. Alternatively, it is possible that the high expression of FN1 observed in both CLP(L) and CLP(P) could result elevated production of fibronectin thereby disrupting the regular fibronectin arrangement and contributing to the development of CLP in conjunction. However, larger samples sizes are required to confirm whether the expression of FN1 is related to the manifestation of specific cleft phenotypes.

3.8.5 Transforming growth factor beta expression

Genes related to the transforming growth beta factor (TGFβ) superfamily have been repeatedly linked with cleft development (Funato and Nakamura, 2017; Kohli and Kohli, 2012). Due to this, the expression multiple *TGF* gene transcripts were assessed across the cleft sample cohort to determine if differences correlated with cleft type. TGFβ ligands are cytokines that can regulate: cell recruitment, proliferation, ECM deposition, differentiation and apoptosis (Penn et al, 2012), all of which are key to normal craniofacial development (Wu and Hill, 2009). During palatogenesis TGFβ ligands are expressed within the developing palatine shelves and surrounding craniofacial structures. *TGFB1* and *TGFB3* are significantly expressed in medial edge epithelium (MEE) of the developing palate prior to fusion whereas *TGFB2* is expressed significantly in the underlying palatal mesenchyme; this expression increases further immediately following contact of the opposing shelves (Fitzpatrick et al, 1990). Following fusion, epithelial expression of *TGFB1* and *TGFB3* is decreased followed by upregulation within the underlying mesenchyme, this is associated with formation of the secondary palate and palatal bones (Fitzpatrick et al, 1990). The role of TGFβ in the formation of the upper lip is limited as there is yet to be study outlining the specific involvement of each isoform prior to fusion of the frontonasal and maxillary prominences. However, TGF signalling is thought to be involved as *TGFBR1* murine knockout (KO) models have been observed with both unilateral and bilateral clefts of the lip (Li et al, 2008). Here it was shown that the majority of samples demonstrated significant upregulation of *TGFB1*, *TGFB2* and *TGFB3* relative to the non-cleft control with *TGFB2* displaying the largest average fold change. Studies have shown that dysregulation of TGFβ expression leads to clefts in murine models. *TGFB2* knockout mice develop clefts of the secondary palate, with extension from the hard palate into the soft palate, in 23% of pups (Sanford et al, 1997). Further, clefts were caused due to disruption of shelf growth and elevation resulting in malposition thus incorrect orientation for opposing shelf

fusion (Sanford et al, 1997), this suggests that patient dysregulation of *TGFB2* may potentially disrupt palatal mesenchyme growth thereby contributing to cleft development. *TGFB3* knockout mouse models also presented the CP phenotype (Proetzel et al, 1995), however unlike with *TGFB2* knockouts palatal shelf elevation and orientation was not disrupted. Rather, clefts were caused due a failure of fusion of opposing MEE surfaces (Proetzel et al, 1997), later it was shown that *TGFB3* null mice display significantly reduced MEE filopodia distribution that potentially interfered with shelf adhesion (Taya et al, 1999). As TGFβ isoforms are structurally similar but functionally diverse, the expression of each is likely to contribute to differing modes of cleft development and potentially cleft phenotype. Here it was shown there was no direct correlation between *TGFB1* and *TGFB2* expression and different cleft types despite significant sample variation. However, as there was significant downregulation of *TGFB3* in CP fibroblasts, when compared with CLP(L), downregulation of *TGFB3* may contribute to CP manifestation, potentially as a result of a failed opposing MEE surface fusion (Proetzel et al, 1997) although analysis with larger sample sized are required to confirm this.

The majority of cleft samples here displayed upregulation of *TGFBR1* and *TGFBR2* relative to the non-cleft control although there were outliers with significantly reduced expression. *TGFBR1* epithelium knockout models resulted in clefts of the soft palate with 100% penetrance due to failure of fusion (Dudas et al, 2006). Further, in CNCC specific *TGFBR1* knockouts clefts were more significant as they encompassed both clefts of the lip and the hard and soft palate (Dudas et al, 2006). In addition, others have demonstrated that deletion of *TGFBR1* within all of the developing facial prominences routinely led to clefts of the lip (Li et al, 2008). Similarly, CNCC specific *TGFBR2* knockouts resulted in incomplete clefts of the secondary palate with 100% penetrance (Yoshihiro et al, 2003). These clefts were not a result of fusional deficiencies as when palatal shelves were artificially placed in proximity during *in vitro* organ culture they were able to fuse normally. Further, CNCC migration was not disrupted and it was

concluded that clefts formed due to perturbed proliferation resulting disruption to shelf growth leading to malposition (Yoshihiro et al, 2003). These knockout studies suggest appropriate expression and regulation of TGFβ receptors are critical to normal shelf growth, position and subsequent fusion, when their expression is disrupted there is the potential to develop clefts. Due to this, the variation in *TGFBR1* and *TGFBR2* expression observed across the sample cohort may have contributed to clefts in some patients. Further, as both receptors were downregulated in RUCLP when compared to LUCLP it is possible expression may be related to cleft laterality although there is currently no other supporting evidence. Although it is possible that disrupted TGFβ signalling contributed to cleft formation in some patients, as CLP is a pathology that can be caused by several different factors, the expression of single TGFβ genes are unlikely to be a good metric to assess why specific cleft phenotypes manifest.

3.8.5.2 Transforming growth factor alpha expression

Although *TGFA* polymorphisms have continually been associated with cleft development (Vieira, 2006), the assessment of basal expression between multiple patients to establish correlations with cleft phenotype manifestation was yet to be conducted. It was found here that the majority of cleft samples were comparable to the non-cleft control and although a subset presented significant downregulation, there were no significant differences between cleft phenotypes. Others have shown that there is an association between differing alleles of *TGFA* and the development of CP (Shiang et al, 1993), whilst patient polymorphisms have not been assessed here it was found that there were no differences in the basal expression between CP fibroblasts and other cleft types. During craniofacial development *TGFA* is expressed within the rapidly proliferating regions of the palatal shelves both prior to fusion and post fusion (Lamaroon and Diewert, 1996) thereby indicating it contributes to normal palatal development. However, *TGFA* null mice do not displays clefts of the lip or palate (Mann et al, 1993) thus

suggesting despite contributing to normal facial development it is not critical. Further, many studies have conflicting reports regarding the involvement of *TGFA* in cleft development (Vieira et al, 2006), although meta-analysis suggested significantly increased risk of CLP and CP development in individual with specific polymorphisms (Lu et al, 2014).Here RUCLP fibroblasts presented significant downregulation compared with LUCLP and BLCLP, this may have potentially contributed cleft laterality although currently no other studies to support this and it is likely that *TGFA* associated cleft development is a result of its interaction with related genes (Letra et al, 2012).

3.9 Conclusion

Despite significant differences in DT, ECM production, *TGF* beta and *TGF* alpha expression between individual patients in the sample cohort, many of the differences could not be reliably attributed to cleft phenotype; rather, individual variation coupled with anatomical origin, or the age of the patient at the time of isolation, may have been contributory factors in the differences observed. However, palatal cleft fibroblasts derived from CLP(P) and CP patients displayed significantly reduced collagen production and *COL1A1* expression coupled with increased *COL3A1* expression when compared to CL fibroblasts. This suggests the normal collagen distribution and ratio of collagen 1:3 may be disrupted potentially contributing to clefts of the palate. Further, RUCLP fibroblasts were shown to display reduced expression of several genetic markers which may favour the manifestation of right laterality. However, repetition with larger patient cohorts are required to support the preliminary findings outlined here.

CHAPTER FOUR:

ANALYSIS OF CLEFT FIBROBLAST MIGRATION

4.1 Analysis of fibroblast wound closure rates between cleft patients

As cell motility permits the re-localisation of cells to sites where they are needed, appropriate migration is fundamental to broad range of physiological processes including embryological development, wound healing and homeostasis. Perturbations to cell motility can have significant effects, particularly during the wound healing process, where the initial rate of migration is related to the degree of myofibroblast differentiation and potentially contributes to fibrosis (Hinz and Gabbiani, 2003; Tomasek et al, 2002). Due to this, cleft fibroblast motility was assessed to determine if specific populations display motility indicative of pathological wound healing which could later be correlated with the cleft type from which they were derived.

Cleft fibroblast closure of the defined cell free area produced by Ibidi inserts, hereafter referred to as a wound closure, was assessed using fibroblast isolated from each patient (Figure 45A-H). It was identified that there was significant variance in wound closure between cultures from different patients (Figure 46). Following the initial removal of the insert at zero hours there was very little variation in uncolonised area between cultures from different patients within the cohort. However, after 12 hours, cells had started to migrate into the cell free region in all patient samples. The largest variance in uncolonised area between patient samples was seen after 24 hours (variance = 0.30mm^2) whereas after 48 hours several cultures occupied the previously cell free region completely whilst others had not but a lower total variance was identified across the patient cohort (variance = 0.13mm^2). After 48 hours a number of the wounds had been closed, due to this the 24-hour time-point was selected in order to calculate the remaining wound area (RWA%). The RWA% was calculated by division of the total uncolonised area at 24h by the initial uncolonised area at 0h and from this cell migration was inferred (Figure 48). More slowly migrating cells exhibited a higher RWA% whilst faster cells had a lower RWA%, hereafter cell migration will also be used to refer to RWA%.

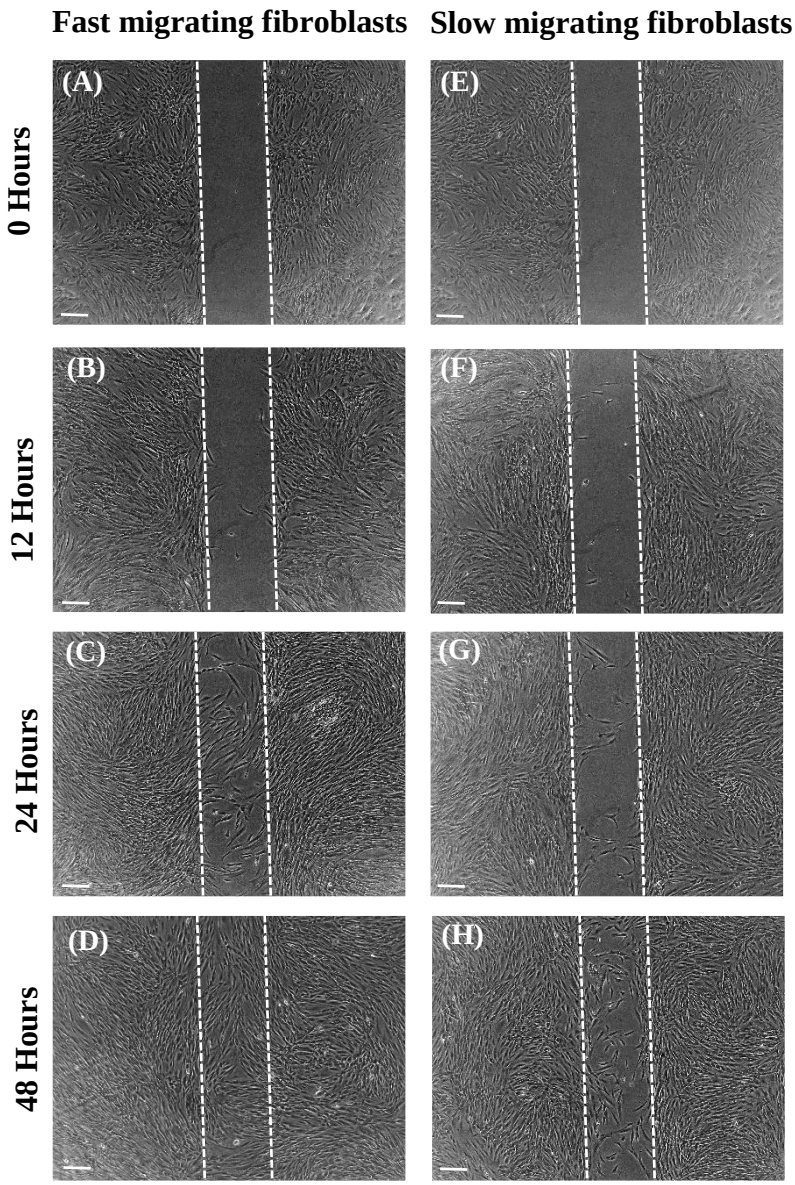

Figure 45: Imaging of cleft fibroblast wound closure of a 500µm cell free region at 0 hours, 12 hours, 24 hours and 48 hours. Immediately following removal of the Ibidi insert there was a comparable well-defined cell free region in all cultures (A and E). At 12h all cultures exhibited some degree of cell migration into the wound (B and F). After 24 hours there was significant migration into the wound in all cultures. However, there were clear differences in the total area of the wound covered in cells with some cultures exhibiting nearly complete wound closure (C), which were labelled fast migrating fibroblasts, whereas others displayed significantly less (G) and were labelled slow migrating fibroblasts. After 48 hours a number of the wounds had been completely closed (D) whereas others still had a large amount of the wound still uncolonised (H). Scale bars = 200µm.

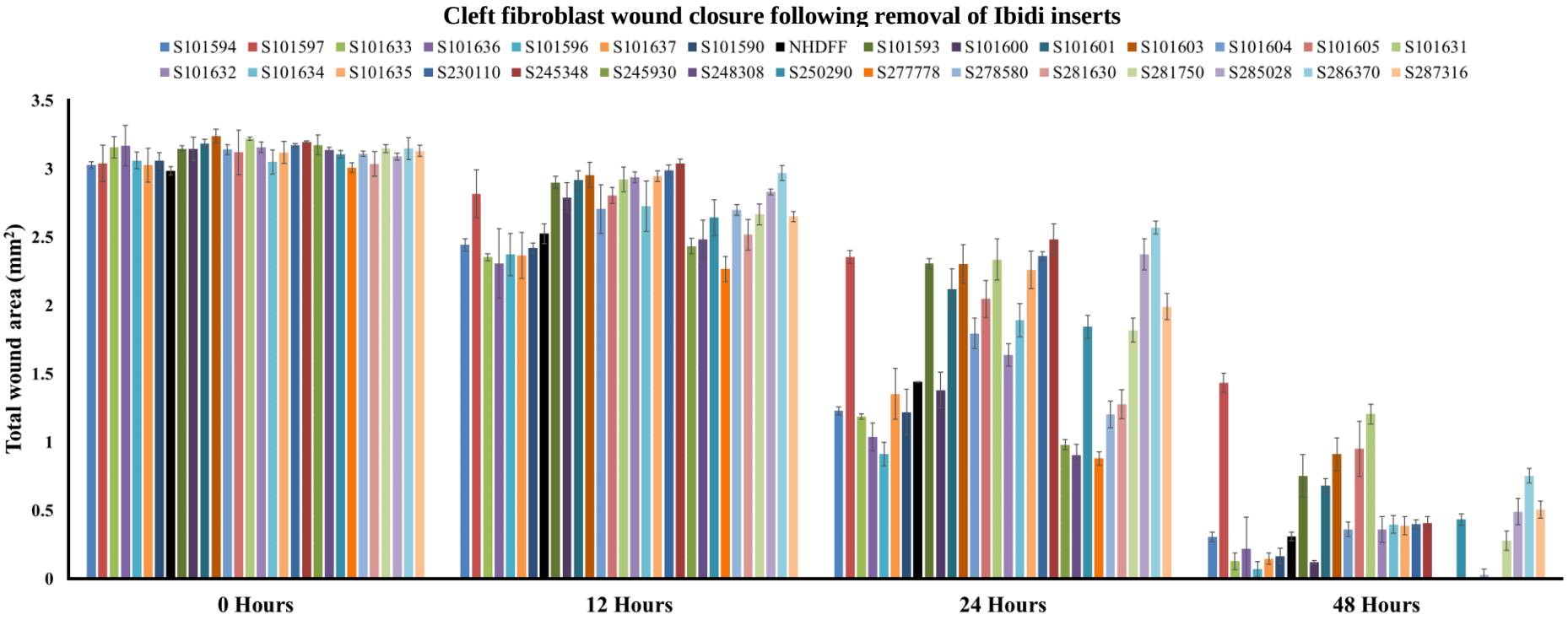

Figure 46: Quantification of cleft fibroblast wound closure for all patients. The total cell free area following removal of the Ibidi insert (0 Hours) was similar for all patients though there were slight non-significant differences. At 0h the maximum area was 3.32mm^2 and the minimum area was 2.89mm^2 thereby demonstrating some slight initial variability in wound area (variance = 0.01mm^2) thus necessitating calculations of RWA% which would account for initial wound variability. Uncolonised area decreased for all patients after 12 hours as fibroblast had begun to migrate into the previously cell free wound, the maximum area was 3.06mm^2 and the minimum was 2.05mm^2, this demonstrated a lack of uniformity in cell migration between fibroblast populations as even at earliest time point assessed here there was significant patient variability. The largest differences in area between patients was observed following 24h after removal of the insert, the maximum area observed was 2.61mm^2 and the minimum was 0.82mm^2 thereby demonstrating large disparities in the wound closure between cleft patient derived fibroblasts; neonatal human dermal foreskin fibroblast (NHDFF) control cells displayed an average remaining area of 1.44mm^2 at 24h thereby displaying an intermediate rate of wound closure. As the variance between all samples was largest at 24 hours post insert removal (variance = 0.301mm^2) this time point to make comparisons between patient-to-patient differences in wound closure. After 48 hours some cleft fibroblasts had completely covered the wound whereas others still had a significant area uncolonised. The maximum area was 1.51mm^2, the NHDFF control had 0.72mm^2 remaining whilst others completely closed (0.00mm^2), suggesting some fibroblasts require significantly longer to complete wound closure thus demonstrating their clear differences in the ability of cleft fibroblasts to migrate into a wound between different cleft patients. This data demonstrates that despite initial similarity in the wound area at 0h cleft fibroblasts derived from different patients cover the wound at significantly different rates (n=9).

4.1.2 Hierarchical cluster analysis based on the percentage remaining wound area after 24 hours (RWA%) for all cleft patients

In order to analyse the differences and similarities in inferred fibroblast migration rates across the patient cohort, all data for each time point was subject to hierarchical cluster analysis which grouped patients according to the similarity of the data sets depicting results as a dendrogram (Figure 47). The data pertaining to the percentage remaining wound area after 24 hours (RWA%) was clustered into two statistically distinct groups; group A which comprised 17 patient samples and group B of 12 patient samples. Within group A sample RWA% ranged between 49.53%-83.34% whereas in group B RWA% ranged between 26.72%-48.88% thereby demonstrating considerable variation within clusters (Figure 48). When the RWA% for each patient's fibroblasts within their respective cluster was averaged it was found that group A had an average RWA% of 68.34% whereas group B had an average RWA% of 37.48% thereby demonstrating that fibroblasts in group A migrated more slowly when compared with those in group B ($p<0.001$) (Figure 49). As the slow migrating fibroblasts in group A comprised of 17 patient samples and the fast migrating fibroblasts in group B comprised of 12 patient samples, when averaging all of the experimental data for analysis and comparison of fast and slow cell populations, based on cluster membership, there was an n number of 51 for the slow group and an n number of 36 for the fast group as assays for each cleft sample were conducted in triplicate.

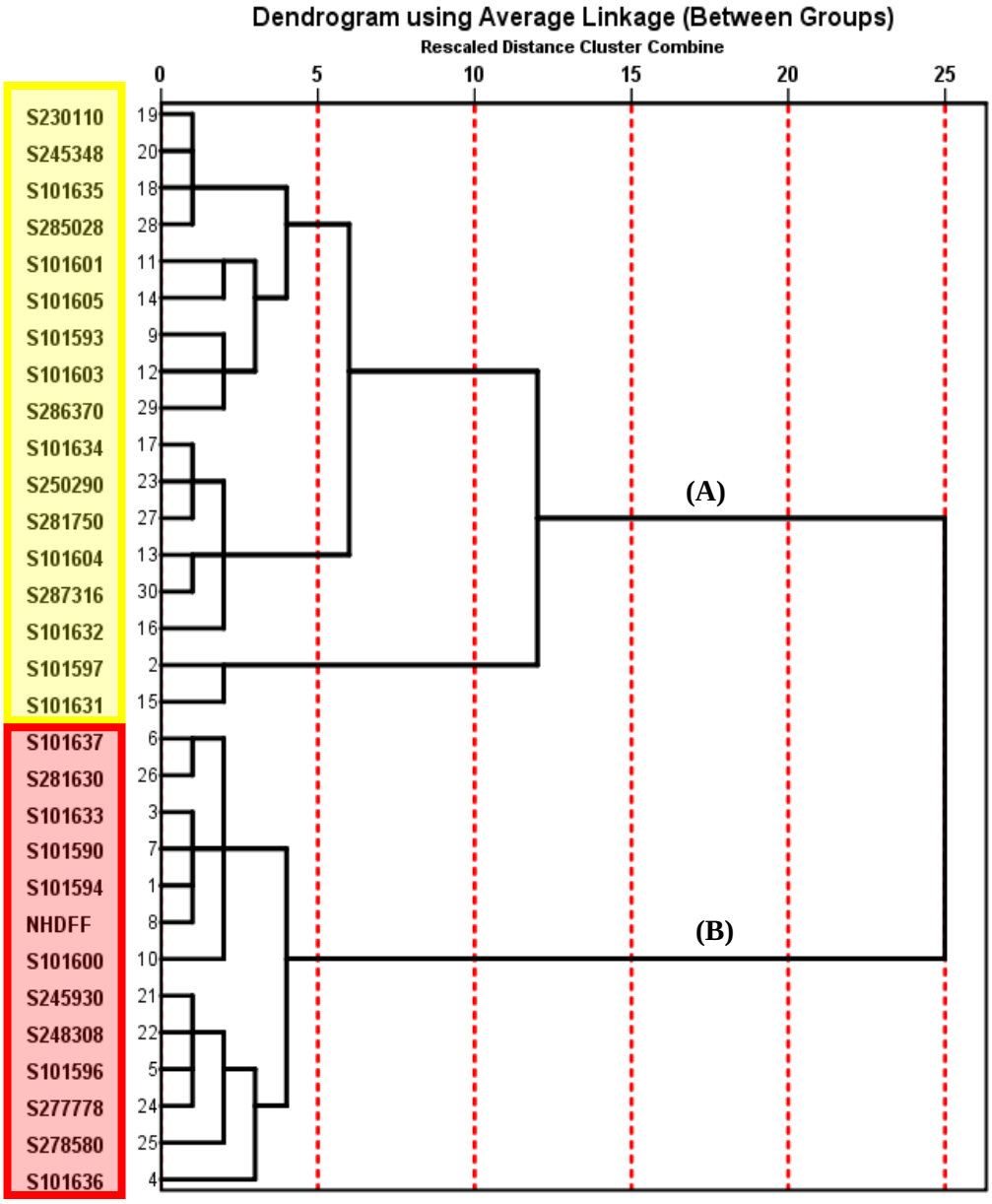

Figure 47: Dendrogram grouping patients based on the wound closure by cleft fibroblast at each time point. Hierarchical cluster analysis was employed to group patients based on the total area of wound closure of the initial 500µm wound at 0h, 12h, 24h and 48h. The number of clusters was not pre-determined thus cluster membership was based on data alone. The clustering method employed was the average linkage method and data was measured using the squared Euclidean distance interval. The dendrogram revealed the presence of two statistically distinct groups, Group A, which comprised 17 samples and group B, which comprised 12 samples and the age matched NHDFF control. This data suggests that cleft fibroblasts differ significantly based on wound closure and can be categorised as fast migrating fibroblasts, which is group B, and slow migrating fibroblasts, which is group A. For ease of comparison, the slow group was coloured yellow and the fast group was coloured red and this was used for all future comparisons.

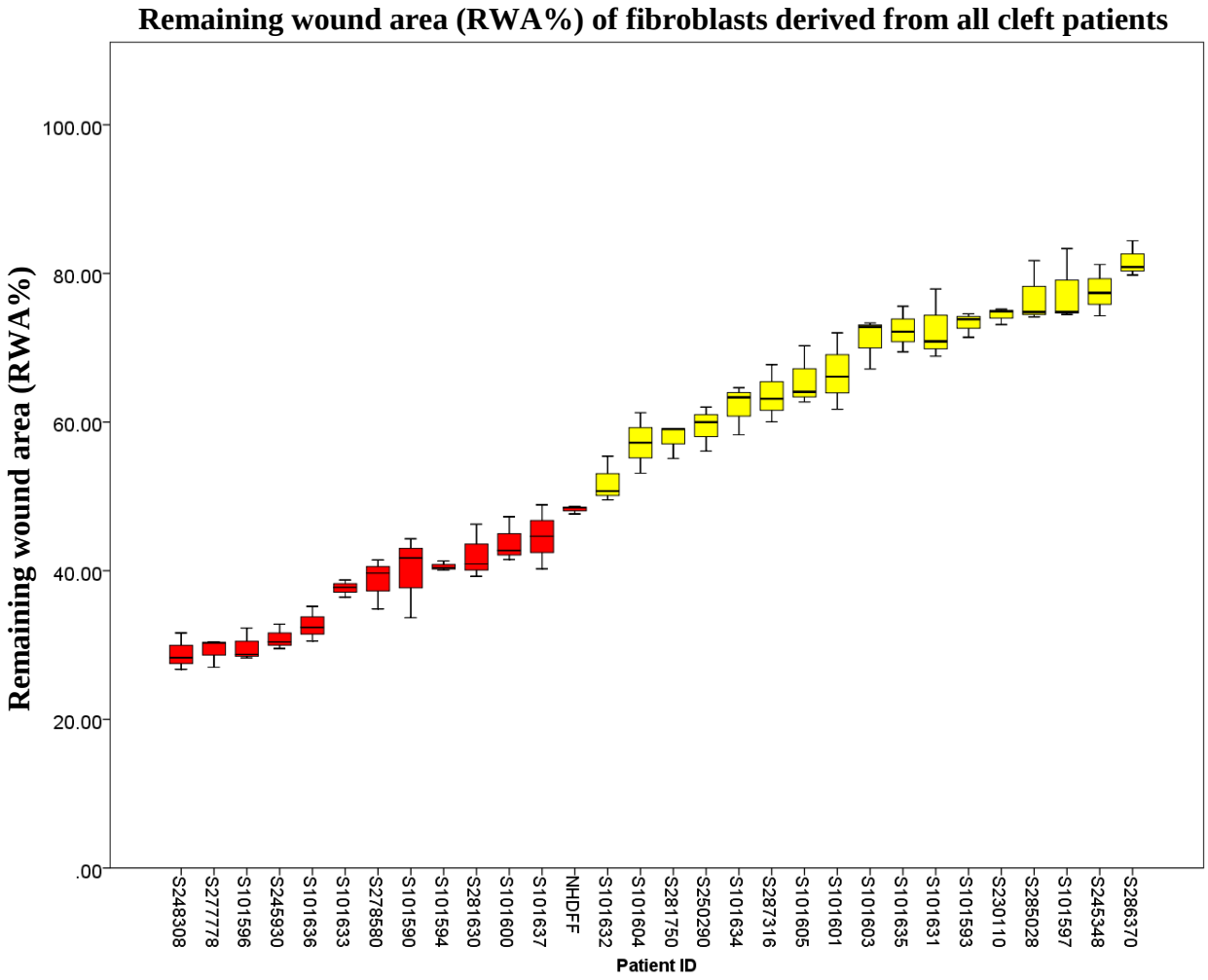

Figure 48: Remaining wound area after 24 hours for all cleft fibroblast samples. Cell migration was expressed as a percentage of the wound area uncolonised at 24 hours when compared with total area at 0 hours, thus accounting for the slight variance in initial starting area. The fibroblast samples have been ordered from fastest migrating (smallest RWA%) to slowest migrating (largest RWA%). The two groups determined by cluster analysis have been coloured based on cluster membership (red = fast; yellow = slow). The NHDFF control was clustered into the fast group however it was the slowest migrating sample within the fast group due to having the largest RWA% after 24 hours (n=9).

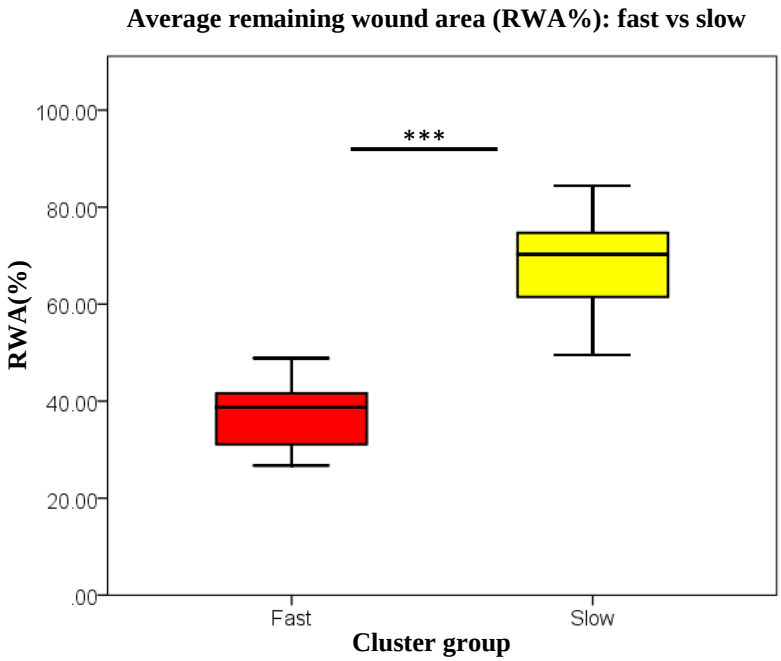

Figure 49: Average RWA% for all cleft fibroblast samples in fast and slow migrating groups. The average RWA% of the fast migrating group was 37.48% whereas the slow group had an average RWA% of 68.34%. This difference in average RWA% was shown to be significant ($p<0.001$) as determined by an independent samples t-test with a two tailed distribution (Fast group: n=36; slow group: n=51).

4.1.3 Analysis of RWA% and cluster membership between cleft types

When comparing the RWA% from fibroblasts derived from patients with different cleft types it was found that fibroblast samples derived from patients with CL displayed significantly lower RWA% when compared with fibroblasts derived from CLP(L) ($p<0.01$), CLP(P) ($p<0.01$) and CP ($p<0.01$) patients (Figure 50A). In addition, all fibroblasts derived from CL patients were clustered within the fast migrating cluster (Figure 50B) thus demonstrating that all CL derived fibroblasts have low RWA% and share a degree of similarity. This data suggests that, in terms of inferred motility rates derived from RWA%, fibroblasts derived from the CL phenotype may be physiologically distinct from fibroblasts derived from other cleft phenotypes due to their elevated migration rates. In addition, cells from CLP(L) patients, which were shown to have significantly less average RWA% when compared with the anatomically similar CL, demonstrated significantly higher RWA% when compared with cells from CLP(P) ($p<0.05$) and CP patients ($p<0.05$). Despite this, cluster analysis placed 3 CLP(L) derived fibroblasts in the fast cluster and 6 in the slow cluster thus demonstrating variability in migratory speeds within this group. Cluster analysis also placed 4 CP derived fibroblasts in the slow cluster and 1 in the fast cluster whereas fibroblasts derived from CLP(P) had 7 in the slow cluster but only 2 in the fast cluster thus suggesting a greater degree of similarity in the RWA% between patients of these cleft types. This data suggests the differences in RWA% observed in fibroblast samples derived from CLP(L), CLP(P) and CP may be potentially due to individual biological variation of primary cells and not the cleft phenotype from which they were derived. Additionally, fibroblasts derived from patients with RUCLP demonstrated significantly lower RWA% when compared with BLCLP ($P<0.05$) but not LUCLP (Figure 50C-D).

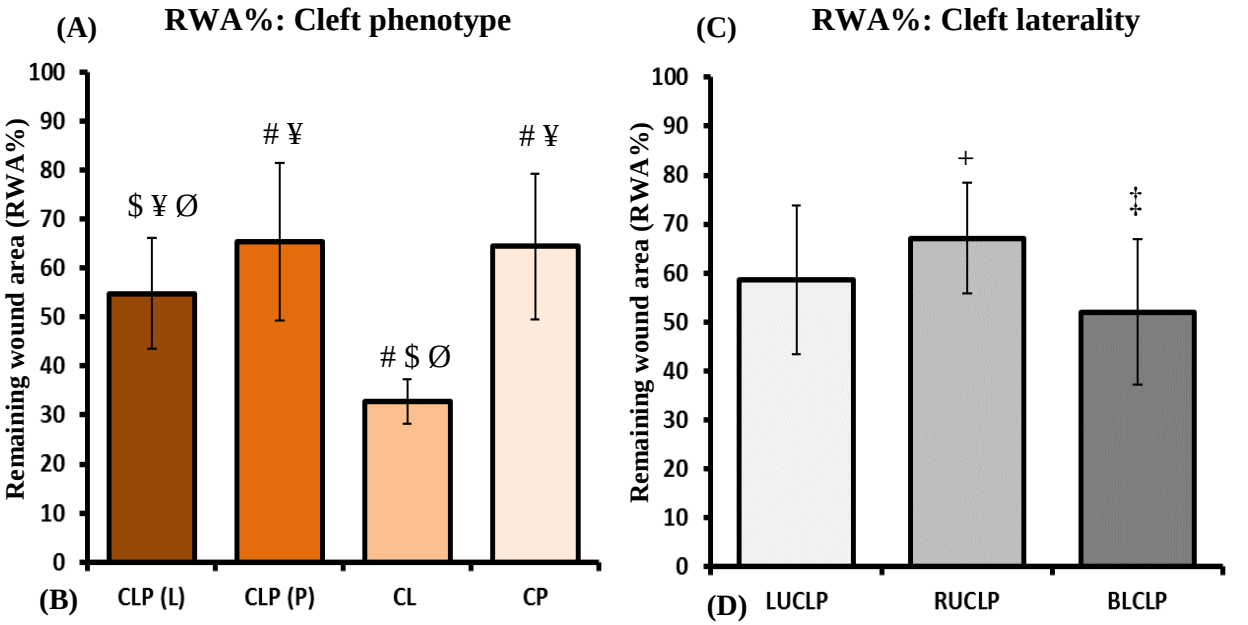

Cleft phenotype		
Type	Fast	Slow
CLP (L)	3	6
CLP (P)	2	7
CL	6	0
CP	1	4

Cleft laterality		
Type	Fast	Slow
LUCLP	2	4
RUCLP	1	6
BLCLP	2	3

Figure 50: Average RWA% between cleft types. (A) Fibroblasts isolated from CLP(P) and CP cleft patient tissues demonstrated significantly slower overall migration when compared with both CLP(L) and CL derived fibroblasts; CL fibroblasts migrated at significantly faster rates than all other cleft types. (B) Fibroblasts from each cleft type were present in both fast and slow migrating groups except CL fibroblasts which were all grouped into the fast migrating cluster. (C) Migration rates between LUCLP and RUCLP patients were similar whilst fibroblasts derived from BLCLP patients were significantly faster than RUCLP but not LUCLP. (D) Fibroblasts were present in both slow and fast clusters regardless of cleft laterality; however, most RUCLP derived fibroblasts were clustered into the slow migrating group. Significant differences were determined by means of student's t-test where: # = $p<0.05$ relative to CLP(L) (n=27); $ = $p<0.05$ relative to CLP(P) (n=27); ¥ =$p<0.05$ relative to CL (n=18); Ø = $p<0.05$ relative to CP (n=15); † = $p<0.05$ relative to LUCLP (n=18); ‡ = $p<0.05$ relative to RUCLP (n=21) and + = $p<0.05$ relative to BLCLP (n=15).

4.2 Assessment of the potential effect of cell proliferation on RWA%

To assess whether cell proliferation contributed to the differences in RWA% observed between cells from the different cleft patients, the RWA% was compared with the doubling time (DT) for each patient (which were previously established through growth curve analysis). It was found that there was significant overlap in the DT between patients in the fast and slow group; the DT in the fast group ranged between 26.32 hours and 30.68 hours whereas the slow group DT ranged between 26.11 and 32.41 (Figure 51A-B). It was shown that there were no significant differences in the average DT between the fast and slow groups. Further, Pearson's correlation analysis revealed that there were no significant correlations between RWA% and DT (correlation coefficient = 0.189) suggesting that DT does not influence RWA%. In addition, an Ibidi wound healing assay was repeated with both Mitomycin C, an agent known to inhibit cell proliferation, treated and untreated fibroblasts and the RWA% was compared (data not presented here). No significant difference between the treated and untreated groups was identified with a student's t-test with two-tailed distribution (p = 0.901).

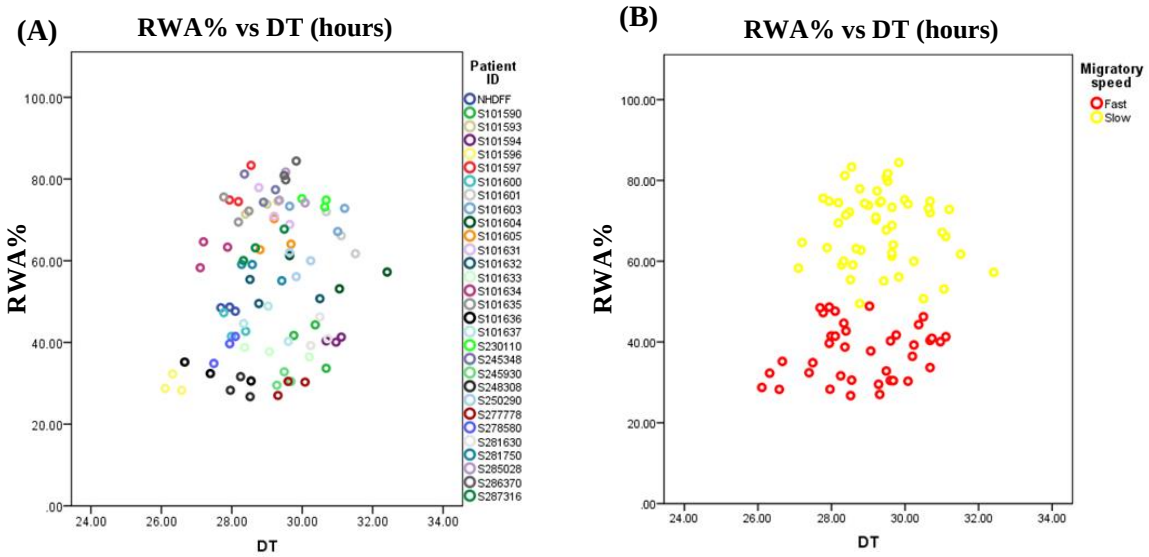

Figure 51: Scatterplots of RWA% vs doubling time. (A) The RWA% and population doubling time for each patient. (B) When patients were clustered based on migratory speed there was significant overlap in the DT between fast and slow groups.

4.3 Analysis of cytoskeletal related components in fast and slow groups

As actin is a major component of the cell cytoskeleton and is fundamental to the processes involved in cell motility, the intracellular cytoskeletal F-actin levels were quantified in fibroblasts from three patients in each of the fast and slow migrating groups. The F-actin levels were normalised to cell number and whilst total F-actin was variable, there was significantly more total F-actin found on average in the fast migrating fibroblasts when compared with the slow migrating fibroblasts ($p<0.001$) as determined by an individual samples t-test with a two tailed distribution (Figure 52A-H). When comparing cleft types, it was shown that there were no significant differences in the total F-actin levels within tissue samples when comparing CP and CL (Figure 53A-G). This suggests that although increased actin may be associated with elevated fibroblast migration, it is unlikely that differences in actin are associated with cleft phenotype and the significantly increased RWA% observed in CL derived fibroblasts relative to other cleft types.

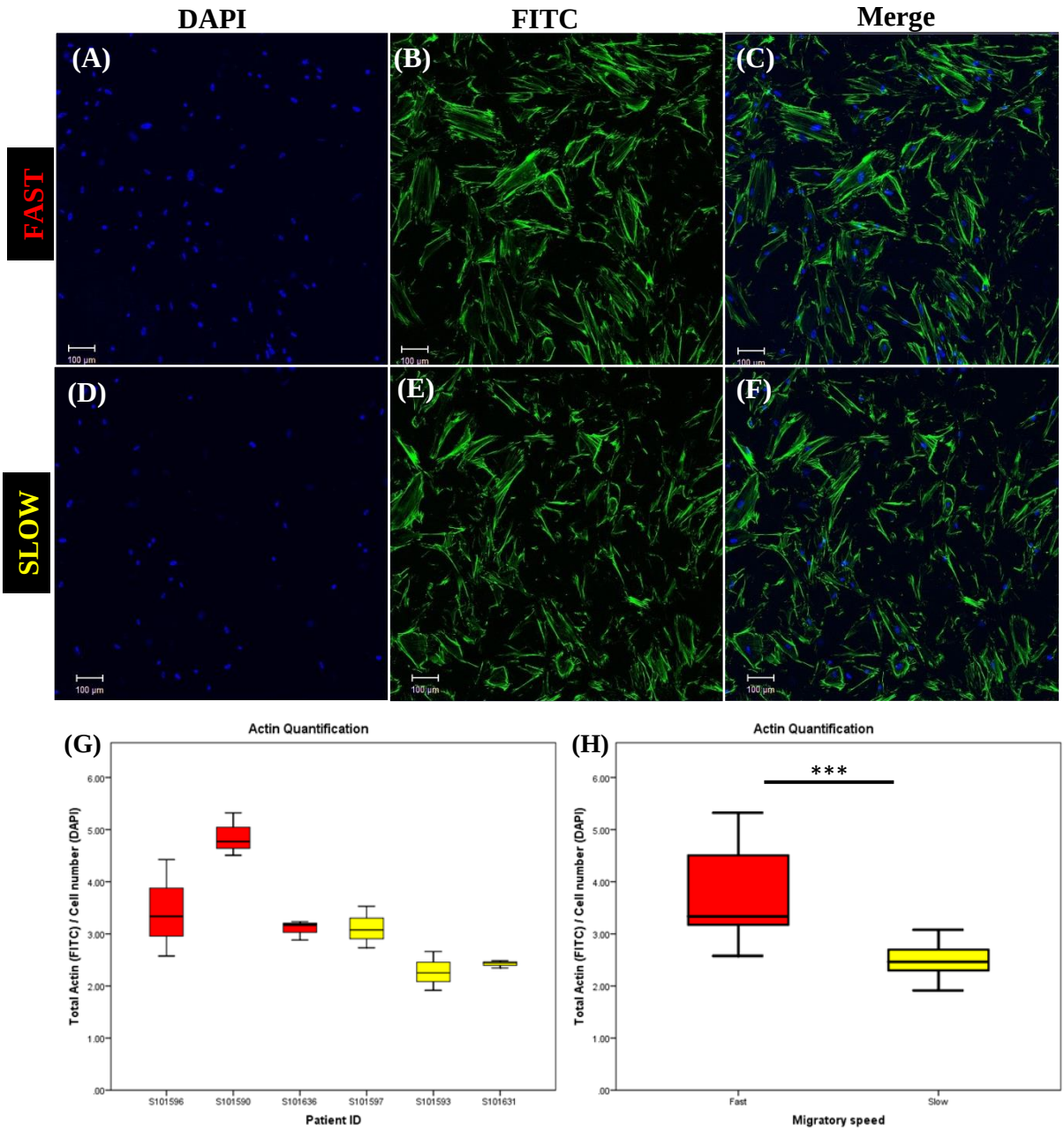

Figure 52: Quantification of total cytoskeletal F-actin levels in both fast and slow cleft fibroblast groups using phalloidin staining. Three patients from both the fast and slow groups were selected for analysis. Representative images from the fast group (A-C) and the slow group (D-F) depicted the locations of individual cell nuclei (DAPI staining cell nuclei blue) the distribution of F-actin within individual cellular cytoskeletons (FITC staining F-actin green). (G) Each patient's actin levels were quantified in terms of integrated density and presented as a ratio of total F-actin to cell number. (F) Averaging data from each group revealed there was a significant difference ($p<0.001$) in F-actin levels between fast and slow groups as determined by an individual samples t-test with a two tailed distribution (n=9).

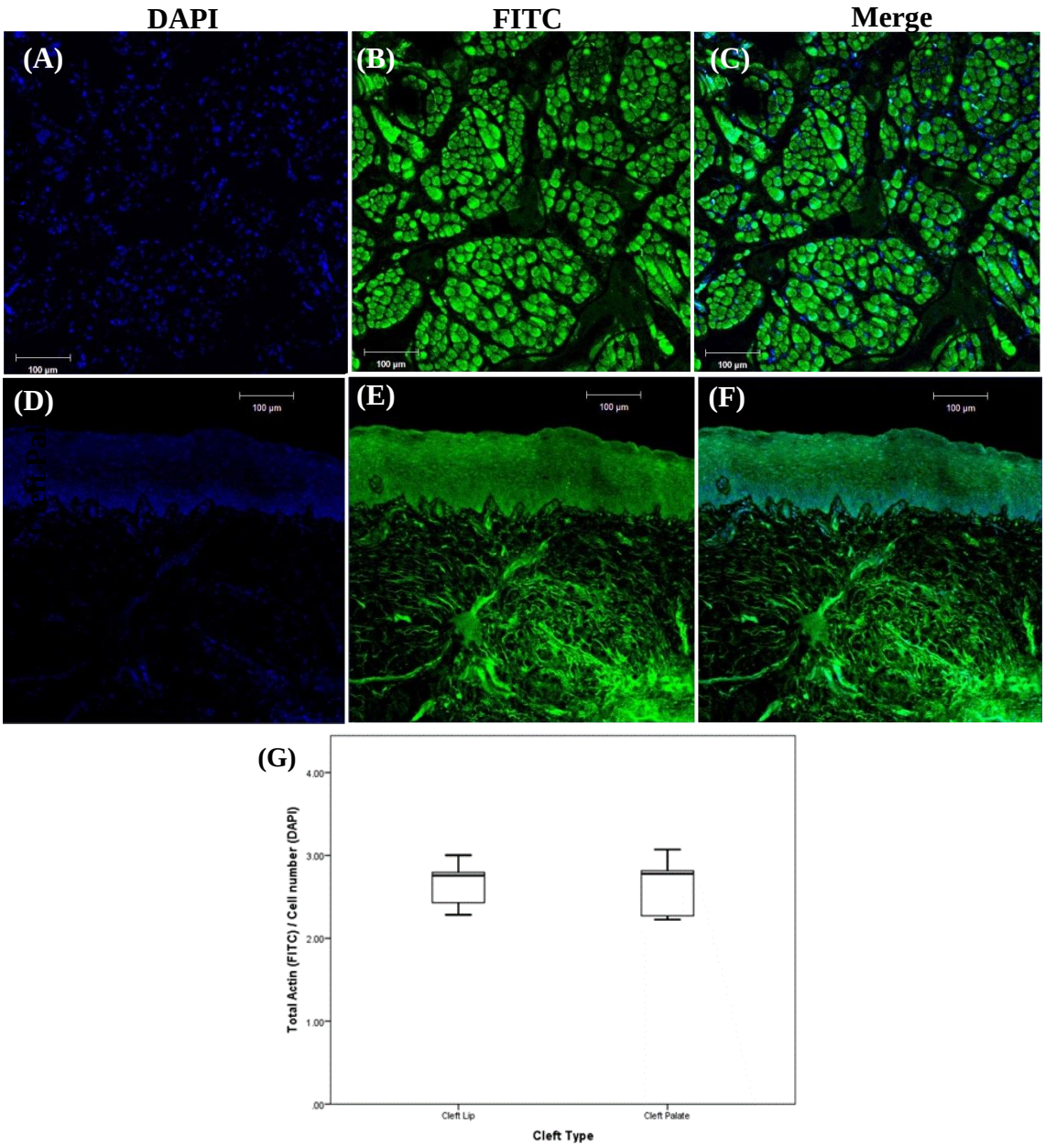

Figure 53: Quantification of total cytoskeletal F-actin levels in both cleft lip and cleft palate tissue sections. (A-C) Mucosal tissue sections from cleft lip and mucosal tissue sections from patients with cleft palates (D-F) were stained with DAPI (blue) and phalloidin bound fluorescein conjugates (green) to reveal the distribution of F-actin within each section. (G) Quantification of F-actin revealed no significant difference in the amount of F-actin present when comparing cleft lip and cleft palate tissue section (n=6).

4.3.1 Assessment of *ACTA1* and *TUBA1* expression

As there were significantly greater total amounts of F-actin per cell within fast migrating fibroblasts relative to slow migrating fibroblasts, actin expression (*ACTA1*) was assessed by means of real time PCR in cleft fibroblasts for all cleft patients. There was considerable variability in the expression levels of *ACTA1* in fibroblasts from the 29 patients as the highest fold change, relative to the age-matched control, was 8.61 whereas the lowest was 1.42. When the patients were grouped according to migratory speed no significant differences were identified between the fast group and the slow group suggesting that *ACTA1* expression was not related to migratory speed (Figure 54A-B). *TUBA1* expression was also assessed as tubulin is also major component of the cytoskeleton and often works in conjunction with actin filaments to aid in motility. Tubulin expression was variable with the fold changes, relative to control, ranging between 5.09 and the lowest being 0.75 thereby suggesting significantly lower expression in some cleft patients. When *TUBA1* expression levels were grouped based on fibroblast migratory speeds the fast migrating fibroblasts generated significantly higher overall expression when compared with the slow migrating fibroblasts ($p<0.01$) as determined by an independent samples t-test with a two-tailed distribution, this suggests that *TUBA1* expression is higher in patients in fast migrating fibroblasts (Figure 55A-B). Spearman's rho analysis showed no correlation between *ACTA1* and *TUBA1* expression (correlation coefficient = 0.041) nor differences in expression of *ACTA1* or *TUBA1* between cleft phenotypes. *TUBA1* expression did differ based on cleft laterality as RUCLP patients exhibited significantly lower expression when compared with both LUCLP and BLCLP ($p<0.01$) (Figure 56A-D).

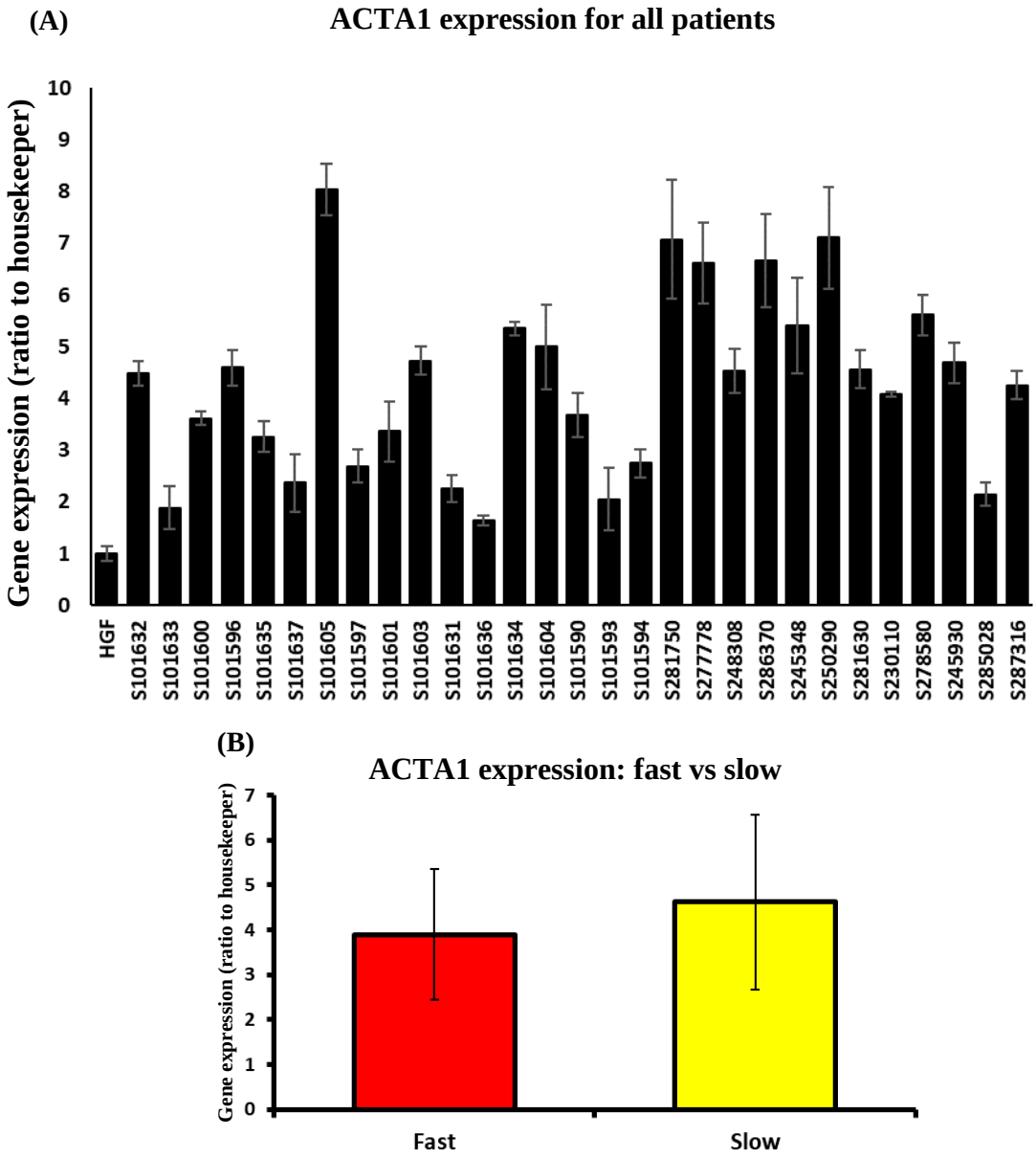

Figure 54: Expression levels of *ACTA1*. (A) Expression levels of *ACTA1* were variable in cells from the whole patient cohort yet the expression levels were all higher than found in the HGF control. The maximum fold change was 8.61 and the minimum was 1.42 indicating considerable patient-to-patient variability. (B) Average expression levels between fast and slow migratory groups revealed that there was no significant difference in *ACTA1* expression as determined by an independent samples t-test with a two tailed distribution. (Fast group: n=36; slow group: n=51).

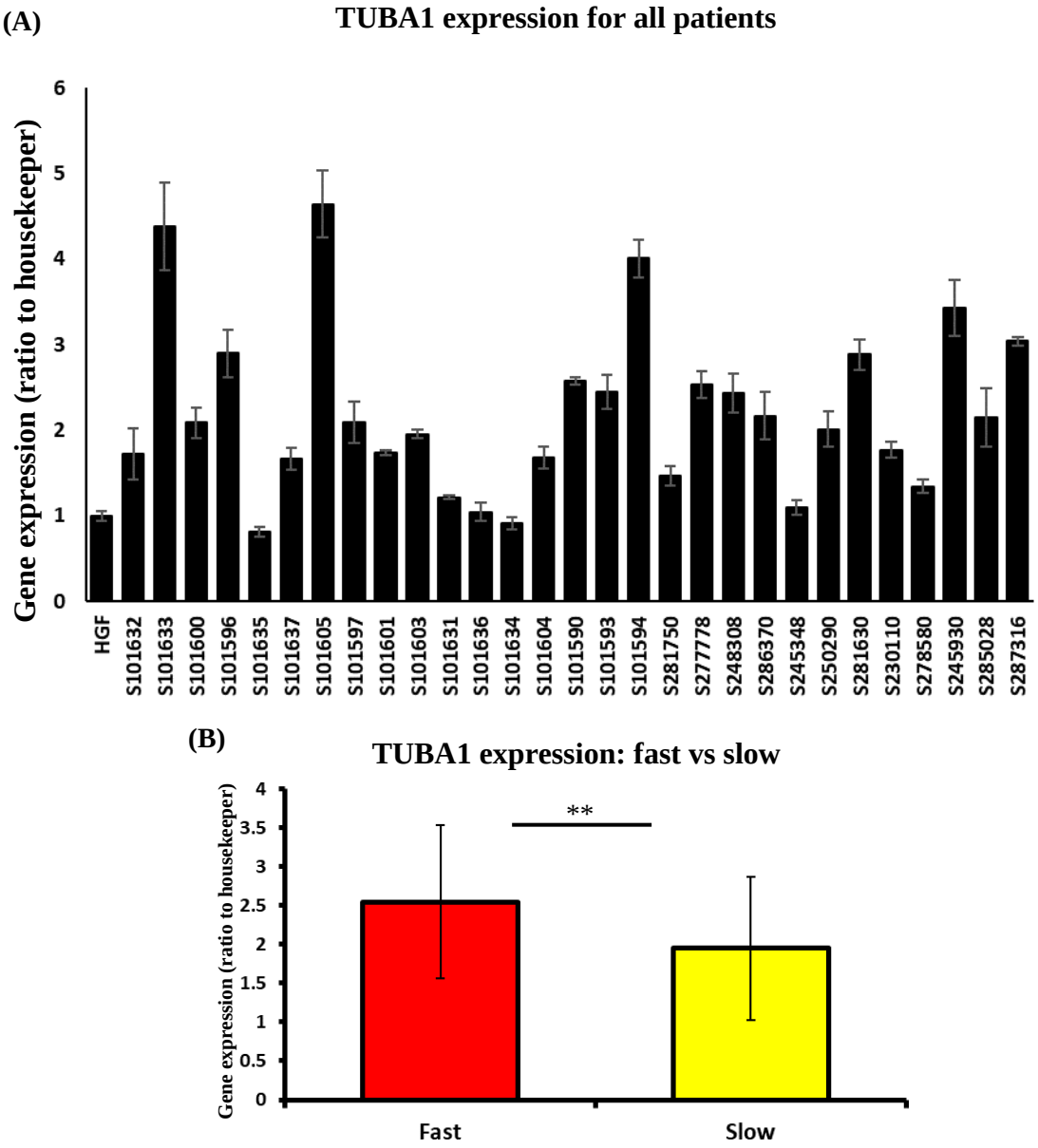

Figure 55: Expression levels of *TUBA1*. (A) Expression levels of *TUBA1* in fibroblasts from the entire patient cohort were variable. Most expression levels were greater than found in the HGF control though there were a number of outliers with lower expression levels. The maximum fold change was 5.09 and the minimum was 0.75 indicating considerable variability between cleft patients. (B) Average expression levels of *TUBA1* revealed that there is a significant difference between fast and slow groups ($p<0.01$) as determined by an independent samples t-test with a two-tailed distribution. (Fast group: n=36; slow group: n=51).

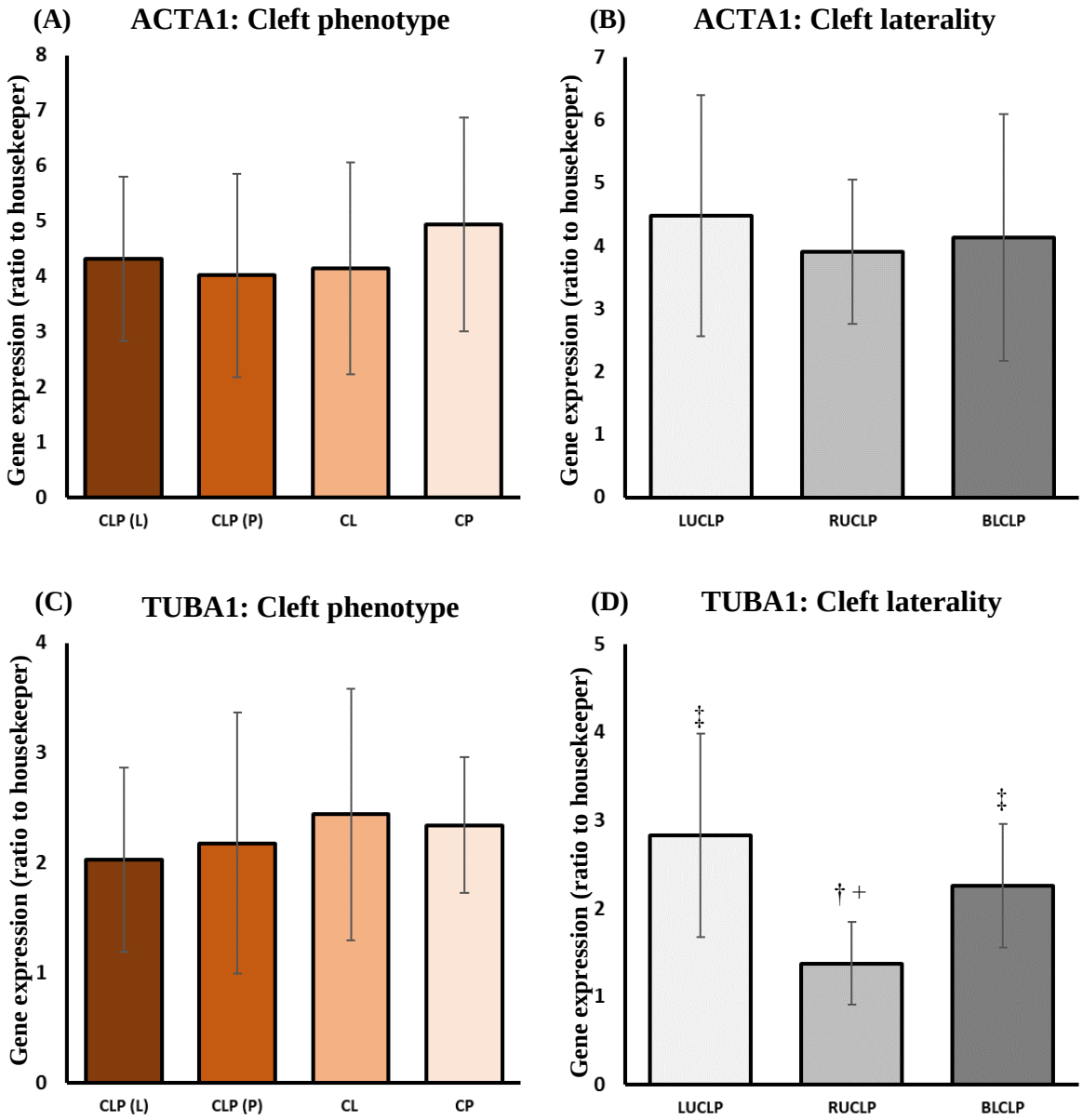

Figure 56: *ACTA1* and *TUBA1* expression between cleft types. (A) *ACTA1* expression was comparable between both cleft types (B) and laterality. (C) There were no significant differences in *TUBA1* expression between cleft types (D) *TUBA1* expression was significantly lower in fibroblasts from patients with RUCLP when compared with both LUCLP and BLCLP. Significant differences were determined by means of student's t-test where: † = $p<0.05$ relative to LUCLP (n=18); ‡ = $p<0.05$ relative to RUCLP (n=21) and + = $p<0.05$ relative to BLCLP (n=15).

4.3.2 Expression of *RAC1, RHOA* and *CDC42*

Regulation of cytoskeletal dynamics, including reorganization of actin and tubulin, is largely controlled by the Rho family of GTPases which interact with downstream effectors to stimulate conformational change; *RAC1*, *RHOA* and *CDC42* are the primary influencers in terms of migration. *RAC1* expression in fibroblasts from each cleft patient revealed large differences in expression levels between samples. Some fibroblasts demonstrated fold changes greater than nine relative to the HGF control, whilst others showed expression levels similar to the control resulting in large standard deviations. There was no significant correlation between RWA% and *RAC1* expression (correlation coefficient = -0.328). It was shown that the *RAC1* expression in fibroblasts from patients with both CL and CP were significantly higher than the cells from patients that demonstrated the CLP(L) phenotype despite CL and CLP(L) both being lip derived fibroblasts (Figure 57A-C). The expression of *RHOA* was just as variable and there was no significant correlation identified between *RHOA* expression and RWA% (correlation coefficient = 0.054). The variability in terms of *RHOA* expression was not identified to be due to the cleft phenotype (Figure 58A-C). The expression of *CDC42* was less variable when compared with *RAC1* and *RHOA* and there was no correlation between *CDC42* expression and RWA% (correlation coefficient = -0.196). With data averaged, CL and CP cleft phenotypes demonstrated significantly higher *CDC42* expression when compared with CLP(P) despite CP and CLP(P) both being palatal derived fibroblasts (Figure 59A-C). When comparing cleft laterality, fibroblasts from patients with RUCLP consistently demonstrated significantly lowered expression of *RAC1*, *RHOA* and *CDC42* when compared with both LUCLP and BLCLP and interestingly, RWA% was also significantly higher in cultures from patients with RUCLP when compared with those with BLCLP suggesting a possible negative correlation. When patients were grouped based on migratory speed, it was found that, despite average expression of *RAC1* being higher in the slow group (p=0.06), there were no significant

differences in *RAC1*, *RHOA* and *CDC42* expression between fast and slow migrating fibroblasts (Figure 60A-C).

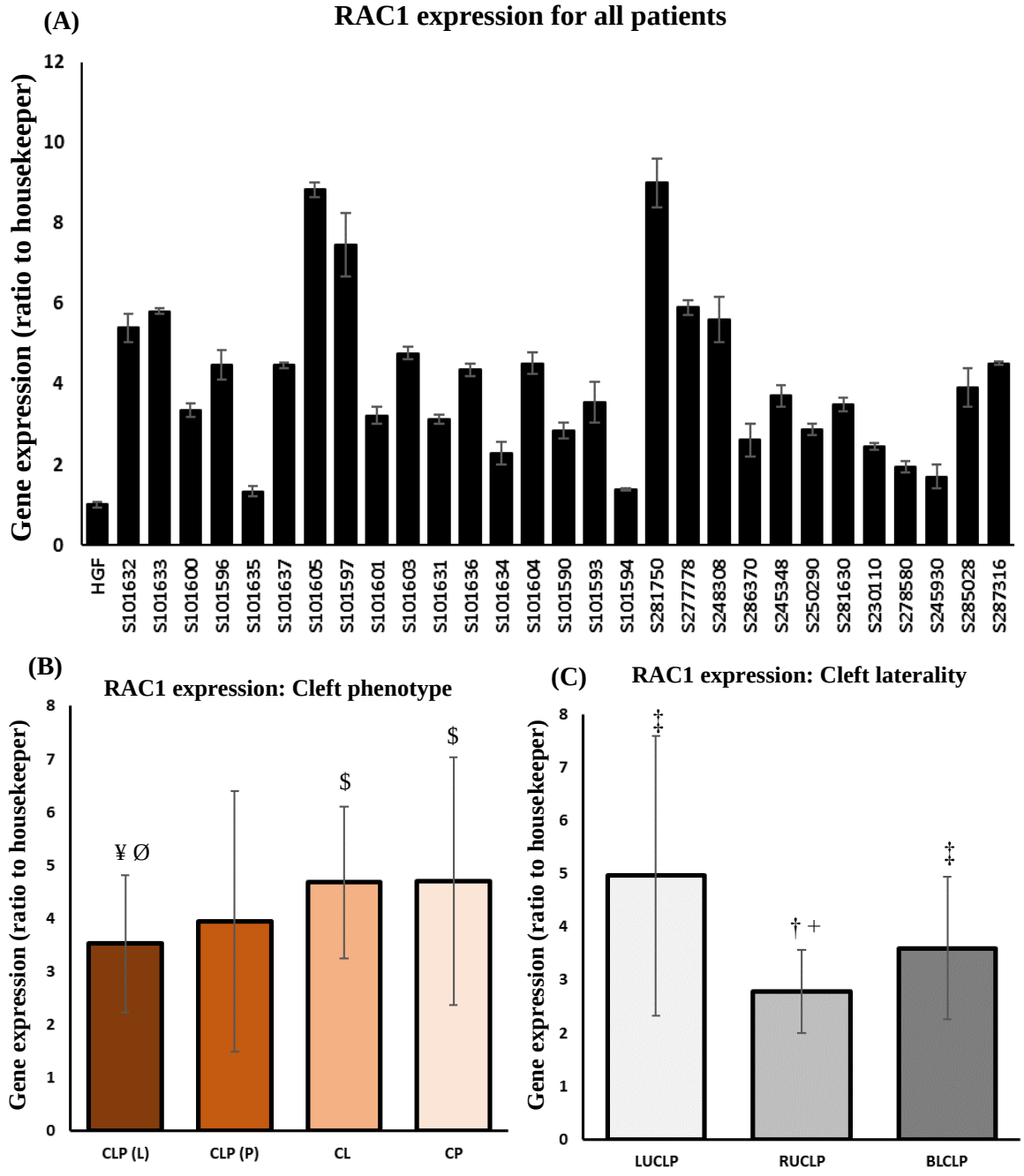

Figure 57: Expression of *RAC1* between cleft patients. (A) expression of *RAC1* was highly variable between cleft patients with a maximum fold change of 9.41 and a minimum of 1.19 indicating considerable differences between patients. (B) CL and CP patients shared similar expression levels *RAC1* both of which were significantly higher than CLP (L). (C) *RAC1* expression was significantly lower in patients with RUCLP when compared with both LUCLP and BLCLP. Significant differences were determined by means of student's t-test where: # = $p<0.05$ relative to CLP(L) (n=27); $ = $p<0.05$ relative to CLP(P) (n=27); ¥ =$p<0.05$ relative to CL (n=18); Ø = $p<0.05$ relative to CP (n=15); † = $p<0.05$ relative to LUCLP (n=18); ‡ = $p<0.05$ relative to RUCLP (n=21) and + = $p<0.05$ relative to BLCLP (n=15).

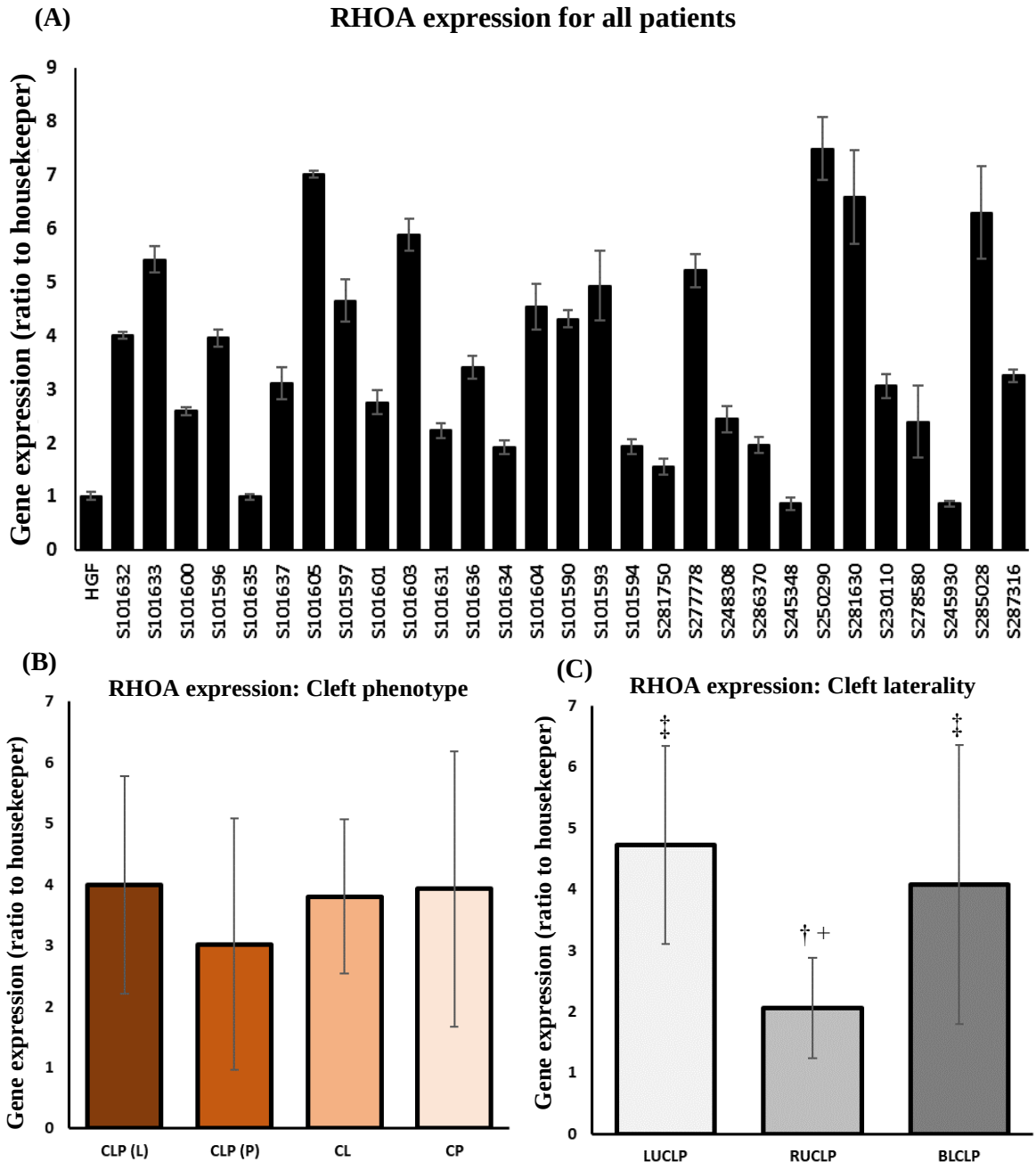

Figure 58: Expression of *RHOA* between cleft patients. (A) overall *RHOA* expression differed considerably in fibroblasts from different cleft patients. The highest fold change was 8.16 and the lowest was 0.77 indicating large patient variation. (B) There were no significant differences in *RHOA* expression between cleft phenotypes. (C) *RHOA* expression was significantly lower in patients with RUCLP relative to both LUCLP and BLCLP. Significant differences were determined by means of student's t-test where: † = $p<0.05$ relative to LUCLP (n=18); ‡ = $p<0.05$ relative to RUCLP (n=21) and + = $p<0.05$ relative to BLCLP (n=15).

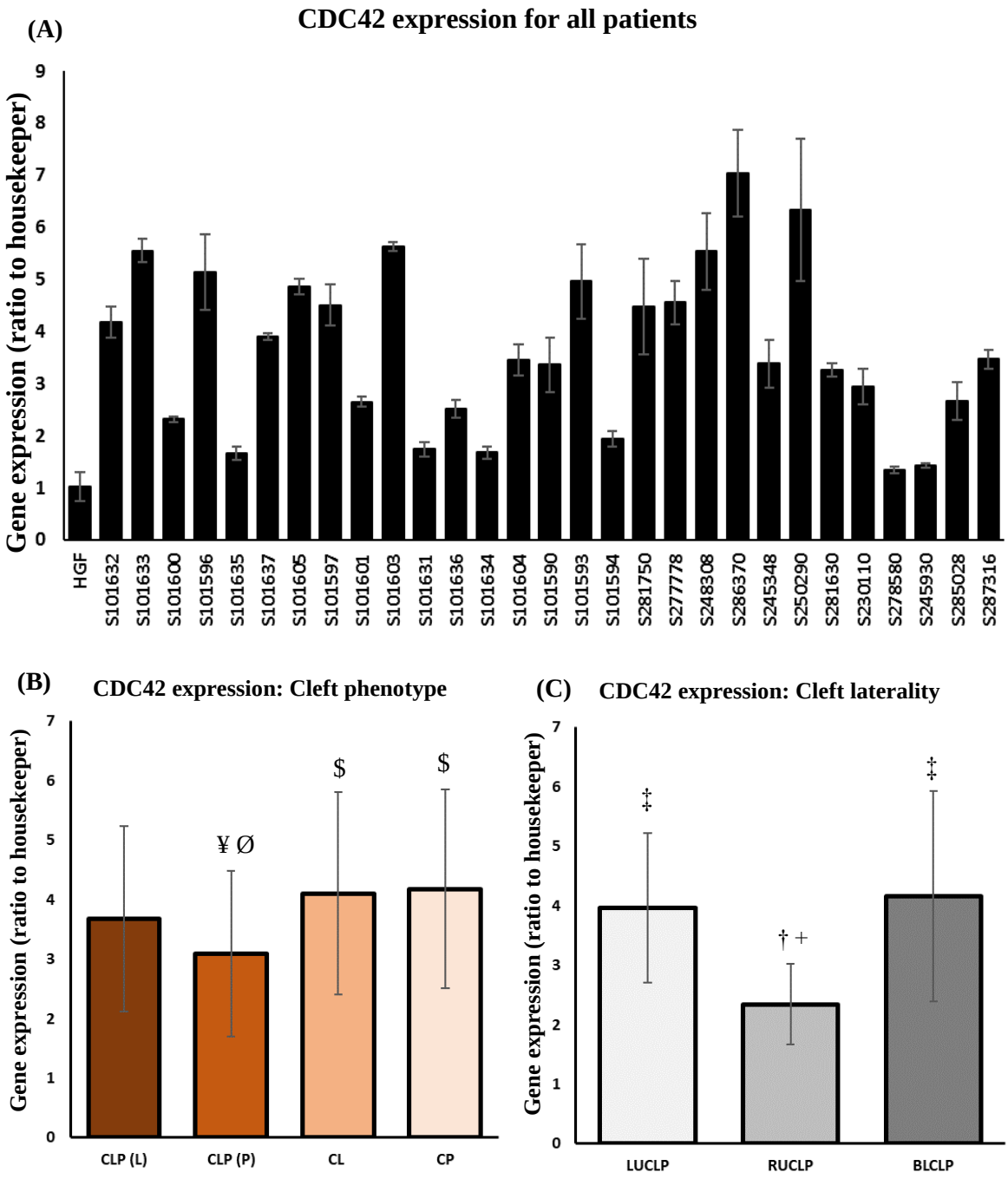

Figure 59: Expression of *CDC42* between cleft patients. (A) There were large variations observed in *CDC42* expression between samples established from different cleft patients outlined by the differences between the highest fold change was of 7.96 and the lowest of 1.29. (B) Patients with CL and CP shared similar levels if expression both of which were shown to be significantly higher than that of CLP (P) but not CLP (L). (C) Patients with RUCLP had significantly lower overall expression when compared with both LUCLP and BLCLP. Significant differences were determined by means of student's t-test where: # = $p<0.05$ relative to CLP(L) (n=27); $ = $p<0.05$ relative to CLP(P) (n=27); ¥ =$p<0.05$ relative to CL (n=18); Ø = $p<0.05$ relative to CP (n=15); † = $p<0.05$ relative to LUCLP (n=18); ‡ = $p<0.05$ relative to RUCLP (n=21) and + = $p<0.05$ relative to BLCLP (n=15).

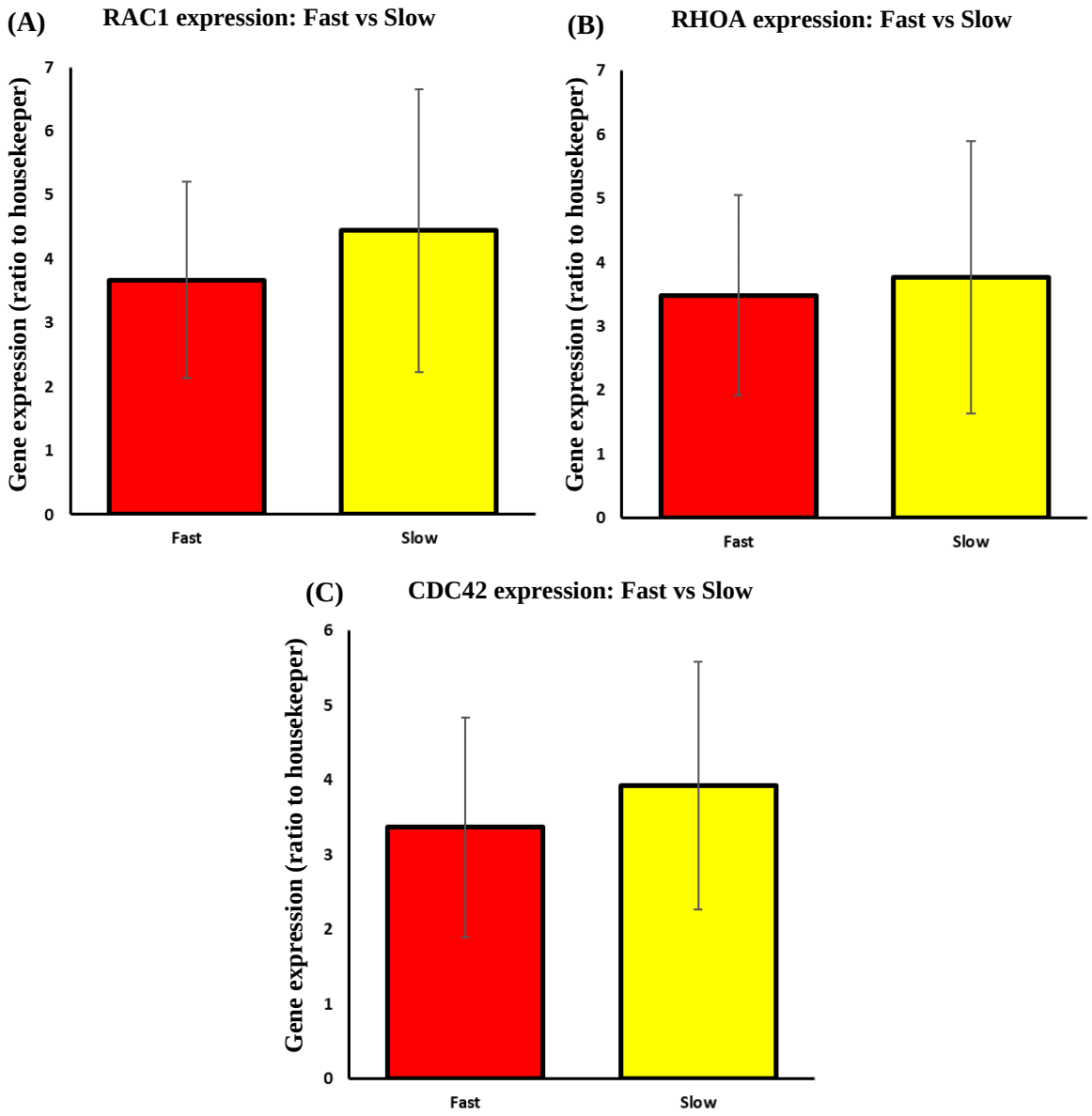

Figure 60: Average expression of *RAC1*, *RHOA* and *CDC42* between patient fibroblast samples clustered into fast and slow migrating groups. (A) Although slow migrating cleft fibroblasts expressed higher *RAC1* on average this was shown to be not statistically significant ($p = 0.06$). (B) *RHOA* expression was similar between fast and slow clusters, as was expression of *CDC42* (C). (Fast group: n=36; slow group: n=51).

4.4 Analysis of ECM production and expression between fast and slow groups

ECM production and expression was compared between fast and slow migrating fibroblasts. Average total collagen protein production, determined by staining mitomycin C treated fibroblast samples with Sirius red after seven days in culture, was greater in fast migrating fibroblasts (mean = 174.53μg) when compared with slow migrating fibroblasts (mean = 162.60μg) and this difference was shown to be significant by means of an independent samples t-test with two-tailed distribution ($p<0.001$). Further, expression of *COL3A1* was significantly lower in the fast group when compared with the slow group thereby suggesting that whilst more rapidly migrating fibroblasts secreted more total collagen overall than the slower migrating fibroblasts, the expression level of *COL3A1* was lower than the slow group. No significant differences were identified between fast and slow migrating fibroblasts for expression of any other collagen types assessed here (Figure 61A-C). Pearson's correlation analysis between RWA% and collagen production reinforced earlier findings as there was a significant negative correlation between RWA% and collagen production (correlation coefficient = -0.454; $p<0.01$) which suggested that cultures with higher RWA%, which migrated at slower rates, also synthesised less collagen whereas cultures with lower RWA%, which had faster migrating fibroblasts, secreted greater amounts of collagen (Figure 62). Glycosaminoglycan production was shown to be similar between fast and slow migrating groups. However, expression of *CSPG4* was significantly lower in the fast group relative to the slow group whereas both *DSE* and *HSPG2* were similar between migratory groups (Figure 63A-D). Whilst expression of elastin was comparable between and slow migrating groups, expression of *FN1* was significantly lower in fast migrating cleft relative to their slow migrating counterpart (Figure 64A-B).

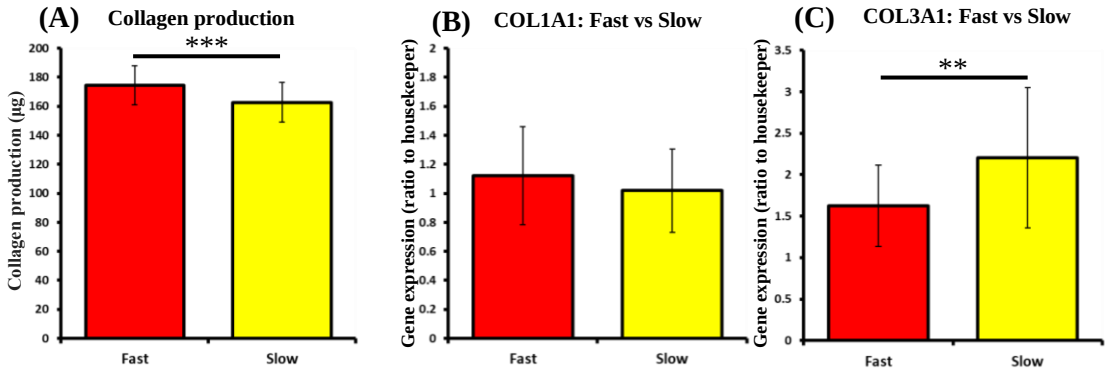

Figure 61: Comparison of collagen production and gene expression between fast and slow migratory groups. (A) Collagen production was generally higher in the fast migratory group when compared with the slow migratory group. This difference was deemed significant ($p<0.001$) by means of Welch's t-test with a two tailed distribution. (B) *COL1A1* expression was similar in both the fast group and slow group with no significant difference. (C) *COL3A1* expression was lower in the fast migratory group when compared with the slow migratory group, this difference was significant ($p<0.01$) as determined by an independent samples t-test with a two tailed distribution. (Fast group: n=36; slow group: n=51).

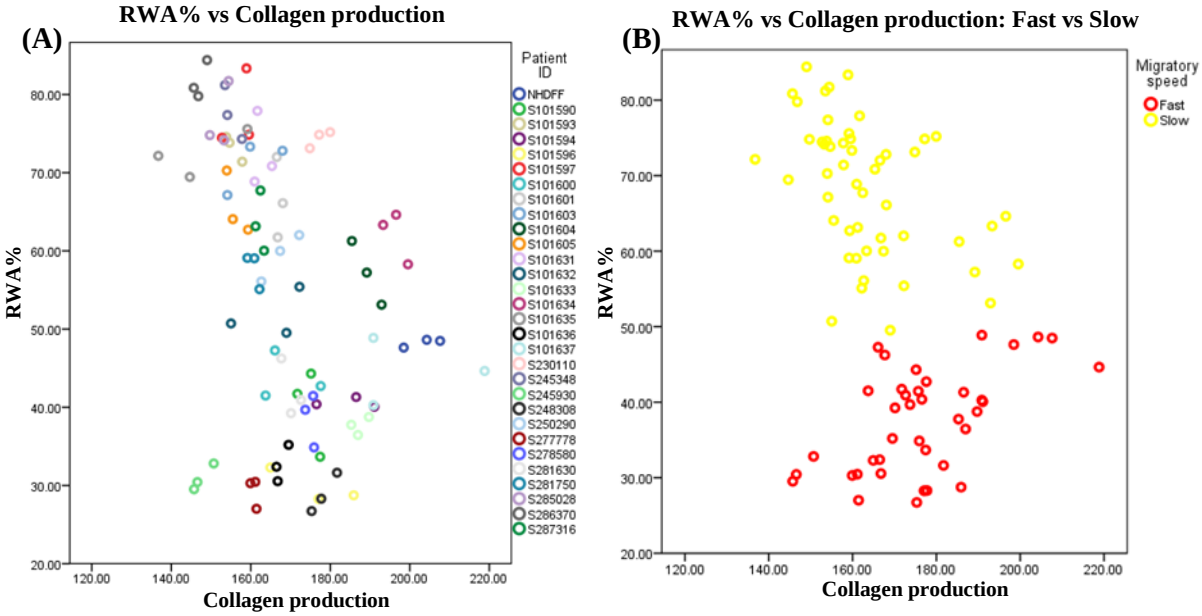

Figure 62: RWA(%) vs collagen production. (A) RWA% and collagen production for all patients compared by means of a scatterplot. (B) RWA% and Collagen production when patient fibroblasts are clustered based on their migratory speed. Data was determined to be non-parametric by means of a shapiro-wilko normality test. Bivariate correlation using Spearman's rho analysis revealed there was a significant negative correlation between RWA% and collagen production (correlation coefficient = -0.454; $p<0.01$). Suggesting patients with a higher RWA%, thus slower migrating cells, have lower total collagen production.

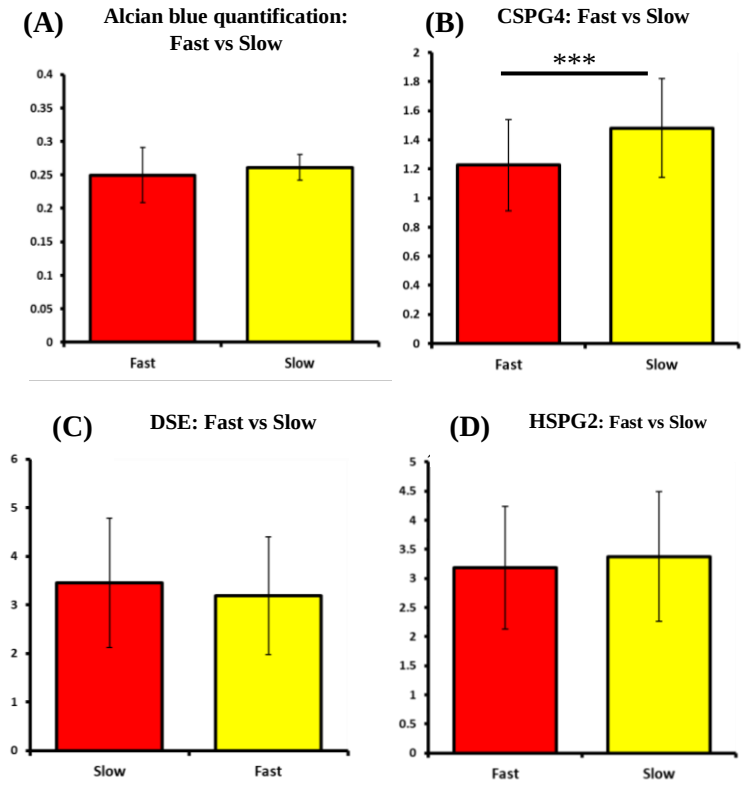

Figure 63: Comparison of sulphated glycosaminoglycan production and expression between fast and slow migratory groups. (A) Sulphated glycosaminoglycan production was similar for both fast and slow groups with no significant difference. (B) *CSPG4* expression was lower in the fast group when compared with the slow group, this difference was significant ($p<0.01$) as determined by the independent samples t-test with two tailed distribution. (C) *DSE* expression was comparable for both the fast and slow migrating groups with no significant difference. (D) *HSPG2* expression was also statistically similar in both the fast and slow migrating. (Fast group: n=36; slow group: n=51).

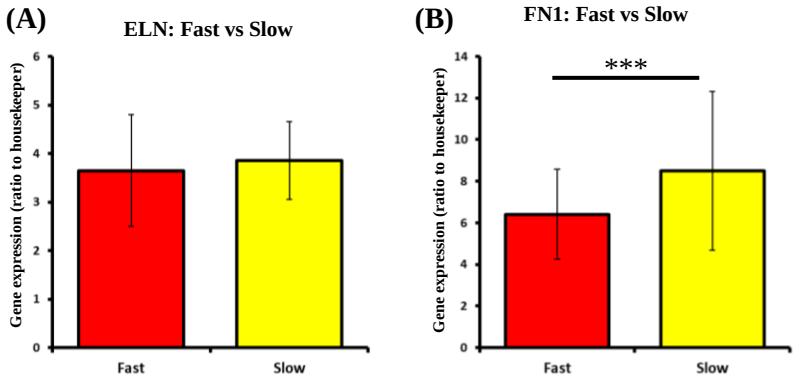

Figure 64: Comparison of *ELN* and *FN1* expression levels between fast and slow migrating groups. (A) *ELN* expression was similar in both fast and slow migrating groups no significant difference. (B) *FN1* expression was lower in the fast migrating group when compared with the slow migrating group, this difference was significant as determined by an independent samples t-test with a two-tailed distribution ($p<0.001$). (Fast group: n=36; slow group: n=51).

4.5 Differences in cytokine release profiles between fast and slow groups

The bicinchoninic acid assay (BCA assay) was employed in order to assess the total amount of protein within serum free cultures of cleft fibroblasts; fibroblasts from three patients in each of the fast and slow migrating groups were assessed so that any differences could be measured. It was found that overall the fast migrating fibroblasts secreted lower total amounts of protein when compared with the slow migrating fibroblasts, this difference was shown to be significant by means of Welch's t-test with two-tailed distribution ($p<0.001$) (Figure 65A-B).

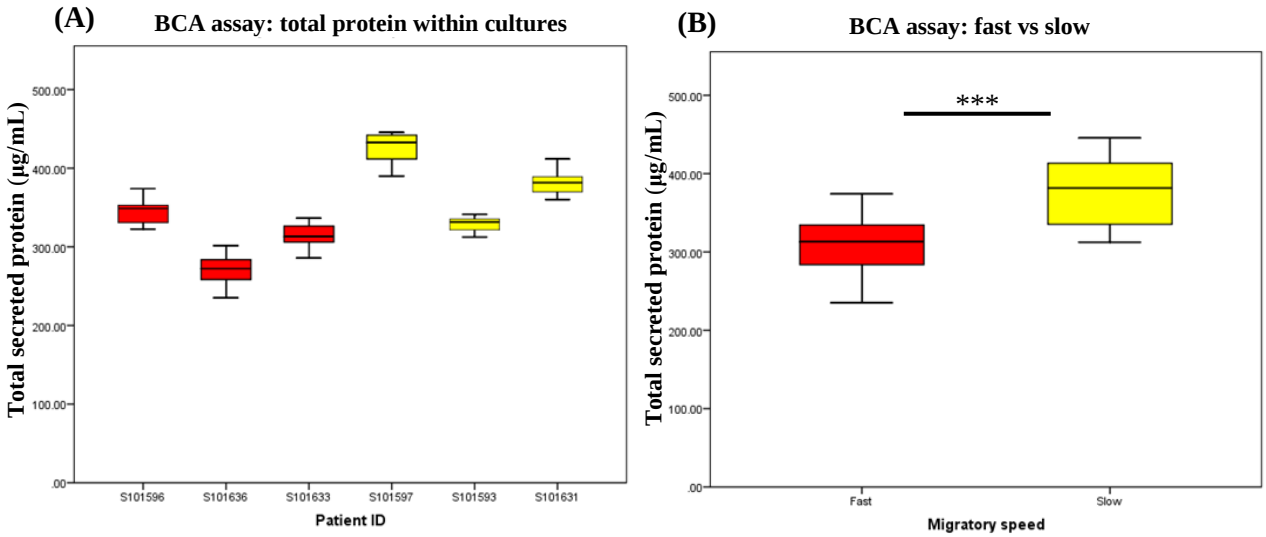

Figure 65: Quantification of total protein secreted by fast and slow migrating fibroblasts. (A) In general, the fast migrating fibroblast secreted lower total protein when compared with slow migrating cells (n=12). (B) When averaged total secreted protein was shown to be significantly lower in the fast migrating group ($p<0.001$) when compared with the slow migrating group as determined by Welch's t-test with two tailed distribution (n=36).

4.5.1 Analysis of the effect of secretome substitution on RWA%

Due to the differences in total secreted protein observed within serum free medium, it was thought that fast and slow migrating cells may have secreted different types and quantities of proteins that could potentially have influenced their behaviour. Secretome substitution assays were conducted whereby fast migrating cells were cultured in the secretome of slow migrating fibroblasts for 24 hours prior to induction of wound healing assays whilst the reverse was also conducted as slow migrating cells were treated with fast migrating fibroblast secretome. It was found that when treated with the fast secretome, slow fibroblast RWA% significantly decreased from 77.56% to 42.63% ($p<0.001$) due to increased wound closure (Figure 66A-C). Conversely, fast migrating fibroblasts were shown to decrease in speed with the RWA% increasing from 29.77% to 44.15% ($p<0.001$) (Figure 67A-C). This data suggested that the variation in the secretome between cleft fibroblasts had a significant effect on the cells ability to migrate into cell free wound area which could have potentially accounted for the significant differences observed in cultures established from the patient cohort.

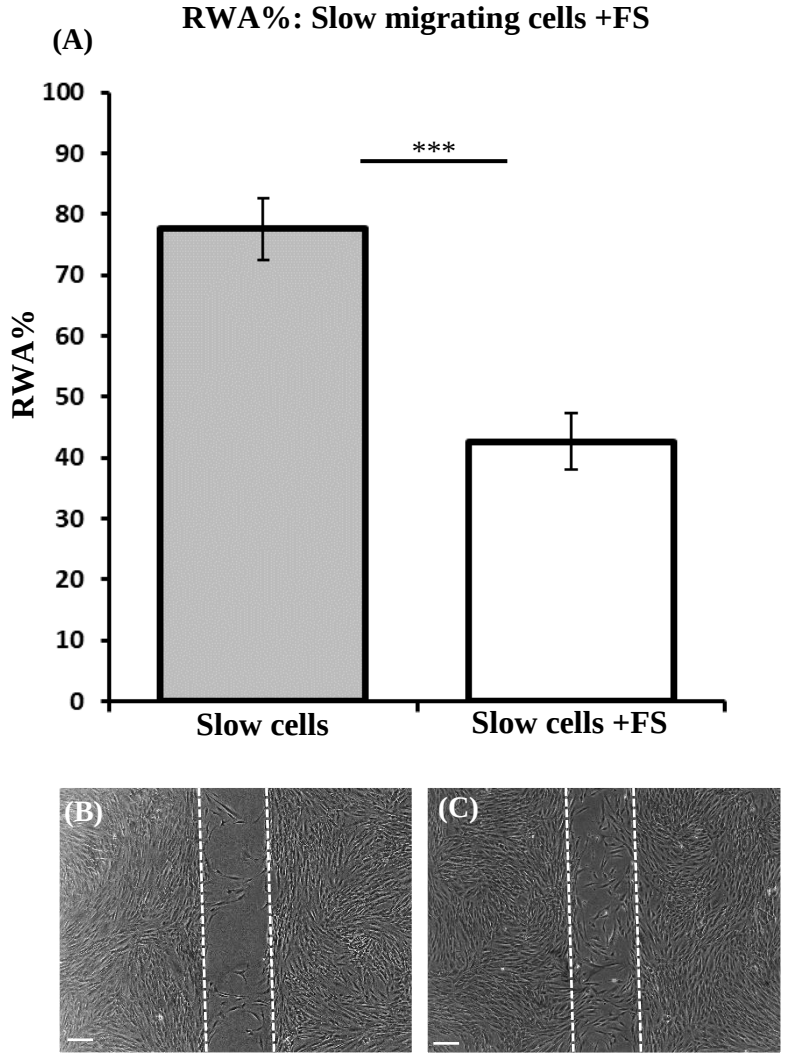

Figure 66: RWA% in slow migrating cells supplemented with fast migrating fibroblast secretome (FS). Following supplementation with FS the RWA% after 24 hours in slow migrating fibroblasts significantly decreased ($p<0.001$) demonstrating an increase in migratory speed (n=9). Scale bars = 100μm.

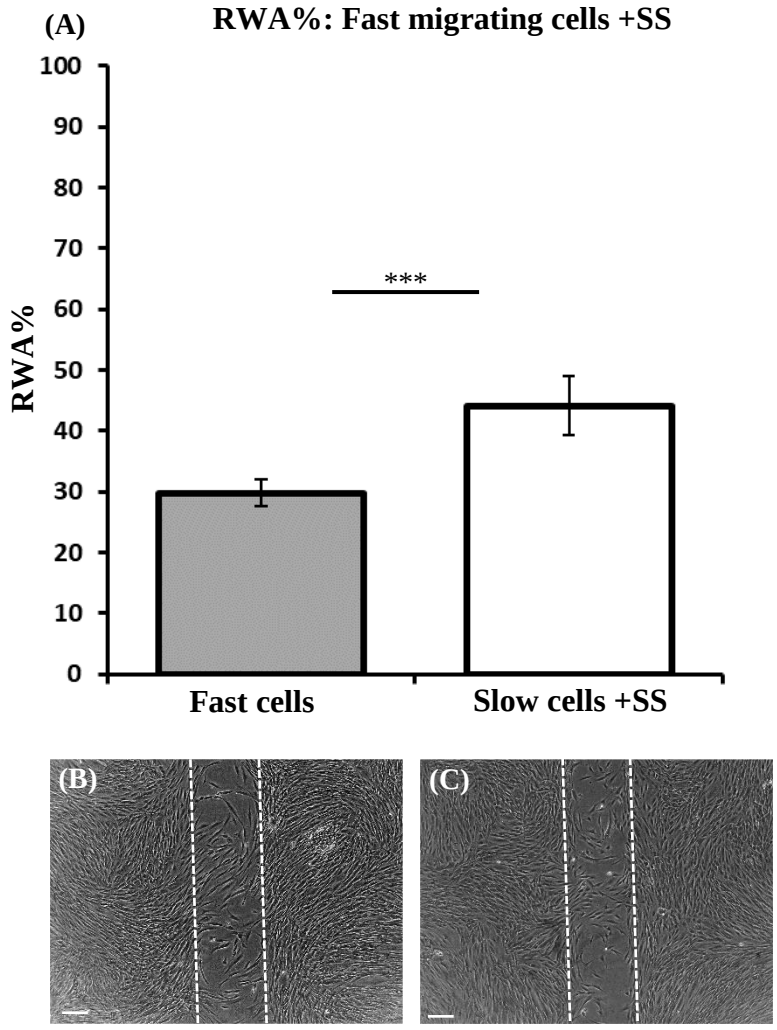

Figure 67: RWA% in fast migrating cells when supplemented with slow migrating fibroblast Secretome (SS). Following supplementation with SS the RWA% after 24 hours in fast migrating fibroblast was significantly increased ($p<0.001$) demonstrating a decrease in migratory speed (n=9). Scale bars = 100μm.

4.5.2 Analysis of fibroblast secretome through use of cytokine arrays

A cytokine array, which assess the relative abundance of 105 different cytokines, was used in order to compare the serum free secretome of fast and slow migrating fibroblasts. Densitometry revealed that there were a number of significant differences (Figure 68A-B). It was found that in the fast group there were a number of cytokines that were present in significantly higher amounts when compared with the slow group, these included: Insulin-like growth factor-binding protein-2 (IGFB2) ($p<0.001$), Growth differentiation factor 15 (GDF15) ($p<0.001$), Dickkopf-related protein 1 (DKK1) ($p<0.001$). Further, Interleukin 6 (IL-6), Interleukin 8 (IL-8), Complement factor D (CFD) and Endoglin (ENG) were absent in the slow group were only secreted by the fast migrating fibroblasts (Figure 69A-G). Conversely, there were a number of cytokines that were produced in significantly higher amounts in the slow migrating group, these included: Monocyte chemoattractant protein 1 (MCP-1) ($p<0.001$), Chitinase-3-like protein 1 (CHI3L1) ($p<0.001$) and Stromal cell-derived factor 1 (SDF-1) ($p<0.05$) (Figure 70A-C).

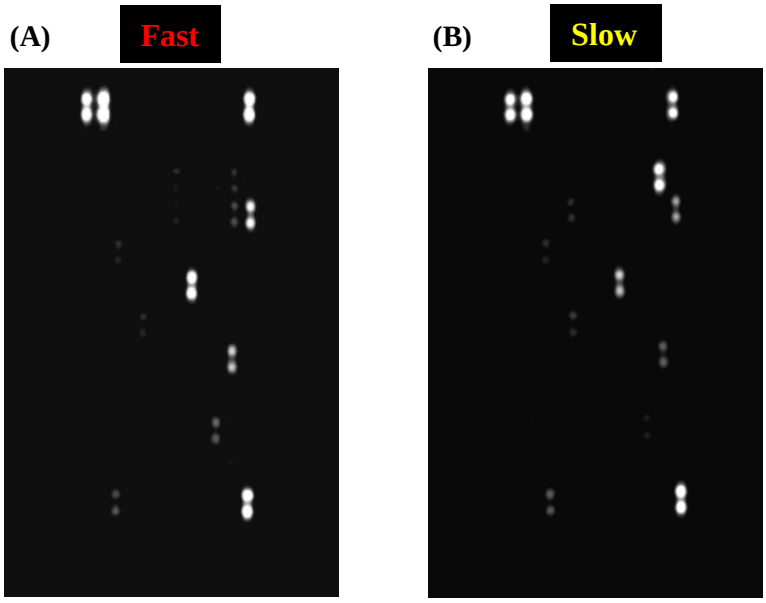

Figure 68: Scans of nitrocellulose membranes following exposure to fast and slow fibroblast Secretome. Different densities were observed at varying location along the membrane that were quantified via densitometry. Each cytokine is spotted in duplicate and two membranes were used for both the fast and slow group (n=4).

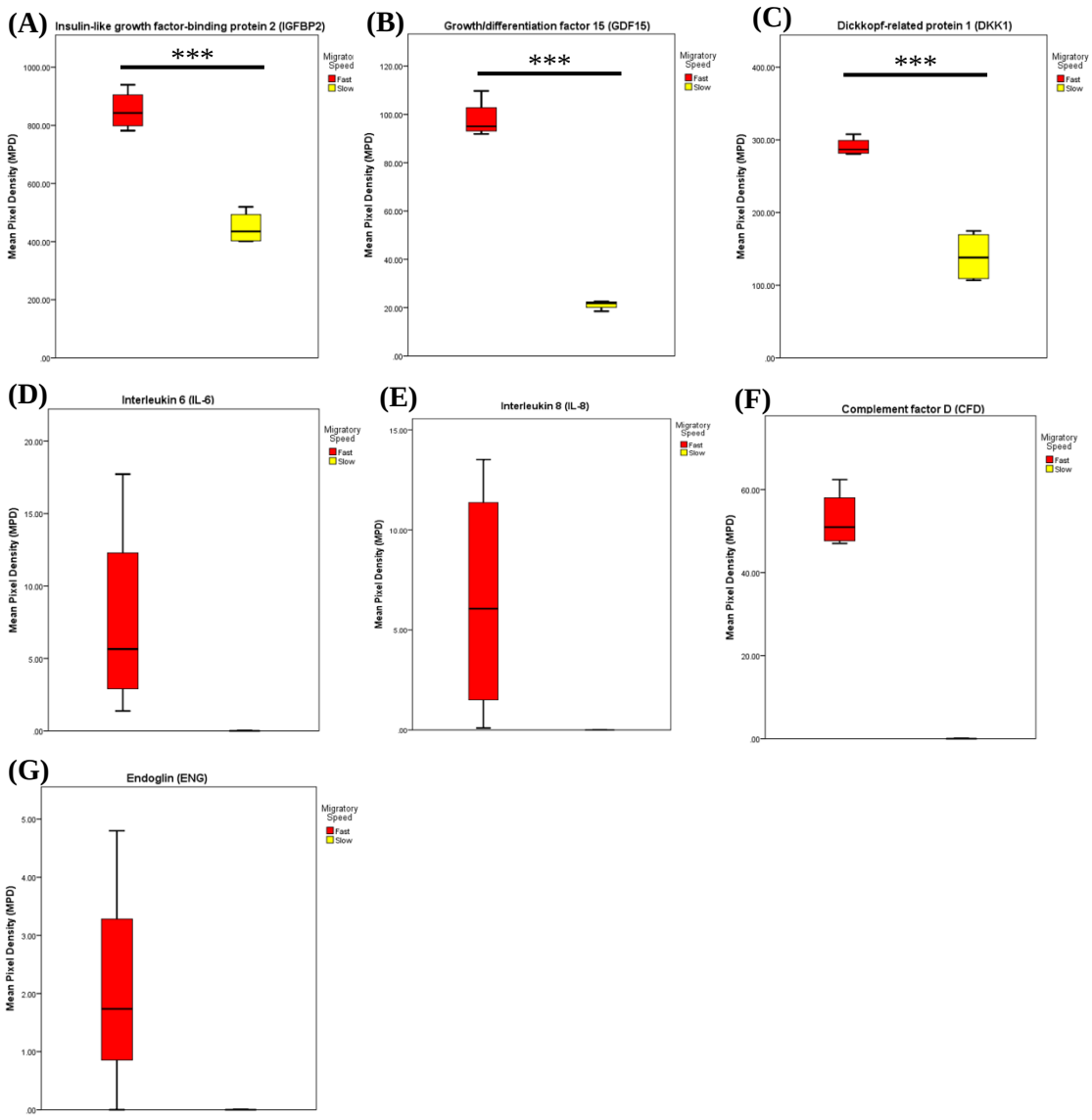

Figure 69: Higher cytokine secretion by fast migrating fibroblasts. A number of cytokines were shown to be secreted in significantly higher amounts from the fast migrating cleft fibroblasts relative to their slow migrating counterparts. These included (A) Insulin-like growth factor-binding protein 2 (IGFB2) (B) Growth differentiation factor 15 (GDF15) and (C) Dickkopf-related protein 1 (DKK1), these differences were significant ($p<0.001$, $p<0.001$ and $p<0.001$ respectively. Furthermore, (D) Interleukin 6 (IL-6), (E) Interleukin 8 (IL-8), (F) Complement factor D (CFD) and (G) Endoglin (ENG) were absent in the slow group were only secreted by the fast migrating fibroblasts, thereby suggesting fast migrating fibroblasts differ considerably in their cytokine release profiles when compared there slow migrating counterparts (Fast group n = 4; slow group n = 4).

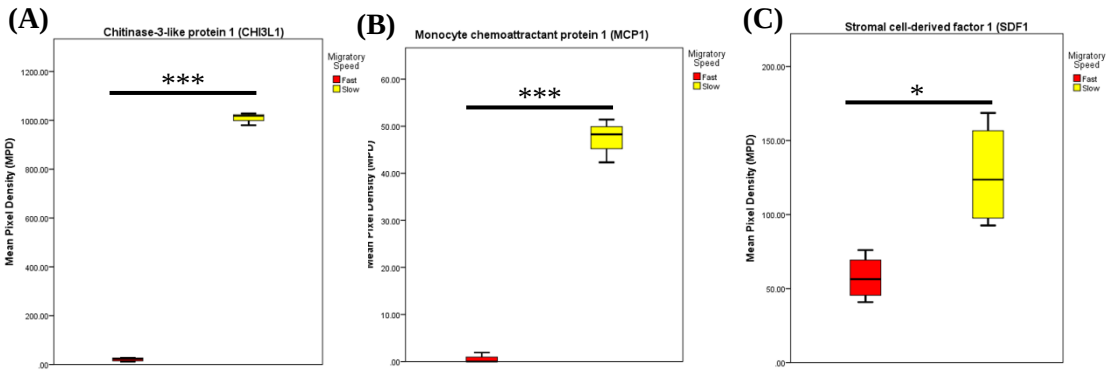

Figure 70: Higher cytokine production by slow migrating fibroblasts. A number of cytokines were secreted in significantly greater amounts by the slow migrating cleft fibroblasts when compared with their fast migrating counterparts. (A) These included: Chitinase-3-like protein 1 (CHI3L1) ($p<0.001$), (B) Monocyte chemoattractant protein 1 (MCP-1) ($p<0.001$) and (C) Stromal cell-derived factor 1 (SDF-1) ($p<0.05$). This data suggests that the cytokine release profiles in fibroblasts derived from the slow migratory group are distinct from there fast migrating counterparts. Fast group n=4; slow group (n=4).

4.6 Human cell motility PCR array analysis

As the fast and slow fibroblasts were shown to differ significantly in their cytokine release profiles and a number of genes involved in cell migration and ECM production, a PCR array comprising 84 genes involved in cell motility was conducted in order to establish how fast and slow groups differed in their expression across a larger gene cohort. Expression levels for the majority of the genes assessed were comparable between fast and slow groups though there were a number of significant differences, these included: Actinin alpha 4 (ACTN4) ($p<0.05$), ARP2 actin-related protein 2 homolog (ACTR2) ($p<0.05$), Hepatocyte growth factor (HGF) ($p<0.05$), Integrin alpha 4 (ITGA4) ($p<0.05$), Matrix metallopeptidase 9 (MMP9) ($p<0.05$), Moesin (MSN) ($p<0.01$), Myosin heavy chain 9 (MYH9) ($p<0.05$) and Ras homolog gene family member B (RHOB) ($p<0.05$). In addition, there were a number of other genes with average fold changes greater than two but not significantly different statistically due to the variation in expression between the members of the fast and slow groups assessed, these genes included: Colony stimulating factor 1 (CSF1), Diaphanous homolog 1 (DIAPH1), Epidermal growth factor receptor (EGFR), Insulin-like growth factor 1 (IGF1), Insulin-like growth factor 1 receptor (IGF1R), Met proto-oncogene (MET), Matrix metallopeptidase 14 (MMP14), Matrix metallopeptidase 2 (MMP2), P21 protein (Cdc42/Rac)-activated kinase 4 (PAK4), Paxillin (PXN) and Ras-related C3 botulinum toxin substrate 2 (rho family, small GTP binding protein Rac2) (RAC2). The fold changes and p-values for the aforementioned genes, as well as the genes that were comparable between the fast and slow group, are shown in the table below.

Gene name	Gene symbol	Accession number	Fold change	p-value
			Relative to Fast migratory group	
Actinin, alpha 1	*ACTN1*	NM_001102	1.12	0.560
Actinin, alpha 3	*ACTN3*	NM_001104	1.35	0.890
Actinin, alpha 4	*ACTN4*	NM_004924	2.09	0.034
ARP2 actin-related protein 2 homolog	*ACTR2*	NM_005722	-1.31	0.045
ARP3 actin-related protein 3 homolog	*ACTR3*	NM_005721	-1.26	0.224
V-akt murine thymoma viral oncogene homolog 1	*AKT1*	NM_005163	1.21	0.800
ADP-ribosylation factor 6	*ARF6*	NM_001663	1.89	0.265
Rho GDP dissociation inhibitor (GDI) alpha	*ARHGDIA*	NM_004309	1.87	0.102
Rho guanine nucleotide exchange factor (GEF) 7	*ARHGEF7*	NM_003899	1.26	0.800
BAI1-associated protein 2	*BAIAP2*	NM_006340	1.32	0.552
Breast cancer anti-estrogen resistance 1	*BCAR1*	NM_014567	1.44	0.709
Calpain 1, (mu/I) large subunit	*CAPN1*	NM_005186	1.86	0.279
Calpain 2, (m/II) large subunit	*CAPN2*	NM_001748	-1.71	0.065
Caveolin 1, caveolae protein	*CAV1*	NM_001753	-1.33	0.424
Cell division cycle 42	*CDC42*	NM_001791	1.05	0.517
Cofilin 1 (non-muscle)	*CFL1*	NM_005507	1.14	0.241
V-crk sarcoma virus CT10 oncogene homolog	*CRK*	NM_016823	1.16	0.655
Colony stimulating factor 1	*CSF1*	NM_000757	2.14	0.252
Cortactin	*CTTN*	NM_005231	-1.07	0.668
Diaphanous homolog 1	*DIAPH1*	NM_005219	2.14	0.125
Dipeptidyl-peptidase 4	*DPP4*	NM_001935	1.55	0.422
Epidermal growth factor	*EGF*	NM_001963	-1.43	0.420
Epidermal growth factor receptor	*EGFR*	NM_005228	2.39	0.258
Enabled homolog	*ENAH*	NM_001008	1.64	0.112
Ezrin	*EZR*	NM_003379	-1.14	0.588
Fibroblast activation protein, alpha	*FAP*	NM_004460	1.44	0.503
Fibroblast growth factor 2	*FGF2*	NM_002006	1.20	0.447
Hepatocyte growth factor (hepapoietin A; scatter factor)	*HGF*	NM_000601	2.95	0.013
Insulin-like growth factor 1	*IGF1*	NM_000618	6.52	0.394
Insulin-like growth factor 1 receptor	*IGF1R*	NM_000875	2.51	0.189
Integrin-linked kinase	*ILK*	NM_004517	1.63	0.112
Integrin, alpha 4	*ITGA4*	NM_000885	-2.43	0.026
Integrin, beta 1	*ITGB1*	NM_002211	1.41	0.348
Integrin, beta 2	*ITGB2*	NM_000211	-1.29	0.428
Integrin, beta 3	*ITGB3*	NM_000212	1.17	0.507
LIM domain kinase 1	*LIMK1*	NM_002314	1.96	0.143

Mitogen-activated protein kinase 1	*MAPK1*	NM_002745	1.07	0.639
Met proto-oncogene	*MET*	NM_000245	3.27	0.072
Matrix metallopeptidase 14	*MMP14*	NM_004995	3.32	0.150
Matrix metallopeptidase 2	*MMP2*	NM_004530	2.66	0.223
Matrix metallopeptidase 9	*MMP9*	NM_004994	1.87	0.010
Moesin	*MSN*	NM_002444	2.10	0.009
Myosin, heavy chain 10, non-muscle	*MYH10*	NM_005964	1.75	0.159
Myosin, heavy chain 9, non-muscle	*MYH9*	NM_002473	3.15	0.010
Myosin, light chain 9, regulatory	*MYL9*	NM_006097	1.55	0.102
Myosin light chain kinase	*MYLK*	NM_053025	-1.24	0.668
P21 protein (Cdc42/Rac)-activated kinase 1	*PAK1*	NM_002576	-1.28	0.126
P21 protein (Cdc42/Rac)-activated kinase 4	*PAK4*	NM_005884	2.52	0.188
Profilin 1	*PFN1*	NM_005022	-1.52	0.113
Phosphoinositide-3-kinase, catalytic, alpha polypeptide	*PIK3CA*	NM_006218	1.38	0.267
Plasminogen activator, urokinase receptor	*PLAUR*	NM_002659	-1.50	0.440
Phospholipase C, gamma 1	*PLCG1*	NM_002660	1.56	0.426
Phospholipase D1,	*PLD1*	NM_002662	1.32	0.709
Protein kinase C, alpha	*PRKCA*	NM_002737	1.78	0.142
Phosphatase and tensin homolog	*PTEN*	NM_000314	1.59	0.494
PTK2 protein tyrosine kinase 2	*PTK2*	NM_005607	1.02	0.927
PTK2B protein tyrosine kinase 2 beta	*PTK2B*	NM_004103	1.01	0.561
Protein tyrosine phosphatase, non-receptor type 1	*PTPN1*	NM_002827	1.60	0.322
Paxillin	*PXN*	NM_002859	4.15	0.071
Ras-related C3 botulinum toxin substrate 1 (rho family, small GTP binding protein Rac1)	*RAC1*	NM_006908	1.15	0.586
Ras-related C3 botulinum toxin substrate 2 (rho family, small GTP binding protein Rac2)	*RAC2*	NM_002872	-2.48	0.279
RAS p21 protein activator (GTPase activating protein) 1	*RASA1*	NM_002890	1.01	0.985
Radixin	*RDX*	NM_002906	-1.14	0.665
Rhodopsin	*RHO*	NM_000539	-1.05	0.801
Ras homolog gene family, member A	*RHOA*	NM_001664	1.01	0.882
Ras homolog gene family, member B	*RHOB*	NM_004040	2.49	0.027
Ras homolog gene family, member C	*RHOC*	NM_175744	1.21	0.175
Rho family GTPase 3	*RND3*	NM_005168	1.21	0.696
Rho-associated, coiled-coil containing protein kinase 1	*ROCK1*	NM_005406	1.42	0.372
SH3 and PX domains 2A	*SH3PXD2A*	NM_014631	1.76	0.403
V-src sarcoma (Schmidt-Ruppin A-2) viral oncogene homolog =	*SRC*	NM_005417	1.51	0.296

Signal transducer and activator of transcription 3	*STAT3*	NM_003150	1.68	0.352
Supervillin	*SVIL*	NM_003174	1.66	0.528
Transforming growth factor, beta 1	*TGFB1*	NM_000660	1.52	0.494
TIMP metallopeptidase inhibitor 2	*TIMP2*	NM_003255	1.90	0.273
Talin 1	*TLN1*	NM_006289	1.84	0.112
Vasodilator-stimulated phosphoprotein	*VASP*	NM_003370	1.60	0.276
Vinculin	*VCL*	NM_003373	1.93	0.150
Vascular endothelial growth factor A	*VEGFA*	NM_003376	-1.62	0.391
Vimentin	*VIM*	NM_003380	-1.05	0.975
WAS protein family, member 1	*WASF1*	NM_003931	1.05	0.982
WAS protein family, member 2	*WASF2*	NM_006990	1.58	0.198
Wiskott-Aldrich syndrome-like	*WASL*	NM_003941	1.02	0.738
WAS/WASL interacting protein family, member 1	*WIPF1*	NM_003387	1.79	0.234

Table 7: Summary of fold changes in gene expression between fast and slow migrating fibroblasts obtained by PCR arrays. Three patients from both the fast and slow migrating group were selected for PCR array analysis, the data was pooled and expressed in terms of an average fold change in the slow migrating group relative to the fast migrating group. Positive fold changes greater than two are marked in red whereas high negative fold changes greater than two are marked in blue. All p-values have also been recorded and any significant differences were marked in red (n=3).

4.7 Analysis of transforming growth factor beta and alpha on cell growth

In order to assess the effect of recombinant TGF's on the growth of cleft fibroblasts, cultures were supplemented with 5nM or 20nM of each growth factor followed by generation of growth curves. It was found that supplementation with both 5nM and 20nM TGFβ1 increased cell growth leading to significantly decreased DT ($p<0.05$ and $p<0.001$ respectively). Conversely, supplementation with TGFβ3 at 5nM decreased cell growth rate leading to significantly increased DT ($P<0.05$) which increased further following supplementation with 20nM ($p<0.001$). Supplementation with both TGFβ2 and TGFα did not significantly influence growth of cleft fibroblasts at any of the concentrations used here (Figure 71A-D).

4.7.1 Comparison of transforming growth factor beta and alpha expression between fast and slow migrating cleft fibroblasts

To asses if there were any differences in the expression of various *TGF* beta and alpha between the fast and slow migrating fibroblasts, samples were grouped and their gene expression was averaged. It was found that *TGFA* expression was significantly upregulated in the fast group when compared with the slow ($p<0.001$). No other TGF gene transcripts were up-regulated in the fast migrating fibroblast group. Conversely, expression of *TGFB3* was significantly downregulated in the fast group when compared with the slow ($p<0.05$). Similarly, *TGFBR1* was also significantly down-regulated in the fast group when compared with the average expression of the slow group ($p<0.05$) thereby suggesting that *TGFA*, *TGFB3* and *TGFBR1* may be involved in the differences observed in wound closure (Figure 72).

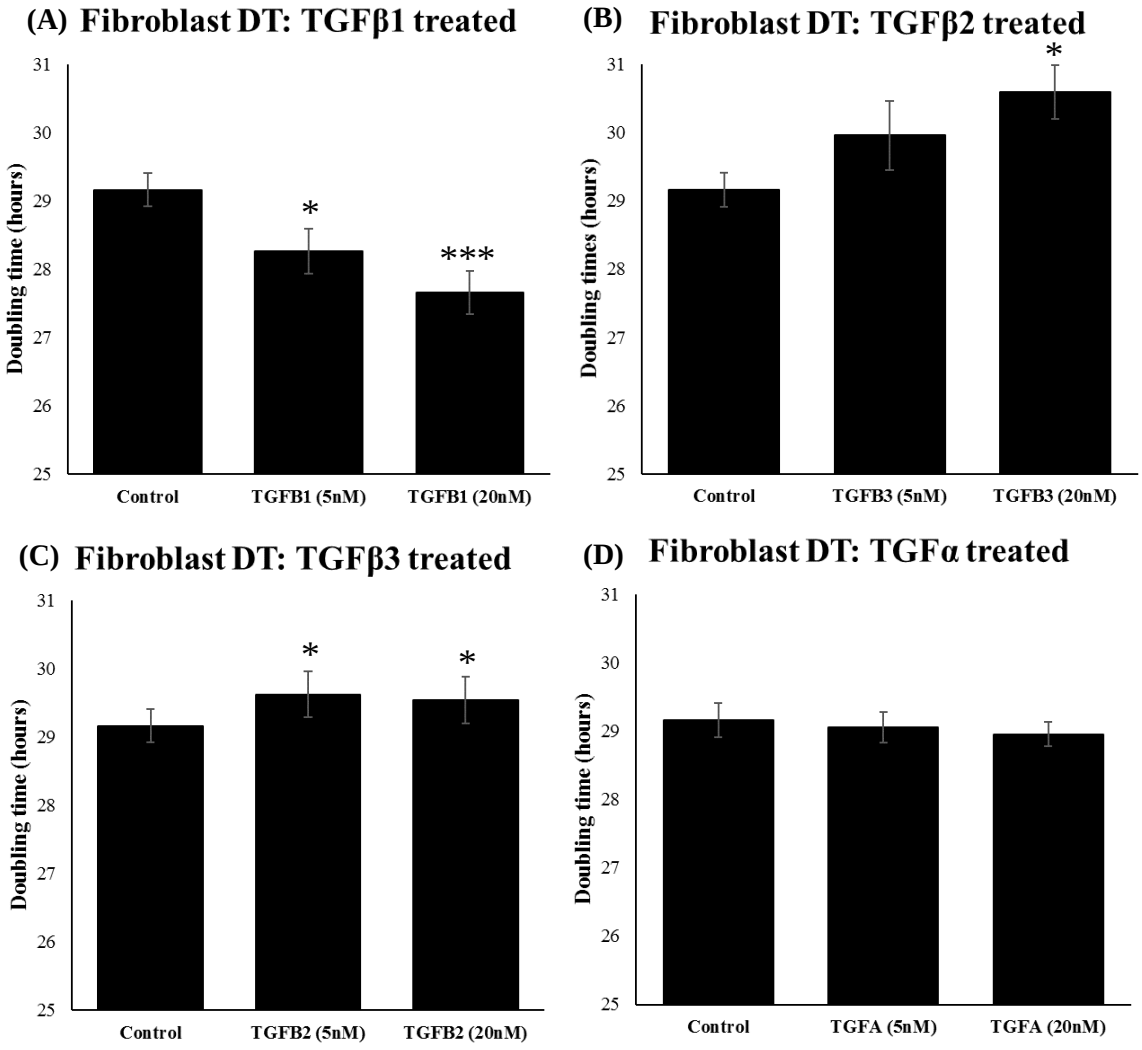

Figure 71: The effect of Transforming growth factor beta and alpha on the population doubling times of cleft fibroblasts. (A) Supplementation with 5nM TGFβ1 significantly decreased DT ($p<0.05$), this is decreased further following supplementation with 20nM ($p<0.001$) demonstrating that TGFβ1 supplementation at the concentrations used here increased the growth of cleft fibroblasts. (B) 5nM TGFβ2 led to an increase in DT however this increase was non-significant, DT did increase further following supplementation with 20nM ($p<0.05$). (C) Supplementation with 5nM TGFβ3 significantly increased DT ($p<0.05$) this increase was maintained following supplementation with 20nM ($p<0.001$). (D) Treating cleft fibroblasts with either 5nM or 20nM TGFA did not significantly influence their DT.

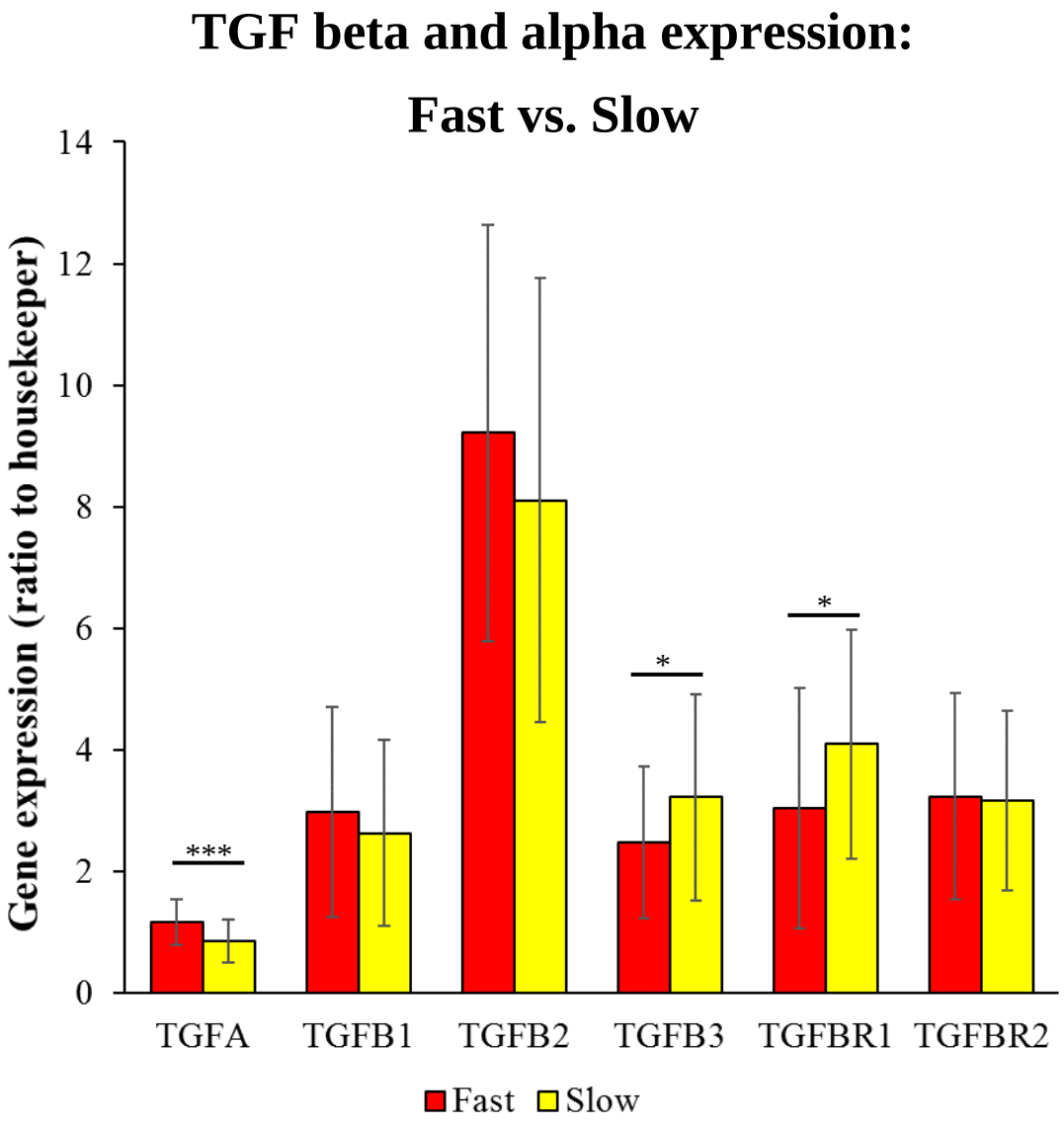

Figure 72: Transforming growth factor beta and alphaexpression between fast and slow migrating fibroblasts. Expression of *TGFA* was significantly higher in the fast group relative to the slow ($p<0.001$). There were no differences between the two groups based on expression of *TGFB2* and *TGFBR2*. However, both *TGFB3* and *TGFBR1* were, on average, expressed in significantly higher amount in the slow group relative to the fast ($p<0.05$). (Fast group n=36; slow group=51).

4.7.2 Analysis of TGF beta and alpha on wound closure after 24 hours

As it was previously shown that expression of *TGFB3* and *TGFA* differed significantly based migratory group, the effect of TGF supplementation at 20nM on the RWA% of cleft fibroblasts was assessed. It was found that supplementation with 20nM TGFβ1 and TGFβ2 did lead to a decrease in wound closure though this not significant relative to the unsupplemented control. Supplementation with 20nM TGFβ3 did lead to a significant increase in the RWA% relative to the control ($p<0.05$). In contrast, the RWA% was very significantly decreased following supplementation of cultures with 20nM TGFα ($p<0.001$) (Figure 73).

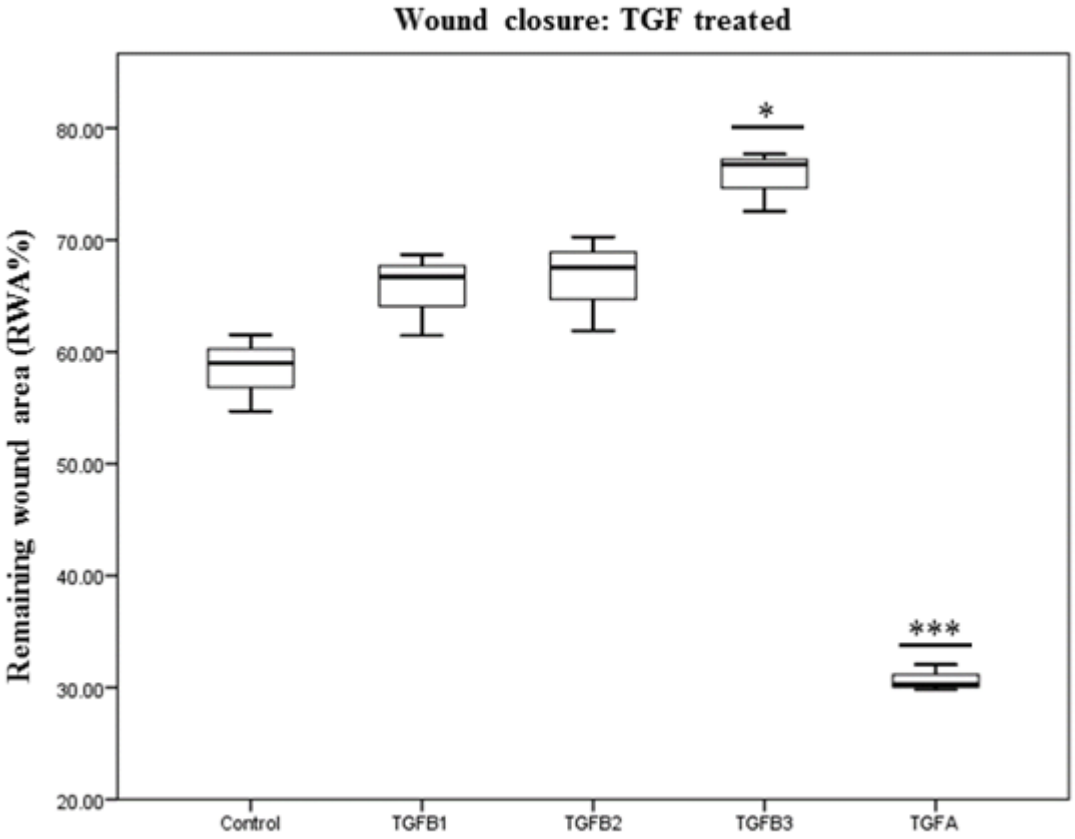

Figure 73: Effect of Transforming growth factor beta and alpha supplementation of on cleft fibroblast RWA%. Supplementation with 20nM TGFβ1 and 20nM TGFβ2 decreased RWA% however this was not statistically significant. Supplementation with 20nM TGFβ3 did lead to a significant decrease in the RWA% ($p<0.05$) suggesting the presence of TGFβ3 decreases the migratory rates of cleft fibroblasts. The RWA% was very significantly decreased following supplementation with 20nM TGFA ($p<0.001$) suggesting that the presence of TGFA significantly increases cell migratory speed in cleft fibroblasts (n=9).

4.7.3 TGF beta and alpha on expression of myofibroblast differentiation markers

ACTA2 expresses alpha smooth muscle actin (α-SMA) which is a commonly used marker for fibroblast to myofibroblast differentiation and was used here to assess the effect of TGF supplementation on cleft fibroblasts differentiation. It was shown here that supplementation with recombinant TGFβ1, TGFβ2, TGFβ3 and TGFα at concentration of 5nM and 20nM all led to significant upregulation of ACTA2 when compared with the unsupplemented control. The largest increase in *ACTA2* expression was observed following TGFβ1 supplementation, this was shown to increase by 7.87-fold following 5nM supplementation and increased to 14.60-fold after treatment with 20nM TGFβ1 (Figure 74). In addition, vimentin (*VIM*), a commonly used fibroblast marker that has also been shown to be upregulated following fibroblast to myofibroblast differentiation, expression was assessed. As with *ACTA2*, *VIM* expression was shown to be significantly upregulated in all TGF supplementation conditions. Further, as with *ACTA2*, the greatest upregulation was observed following TGFβ1 supplementation which increased by 5.76-fold under the 5nM condition and 6.32-fold following treatment with 20nM. This data indicates that TGF supplementation can induce cleft fibroblast-to-myofibroblast differentiation and TGFβ1 was the most potent inducer of this differentiation (Figure 75).

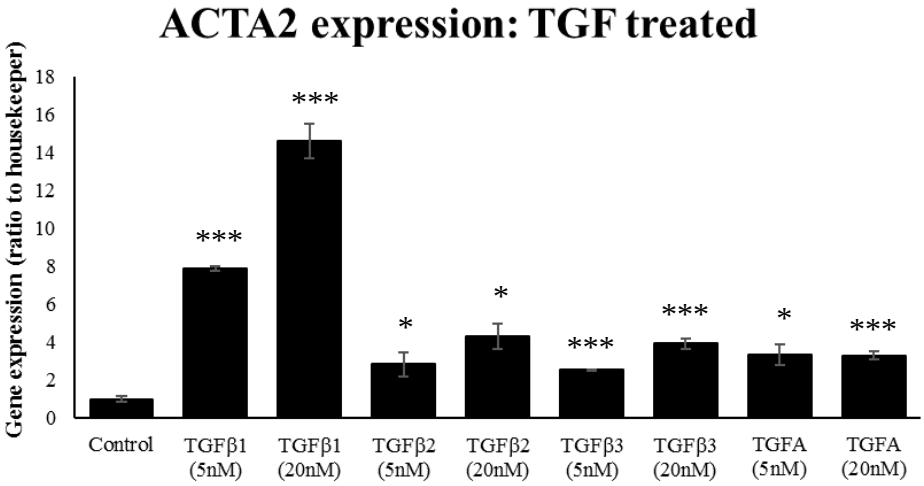

Figure 74: Effect of transforming growth factors beta and alpha on *ACTA2* expression. Supplementation with 5nM TGFβ1 significantly increased the expression of *ACTA* in cleft fibroblasts ($p<0.001$); this increased further following supplementation with 20nM ($p<0.001$) suggesting that the presence of TGFβ1 induced cleft fibroblast to myofibroblast differentiation. Supplementation with TGFβ2 (5nM and 20nM) both resulted in significant upregulation of *ACTA2* but not the extent of TGFβ1 ($p<0.05$). TGFβ3 (5nM and 20nM) and *TGFA* (5nM and 20nM) also significantly increased expression of *ACTA2* by however this increased expression was significantly lower than that of TGFβ1 treated cultures (n=3).

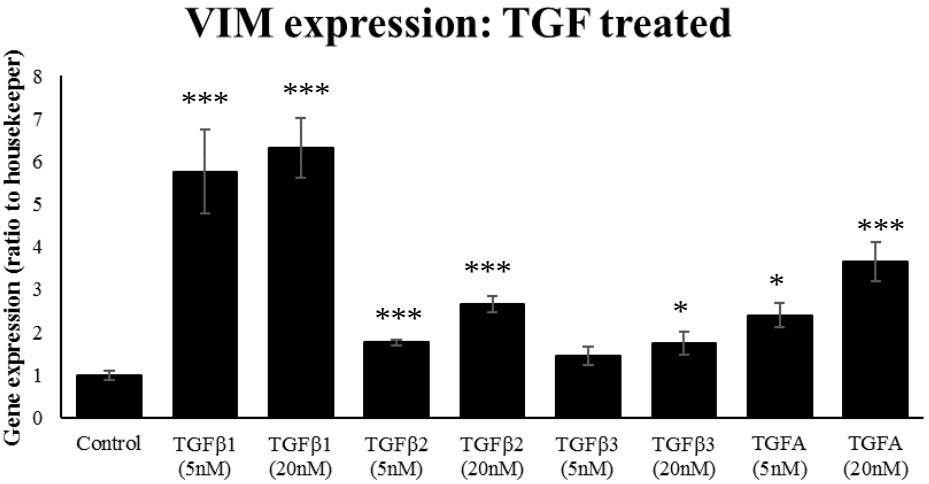

Figure 75: Effect of transforming growth factor beta and alpha on *VIM* expression. Cultures treated with 5nM and 20nM TGFβ1 displayed significant upregulation of VIM when compared with the untreated control ($p<0.001$); there was no significant difference between the 5nM and 20nM treatment conditions. *VIM* was also upregulated in cultures treated with 5nM TGFβ2, this was upregulated further with 20nM ($p<0.001$). Cleft fibroblasts treated with 5nM TGFβ3 did not significantly upregulate *VIM* however significant increases were observed with 20nM supplementation ($p<0.05$). Treatment with 5nM *TGFA* significantly increased expression of *VIM* relative to the control ($P<0.05$); this expression was increased further following treatment with 20nM ($P<0.001$) (n=3).

4.7.4 TGF beta and alpha and cleft fibroblast collagen production and expression

Total collagen production by mitomycin C growth inhibited cleft fibroblasts following supplementation with TGF's was assessed by means of Sirius red staining. Both TGFβ1 and TGFα supplementation at 5nM led to significantly increased production of collagen when compared with the unsupplemented control ($p<0.001$ and $p<0.001$ respectively), TGFβ1 did not cause collagen production to increase further following treatment with 20nM although 20nM TGFα did lead to increased collagen production when compared with its 5nM counterpart. TGFβ2 did not significantly influence collagen production in concentrations of 5nM or 20nm, however supplementation with 5nM TGFβ3 led to a significant decrease in collagen production ($p<0.001$) which was shown to decrease further following treatment with 20nM ($p<0.05$) (Figure 76).

Supplementation with TGFβ1 at concentration of 5nM and 20nM resulted in significant upregulation of both *COL1A1* and *COL3A1*, this was also observed following supplementation with TGFβ2 however both genes were not upregulated to the extent observed following treatment with TGFβ1. Supplementation of cleft fibroblasts with TGFβ3 at 5nM led significant downregulation of *COL1A1* but not *COL3A1*, *COL3A1* expression was significantly decreased following TGFβ3 treatment at 20nM as was *COL1A1*. *COL1A1* expression was comparable with the control following treatment with both 5nM and 20nM TGFA whereas both of these concentrations resulted in significant upregulation of *COL3A1* (Figure 77 and Figure 78).

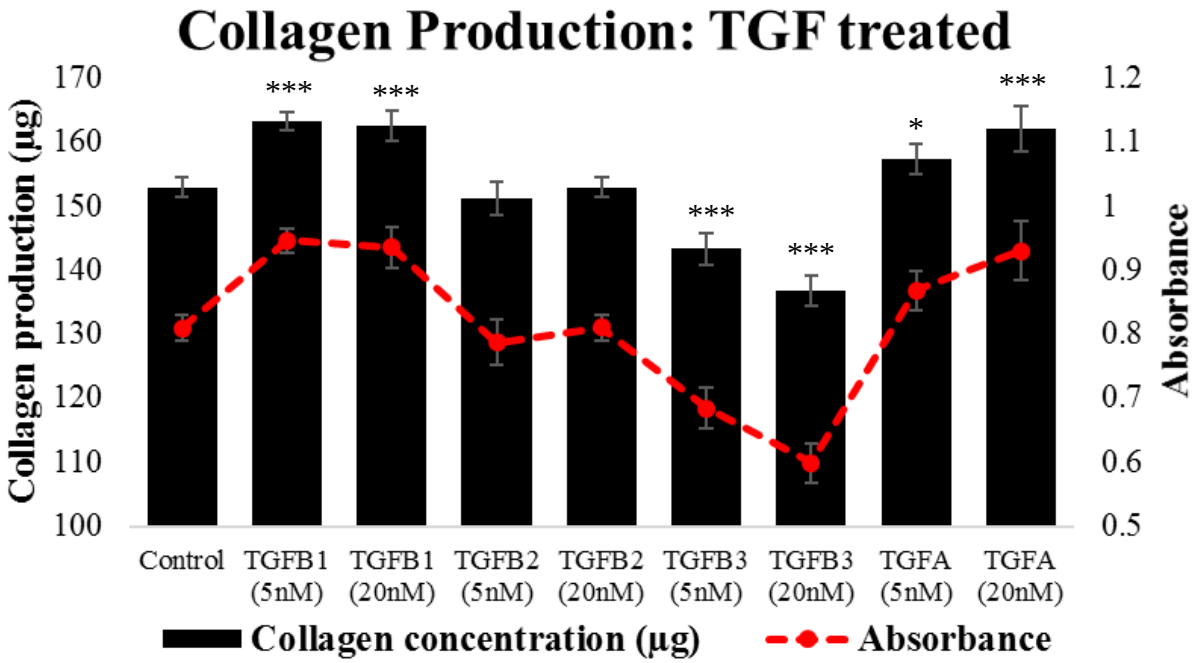

Figure 76: Effect of transforming growth factor beta and alpha on collagen production Supplementation with TGFβ1 (5nM and 20nM) significantly increased the total collagen, produced by mitomycin C growth inhibited cleft fibroblasts, relative to the control which comprised of growth inhibited cleft fibroblasts that were not supplemented with exogenous transforming growth factors ($p<0.001$ and $p<0.001$ respectively); there was no significant difference between the 5nM and 20nM conditions. There were no significant differences in collagen production between fibroblasts treated with TGFβ2 and the control. Cultures treated with 5nM TGFβ3 produced significantly decreased levels of collagen ($p<0.001$); this decreased further following supplementation with 20nM ($p<0.05$). Treatment with 5nM TGFA led to significantly increased collagen production ($p<0.05$) which increased further following supplementation with 20nM ($p<0.001$) (n=6).

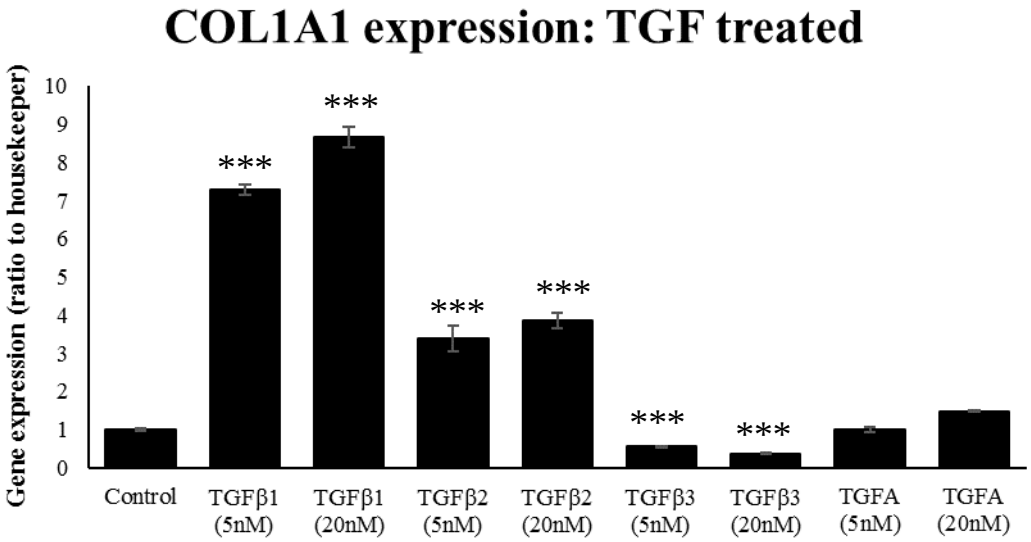

Figure 77: Effect of transforming growth factor beta and alpha on *COL1A1* expression. TGFβ1 supplementation had the greatest effect on *COL1A1* expression. *COL1A1* was significantly upregulated following supplementation with 5nM ($p<0.001$); expression was increased further with 20nM ($p<0.001$). *COL1A1* was also upregulated following supplementation with both 5nM and 20nM TGFβ2 ($p<0.001$). Supplementation with 5nM TGFβ3 significantly decreased *COL1A1* expression ($p<0.001$); this was decreased further 20nM. Cultures supplemented with 5nM and 20nM TGFA displayed expression profiles comparable to that of the unsupplemented control (n=3).

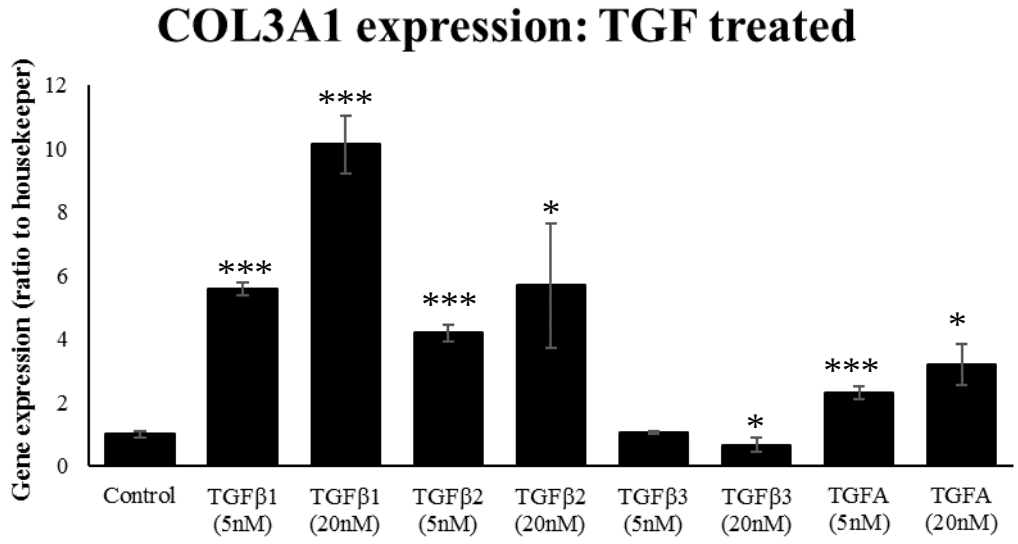

Figure 78: Effect of transforming growth factor beta and alpha on *COL3A1* expression. *COL3A1* was significantly upregulated following treatment with 5nM TGFβ1 ($p<0.001$); this was increased further with 20nM ($p<0.01$). *COL3A1* was also upregulated following treatment with 5nM and 20nM TGFβ2. Supplementation with 5nM *TGFB3* did not lead to any significant change in expression of *COL3A1* however expression was significantly decreased in the presence of 20nM TGFβ3 ($p<0.05$). *COL3A1* was significantly upregulated following 5nM TGFα supplementation ($p<0.001$), this was also increased with 20nM however due to larger stdev the significance relative to the control decreased ($p<0.05$) (n=3).

4.8 Discussion

Following cleft repair, a subset of patients develop post-operative complications. For example, oronasal fistula (ONF) is characterised by reinstatement of the link between the oral and nasal cavities postoperatively and on average effects approximately 8.6% of cleft patients, although patients with combined CLP are at increased risk (Hardwicke et al, 2014). The cause of post-operative complications can be varied and a number of potential contributory factors have been suggested, which include: size and width of the cleft (Khanna et al, 2012), surgical protocol (Zhang et al, 2017), differences between clinicians (Sitzman et al, 2017), age (Williams et al, 2001) and body weight (Fillies et al, 2007). However, although multiple factors can influence the risk of post-operative complications, it has been suggested that pathological wound healing may be the principle contributor (Chitturi et al, 2015; Beyeler et al, 2014). Hypertrophic scarring (HTS), which affects approximately 25% of cleft patients (Soltani et al, 2012), is a result of persistent pathological deposition of ECM by local fibroblast which contribute to post-operative complications through pathological wound contracture, increased tension at suture lines and reduced tissue integrity at the site of the repair. As many of the genes associated with cleft development are also involved in wound healing (Dixon et al, 2011), it is possible that the abnormal wound healing observed in some patients may be due to the disruption of normal fibroblast behaviour caused by the genetic predisposition that led to the formation of CLP.

4.8.1 Cleft fibroblasts and cell migration

Fibroblasts are central to normal wound healing, migrating into a wound from surrounding tissues thereby exerting tractional forces between their cell body and ECM molecules to which they are attached, leads to increased rigidity between fibroblast-ECM contacts and increased intercellular stress resulting in a myofibroblast differentiation response (Hinz and Gabbiani, 2003). Myofibroblasts are also key secretors of ECM macromolecules, including collagens, and

are the major contributors to wound contracture. As the initial fibroblast migration rate is directly related to the rate of myofibroblast differentiation, which in turn is associated with mechano-transduction of contractile forces that lead to wound contracture, the initial fibroblast migration rate is central to ECM deposition and wound contraction (Tomasek et al, 2002). To date, one other study has compared cell migration of fibroblasts isolated from different cleft patients (Beyeler et al, 2014). However, only cleft lip fibroblasts, isolated from patients with CLP, were assessed, thereby limiting the data to a single cleft type. Further, scratch wound assays, which have significant drawbacks that can influence analysis of cell migration, were utilised to calculate a rate of wound closure (RWC%). Beyeler et al (2014) found that of the 16 primary cleft fibroblast cell lines assessed, 10 shared comparable RWC%, whereas 5 migrated significantly faster and 1 migrated significantly slower. The patients were separated into three distinct groups which were: fast, intermediate and slow, as only one patient was in the slow group it was deemed an outlier and excluded from analysis. It was found that average RWC% between fast and intermediate groups were statistically different ($p<0.001$) (Beyeler et al, 2014). Similarly, the present study identified two distinct groups in terms of cell migration, fast and slow, which were also statistically distinct. However, these migratory groups did not correlate with cleft type although CL derived fibroblast were all clustered into the fast group and demonstrated elevated motility. As fibroblasts isolated from different cleft patients migrate at differing rates, this variance in motility could potentially be a significant contributory factor in the pathological wound healing found in some cleft patients; particularly CL patients which present a 25% risk of HTS (Soltani et al, 2012). Further, this may account for why different patients undergoing the same cleft repair by the same surgeon often display distinct surgical outcomes (Soltani et al, 2012). Cell migration is accelerated in fibroblasts isolated from HTS (Deng et al, 2018); in addition, fibroblasts isolated from keloid scar tissue also have significantly increased migratory rates compared with both extralesional fibroblasts, at the

periphery of the keloid scar and normal dermal fibroblasts within the same patient (Syed and Bayat, 2012). As both HTS and keloid scars arise as a result of pathological wound healing, it is significant that both of these tissue types contain fibroblasts with increased migration rates. It may be possible that cleft fibroblasts that demonstrate faster migration, could also contribute to defective wound healing due to greater exertion of tractional forces leading to elevated myofibroblast differentiation thus greater secretion of ECM and potentially HTS formation.

4.8.2 ECM deposition and expression by cleft fibroblasts

The provisional ECM secreted by fibroblasts comprises largely of collagen and fibronectin (Werner and Grose, 2003), this process is similar in both normal and pathological wound healing, however, the hallmarks of pathological healing, such as fibrosis and subsequent formation of HTS, include excessive myofibroblast differentiation and collagen production. As stated previously, the increased migration rates in the fast migrating cleft fibroblast group could potentially lead to greater myofibroblast differentiation; however, it was also shown here that the fast migrating fibroblasts secreted a significantly higher amount of total collagen. This increased collagen production is important as it has been shown that HTS tissue histologically contains a significant overabundance of collagen when compared with normally healed tissue (Gauglitz et al, 2010). This increase in production primarily comprises of Collagens type I and III (Niessen et al, 1999); however, here it was shown that fast migrating fibroblasts, despite secreting more total collagen, expressed *COL1A1* at levels comparable with the slow group whereas *COL3A1* had significantly lower overall expression in the fast group when compared with the slowly migrating fibroblasts. Although many studies report increased collagen I and III in HTS (Zhang et al, 1995), there are many conflicting reports, with some suggesting that only type III is upregulated and not type I (Oliveira et al, 2009). However, some have reported that HTS consist primarily of type I collagen and type III collagen is found at higher ratios in

normal tissues (Grieb et al, 2011; Cheng et al, 2011), which correlates with results obtained here. This potentially suggests that patients with faster migrating fibroblasts may be at elevated risk of pathological wound healing. The conflicting reports regarding collagen composition and HTS may be due to innate differences between oral and dermal fibroblasts (Shannon et al, 2006) as some report oral fibroblasts demonstrate an enhanced ability to re-organise ECM (Stephens et al, 1996). Coupled with increased motility, cleft lip fibroblasts produced significantly greater total collagen and *COL1A1* expression relative their palatal counterparts. As these are both hallmarks of pathological wound healing and HTS, it could be stipulated that patients with the CL phenotype may be at elevated risk of pathological wound healing. This correlates with others demonstrating that patients with CL develop HTS in 25% of patients (Soltani et al, 2012) as opposed to the 8.6% risk of ONF formation following CP repairs (Hardwicke et al, 2014).

Cleft fibroblasts from the slow migrating groups demonstrated significant upregulation of fibronectin (*FN1*) compared with their fast counterparts. Fibronectin is a glycoprotein that is assembled into the ECM, where it functions as a scaffold and a signalling molecule, to aid in cell adhesion and migration (Ishise et al, 2015). During early wound healing fibronectin is fundamental to the production of the fibrin clot (Fieguth et al, 2003), this provisional matrix is essential for initial fibroblast migration into the wound as when absent fibroblast migration into the wound bed is decreased by 80% (Greiling and Clark, 1997). Although fibronectin is critical to normal wound healing, histological sections of HTS tissue display significant deposition of fibronectin with HTS derived fibroblasts secrete significantly greater amounts of fibronectin (Kischer and Hendrix, 1983; Kischer et al, 1989). Contrary to what would be expected, the present study demonstrated that slow migrating fibroblasts exhibited upregulation of *FN1* suggesting it may contribute to HTS in those patients. Equally, decreased expression of *FN1* by the fast group, which is the presumed pathological group, could be significant as there are likely many compounding factors that converge and contribute to abnormal wound healing.

4.8.3 Involvement of cytoskeletal components in cleft fibroblast migration rates

In order to establish why cleft fibroblasts presented significantly different RWA%s, structural differences in the cell cytoskeleton were investigated. It was found that fast migrating cleft fibroblast, on average, contained significantly more total cellular f-actin when compared with the slow migrating cleft fibroblasts ($p<0.001$), although this did not correlate with increased actin expression. Similarly, others have shown that fast migrating cleft fibroblasts have significantly larger lamellipodia, due to a more organised actin network within the fibroblasts, compared with their slower migrating counterparts (Beyeler et al, 2014), however total actin was not quantified and differences were determined by analysis of a single patient from each group. The cell cytoskeleton is also comprised of polymers of tubulin, which form microtubules that are critical to normal locomotion of adherent cells. Microtubules are dynamic and are in a constant state of polymerisation and depolymerisation to regulate locomotion. These structures are present in large concentrations at the rear of the cell and are pivotal in the disassembly of focal adhesion complexes with underlying matrix (Ezratty et al, 2005) in response to contractile forces produced by actin at the leading edge of the cells. It was found in the present study that *TUBA1* was significantly downregulated in slow fibroblasts when compared with the fast counterparts, due to the critical role of tubulin in cell dynamics this down regulation may have resulted in decreased tubulin production by slow migrating cell and potentially contributed to the decreased migration rates. Chinese hamster ovary (CHO) cells treated with nocodazole, a microtubule inhibitor, have demonstrated the importance of tubulin in directed cell migration. Treatment with 1nM nocodazole, a concentration that supresses microtubule dynamics, led to a significant decrease in migration rates. However, in the presence of 70nM nocodazole, a concentration that leads to complete breakdown of the microtubule network, cells were still able to migrate, although the directionality of migration was significantly perturbed as cells did not migrate towards a scratch wound due to disrupted cellular polarity (Ganguly et al, 2012;

Baudoin et al, 2008). As slow migrating fibroblasts downregulated tubulin it is possible that the cells may have disrupted directional motility. This could lead to fewer cells migrating into the empty area created by the Ibidi insert, meaning the differences observed in migration rates were not due to migratory speed but rather an inability to control the direction of motility towards uncolonised areas, thereby generating a perceived decrease in migratory rate.

Cytoskeletal dynamics, including reorganisation of actin and tubulin, is regulated by the Rho family of GTPases, which are proteins that act as molecular switches within the cell where they stimulate cytoskeletal conformational change through interaction with downstream effectors (Zhao and Manser, 2005). In terms of fibroblast motility *RAC1*, *RHOA* and *CDC42* are the primary influencers (Nobes and Hall, 1995; Lawson et al, 2017), however here it was shown that their expression was comparable between fast and slow groups therefore are unlikely contributory factors in the disparity seen in RWA%.Intracellular regulation of cytoskeletal dynamics is achieved by the above GTPases interacting with the downstream effectors Wiskott–Aldrich syndrome protein (*WASP*), which are effectors for *CDC42*, and *WASP*-family verprolin homologue (*WAVE*), which are involved in RAC-induced actin dynamics (Bompard and Caron, 2004; Symons et al, 1996). This interaction induces effector protein conformational change which subsequently activates the Arp2/3 complexes that mediates f-actin polymerisation through formation of nucleation cores which are precursors to actin filaments (Kurisu and Takenawa, 2009). This process contributes to cell polarity in the initial stages of cell migration through formation of lamellipodia at the leading edge of the cell, which help propel the cell in a forward direction (Steffen et al, 2013). Despite their being no differences in the expression of *WASP* and *WAVE* between fast and slow groups, the main function of *WASP* and *WAVE* proteins is to activate the *ARP2* and *ARP3* proteins thereby permitting formation of the ARP2/3 complex, it was shown here that *ARP2* gene expression was significantly downregulated in the slow migrating fibroblasts (see table 7). The ARP2/3 complex is the principal component in the

formation of new actin filaments at the leading edge of the cells. The complex binds to the lateral borders of existing filaments where it acts as a nucleation core by anchoring at 70° angle, relative to the parent filament and acts as a site for continued actin polymerization leading to formation of new filaments. Growth of the daughter filament is halted by capping proteins, when the filament reaches the desired length, allowing the daughter filament to act as a new binding site for ARP2/3 thereby exponentially expanding the actin network at the leading edge of the cell and aiding in propelling the cell forward (Mullins et al, 1998; Pollard and Beltznar, 2002). As slow migrating cleft fibroblasts were shown to express significantly lower amounts of *ARP2*, a critical component of the ARP2/3 complex, it is possible that decreased migration rates were a result of decreased nucleation of new actin filaments at the leading edge, this would also correlate with reduced total actin observed in slow migrating fibroblasts by phalloidin staining. This is supported by recent research that has found that *ARP2* depleted murine fibroblasts demonstrated a loss of lamellipodial formation and reduced migration rates, both of which were normalised following *ARP2* restoration (Congying et al, 2012). *RHOB* is a small GTPase that coordinates interaction with several complexes which contribute to: actin polymerisation, membrane protrusion, cell migration and cell adhesion (Vega and Ridley, 2018). RHOB downregulation has been reported to have an inverse correlation cell motility in multiple cell types with RhoB depletion leading to elevated motility but reduced cell spreading and lamellipodial extension; potentially due to perturbed focal adhesion contact with the underlying substratum (Vega et al, 2012). As PCR array analysis revealed that *RHOB* expression was significantly upregulated in the slow migrating cleft fibroblasts it is possible that the potential increased production of *RHOB* proteins by slow cells could have contributed to their decreased migratory capabilities.

Patients with CL demonstrated significantly faster RWA% when compared with all other cleft types although expression of *ACTA1*, *TUBA1*, *RAC1*, *RHOA* and *CDC42* were not shown to be

significantly different when compared with all other cleft types. Due to this the mechanism behind the increased RWA% of CL patients is currently unknown, although the other cytoskeletal regulators such as upstream regulators of ARP 2/3 complex activity should be assessed as potential contributors. When comparing clefts of the lip with differing laterality, it was found that RUCLP derived fibroblasts had significantly decreased *CDC42* and *RHOA* expression relative to LUCLP and BLCLP whilst also demonstrating significantly lower *RAC1* expression relative to LUCLP. These differences are of note as RUCLP fibroblasts also had slower RWA% compared with LUCLP and BLCLP fibroblasts. Therefore, it is possible that the decreased RWA% observed in RUCLP was due to disrupted cytoskeletal dynamics due to decreased expression of *RAC1, CDC42* and *RHOA* though further assessment of downstream effectors should also be assessed and compared between clefts of differing laterality. Increased migratory speed may be associated with pathological wound healing, as RUCLP have slower RWA%, from which decreased migration rates can be inferred, it is possible that these patients may be at decreased risk of post-operative complications. However, one study has shown that there is no difference in HTS formation between patients with ULCLP and BLCLP with relative incidence rates of 24.1% and 28.6% respectively, although no distinctions were made between RUCLP and LUCLP (Soltani et al, 2012) which should be addressed in future studies.

4.8.4 Differences in protein production between fast and slow cleft fibroblasts

Due to the involvement of fibroblasts in multiple physiological behaviours they are able to secrete an array of diverse cytokine that can influence cell behaviour. It was shown here that the fast migrating fibroblast group secreted greater total protein relative to the slow. Further, secretome substitution assays demonstrated that secreted cytokines were able to both increase and decrease the RWA% of slow and fast migrating fibroblast respectively. Others have also demonstrated the stimulatory effects of conditioned media, human dermal fibroblasts (HDF)

treated with conditioned media from human immortalized keratinocytes (HaCaT) stimulated cell migration (Li et al, 2014). Further, HDF supplementation with bone marrow mononuclear cell (BM-HNC) secretome significantly increased migration thus closure of scratch wounds (Menendez et al, 2017). The inhibitory effect of conditioned media has also been demonstrated as mesenchymal stem cells (MSC) secretome significantly decreased the migration of corneal fibroblasts (Watson et al, 2009). This demonstrate the secretome derived from different cell types can influence fibroblast behaviour. However here, secretome substitution from cells of the same type, significantly influenced RWA%, suggesting the presence of differing cytokines within the secretome could have influenced cleft fibroblast motility in an autocrine fashion.

Cytokine arrays were conducted to identify how fast and slow fibroblasts differed in terms of their secreted cytokine profiles. Fast migrating cleft fibroblasts produced significantly greater amounts of Insulin-like growth factor (IGF) binding protein-2 (IGFbP2) when compared with their slow counterparts. IGFBP2 is a secreted cytokine that is involved in the regulation of the cell behaviours induced by IGF-1 through its antagonistic function (Firth and Baxter, 2002). IGF-1 has repeatedly been shown to potent stimulator of cell migration in multiple cell types (Guvakova, 2007), whilst the main function of IGBP2 is to compete for IGF-1 receptor binding sites, recent research has shown that it can also stimulate cell motility. HDF's that were cultured with both IGFBP2 and IGFBP2 fragments were shown to increase cell migration rates by 50% compared with controls (Brandt et al, 2014); further, inhibition of IGFB2 in fibroblast-like synoviocytes (FLS) were shown to significantly decrease their rate of migration (Wang et al, 2017). Though the precise mechanism of the stimulatory effect of IGBP2 on cell migration is currently undefined, it has been shown that IGFBP2 potently binds to proteoglycans and glycosaminoglycans (Kawai et al, 2011). Further, when IGFBP2 treated fibroblasts were pre-treated with α5β1, an integrin that binds to ECM macromolecules, motility deceased to levels comparable with that of the control, suggesting that the mechanism behind increased migration

rates was due to alteration to the way cells adhered to the surrounding ECM (Brandt et al, 2015). Therefore, increased IGBP2 secretion observed in fast cleft fibroblasts may contribute to their elevated motility due to alteration to cell-ECM interactions. Growth differentiation factor 15 (GDF15), was also shown to be secreted in higher amounts by fast fibroblasts. Although the precise role of GDF15 remains undefined, it is known to be upregulated in response to cellular stress and disease thereby stimulating changes in cell behaviours including growth, apoptosis and invasion (Baek and Eling, 2019. For example, GDF15 contributes to malignant progression of a number of cancers by stimulating tumour cells to migrate into surrounding tissues (Corre et al, 2013). SNU-216 cells, a gastric cell line, displayed increased invasiveness due to overexpression of GDF15 (Lee et al, 2003) whereas prostate cancer cells displayed increased motility due to reorganization of the cytoskeletal actin network in response to GDF15 (Senapati et al, 2010). Due to this, increased GDF15 secretion may have contributed to the elevated motility observed in the fast fibroblast group potentially due to influences on the actin cytoskeleton as it was also shown here that they contained greater intercellular actin. Dickkopf-related protein-1 (Dkk1), which plays a critical role in craniofacial development due to its function as an antagonist to Wnt signalling molecules (Nie, 2005), was elevated in the fast migrating group. Wnt signalling molecules are potent inducers of cell migration in a range of cell types, including neural crest cells which are involved in development of the lip and palate (Schambony and Wedlich, 2013); thus, variation in Dkk1 production may contribute to the development of CLP. Pax9 negative mice, which exhibit the CP phenotype, demonstrated corrected palatal fusion thus inhibition of the CP phenotype, following intravenous delivery Dkk1 inhibitors to prenatal mice during the palatogenesis developmental period (Jia et al, 2017). It was suggested that corrected palatal fusion was likely due to restoration of Wnt signalling within the palatal mesenchyme as Dkk1 inhibitors acted as Wnt agonists. Further, as overproduction of Dkk1 increased the motility of carcinoma cell lines by interference with Wnt

signalling (Chen et al, 2013; Pang et al, 2017) it is possible that increased Dkk1production by the fast group may have contributed to their elevated motility via disruption to wnt signalling.

The slow cleft fibroblast group secreted increased monocyte chemoattractant protein-1 (MCP-1), a potent inflammatory chemokine produced by multiple cells types including fibroblasts (Yoshimura and Leonard, 1990). Whilst the main function of MCP-1 is to regulate monocyte migration during an inflammatory response, MCP-1 has also been shown to exert an anti-fibrotic effect in human foetal fibroblasts by downregulation of ECM proteins involved in fibrosis, including: collagen-1 by 75%, and fibronectin by 40% (Kalderen et al, 2014). Further, MCP-1 treated fibroblasts significantly downregulated α-Smooth muscle actin (α-SMA), a myofibroblast differentiation marker, relative to control samples (Kalderen et al, 2014). This suggests MCP-1 is an inhibitor of excessive ECM production and fibroblast-to myofibroblast differentiation, which are both contributors to fibrotic scar formation. As slow cleft fibroblasts secreted lower total collagen when compared with their fast counterparts, it is possible that an increased MCP-1 production was a contributory factor. Further, as slow migrating fibroblasts exert less tractional force on the surrounding ECM, which reduces subsequent myofibroblast differentiation, it is possible that patients with decreased migratory rates may be at lowered risk of pathological wound healing therefore subsequent development of HTS and ONF. As the cytokine release profiles between fast and slow cleft fibroblast differed considerably, with a number shown to significantly influence motility, the disparity between migratory groups may have due to variability in intrinsic cytokine release followed by autocrine responses.

4.8.5 Effect of transforming growth factor beta and alpha on cleft fibroblast behaviour

Transforming growth factors are critical to normal wound healing as they stimulate or inhibit key processes including cell recruitment, proliferation, ECM deposition and wound contracture (Penn et al, 2012). Pathological wound healing following cleft repair is a considerable issue as

it can lead to the formation of hypertrophic scars (HTS) and contribute to the formation of oronasal fistulae. Myofibroblasts are critical to normal wound healing but their overabundance can be pathological and contribute considerably to fibrosis. As outlined previously the initial rate of fibroblast migration into and across a wound contributes to myofibroblast differentiation due to increased tractional force at the wound site, this increased mechanical stress leads to ECM stiffness and stimulate differentiation (Hinz and Gabbiani, 2003). However, transforming growth factor β1 (TGFβ1) can also contribute to differentiation to the myofibroblast phenotype (Thannickal et al, 2003) which is characterised by upregulation of *ACTA2* (α-SMA) (Evans et al, 2003). Here cleft fibroblasts treated with TGFβ1 at concentration significantly upregulated *ACTA2* in a dose dependant manner thus indicating fibroblast-to-myofibroblast differentiation similar to what other have shown (Evan et al, 2003). As TGFβ1 is a potent differentiation factor in cleft fibroblasts it is possible that the cleft patients with increased TGFβ1 expression, across the highly variable cohort, may be at increased risk of HTS due to premature differentiation as a result of increased *TGFB1* production. Fibroblasts isolated from HTS also upregulate *TGFB1* relative to their normal counterparts (Wang et al, 2001). In addition, following treatment with TGFβ1, cleft fibroblasts produced greater amounts of total collagen which coincided with upregulation of *COL1A1* and *COL3A1*, which is comparable to what other have found (Petrov et al, 2002). This is interesting as myofibroblast are associated with increased ECM production (Hinz et al, 2007) and increased collagen is a hallmark of HTS thereby offering further evidence that patients with elevated *TGFB1* expression may be at greater risk of fibrosis.

TGFA expression was significantly higher in fibroblasts isolated from patients in the fast group compared with the slow. Further, cleft fibroblast supplementation with 20nM *TGFA* resulted in drastically increased RWA%, relative to unsupplemented controls, thereby demonstrating its stimulatory effect on cleft fibroblast migration. One other study has assessed cleft fibroblast motility, findings correlate with the present study as *TGFA* was significantly upregulated in fast

migrating cleft fibroblasts and the addition of TGFα at 5nM significantly increased the wound closure of slow migrating fibroblasts (Beyeler et al, 2014). In addition, supplementation with TGFα inhibitors, resulted in reduced wound closure of fast migrating fibroblasts thus it was concluded that TGFα plays an important role in cleft fibroblast motility which could potentially translate to reduced fibrosis in some patients (Beyeler et al, 2014). The present study also demonstrated that supplementation with TGFα led to increased collagen production and *COL3A1* expression. Others have shown mature hypertrophic scars, within which increased collagen deposition is characteristic, expressed significantly higher collagen type III within the dermis relative to non-hypertrophic scars (Oliveira et al, 2014). This suggests that elevated TGFα is likely involved in cleft fibroblast motility and stimulates increased collagen secretion which could result in greater likelihood of HTS formation in some patients.

Following supplementation with TGFβ3 cleft fibroblasts demonstrated significantly decreased RWA%, others have also shown that TGFβ3 has an anti-motility effect on dermal fibroblasts (Bandyopadhyay et al, 2006). This anti-motility effect potentially accounts for why fibroblasts in the slow cluster exhibited increased expression of TGFβ3 which potentially contributed to their decreased wound closure. As migration rates are related to myofibroblast differentiation it is also possible that these patients are at decreased risk of fibrosis due to increased production of TGFβ3 potentially reducing wound site migration rates. TGFβ3 has been shown to have an antagonistic effect in the formation of scars as it was shown that intradermal delivery of TGFβ3 at a murine wound sites led to a decreased presence of fibrotic markers (Waddington et al, 2010). Further, delivery of exogenous TGFβ3 to the wound site following cleft lip repair on a murine model resulted in decreased expression of smooth muscle actin and reduced collagen deposition (Hosokawa et al, 2003). This supports the results found here as following supplementation with TGFβ3, *COL1A1* expression was downregulated as was expression of *COL3A1*, both of which correlated with significantly decreased total collagen production. This

data suggests that TGFβ3 potentially has a protective role against fibrosis and resultant HTS. Due to this, the increased expression of *TGFB3* seen in some fibroblasts may result in a decreased risk of pathological wound healing in the patients from which they were isolated. However, HTS is a complex process and is likely not the result of expression of single genes rather the interaction and regulation multiple associated genes are the likely cause. Long-term follow-up assessments following cleft repair are required, with larger patient cohorts, to assess if there are any significant correlations with TGF expression and patient outcome.

4.9 Conclusion

Fibroblasts isolated from cleft patients differed significantly in terms of their RWA% and were grouped into two distinct migratory clusters: fast and slow, with fibroblasts from the fast group secreting greater total collagen. The non-cleft NHDFF control was clustered into the fast group but due to the fundamental differences between oral and dermal fibroblasts they may not be comparable. Although migratory speed did not correlate with cleft phenotype, CL derived fibroblast all presented elevated motility and were all clustered into the fast group. Further, CL fibroblast secreted greater total collagen and upregulated *COL1A1*. As increased migration and collagen secretion are hallmarks of HTS, it is possible patients with faster migrating fibroblast, including those derived from CL, may be at greater risk of pathological wound healing, this correlates with the elevated risk of HTS in patients following CL repair (Soltani et al, 2012). Although fast migrating fibroblasts did not differ in terms of expression of the cytoskeletal regulators *RAC1*, *RHOA* and *CDC42*, they contained increased intercellular actin which correlated with upregulation of *ARP2*, a component of the ARP 2/3 complex which acts as an actin nucleator, thereby suggesting elevated motility may be due to altered cytoskeletal dynamics. However, the two migratory groups also differed in terms of their cytokine release profiles which could have potentially influenced cell motility in an autocrine manner, thereby suggesting distinct physiological differences between the two groups.

CHAPTER FIVE:

THE INFLUENCE OF FOLIC ACID ON CLEFT FIBROBLAST BEHAVIOUR

5.1 Folic acid and cell growth

Folate deficiency has been repeatedly associated with the development of orofacial clefts (Jahanbin et al, 2019); however, despite this, the underlying physiological function that folic acid (FA) contributes to in order to induce its protective role is undefined. Here a broad range of cell responses to FA supplementation was assessed *in vitro* to identify cell behaviours that are induced by the presence of elevated FA thereby identifying potential underlying cell behaviours that may contribute to cleft prevention. To assess the effect of FA concentration on the growth of cleft fibroblasts, isolated from the fast (S101596) and slow (S101597) migratory groups established previously, growth curves were generated with an FA negative control (FA-ve), which had the same DMEM formulation but excluded FA, and in the presence of FA at concentrations of: 20nM, 10µM, 20µM and 30µM from which doubling times were calculated. Fibroblasts supplemented with physiological concentrations of FA (20nM) generated comparable cell numbers to that of the FA-ve control, throughout the assay period, indicating that at this concentration FA did not appear to influence cell growth. Despite all cultures being seeded at the same concentration ($5x10^4$), fibroblast growth following culture with 10µM FA was accelerated ($p<0.01$), cell number increased further in the presence of 20µM FA, though not significantly (Figure 79A-B). However, growth was significantly reduced in medium containing 30µM FA ($p<0.01$). Fibroblasts derived from the fast and slow migratory groups shared similar responses to the presence of FA. The growth increases observed in the presence of 10µM and 20µM FA was also observed in the non-cleft neonantal human dermal foreskin fibroblasts (NHDFF) control (figure 79C), indicating this folate response was not specific to cleft fibroblasts. Population doubling times (DT) mirrored growth curve models. Physiological concentrations (20nM) FA did not influence DT. However, 10µM and 20µM resulted in significant ($p<0.01$) decreases in DT in both fast (figure 80A) and slow groups (figure 80B) relative to the control. Fibroblasts treated with 30µM displayed significantly longer DT in both

migratory groups (P<0.001). This general trend was also observed in the NHDFF control (figure 80C).

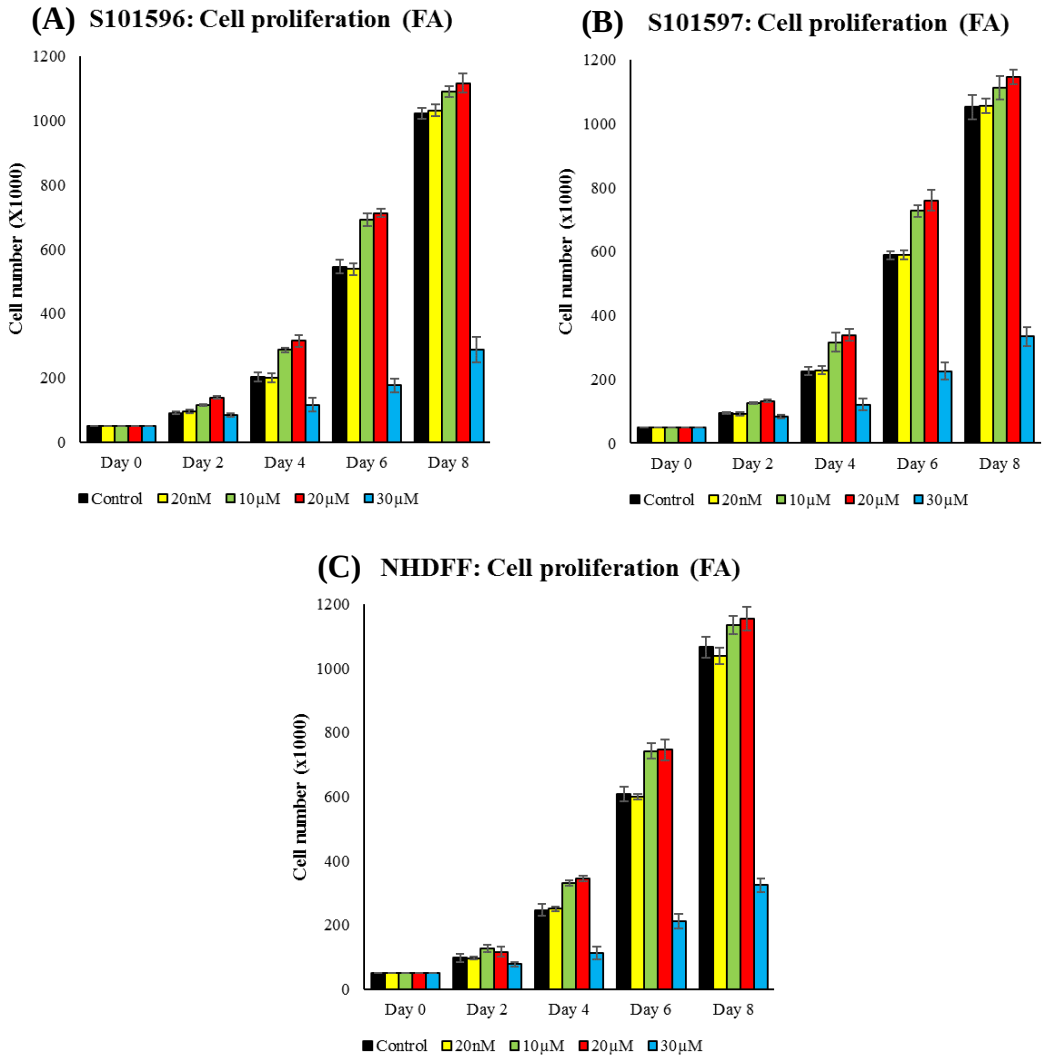

Figure 79: Effect of folic acid on the growth of cleft fibroblasts. At day 0 the same number of cleft fibroblasts were seeded with the only differences between cultures being the concentration of FA provided. After 2 days in culture there were marginal (non-significant) increases in the cell numbers present in cultures treated with 10µM and 20µM FA. After 4 days in culture cells treated with 20nM FA displayed cell numbers comparable with those of control cells whereas fibroblast treated with 10µM and 20µM FA were significantly higher in cell number ($p<0.05$ and $p<0.05$, respectively) however cultures treated with 30µM displayed significantly lower cell number ($p<0.01$). This increased growth rate in cultures treated 10µM and 20µM FA continued up until day 8 whereas growth in 30µM was significantly decreased. This general trend was observed in both fast and slow migrating fibroblasts as well as in non-cleft control cells (NHDFF) (n=12).

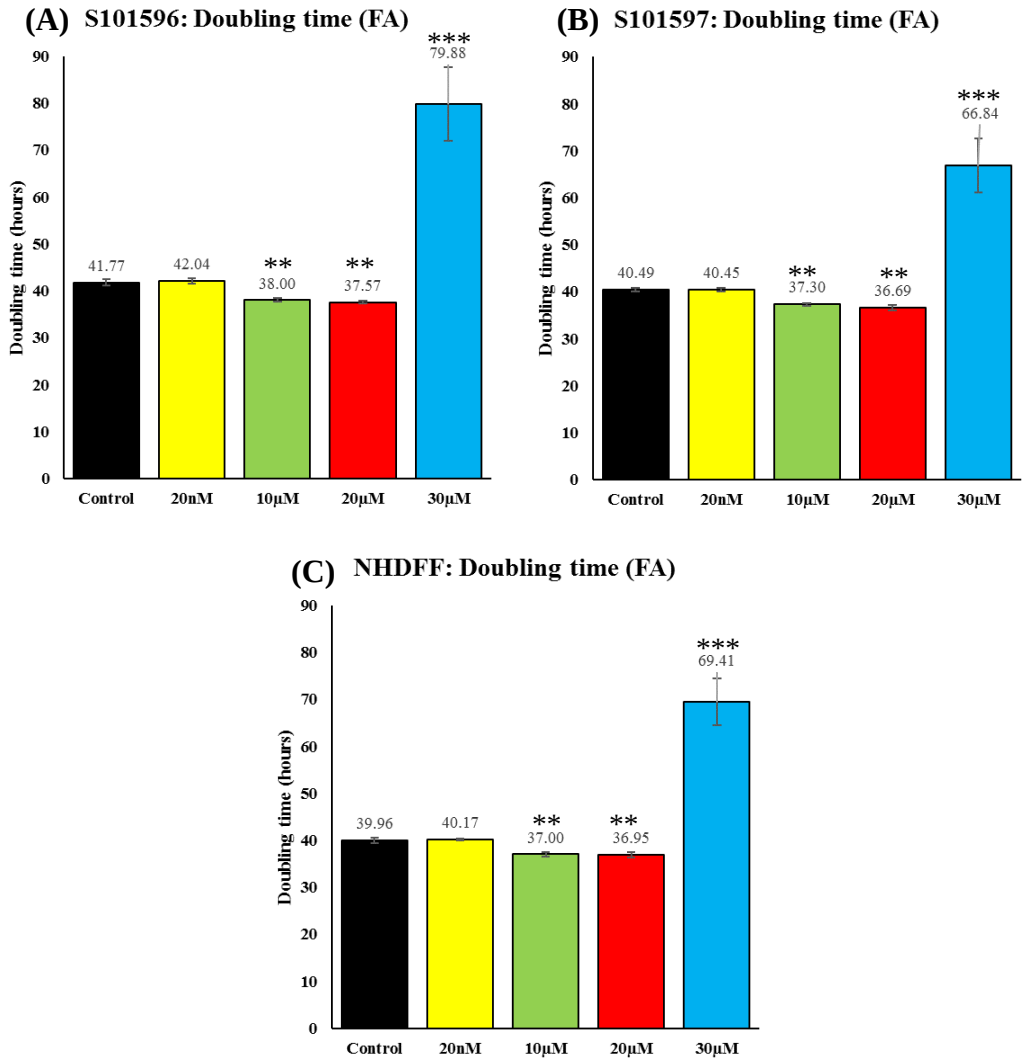

Figure 80: Effect of folic acid on cleft fibroblast doubling time. (A) Doubling times were comparable between untreated control cells and cells treated with 20nM FA, which demonstrated that at physiological concentration FA did not influence cleft fibroblast growth rates. Doubling times were significantly lower in cultures treated with 10µM and 20µM ($p<0.01$ and $p<0.01$ respectively) thus demonstrating an increase in cell growth however there was no significant difference between 10µM and 20µM treated cultures. Cleft fibroblasts treated with 30µM FA displayed significantly decreased population doubling times ($p<0.001$) when compared with the control group demonstrating that at this concentration FA had an adverse effect on cell growth. This general trend was observed in both the fast (S101596) and slow (S101597) (B) migrating fibroblasts as well as in non-cleft NHDFF control (C) (n=3).

5.2 Influence of folic acid on formazan production by cleft fibroblasts

In the absence of FA fast migrating cells exhibited lower overall absorbance values, this was increased in the presence of physiological concentrations of FA (20nM)(non-significant). When cleft fibroblasts were cultured with 10µM and 20µM FA, absorbance values were significantly higher than both the control ($p<0.01$ and $p<0.01$) and the 20nM condition ($p<0.01$ and $p<0.01$). Supplementation with 30µM led a marked decrease in metabolic activity when compared with the 10µM FA ($p<0.05$) and 20µM ($p<0.01$) conditions although absorbance values were still significantly greater than the FA-ve control ($p<0.05$) (figure 81A). Slow migrating fibroblasts (S101597) displayed a different response to FA. Following 10µM supplementation, fibroblasts exhibited significantly increased absorbance relative to both the control ($p<0.01$) and the 20nM group ($p<0.01$). However, both 20µM and 30µM conditions displayed absorbance comparable with the control and significantly lower than 10µM FA ($p<0.01$ and $p<0.05$) (figure 81B).

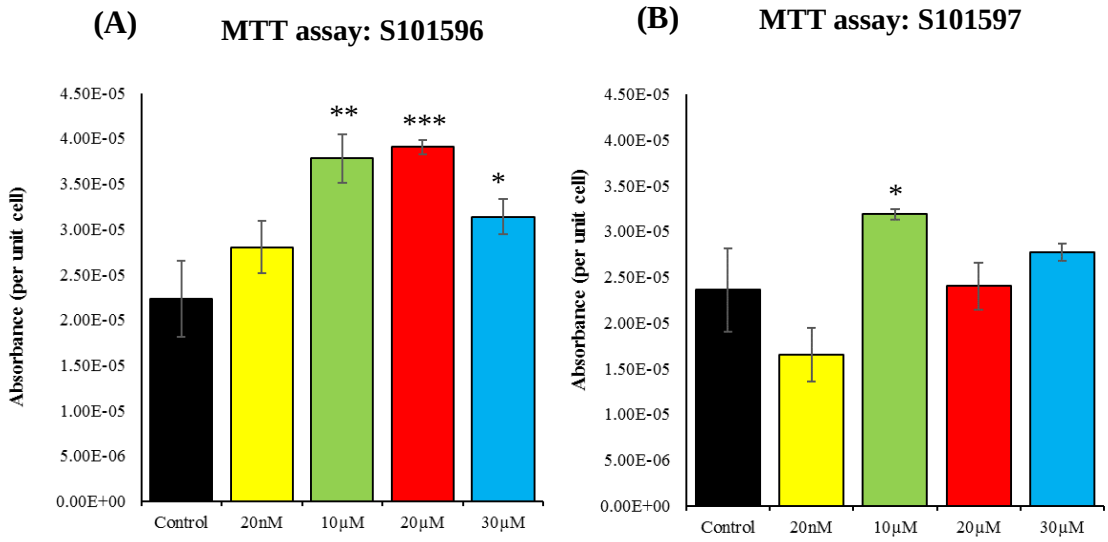

Figure 81: Effect of folic acid on formazan production by cleft fibroblasts. (A) The metabolic activity per cell in the fast migrating group was comparable for untreated control cells and cells treated with 20nM FA, however treating cells with 10µM, 20µM and 30µM FA significantly increased the metabolic activity per cell ($p<0.01$, $p<0.001$ and $p<0.05$ respectively). (B) Following treatment with 10µM FA metabolic activity was significantly increased ($P<0.05$) when compared with the control however there was no significant difference between the control and the 20µM FA and 30µM FA treated cleft fibroblasts.

5.3 Influence folic acid supplementation on wound closure

Changes in wound closure in the presence of a range of concentrations of FA was measured by means of an Ibidi migration assay. Cleft fibroblast from the fast migratory group were found to exhibit similar migratory rates between the control and the 20nM FA supplemented group indicating that despite being the normal physiological concentration of FA it did not have any significant effect on migration rates *in vitro*. Cleft fibroblast migration in the presence of 10μM FA was significantly decreased when compared with both the control ($p<0.01$) and 20nM FA ($P<0.01$) exposure. Treatment with 20μM and 30μM FA led to a further reduction in migratory speed and was significantly slower than the 10μM FA exposure group ($p<0.05$) (figure 82A). This data demonstrated that the addition of FA to fast migrating fibroblasts, in concentrations of 10μM, 20μM or 30μM, led to a significant decrease in migratory speed over a duration of 24 hours. Slow migrating fibroblasts did not demonstrate any significant change in RWA% in response to FA (figure 82B).

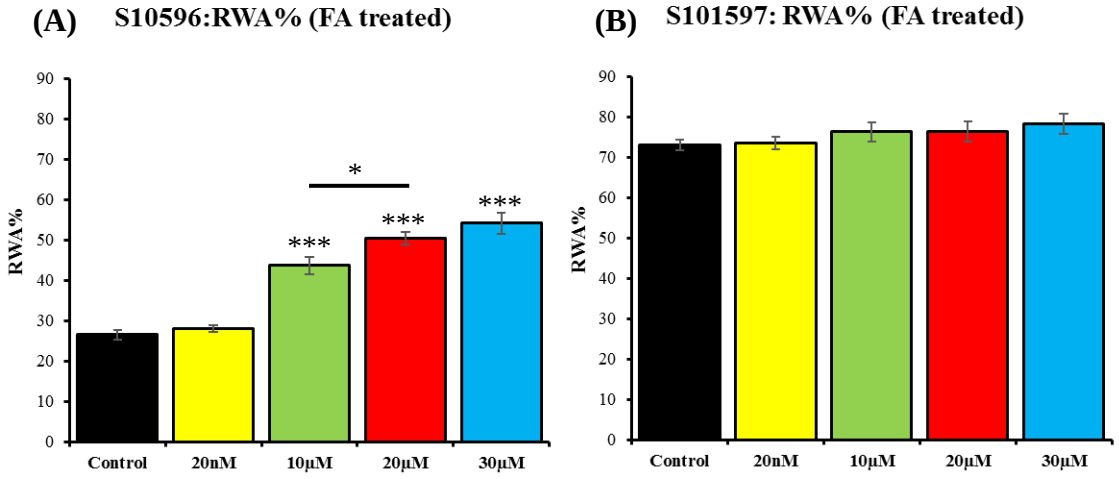

Figure 82: Effect of folic acid supplementation on RWA%. (A) Supplementation with 20nM FA did not lead to any significant change in wound closure However, supplementation with 10μM, 20μM and 30μM FA significantly increased RWA% due to decreased migratory speed when compared with untreated controls ($p<0.001$). Supplementation with 20μM FA led to a significant decrease in RWA% when compared with 10μM ($p<0.05$), there was no significant difference between 20μM and 30μM treated groups. (B) In the slow migrating group supplementation with 20nM, 10μM, 20μM and 30μM FA did not lead to a significant decrease in migratory speed (n=9).

5.3.1 Effect of folic acid on genes related to cell migration

Exposure to a range of concentrations of FA prior to RNA isolation from cultured fibroblasts resulted in a number of changes to the expression levels of *ACTA1* and *TUBA1*, which are regulators of actin and tubulin production and are involved in the mechanical process of cell migration. Supplementation with 10μM FA led to a significant decrease in the expression of both *ACTA1* ($p<0.01$) and *TUBA1* ($p<0.01$) in fast migrating cleft fibroblasts (Figure 83A-B). However, increasing concentrations of FA to 20μM and 30μM did not have any significant effect on *ACTA1* or *TUBA1* expression levels relative to the 10μM treatment condition. Slow migrating fibroblasts had decreased *ACTA1* expression in response to 10μM FA though this decrease was not significant. Increasing FA concentrations to 20μM and 30μM resulted in a significant downregulation of *ACTA1* compared with the FA-ve control ($p<0.05$ and $p<0.01$ respectively). Furthermore, cleft fibroblasts treated with 10μM and 20μM FA had significantly decreased expression of *TUBA1* ($p<0.05$ and $p<0.05$). However, supplementation with 30μM FA did not lead to a significant decrease in *TUBA1* expression, relative to the control, despite minimal downregulation (Figure 83C-D). These data indicated that *ACTA1* and *TUBA1* expression was downregulated in response to relatively high concentrations of FA.

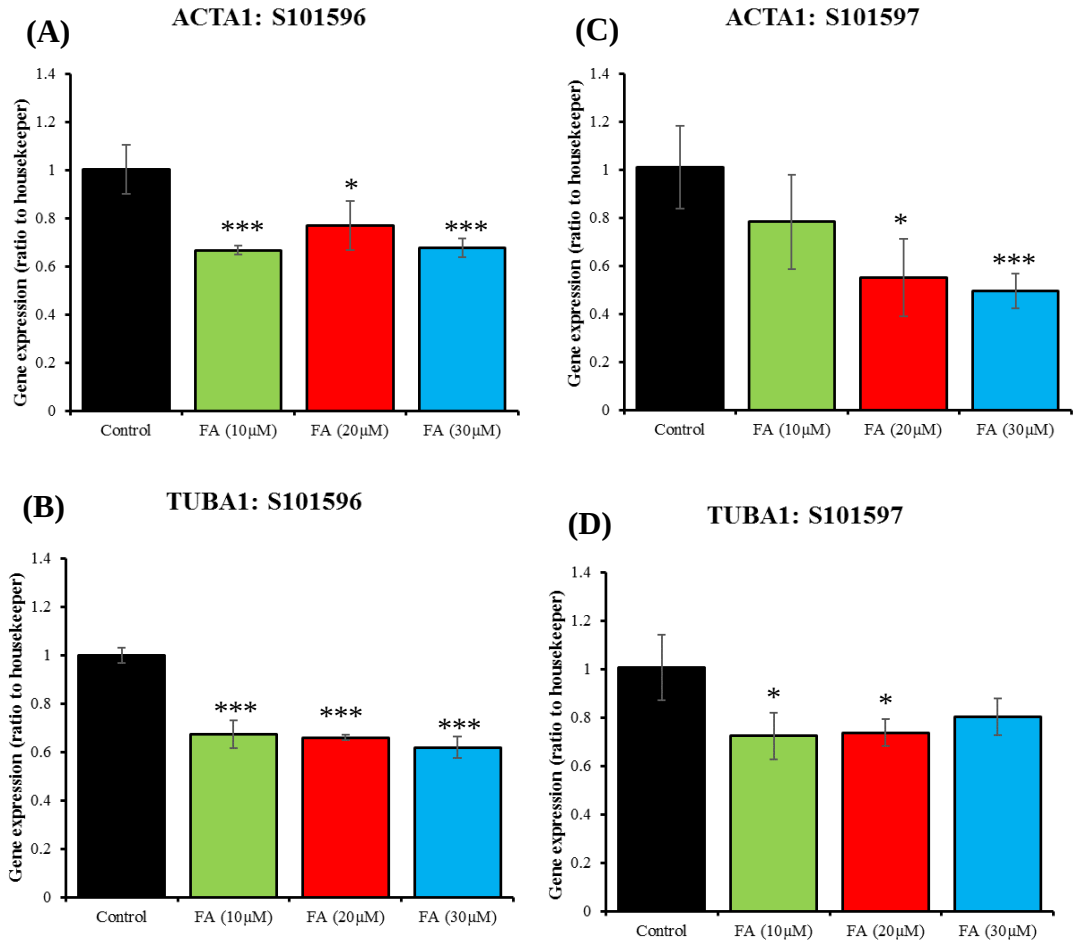

Figure 83: Effect of folic acid on gene expression of cytoskeletal-related molecules. (A) *ACTA1* expression and *TUBA1* expression (B) was significantly decreased in the 10µM FA treated groups ($p<0.001$ and $p<0.001$). This decrease was also detected in both 20µM and 30µM groups, though all treated groups displayed similar expression levels. (C) *ACTA1* expression in fibroblasts from the slow migrating group was lower when treated with 10µM FA however this was non-significant. Supplementation with 20µM and 30µM FA led to a significant decrease in expression levels when compared with an untreated control ($p<0.05$ and $p<0.01$ respectively). (D) Supplementation with 10µM and 20µM FA resulted in a significant decrease in *TUBA1* expression ($p<0.05$ and $p<0.05$) however supplementation with 30µM FA did not lead to a significant decrease in *TUBA1* expression levels (n=3).

5.4 Effect of folic acid on cell adherence and cell non-adherence

To determine the effect of FA on the adhesion of cleft fibroblast, cells were seeded at $5x10^5$ with range of concentrations of FA and after 24 hours and the number of adherent and non-adherent cells were counted. Two controls were used, one comprised of the normal formulation of DMEM (which contains approximately 9μM FA) whilst the second was the modified FA-ve culture medium that has been used for all other folate supplementation assays.

In terms of cell adhesion, fast migrating fibroblasts (S101596) exhibited significantly higher numbers of adherent cells in the FA+ve control when compared with the FA-ve control ($p<0.01$). These data were supported by quantification of the numbers of non-adherent cells which were significantly higher in the FA-ve control when compared with FA+ve ($p<0.01$), indicating that the presence of FA within the normal formulation of culture medium was critical for optimal cell adhesion. Supplementation with 20nM FA did not significantly influence the number of adherent cells as values were comparable with those of the FA-ve control demonstrating that this concentration did not have a significant effect on cell adhesion. However, supplementation with 10μM and 20μM FA caused significantly greater numbers of cells to be adherent after 24 hours when compared with the FA-ve control ($p<0.05$) although values were comparable with the FA+ve control (Figure 84A-C). This was mirrored in the quantification of the number of non-adherent cells as both conditions produced significantly lower number of non-adherent cells when compared with the FA-ve control. Though somewhat unexpected the presence of 30μM FA significantly decreased cell adhesion rates, the numbers of adherent cells were significantly lower than the 10μM and 20μM FA conditions ($p<0.01$ and $p<0.01$ respectively). In addition, the presence of 30μM FA led to numbers of non-adherent cells that were significant higher than all other FA treated groups and the FA-ve control ($p<0.01$). The same general trends were observed in the slow migrating cells (S101597), though

the numbers of non-adherent cells in the 30µM condition were comparable with that of the FA-ve group. Non-cleft cells also exhibited a similar response to FA in the concentration ranges used. Taken together these data demonstrated that the presence of FA was critical for cell adhesion in both cleft and non-cleft fibroblasts although 30uM FA had an adverse effect on cell adhesion (Figure 85A-C).

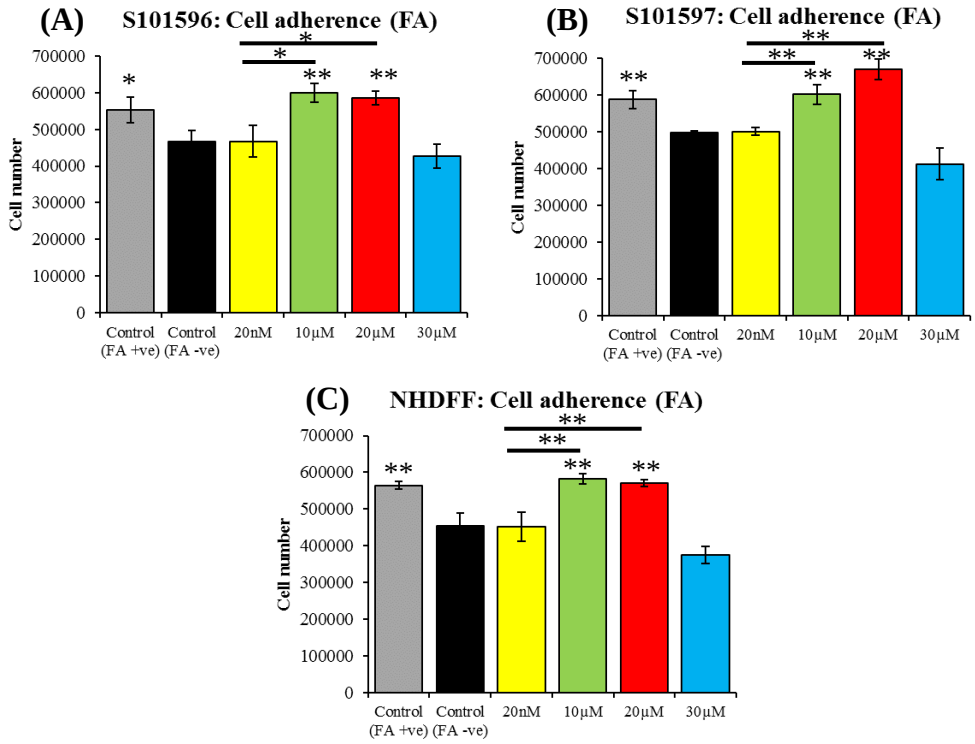

Figure 84: Effect of folic acid supplementation on cell adherence. (A) The number of adherent cells was significantly lower ($p<0.05$) in the FA negative control (FA-ve) when compared with the FA positive control (FA+ve) suggesting that FA is important for optimal cell adhesion. The number of adherent cells was comparable between the FA-ve control and the cells supplemented with 20nM FA, however the supplementation with 20nM did lead to lower total adherent cells when compared with the FA+ve control ($p<0.01$). Following supplementation with 10µM and 20µM the number of adherent cells were comparable to that of the FA+ve control but significantly higher than the FA-ve control ($P<0.05$). When treated with 30µM FA cleft fibroblasts exhibited lower levels of cell adherence when compared with the cells supplemented with 10µM ($p<0.01$) and were similar to that of the FA-ve control. This general pattern of adhesion was also observed in the slow migrating group (B) and the non-cleft cells (C) (n=3).

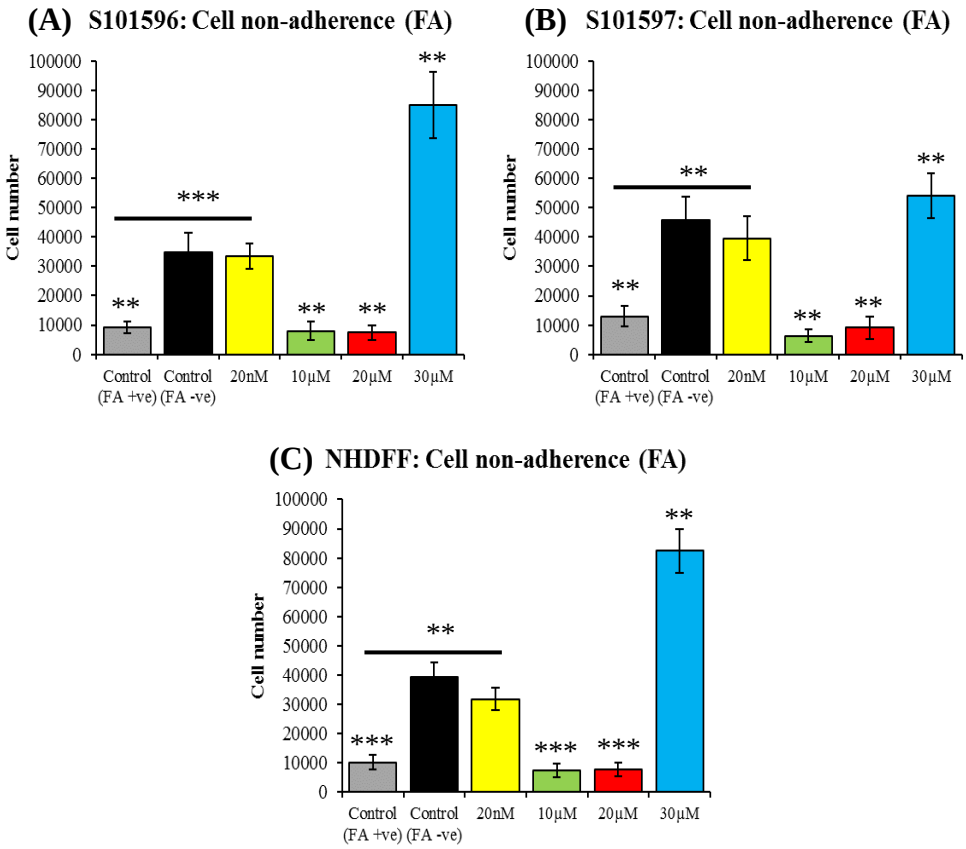

Figure 85: Effect of folic acid supplementation on cell non-adherence. (A) The number of non-adherent cells was significantly lower in the FA+ve control when compared with the FA-ve control ($p<0.01$). Supplementation with 20nM FA did led to non-adherent cell number comparable to the FA-ve control but significantly higher than that of the FA+ve control ($P<0.001$). Cultures supplemented with 10µM and 20µM led to significantly fewer non-adherent cells when compared with FA-ve ($P<0.01$) however cell numbers were comparable to that of the FA+ve control. Cleft fibroblasts treated with 30µM FA were significantly more non-adherent when compared with both the FA-ve control and FA+ve control ($p<0.01$ and $p<0.05$ respectively). (B) Similar trends were observed in slow migrating fibroblasts (S101597) and in NHDFF (C) however in S101597 there was no significant difference between supplementation with 30µM FA and the FA-ve control (n=3).

5.4.1 Effect of folic acid on cell-to-cell adhesion

The effect of FA on cell-cell adhesion was assessed by seeding $5x10^4$ fluorescently labelled cleft fibroblasts onto confluent monolayers of the same cell type followed by measuring the relative fluorescence of the supernatant, which contained all of the labelled non-adherent cells, after 24 hours. The FA-ve control exhibited the highest fluorescence which indicated the largest number of non-adherent cells (Figure 86A) this was confirmed following quantification of cell numbers using a standard curve (Figure 86B). Supplementation with 20nM FA led to a reduction in fluorescence relative to the control, following quantification this decreased signal translated to significantly decreased non-adherent cell number ($p<0.05$). Exposure to 10µM, 20µM, and 30µM FA significantly lowered fluorescence compared with the control ($p<0.01$). This data suggests that the presence of FA within the culture medium improved the ability of cleft fibroblasts to adhere to cells of the same type.

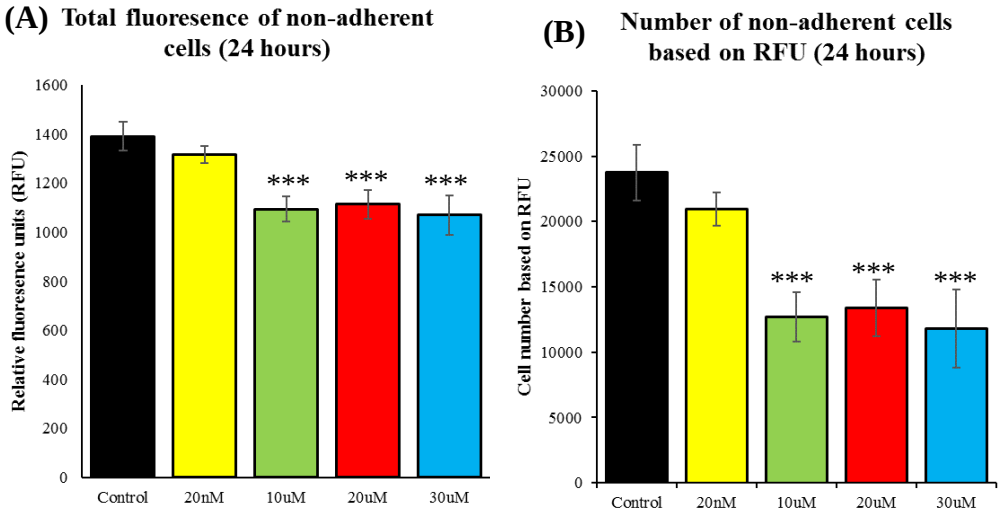

Figure 86: Effect of folic acid supplementation on cell-cell adhesion. (A) FA negative control cultures exhibited the highest RFU based on the number of remaining stained non-adherent cells in the cell supernatant after 24 hours. Supplementation with 20nM FA did not lead to any significant differences in RFU relative to the control. However, supplementation with 10µM, 20µM and 30µM led to a significant reduction in RFU when compared with the FA-ve control ($p<0.001$, $p<0.001$ and $0<0.001$ respectively), indicating the presence of FA increases cell-to-cell adhesion rates. (B) 20nM FA did lead to significant reduction in the number non-adherent cells after 24 hours when compared with the control ($P<0.05$). 10µM, 20µM and 30µM FA led to a greater decrease in non-adherent cells when compared with both the control and the 20nM group ($p<0.001$, $p<0.001$ and $p<0.001$ respectively). There were no significant differences between 10µM, 20µM and 30µM FA conditions (n=6).

5.4.2 Effect of folic acid on expression of genes related to cell adhesion

Due to the effect of FA on the adhesive ability of cleft fibroblast, gene expression analysis was conducted on a number of transcripts that are associated with cell adhesion. In the fast migrating group (S101596) intercellular adhesion molecule-1 (*ICAM1*) was significantly upregulated ($p<0.01$) following supplementation with 10μM FA with a 4-fold change relative to the FA-ve control. Increasing FA concentration to 20μM and 30μM did not lead to further increases in expression (Figure 87A). Vascular cell adhesion molecule 1 (*VCAM1*) was also significantly upregulated in the presence of 10μM and 20μM FA ($p<0.01$ and $p<0.01$) with an approximate 4-fold change relative to the control, 30μM FA led to a further increase in expression of *VCAM1* with an approximate 5-fold change which was significantly higher than both the 10μM and 20μM conditions (Figure 87B). Paxillin (*PXN*) expression was shown to be significantly higher than the FA-ve control following exposure to 10μM and 20μM FA however the fold change of 1.5 was much lower than the increase observed with *ICAM1* and *VCAM1*, supplementation with 30μM FA did not lead to a significant increase in *PXN* expression relative to the control (Figure 87C). Fibroblasts from the slow migrating group (S101597) also showed upregulation of *ICAM1* in the presence of 10μM FA; however, this was increased further to a 5-fold change in the presence of 20μM FA (Figure 87D). *VCAM1* was also upregulated in all experimental conditions though the fold change was lower (approximately 3.5) (Figure 87E). *PXN* expression was not affected by FA in any of the concentrations assessed with expression levels comparable with that of the FA-ve control.

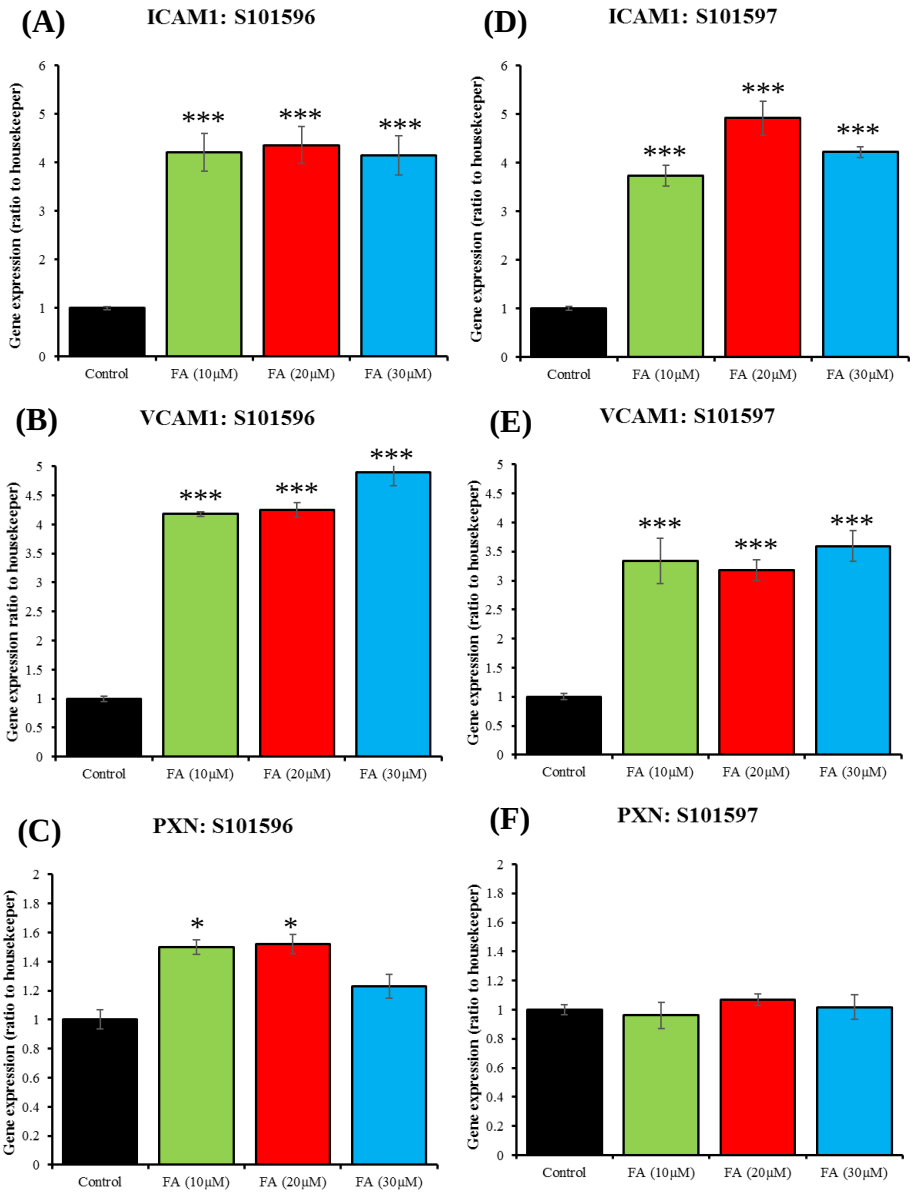

Figure 87: Effect of folic acid supplementation on cell adhesion related gene expression. Fast migrating cells: (A) *ICAM1* expression was significantly increased following supplementation with 10µM, 20µM and 30µM FA ($p<0.001$); there was no significant differences between supplemented conditions. (B) *VCAM1* expression was significantly upregulated in all supplemented conditions when compared with the control ($p<0.001$), however 30µM FA led to significantly higher expression when compared with 10µM and 20µM exposure ($p<0.05$). (C) *PXN* expression was significantly higher in the 10µM and 20µM FA conditions when compared with the control however there was no significant difference between 30µM FA exposure and the control. Slow migrating cells: (D) All experimental conditions displayed significantly higher *ICAM1* expression compared with the untreated control ($p<0.01$) however 20µM FA exposure resulted in significantly higher expression levels when compared with 10µM and 30 µM FA exposure. (E) *VCAM1* expression was significantly higher in the 10µM, 20µM and 30µM exposure conditions when compared with the FA-ve control, there were no differences between groups. (F) There were no differences between *PXN* expression in the control and the FA treated conditions (n=3).

5.5 Effect of folic acid on expression of RAC1, RHOA and CDC42

As FA influences both cell adhesion and cell motility, expression of genes associated with these cell activates were determined. Rac family small GTPase-1 (*RAC1*) was significantly down-regulated, when compared with the control, in response to 10μM, 20μM, and 30μM FA ($p<0.01$) in the fast migrating groups (Figure 88A). Ras-homolog gene family member-A (*RHOA*) was significantly upregulated ($p<0.01$) with an average 2.5-fold change relative to the control following supplementation with 10Mm, 20μM, and 30μM FA (Figure 88B). Cell division control protein 42 (*CDC42*) expression was also significantly up-regulated in response to 10μM ($p<0.01$) 20μM ($p<0.05$) and 30μM ($p<0.01$) FA however, the average fold-changes were only approximately 1.5 (Figure 88C). Although the slow migrating fibroblast sample shared a similar pattern of expression there were a few differences. *RAC1* was significantly down-regulated in response to 10μM and 20μM FA exposure and expression was down-regulated further in response to 30μM FA (Figure 88D). *RHOA* was upregulated in response to 10μM and 20μM FA exposure with an average 3-fold change this was reduced to 2.5-fold in the 30μM FA group (Figure 88D). *CDC42* was upregulated in response to 10μM FA (fold-change approximately 1.5) and expression increased further following exposure to 20μM and 30μM FA (fold change approximately 2) (Figure 88F). These data suggested that the expression levels of *RAC1*, *RHOA* and *CDC42* genes were significantly influenced by FA exposure at high concentrations, which may have exerted an effect on cell adhesion and migration.

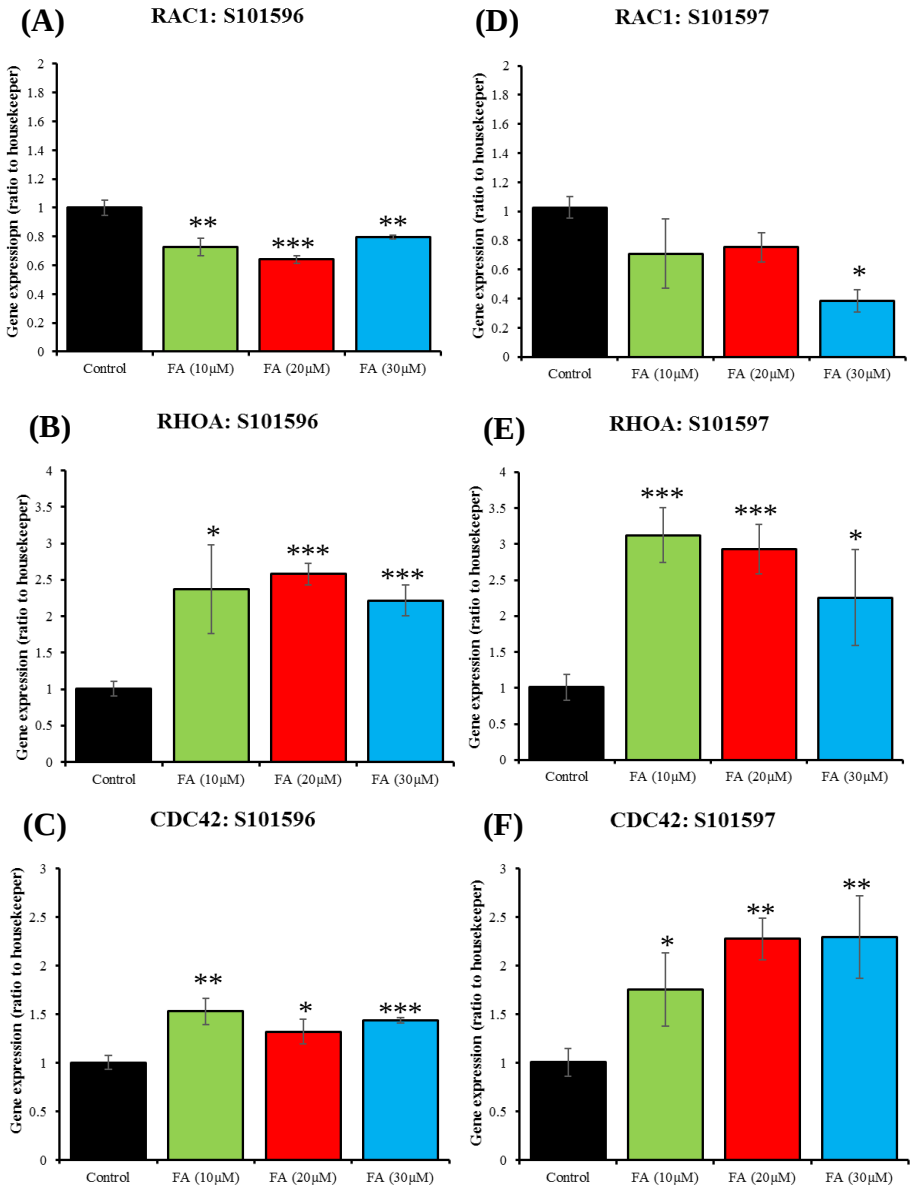

Figure 88: Effect of folic acid supplementation on *RAC1*, *RHOA* and *CDC42* gene expression. Fast migrating cells: (A) *RAC1* expression was significantly down-regulated following supplementation with 10µM, 20µM and 30µM FA ($p<0.01$; $p<0.001$; $p<0.01$); there were no significant differences between treated groups. (B) *RHOA* expression was significantly up-regulated in all FA treated groups ($p<0.05$; $p<0.001$; $p<0.001$) however there were no significant differences between treatment conditions. (C) *CDC42* expression was upregulated in the 10µM ($p<0.01$), 20µM ($p<0.05$) and 30µM ($p<0.001$) treated groups when compared with the control. Upon supplementation with FA, similar patterns of *RAC1*, *RHOA* and *CDC42* expression were observed in the cells from the slow migrating group (D-F) (n=3).

5.6 Influence of folic acid on collagen production and expression

The response of cleft fibroblasts to FA in terms of collagen production was assessed by means of Sirius red staining followed by quantification of the adherent dye. With S101596 cells, it was found that supplementation with the physiological concentration of FA (20nM) did not result in any significant change in collagen production relative to the FA-ve control. However, FA in concentrations of 10μM led to a significant increase in total collagen production ($p<0.01$) while increasing the concentration to 20μM and 30μM did not lead further increased (Figure 89A). Despite producing a greater amount of collagen overall, S101597 cells shared a similar response to FA supplementation. Treatment with 20nM produced similar levels of collagen as the control, whereas, supplementation with 10μM, 20μM and 30μM FA led to significantly higher total collagen but no differences between FA exposure concentrations (Figure 89B).

The influence of FA on collagen gene expression was also measured by means of real-time polymerase chain reaction. In S101596 cleft fibroblasts the addition of 10μM FA resulted in a significant increase ($p<0.01$) *COL1A1* expression which increased further in the presence of 20μM ($p<0.05$) but not 30μM (Figure 90A). *COL3A1* was significantly upregulated in the presence of 10μM FA ($p<0.05$) though to a lesser degree than *COL1A1*, this was increased further in response to 20μM and 30μM FA though not significantly (Figure 90C). In S101597 cleft fibroblasts cultures *COL1A1* expression was also upregulated in response to 10μM FA ($p<0.01$) although to a much greater degree; there was no significant change in *COL1A1* expression following exposure to 20μM and 30μM FA groups relative to the 10μM FA (Figure 90B). *COL3A1* was significantly upregulated ($p<0.01$) in response to 10μM and 20μM FA (approximately 2.5-fold change relative to the FA-ve control), this decreased to an approximate 2-fold change in response to 30μM FA (Figure 90D).

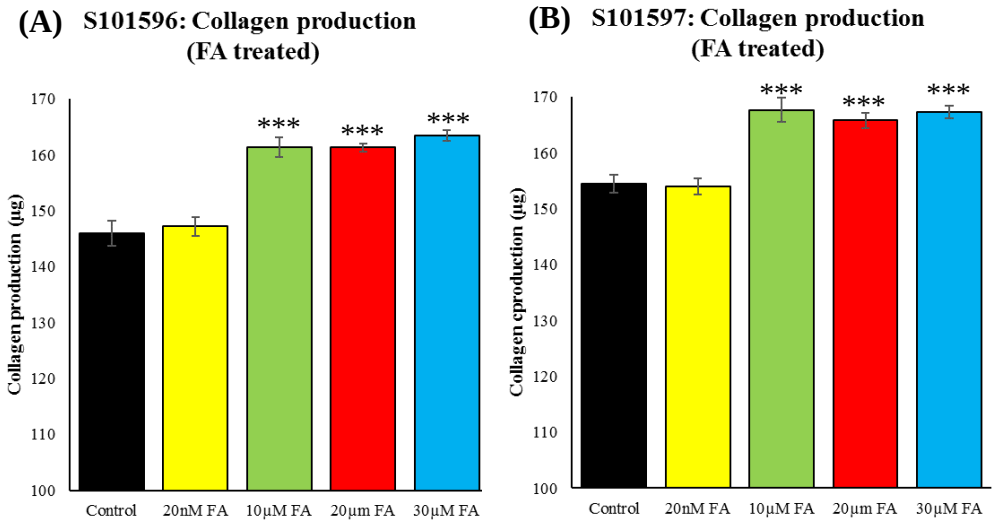

Figure 89: Folic acid supplementation and cleft fibroblast collagen production. (A) Supplementation with 20nM FA did not significantly alter collagen production in both cell types. However, elevated FA exposure (10µM, 20µM and 30Mm) significantly increased collagen production ($p<0.01$), though there were no significant differences between treatment conditions. (B) Similar trends were observed in the slow migrating group (S101597) although overall collagen production was higher in this group.

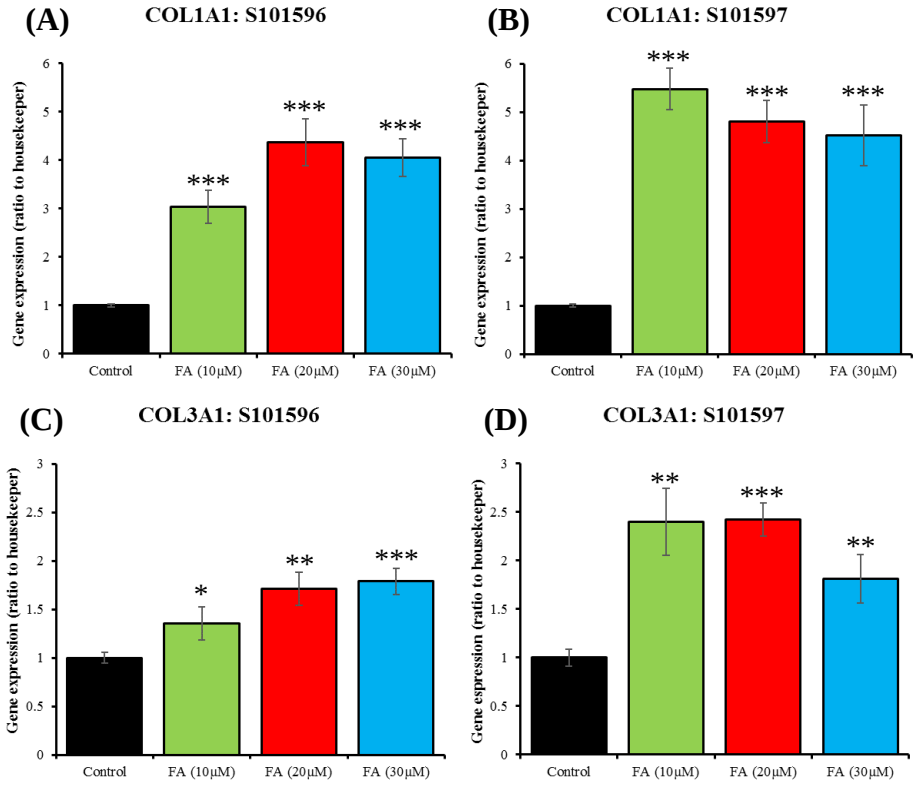

Figure 90: Folic acid supplementation and cleft fibroblast collagen gene expression. (A-B) Supplementation at 10µM, 20µM and 30µM FA significantly increased *COL1A1* expression in both the fast (S101596) and slow (S101597) migrating groups ($P<0.001$ and $p<0.001$ respectively). (C) Supplementation with 10µM FA caused a significant increase in *COL3A1* expression in the fast group ($p<0.05$), this upregulation increased at elevated FA exposures ($p<0.01$ and $p<0.001$). (D) Upon FA supplementation, *COL3A1* expression was higher in the slow migrating groups; 10µM and 20µM FA significantly increased *COL3A1* expression though this decreased following supplementation with 30µM. (n=3).

5.6.1 Effect of folic acid on sulphated GAG production and gene expression

Alcian blue staining was assessed following incubation of with varying concentrations of FA to quantify the amount of sulphated glycosaminoglycans (GAGs) produced over a seven-day period. S101596 fibroblasts demonstrated comparable absorbance values between the FA-ve control and the 20nM FA supplemented condition, indicating that at this concentration FA did not influence GAG production. Incubation with 10μM caused a significant increase in sulphated GAG production ($p<0.01$), this increased further following supplementation with 20μM though not significantly. Exposure to 30μM FA led to a significant decrease in GAG production with levels lower than that of the FA-ve control (Figure 91A). The S101597 cleft fibroblasts produced significantly lower amounts of sulphated GAGs although a similar response to FA was observed. The FA-ve control and the 20nM condition produced similar amounts of GAG whereas production was increased following the addition of 10μM FA. However, unlike S101596 absorbance was decreased following the addition of 20μM and this was decreased further following the addition of 30μM (Figure 91B). These data indicated that although physiological concentration of FA did not appear to influence sulphated GAG production the application of 10μM FA may have had a positive effect on production whilst higher concentrations may have caused to a significant reduction in GAG production.

Expression of markers associated with sulphated glycosaminoglycan production was assessed to ascertain cell responses to FA. Chondroitin sulphate proteoglycan 4 (*CSPG4*) expression was significantly downregulated in response to 10μM, 20μM and 30 FA ($p<0.01$) in both S101596 and S101597 although the latter produced lowered expression overall; there was no significant difference in expression between treated groups (Figure 92A-B). Heparin sulphate proteoglycan 2 (*HSPG2*) was not downregulated in response to 10μM FA in the S101596 group. However, expression was significantly downregulated in response to 20μM and 30μM FA supplementation ($p<0.01$) (Figure 92C). Similarly, *HSPG2* expression remained comparable

with the FA-ve control in the S101597 group in response to 10µM and 20µM FA but was downregulated in response to 30µM ($p<0.01$) (Figure 92D). Dermatan sulphate epimerase (*DSE*) expression was not significantly influenced by the presence of FA at any of the concentrations used in both S101596 and S101597 cleft fibroblasts (Figure 92E-F).

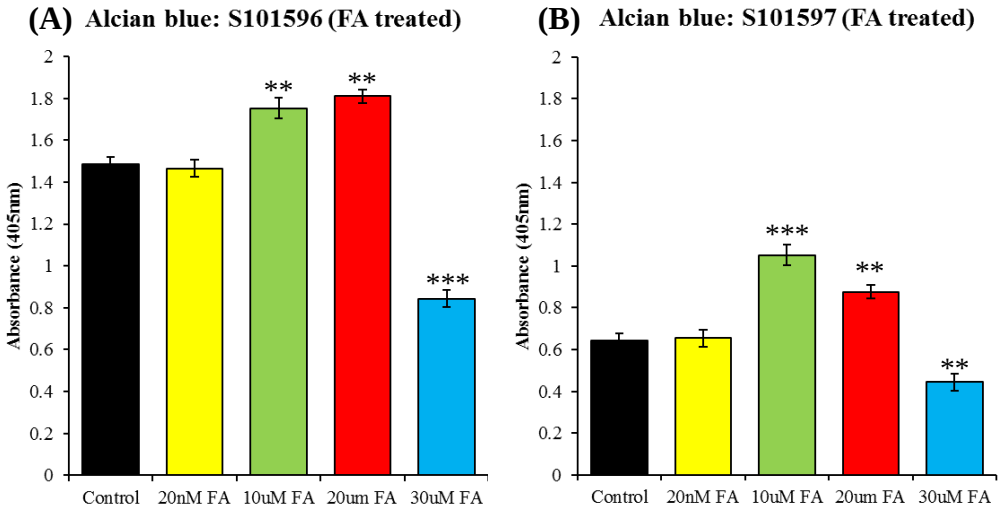

Figure 91: Effect of folic acid supplementation on glycosaminoglycan production. (A) Supplementation with 20nM FA did not significantly affect the amount of GAGs produced based on absorbance readings. However, following supplementation with 10µM and 20µM FA absorbance was significantly increased ($p<0.01$); absorbance was again decreased to levels comparable with that of the control in the 30µM condition. (B) The slow migrating cell types assessed here produced lower overall GAGs when compared with the fast group. GAG production significantly increased following supplementation with 10µM FA ($p<0.001$) it was also increased in the presence of 20µM and 30µM but to a lesser degree than that of 10µM.

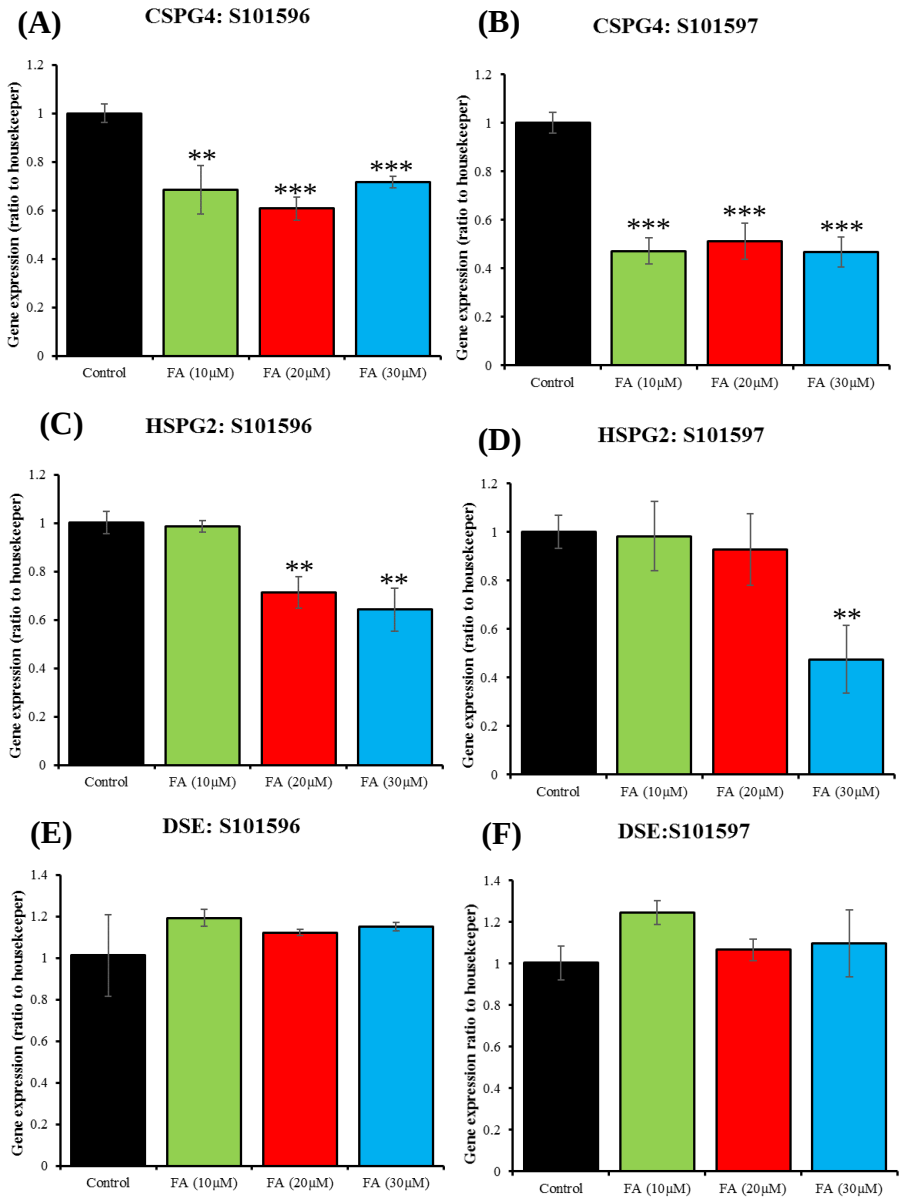

Figure 92: Effect of folic acid supplementation on glycosaminoglycan gene expression. (A-B) *CSPG4* was significantly downregulated following supplementation with 10µM, 20µM and 30µM FA ($p<0.01$) in both the fast and slow migrating groups however the slow migrating group exhibited lower overall expression; there was no significant differences between treatment conditions. (C) Supplementation with 10µM does not lead to any significant change in *HSPG2* expression however supplementation with 20µM and 30µM led to a significant decrease in *HSPG2* expression ($p<0.01$). (D) In the slow migrating groups *HSPG2* expression was not significantly different following supplementation with 10µM or 20µM FA however treatment with 30 µM FA resulted in a significant downregulation of *HSPG2*. (E-F) Supplementation with 10µM, 20µM and 30µM did not cause any significant change in *DSE* expression in either the fast or slow migratory groups (n=3).

5.6.2 Expression of other extracellular matrix related molecules in response to folic acid

Fibronectin 1 (*FN1*) expression was not significantly influenced by the presence of FA in S101596 fibroblast cultures (Figure 93A). However, *FN1* expression was significantly upregulated in S101597 fibroblasts in response to 10μM, 20μM and 30μM FA ($P<0.05$) (Figure 104B). Elastin (*ELN*) expression was significantly downregulated in S101596 fibroblasts in response to 10μM FA ($p<0.01$) but at concentrations of 20μM and 30μM FA expression levels were comparable with that of the control (Figure 93C). Conversely, in S101597 fibroblasts supplementation with 20μM and 30μM FA led to a significant downregulation of ELN ($p<0.01$) (Figure 93D). Laminin subunit alpha 1 (*LAMA1*) expression was not affected by the presence of FA as expression levels were comparable with those of the FA-ve control in both cell populations (Figure 93E-F).

5.7 Effect of folic acid on expression of markers associated folate with metabolism

Folate hydrolase 1 (*FOLH1*) was upregulated in both S101596 and S101597 with increasing FA concentrations. However, the fast migrating cell type had higher fold changes in *FOLH1* expression relative to the slow group. Further, there were no differences observed in expression based on FA concentrations as 10μM, 20μM and 30μM had similar fold changes (Figure 94A-B). Methylenetetrahydrofolate reductase (*MTHFR*) expression was also upregulated following supplementation with 10μM, 20μM and 30 FA relative to the FA-ve control in both S101596 and S101596. However, as with *FOLH1*, fold changes were higher in the fast group whilst there were no significant differences between FA treated groups (Figure 94C-D).

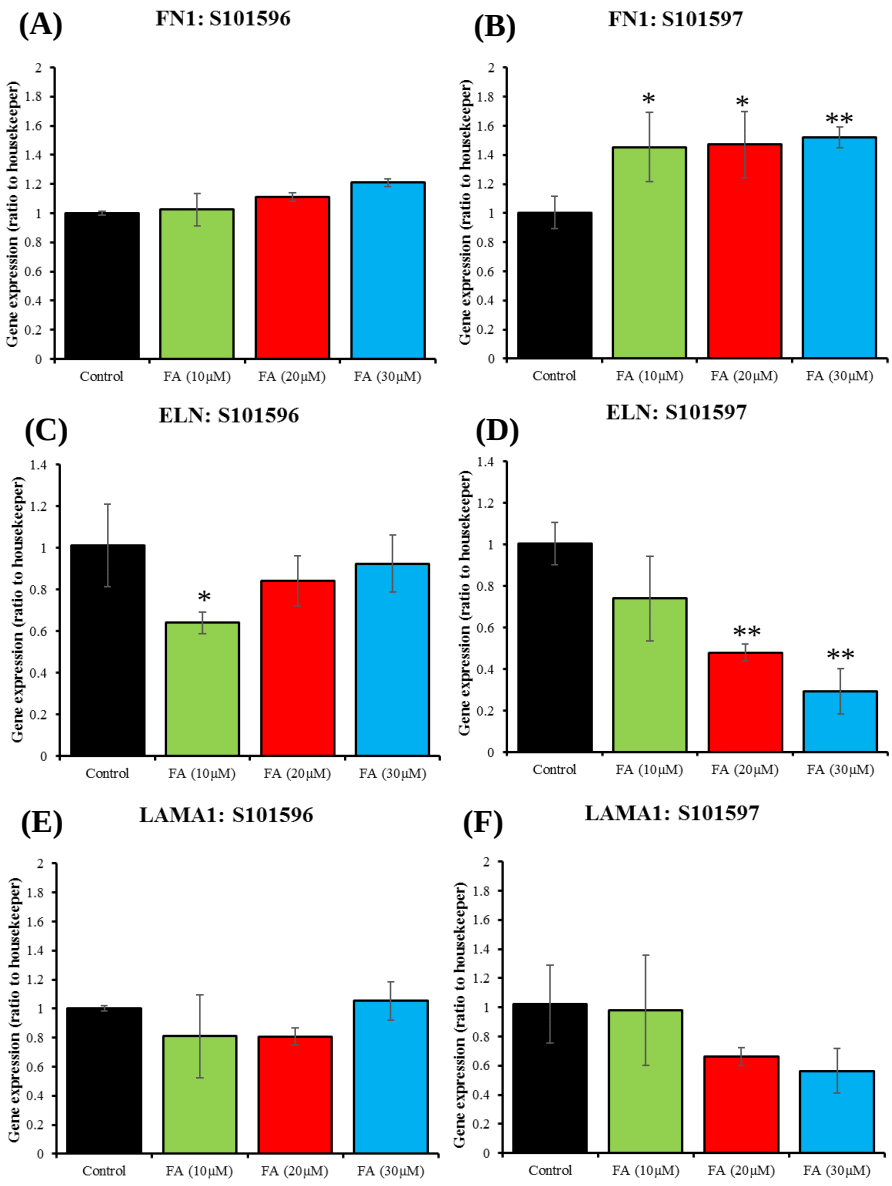

Figure 93: Effect of folic acid supplementation on expression of extracellular matrix related molecules. (A) *FN1* expression was comparable between 10µM, 20µM and 30µM FA treated cleft fibroblasts and the FA-ve control. (B) In the slow migratory group treatment with 10µM, 20µM and 30µM FA leads to a significant increase in *FN1* expression ($p<0.05$); there were no significant differences between treatment conditions. (C) *ELN* expression was significantly downregulated following supplementation with 10µM however there was no significant difference between the control and the 20µM and 30µM treatment conditions. (D) Supplementation with 10µM led to a non-significant decrease in *ELN* expression in the slow migratory group, this expression decreased significantly following treatment with 20µM and 30 µM ($p<0.01$). (E-F) There were no significant differences in *LAMA1* expression between the FA-ve control and FA treated cultures for both the fast and slow migratory groups (n=3).

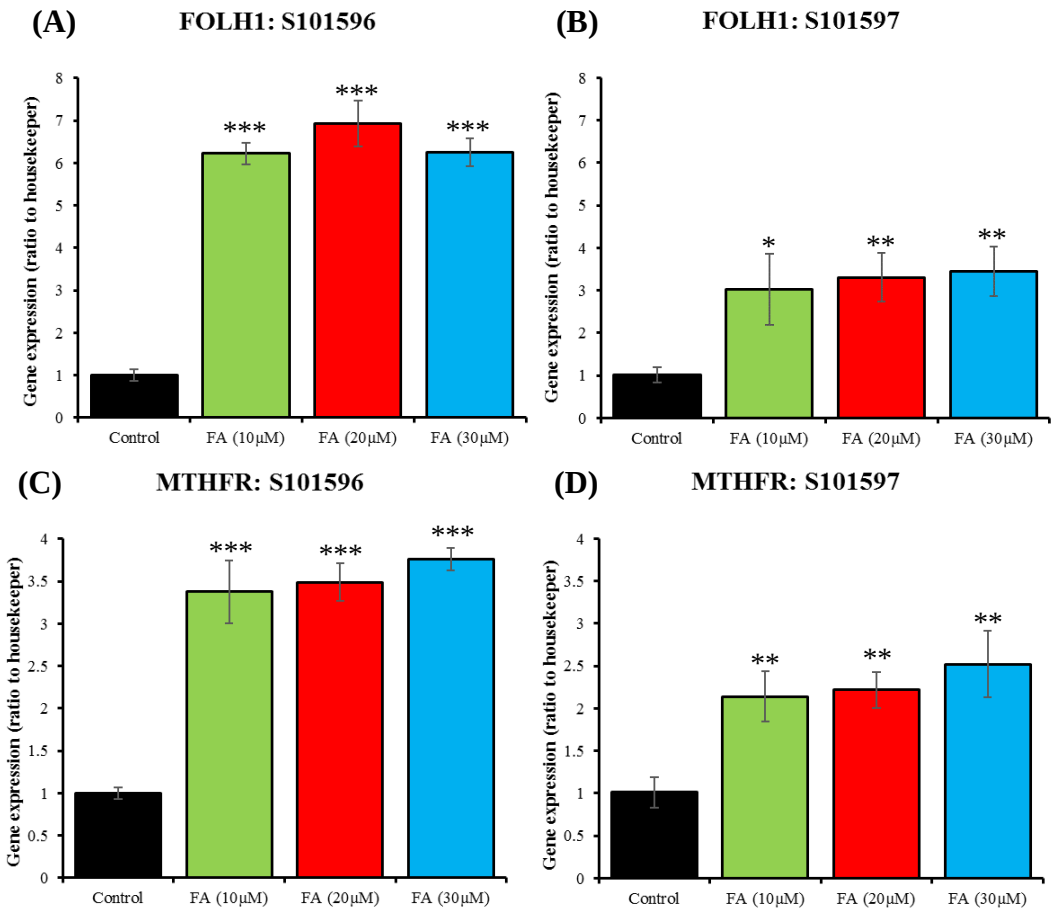

Figure 94: The effect of folic acid supplementation on genes involved in folate metabolism. (A) *FOLH1* expression was significantly upregulated following supplementation with 10µM, 20µM and 30µM FA in the fast migrating cells (fold change approximately 6-7) ($p<0.001$); there was no significant difference between supplemented groups. (B) *FOLH1* was also upregulated in the slow cells however the fold changes were smaller than in S101596 (fold change of approximately 3-3.5) with no differences between FA treatment conditions. (C) *MTHFR* was significantly upregulated relative to the FA control in all 3 experimental conditions ($p<0.001$) (fold change approximately 3.5-4). (D) *MTHFR* was also upregulated in the slow migrating groups following FA supplementation ($p<0.01$) (fold change approximately 2-2.5); variation in FA conditions did not influence expression.

5.8 Discussion

Maternal dietary intake of folic acid (FA) has been continually associated with potential preventative roles in cleft development (Van-Rooji et al, 2004) with a recent comprehensive meta-analysis concluding maternal FA supplementation significantly reduced the risk of all cleft phenotypes (Jahanbin et al, 2019). Despite this, there is currently little data pertaining to the regulatory and behavioural influences FA may have on cleft fibroblasts which could be altered and potentially influence clefting during foetal development. Therefore, the purpose of this study was to identify a broad array of behaviours that may be influenced by the presence of FA thus providing new insights into the potential cellular and molecular mechanisms by which FA may be involved in cleft prevention. Overall, the data indicated that FA can affect a range of cell activities including: growth, migration, adhesion, ECM deposition and gene expression. However, FA supplementation in normal physiological concentrations (20nM), did not induce significant change in the aforementioned cell responses, suggesting physiological concentrations of FA might be too low to bring about an observable cellular response in the assays used. However, elevated concentrations of FA induced measurable differences in cell behaviour relative to controls. This is important as pregnant mothers are advised to supplement their diets with a much higher folate intake than normal, (up to 1000µg/day as opposed to 400µg/day (WHO, 2004), both periconceptually and during their first trimester of pregnancy which would likely increase serum folate levels significantly (Chitayat et al, 2016). Despite the potential benefit of excess dietary folate, it was found here that supplementation with 30µM FA often caused a decrease in the positive effects observed at other FA concentrations, which may be due to potential cytotoxicity of FA at this concentration. However, it is important to note these assays were conducted *in vitro* thus any effect folate supplementation had on cell cultures may not translate to altered physiological behaviours during foetal development *in utero*, thus the results may not translate to any preventative roles in cleft development.

5.8.1 Effect of folic acid supplementation on cell growth, migration and adhesion

During craniofacial development pluripotent cranial neural crest cells (CNCCs) delaminate and migrate from the neural tube into regions that will form the frontonasal prominence, maxillary and mandibular prominences. CNCCs undergo rapid proliferation and differentiation, causing prominences to increase in size resulting in formation of the craniofacial structures. Controlled cell migration, through the process of adhesion and detachment, to the correct anatomical site followed by proliferation are therefore critical to normal facial development. Thus, factors that can influence these behaviours must be carefully regulated to ensure normal development. Cleft fibroblast growth of was increased in the presence of 10μM and 20μM; further, non-cleft control cells (NHDFF's) also responded to FA by increasing proliferative rate. This stimulatory effect is likely due to the cellular requirement of FA to act as a carbon donor for *de novo* nucleotide synthesis of thymidine and the purines, adenine and guanine (Stover and Field, 2011). As the rate of proliferation is elevated during development, FA deficiency may be a limiting factor due to reduced cellular nucleotide concentrations which are required for DNA replication (Bailey et al, 1999). Others have shown proliferation is reduced in FA deficient cultures whereas growth is stimulated by the presence of FA (Hwang et al, 2018). Further, murine knockout models, which develop neural tube defects due to impairment in neuro-epithelial proliferation, presented rescued proliferation, comparable to controls, in the presence of FA (Ichi et al, 2010). As neuro-epithelial cells are CNCC precursors and FA has been shown to simulate proliferation in a range of cell types, including cleft fibroblasts and NHDFFs, it is possible maternal FA deficiency may perturb CNCC proliferation within the facial growth centres, thereby contributing to cleft development due to the embryos reliance on maternal FA intake.

Changes in the adhesive ability of local cell populations is required during CNCC delamination from neural tube and during migration towards the sites that will become the facial growth

centres. Here it was demonstrated that the presence of FA had a positive effect on cell-substrate and cell-cell adhesion relative to FA-ve controls; further, this correlated with upregulation genes associated with cell adhesion. FA within culture medium has been shown to influence cell adhesion in multiple studies; however, it usually induces decreased adhesion, or has no effect, as opposed to the increase observed with cleft fibroblasts here. Indeed, Hoover (1977) found that populations of embryonic neural retinal cells had significantly decreased cell adhesion in the presence of 3.5mM FA (75%) and 0.7mM (43%). Branda and Tracy (1990) found that there were greater numbers of adherent melanoma cells in FA deficient cultures, relative to FA supplemented, whereas carcinoma colon epithelial cells were unaffected in terms of adhesion when exposed to 10uM FA (Ting et al, 2018). Although much of the literature seems to suggest FA has a negative impact on adhesion, the present study represents the first instance that the influence of FA on cleft fibroblast adhesion has been assessed and it was shown to have a positive effect. As GTPases are pivotal to cellular adhesion and motility, there activation/deactivation may significantly affect the adhesiveness of fibroblasts. The actin cytoskeleton interacts with the underlying substrate primarily through actin stress fibres which transmit mechanical forces between the substrate and the cell at focal adhesions. It was shown in 3T3 fibroblasts that RhoA drives the formation of stress fibres and focal adhesions, which anchor the cell to the substrate; further, stress fibre and focal adhesion formation was blocked when RhoA activity was inhibited (Ridley and Hall, 1992). As *RHOA* was upregulated in cleft fibroblasts in the presence of FA, it is possible that FA stimulates *RHOA* mediated actin formation leading to the production of focal complexes which improve their adhesiveness

The migratory route adopted by CNCCs during migration from the neural folds is guided by a highly preserved molecular blueprint that ensures migration towards developing craniofacial sites through induction of a number of molecular pathways coupled with regulation of cellular responses to the extracellular milieu (Hall, 2009). The presence of elevated FA within cleft

fibroblast cultures significantly reduced migration; this was coupled with downregulation of *ACTA1* and *TUBA1*. Actin filaments and microtubules comprise the major components of the cell cytoskeleton which is pivotal in controlling cell locomotion, this appears to be especially important during craniofacial development as altered cytoskeletal polymerization has been shown to lead to alterations to cell shape disrupting neural tube closure and consequently facial development (Sadler et al, 1982; Moephuli et al, 1997). Downregulation of both actin and tubulin may account for the decreased cell migration rates especially when considering that there is a direct association between intercellular actin and folate metabolism as it was shown following disruption of the actin cytoskeleton there was an increase in the number of cellular folate surface receptors followed by increased intercellular folate metabolism (Lewis et al, 1998). As maternal FA intake has been associated with cleft prevention, altered expression of actin and tubulin, coupled with the resultant influence on migratory rates, in response to folate, may influence CNCC migration from the neural tube. However, further research is needed to identify the precise CNCC response to FA in terms of migration. Others have concluded that FA has a similar anti-migratory effect thereby supporting the results obtained here as 10μM FA was shown to inhibit endothelial cell migratory rates and decrease lamellipodial formation as a result of modulation of RhoA activity (Hou et al, 2013; Chou et al, 2013). Rho GTPases are major regulators of cytoskeletal dynamics thereby influencing the behaviours of actin and tubulin during cell locomotion. FA supplementation led to significant downregulation of *RAC1* in cleft fibroblasts relative to FA-ve controls. RAC1 is ubiquitously expressed and is pivotal to cell locomotion as Rac proteins are reportedly expressed at the front of the cell and drives cell motility via formation of lamellipodial extensions which function to interact with the extracellular environment, direct cell polarity and propel the cell in a forward direction (Thomas et al, 2010). Due to this, downregulation of *RAC1* in the presence of FA may have contribute to the decreased migratory rates observed in FA treated fibroblasts. Furthermore, as *RAC1*

expression was altered in both cleft and non-cleft NHDFF fibroblasts it is plausible that CNCCs may have similar responses to FA during craniofacial formation which may potentially contribute to OFC prevention though this needs to be explored further. If the pluripotent CNCCs present disrupted motility in response to FA deficiency, it could influence fibroblast concentrations within that facial growth centres, potentially perturbing ECM deposition thereby disrupting normal tissue expansion potentially contribute to cleft development.

5.8.2 The effect of folic acid on the production of extracellular matrix

The ECM comprises the local microenvironment that cells must interact with to carry specific cellular functions whilst providing a medium through which adhesion, migration, proliferation and extracellular signalling can occur. Collagens are the major fibrillary component of the ECM and impart mechanical integrity to the surrounding cells and tissues whilst also acting as point of guidance for directed cell migration (Zetter and Brightman, 1990). This is achieved through collagens contribution to tissue rigidity as cellular mechano-sensing can identify substrate rigidity and adjust motility through the process of durotaxis (Lo et al, 2000); however, chemo attractive forces also contribute to CNCC migrational directionality (Rogers et al, 2012). The presence of FA was shown here to significantly increase collagen production and expression of both *COL1A1* and *COL3A1*. Providing similar folate responses occur during embryological development, fibroblasts could be stimulated to express and secrete elevated fibrillar collagens *in utero*. This could potentially contribute to the CNCC motility, which display rapid migration that is stimulated by the underlying ECM (Henderson and Copp, 1997). This is due to the presence of collagens and fibronectin, which are expressed and synthesised along the precise pathways of CNCC migration thereby permitting directed motility to the facial growth centres through continued attachment and detachment with underlying fibres (Henderson and Copp, 1997; Perris, 1997). Others have also demonstrated the stimulatory role of FA in terms of

collagen production, although the mechanism has not yet been determined. For example, FA supplementation in collagen embedded dermal fibroblasts significantly increased collagen synthesis expression of *COL1A1* (Fischer et al, 2011). Further, diabetic mice, which demonstrated impaired wound healing and reduced collagen deposition, were shown to display cell proliferation, collagen deposition and tissue regeneration comparable to that of their non-diabetic counterparts following daily 3mg/KG FA dosing (Zhao et al, 2018). As during embryological development of the palate collagen type I is highly expressed in CNCCs within the palatal mesenchyme thereby significantly contributing towards development of the hard and soft palate (Oka et al, 2012).Fibronectin (*FN1*) was also to be upregulated by cleft fibroblasts in the presence of FA. As with collagen, cell attachment and guided migration of early embryonic cells is contributed to by the presence of underlying fibronectin as it has been shown that FN is present along the migratory pathways taken by neural crest cells (Nawgreen and Thiery, 1980) and that integrin mediated NCC binding to FN is critical for normal motility (Strachan and Condic, 2008). In addition, following the injection of peptides, that were complimentary to fibronectin binding domains, into chick embryos, the migratory path of CNCCs was significantly perturbed due to the saturation of fibronectin binding sites thereby preventing their interaction with CNCC leading to abnormal craniofacial development (Boucaut et al, 1984). This demonstrates the critical importance of appropriate fibronectin regulation to normal development. As the presence of FA has been shown to lead to upregulation of collagen and fibronectin, it is possible that the potential protective role FA has in the prevention of clefts is, in part, due to its stimulation of ECM deposition

5.8.3 The effect of folic acid on genes related to folate metabolism

Closely linked with the folate metabolism cycle, which is required to permit FA derivatives to function as acceptors and a donors of carbon units thereby enabling: synthesis of nucleotides,

amino acid metabolism and oxidation reactions (Blom et al, 2006), is the methionine cycle, which leads the production of homocysteine (HCY) and is required to form cysteine and other related proteins. Plasma HCY levels are largely determined by plasma concentrations of FA as it is required to convert HCY back into methionine; this is relevant as elevated HCY (hyper-homocysteinemia) is linked to perturbed foetal development (Taparia et al, 2007) including neural tube defects (Imbard, 2013) and orofacial clefts (Wong et al, 1999). In the present study, following supplementation with FA, *MTHFR*, which is responsible for conversion of 5,10–MTHF to 5-MTHF, was significantly upregulated. *MTHFR* upregulation is significant as it regulates serum HCY concentrations by inducing demethylation of 5-MTHF to THF thereby converting HCY into methionine as part of a secondary reaction (Selhub, 1999). HCY has been shown to be elevated in non-syndromic CLP patients relative to control patients (Abdulla et al, 2016; Rooji et al, 2003; Kumari et al, 2013) and elevated maternal serum HCY was associated with increased risk of both CLP and CPO (Little et al, 2007). One study demonstrated the serum HCY was 9.5μ/L in control group whereas it was significantly higher in the cleft groups (18.4μ/L) (Abdulla et al, 2016). Elevated HCY levels were also shown to affect the behaviour of CNCC by altering their growth and migration from the neural tube coupled with CNCC differentiation; FA supplementation was shown to reverse this due to reduction in HCY levels by conversion to methionine (Boot et al, 2003). Furthermore, *FOLH1* which contributes to cellular uptake of 5-MTHF, was also upregulated here following supplementation of cleft fibroblasts with FA, this would suggest more efficient cellular folate delivery. As folate deficiency has been shown to alter expression of genes relating to cell signalling, cytoskeletal components and the ECM (Katula et al, 2007) it is possible that the increased FA uptake as a result of *FOLH1* upregulation may contribute to normal cell behaviour. Taken together these data suggest that the presence of FA increases expression of *MTHFR* which, coupled with the presence of elevated serum folate levels, promotes the conversion of HCY into methionine. As

HCY concentrations have repeatedly been shown to be elevated in both mothers who are FA deficient it is possible that the protective effect against cleft formation that is observed following FA supplementation is due, at least in part, to reduction of HCY by means of the folate and methionine pathways. Although homocysteine has been repeatedly associated with cleft formation, most of the studies conducted have suffered from small sample sizes and low statistical power therefore large scale studies are needed within which HCY levels within FA deficient and FA sufficient mothers are assessed and correlated with the risk of foetal OFC.

5.9 Conclusion

The presence of folic acid was shown here to influence a range of cleft fibroblast behaviours. *FOLH1*, which contributes to cellular folate metabolism, was upregulated thereby suggesting the presence of FA may result in more efficient cellular folate delivery. In addition, adhesion of cleft fibroblasts was elevated whilst their migratory speed was reduced, this may have been due to the variations observed in Rho GTPase expression in the presence of FA; specifically, upregulation of *RHOA*, which is involved in the formation of adhesive focal complexes, and downregulation of *RAC1*, which contributes lamellipodial extension thus directed cell motility. The expression of ECM associated genes, including regulators of collagen and fibronectin, were also upregulated. This could potentially result in elevated ECM deposition during development which could play a protective role as both collagen and fibronectin are required along cellular migratory pathways and are also essential to the mechanical integrity of developing tissues. As FA stimulated a diverse range of cell behaviours within populations of cleft fibroblasts it is possible that CNCCs, which are the principle cell type in craniofacial development, would also be influenced in a similar manner. Perturbations to these behaviours within FA deficient mothers may contribute to OFC development thereby suggesting that FA plays a protective role by contributing to normal cell behaviour; however further research is required into the FA response of human CNCCs before such a conclusion can be made.

CHAPTER SIX:

GENERAL DISCUSSION AND CONCLUDING REMARKS

6.1 General discussion

Due to the high incidence of cleft lip and cleft palate forming in isolation, there has been considerable speculation as to whether CP, CL and CLP are disparate clinical entities with differing physiological aetiologies. Normal facial development occurs in a regulated sequential pattern. Following delamination from the neural tube, the rapidly migrating and proliferating CNCCs migrate to the sites that will become frontonasal prominence and into the pharyngeal arches. Outgrowth of the first pharyngeal arch eventually leads to its separation into the paired mandibular processes and the paired maxillary processes. Medial growth of the mandibular processes leads to fusion at the midline, forming the mandible, whereas medial growth of the maxillary processes leads to fusion with the lateral nasal process, which differentiates from the frontonasal process, eventually forming the intermaxillary segment which gives rise to the philtrum, upper lip and the primary palate (Senders et al, 2003; Lan et al, 2015); disruption during this process can lead to the formation of either unilateral or bilateral clefts lip. Following this, bilateral outgrowths from the maxillary processes form the palatal shelves, which fuse to form the midline epithelial seam and eventually the definitive palate (Yu et al, 2009); disruption at this stage can lead to clefts of the palate. Due to the formation of the lip and palate being distinct embryological events, it is possible that formation of cleft lip and the palate are formed due to physiologically distinct mechanisms. However, it is also possible that cleft lip and palate, when forming in conjunction, is a more severe manifestation of the same physiological defect, with the same causation, but at a greater degree of severity (Shkoukani et al, 2013).

The present study is the first to characterise and compare fibroblasts derived from differing cleft phenotypes, in terms of their behaviour *in vitro*, to determine whether fibroblasts isolated from differing cleft types are physiologically distinct. It was highlighted here that there were many behavioural and genetic differences between fibroblast isolated different patients within the

cohort. However, these differences often did not correlate with cleft type; therefore, the variation in fibroblast behaviour could not be attributed to the potential genetic deviations that resulted in the manifestation of the cleft type. Rather, the differences observed in fibroblast behaviour were likely due to the distinct individual genetic profiles of the patients undergoing the repair. However, RUCLP fibroblasts were shown to consistently downregulate a number of genes associated with ECM production and TGF expression compared with both LUCLP and BLCLP. It is thus possible fibroblasts derived from the CL with right laterality are genetically distinct and potentially have distinct aetiological origins. Left laterality is more common than right laterality (Nagase et al, 2011; Conway et al, 2015) and currently it is unknown why there is left dominance with regards cleft lip development (Vieira and Dattilo, 2018). It is possible that the down-regulation of ECM associated genes observed here may lead to interference with the normal positioning of the facial processes prior to fusion thereby contributing to formation of RUCLP. However, samples sizes for the present study were small; therefore, the results obtained here are preliminary and cannot be deemed conclusive or representative of all cleft patients. Large-scale studies that analyse an array of genetic markers associated with cleft development are required to definitively determine if RUCLP fibroblasts are genetically distinct from their LUCLP and BLCLP counterparts. Determination of aetiological differences between cleft types is important, as if clefts of differing types and laterality are aetiologically distinct they should be studied as separate conditions. Currently a portion of the literature adopts simplistic qualitative classification systems and often the cleft type is not reported. This is problematic as that data obtained may not relatable to patients with different cleft types.

6.2 Limitations of the study

Although the patient selection criteria excluded individuals with syndromic forms of CLP, only patients which displayed overt symptoms of known syndromes were excluded from the study.

Further, following sample collection, all samples were anonymised thus any individual patients that were diagnosed with syndromic CLP following their cleft repair, would have been included in this study due the patient's post-operative diagnosis being unknown. This is problematic as it leads to the possibility that a number of samples may not have been comparable to the remainder of the patient cohort due to potentially having distinct aetiological origins. Future analysis of cleft samples should include genetic testing for known syndromic forms of CLP with post-operative reviews to definitively determine sample homogeneity. In addition, although multiple samples were isolated from each cleft phenotype, the precise anatomical origin of each individual sample was not controlled, this was due to tissue availability being limited to that which was not required for the repair. As clefts of the same type can differ in terms of their dimensions, there is often differing tissue requirements for each repair as they may involve implementation of differing surgical protocols for different patients. As the clinician must prioritise the surgical repair the precise tissue isolation site could not be controlled. This may have led to a degree of heterogeneity within samples derived from the same cleft types as different regions of the lip and palate were donated for analysis, this must be taken into account as it is possible that the variations in cell behaviour observed between samples may have been due to the differing anatomical origins of the samples. In addition, despite efforts to obtain as many samples a possible for each cleft phenotype, the number of samples was limited between a minimum of five, for isolated CP, and a maximum of 9, for both lip and palate derived CLP samples. Due to this, the number of replicates for each cleft type was too low to make and definitive conclusions; rather, potential associations and differences could only be outlined.

There was significant difficulty in obtaining a true age-matched and anatomical-matched control with which cleft fibroblast behaviour could be compared. This was due to the ethical issues in obtaining healthy donor tissue from the lip or palate of non-cleft patients. Due to this,

human gingival fibroblasts (HGF) were selected as control cells for PCR applications due to being readily available human oral fibroblasts. Many of the genetic markers assessed in the present study were shown to be significantly upregulated across the sample cohort when compared with the non-cleft HGF control. This could potentially suggest that disrupted gene expression may be due to the pathological nature of the fibroblasts and that aberrant gene expression of ECM associated genes is a hallmark of cleft derived fibroblasts. However, the control used here was derived from adult gingival tissue therefore it did not share the same anatomical origin of cleft fibroblasts which were isolated from either the lip or palate. The anatomical origin of fibroblasts can have a significant influence on their behaviour, it has been shown that gingival fibroblast cell lines express significantly increased expression of inflammatory and ECM markers whilst significantly decreased expression of TGF signalling markers when compared with dermal fibroblasts (Mah et al, 2014). Further, there can be significant variation in the expression between different fibroblast population within the oral cavity as it has been shown that periodontal ligament fibroblasts produced significantly greater amounts of ECM proteins relative to their gingival fibroblast counterparts (Hou et al, 1995) furthermore differences between populations of oral fibroblast populations are also significant when derived from the same donor (Palioto et al, 2002). This suggests that anatomical differences between the HGF control used here and the cleft fibroblasts may account for many of the significant differences observed between the control and cleft samples. Equally the HGF control was derived from adults whereas cleft fibroblasts were isolated from infants typically aged between three and nine months. As with anatomical origin the age of the patient from which the fibroblasts are derived can also have a significant effect. It has been shown that that neonatal fibroblasts differed from adult fibroblasts in terms of expression of genes associated with ECM deposition, morphogenesis and cell adhesion (Mateu et al, 2016). This suggests that the disparity in gene expression observed between the HGF control and cleft fibroblasts may

be due the age of the patient from which they were isolated. A minority of studies pertaining to cleft fibroblast behaviour have managed to obtain neonatal fibroblasts from non-cleft oral tissues. When assessing the effect of diphenylhydantoin (PHT), a drug that induces CP, control fibroblasts were obtained from infants undergoing surgery for palatal trauma (Bosi, et al, 1998). Similarly, when assessing the effects of nicotine on cleft fibroblasts, control fibroblasts obtained from infants with palatal trauma were used (Baroni et al, 2009). However, obtaining this type of control tissue was not possible in the present study as infants with oral trauma are uncommon and any cases would be treated as a matter of urgency before parental consent could be obtained. Others have also compromised on control fibroblasts, when assessing cleft fibroblast behaviour neonatal human dermal foreskin fibroblasts have been used (Beyeler et al, 2014) as well as adult dermal fibroblasts (Zivicova et al, 2017). Due to the absence of a true age matched and anatomical matched control, the data generated here, which compared gene expression and cell behaviour with controls, may not be valid as the behaviour of the controls utilised here may not be indicative of how non-pathological age and anatomical matched fibroblasts would behave, thus definitive conclusions cannot be made. Future studies that comparatively assess cleft fibroblast behaviour should incorporate the use of multiple controls such as those isolated from neonates with oral trauma.

6.3 Conclusion and recommendations for future work

The data presented in this thesis suggest that individual cleft patients can vary significantly both in cell behaviour, such as motility and ECM deposition, and in their gene expression profiles. These disparities in fibroblast behaviour and gene expression may be potential contributing factors in the pathological wound healing seen in some patients following cleft repair, this could potentially account for why different patients with the same cleft type and surgical treatment protocol present significantly different clinical outcomes. Despite the differences in cleft

fibroblast behaviour observed here, there was limited correlation with cleft phenotype thus fibroblast behaviour could not be reliably correlated with the type of cleft that manifested. However, fibroblasts derived from cleft lip in isolation presented cell behaviours consistent with the hallmarks of HTS, including elevated motility and collagen deposition, thus these patients may be at increased risk of pathological wound healing relative to the other cleft types assessed here. The results obtained in this thesis highlight a number of areas that should be explored further. Therefore, recommendations for future cell based cleft research include:

- Cleft tissues, from which fibroblasts were isolated, comprise of organised ECM with three dimensional distribution and multiple cell types. As cleft fibroblasts derived from these tissues revealed significant patient-to-patient differences is the ECM production, it would be interesting to assess ECM distribution within tissue samples, through use of histological staining immunostaining methodologies, followed by quantification. This could potentially reveal the physical ECM distribution within pathological cleft tissue between patients and can subsequently be compared between cleft types. Tissue that is both age-matched and anatomically-matched, potentially derived from infants with oral trauma, should be used as controls.
- Cleft fibroblasts samples were shown to split into two statistically distinct groups in terms of wound closure, fast and slow. Cleft patients with fast migrating fibroblast could potentially be at increased risk of pathological wound healing due to premature myofibroblast differentiation leading to elevated ECM deposition. Future studies should characterise fibroblasts based on motility, as conducted here, but also carry out long term follow up patient examinations in order to assess clinical outcome (i.e. development of ONF or HTS) which can subsequently be correlated with the migratory behaviour of their fibroblast *in vitro*. This would provide evidence as to whether increased motility is related to pathological wound healing in surgical cleft repair.

Further, fibroblasts could be isolated from tissue samples taken from patients undergoing revision surgery due to development of ONF. The behaviour of ONF fibroblasts could then be compared to previously established fibroblast behaviour across the sample cohort in order to establish which markers are associated with increased risk of ONF development.

- Following exposure to folic acid, cleft fibroblasts significantly upregulated *MTHFR* and *FOLH1*, both of which are markers involved in the folate metabolism pathway and are linked to the methionine pathway. As the fundamental process of the methionine pathway is to convert homocysteine into methionine, and homocysteine has been associated with cleft development, the effect of folic acid on other genetic markers associated with both folic acid and methionine pathways should be studied further to uncover how exposure can influence cell behaviour and potentially cleft development.
- Epithelial cells have a significant role in normal craniofacial development. For example, in normal palate formation the opposing palatal shelves, which are covered in epithelium, merge due to the superficial interaction of epithelial cells to form the midline epithelial seam. As cleft tissues derived from patients comprise of heterogeneous cell populations future studies should isolate epithelial cells from these tissues and conduct further analysis, particularly of cell-adhesion molecules. It would be interesting to assess if adhesion molecule expression is different between patients with cleft palate only, which had failed palatal shelf fusion, and those with cleft lip, which had successful shelf fusion.

Bibliography

ABDULKAREEM, A. A., SHELTON, R. M., LANDINI, G., COOPER, P. R. & MILWARD, M. R. 2017. Periodontal pathogens promote epithelial-mesenchymal transition in oral squamous carcinoma cells in vitro. *Cell adhesion & migration,* 12**,** 127-137.

ABDULLA, R., TELLIS, R. C., ATHIKARI, R. & KUDKULI, J. 2016. Evaluation of homocysteine levels in individuals having nonsyndromic cleft lip with or without palate. *Journal of oral and maxillofacial pathology: JOMFP,* 20**,** 390-394.

ABERCROMBIE, M. 1978. Fibroblasts. *Journal of clinical pathology. Supplement (Royal College of Pathologists),* 12**,** 1-6.

ABRISHAMCHIAN, A. R., KHOURY, M. J. & CALLE, E. E. 1994. The contribution of maternal epilepsy and its treatment to the etiology of oral clefts: a population based case-control study. *Genet Epidemiol,* 11**,** 343-51.

ACHARYA, P. S., MAJUMDAR, S., JACOB, M., HAYDEN, J., MRASS, P., WENINGER, W., ASSOIAN, R. K. & PURE, E. 2008. Fibroblast migration is mediated by CD44-dependent TGF beta activation. *J Cell Sci,* 121**,** 1393-402.

ACKERMANS, M. M., ZHOU, H., CARELS, C. E., WAGENER, F. A. & VON DEN HOFF, J. W. 2011. Vitamin A and clefting: putative biological mechanisms. *Nutr Rev,* 69**,** 613-24.

ACUNA-GONZALEZ, G., MEDINA-SOLIS, C. E., MAUPOME, G., ESCOFFIE-RAMIREZ, M., HERNANDEZ-ROMANO, J., MARQUEZ-CORONA MDE, L., ISLAS-MARQUEZ, A. J. & VILLALOBOS-RODELO, J. J. 2011. Family history and socioeconomic risk factors for non-syndromic cleft lip and palate: a matched case-control study in a less developed country. *Biomedica,* 31**,** 381-91.

AGREN, M. S., STEENFOS, H. H., DABELSTEEN, S., HANSEN, J. B. & DABELSTEEN, E. 1999. Proliferation and mitogenic response to PDGF-BB of fibroblasts isolated from chronic venous leg ulcers is ulcer-age dependent. *J Invest Dermatol,* 112**,** 463-9.

ALBERTS B, JOHNSON A, LEWIS J.A, MORGAN D, RAFF M, ROBERTS K, WALTER P 2015. *Molecular Biology of the Cell*. 6th edition. New York: Garland Science.

AMARATUNGA, N. A. 1988. Occurrence of oronasal fistulas in operated cleft palate patients. *J Oral Maxillofac Surg,* 46**,** 834-8.

ANANI, R. A. & ALY, A. M. 2012. Closure of palatal fistula with local double-breasted mucoperiosteal flaps. *J Plast Reconstr Aesthet Surg,* 65**,** e237-40.

ANANTHAKRISHNAN, R. & EHRLICHER, A. 2007. The forces behind cell movement. *International journal of biological sciences,* 3**,** 303-317.

ANDERSON, T. W., VAUGHAN, A. N. & CRAMER, L. P. 2008. Retrograde flow and myosin II activity within the leading cell edge deliver F-actin to the lamella to seed the formation of graded polarity actomyosin II filament bundles in migrating fibroblasts. *Molecular biology of the cell,* 19**,** 5006-5018.

ANNIGERI, V. M., MAHAJAN, J. K., NAGARKAR, A. & SINGH, S. P. 2012. Outcome analysis of palatoplasty in various types of cleft palate. *Journal of Indian Association of Pediatric Surgeons,* 17**,** 157-161.

AZARBAYJANI, F. & DANIELSSON, B. R. 2001. Phenytoin-induced cleft palate: evidence for embryonic cardiac bradyarrhythmia due to inhibition of delayed rectifier K+ channels resulting in hypoxia-reoxygenation damage. *Teratology,* 63**,** 152-60.

BAEK, S. J. & ELING, T. 2019. Growth differentiation factor 15 (GDF15): A survival protein with therapeutic potential in metabolic diseases. *Pharmacol Ther,* 198**,** 46-58.

BAGALAD, B. S., MOHAN KUMAR, K. P. & PUNEETH, H. K. 2017. Myofibroblasts: Master of disguise. *Journal of oral and maxillofacial pathology: JOMFP,* 21**,** 462-463.

BAILEY, L. B. & GREGORY, J. F., 3RD 1999. Folate metabolism and requirements. *J Nutr,* 129**,** 779-82.

BAINBRIDGE, P. 2013. Wound healing and the role of fibroblasts. *J Wound Care,* 22**,** 407-8, 410-12.

BANDYOPADHYAY, B., FAN, J., GUAN, S., LI, Y., CHEN, M., WOODLEY, D. T. & LI, W. 2006. A "traffic control" role for TGFbeta3: orchestrating dermal and epidermal cell motility during wound healing. *The Journal of cell biology,* 172**,** 1093-1105.

BARBOSA MARTELLI, D. R., MACHADO, R. A., OLIVEIRA SWERTS, M. S., MENDES RODRIGUES, L. A., DE AQUINO, S. N. & JÚNIOR, H. M. 2012. Non sindromic cleft lip and palate: relationship between sex and clinical extension. *Brazilian Journal of Otorhinolaryngology,* 78**,** 116-120.

BARONI, T., BELLUCCI, C., LILLI, C., PEZZETTI, F., CARINCI, F., LUMARE, E., PALMIERI, A., STABELLINI, G. & BODO, M. 2010. Human cleft lip and palate fibroblasts and normal nicotine-treated fibroblasts show altered in vitro expressions of genes related to molecular signaling pathways and extracellular matrix metabolism. *J Cell Physiol,* 222**,** 748-56.

BARRIENTOS, S., STOJADINOVIC, O., GOLINKO, M. S., BREM, H. & TOMIC-CANIC, M. 2008. Growth factors and cytokines in wound healing. *Wound Repair Regen,* 16**,** 585-601.

BAUDOIN, J. P., ALVAREZ, C., GASPAR, P. & METIN, C. 2008. Nocodazole-induced changes in microtubule dynamics impair the morphology and directionality of migrating medial ganglionic eminence cells. *Dev Neurosci,* 30**,** 132-43.

BAUM, C. L. & ARPEY, C. J. 2005. Normal cutaneous wound healing: clinical correlation with cellular and molecular events. *Dermatol Surg,* 31**,** 674-86; discussion 686.

BEN-KHAIAL, G. S. & SHAH, R. M. 1994. Effects of 5-fluorouracil on collagen synthesis in the developing palate of hamster. *Anti-Cancer Drugs,* 5**,** 99-104.

BENKO, S., FANTES, J. A., AMIEL, J., KLEINJAN, D. J., THOMAS, S., RAMSAY, J., JAMSHIDI, N., ESSAFI, A., HEANEY, S., GORDON, C. T., MCBRIDE, D., GOLZIO, C., FISHER, M., PERRY, P., ABADIE, V., AYUSO, C., HOLDER-ESPINASSE, M., KILPATRICK, N., LEES, M. M., PICARD, A., TEMPLE, I. K., THOMAS, P., VAZQUEZ, M. P., VEKEMANS, M., ROEST CROLLIUS, H., HASTIE, N. D., MUNNICH, A., ETCHEVERS, H. C., PELET, A., FARLIE, P. G., FITZPATRICK, D. R. & LYONNET, S. 2009. Highly conserved non-coding elements on either side of SOX9 associated with Pierre Robin sequence. *Nat Genet,* 41**,** 359-64.

BERG, M. J. 1999. The importance of folic acid. *J Gend Specif Med,* 2**,** 24-8.

BEYELER, J., SCHNYDER, I., KATSAROS, C. & CHIQUET, M. 2014. Accelerated wound closure in vitro by fibroblasts from a subgroup of cleft lip/palate patients: role of transforming growth factor-alpha. *PLoS One,* 9**,** e111752.

BILLE, C., OLSEN, J., VACH, W., KNUDSEN, V. K., OLSEN, S. F., RASMUSSEN, K., MURRAY, J. C., ANDERSEN, A. M. & CHRISTENSEN, K. 2007. Oral clefts and life style factors--a case-cohort study based on prospective Danish data. *Eur J Epidemiol,* 22**,** 173-81.

BIRNBAUM, S., LUDWIG, K. U., REUTTER, H., HERMS, S., STEFFENS, M., RUBINI, M., BALUARDO, C., FERRIAN, M., ALMEIDA DE ASSIS, N., ALBLAS, M. A., BARTH, S., FREUDENBERG, J., LAUSTER, C., SCHMIDT, G., SCHEER, M., BRAUMANN, B., BERGE, S. J., REICH, R. H., SCHIEFKE, F., HEMPRICH, A., POTZSCH, S., STEEGERS-THEUNISSEN, R. P., POTZSCH, B., MOEBUS, S., HORSTHEMKE, B., KRAMER, F. J., WIENKER, T. F., MOSSEY, P. A., PROPPING, P., CICHON, S., HOFFMANN, P., KNAPP, M., NOTHEN, M. M. & MANGOLD, E.

2009. Key susceptibility locus for nonsyndromic cleft lip with or without cleft palate on chromosome 8q24. *Nat Genet,* 41**,** 473-7.

BJORNSSON, S. 1993. Simultaneous preparation and quantitation of proteoglycans by precipitation with alcian blue. *Anal Biochem,* 210**,** 282-91.

BLIOKH, Z. L., DOMNINA, L. V., IVANOVA, O. Y., PLETJUSHKINA, O. Y., SVITKINA, T. M., SMOLYANINOV, V. A., VASILIEV, J. M. & GELFAND, I. M. 1980. Spreading of fibroblasts in medium containing cytochalasin B: formation of lamellar cytoplasm as a combination of several functional different processes. *Proc Natl Acad Sci U S A,* 77**,** 5919-22.

BLOM, H. J., SHAW, G. M., DEN HEIJER, M. & FINNELL, R. H. 2006. Neural tube defects and folate: case far from closed. *Nat Rev Neurosci,* 7**,** 724-31.

BODE, M. 2000. *Characterization of Type I and Type III Collagens in Human Tissues*, Oulun yliopisto.

BODO, M., BARONI, T., CARINCI, F., BECCHETTI, E., BELLUCCI, C., PEZZETTI, F., CONTE, C., EVANGELISTI, R. & CARINCI, P. 1999. TGFbeta isoforms and decorin gene expression are modified in fibroblasts obtained from non-syndromic cleft lip and palate subjects. *J Dent Res,* 78**,** 1783-90.

BOMPARD, G. & CARON, E. 2004. Regulation of WASP/WAVE proteins: making a long story short. *J Cell Biol,* 166**,** 957-62.

BOOT, M. J., STEEGERS-THEUNISSEN, R. P., POELMANN, R. E., VAN IPEREN, L., LINDEMANS, J. & GITTENBERGER-DE GROOT, A. C. 2003. Folic acid and homocysteine affect neural crest and neuroepithelial cell outgrowth and differentiation in vitro. *Developmental dynamics: an official publication of the American Association of Anatomists,* 227**,** 301-308.

BOSI, G., EVANGELISTI, R., VALENO, V., CARINCI, F., PEZZETTI, F., CALASTRINI, C., BODO, M. & CARINCI, P. 1998. Diphenylhydantoin affects glycosaminoglycans and collagen production by human fibroblasts from cleft palate patients. *J Dent Res,* 77**,** 1613-21.

BOUCAUT, J. C., DARRIBERE, T., POOLE, T. J., AOYAMA, H., YAMADA, K. M. & THIERY, J. P. 1984. Biologically active synthetic peptides as probes of embryonic development: a competitive peptide inhibitor of fibronectin function inhibits gastrulation in amphibian embryos and neural crest cell migration in avian embryos. *J Cell Biol,* 99**,** 1822-30.

BRANDA, R. F. & TRACY, P. B. 1990. Effects of nutritional folate deficiency on the adhesive properties of murine melanoma cells. *Cancer Letters,* 55**,** 95-102.

BRANDT, K., GRÜNLER, J., BRISMAR, K. & WANG, J. 2015. Effects of IGFBP-1 and IGFBP-2 and their fragments on migration and IGF-induced proliferation of human dermal fibroblasts. *Growth Hormone & IGF Research,* 25**,** 34-40.

BREUGEM, C. C. & MINK VAN DER MOLEN, A. B. 2009. What is 'Pierre Robin sequence'? *J Plast Reconstr Aesthet Surg,* 62**,** 1555-8.

BRINKLEY, L. L. & MORRIS-WIMAN, J. 1987. Effects of chlorcyclizine-induced glycosaminoglycan alterations on patterns of hyaluronate distribution during morphogenesis of the mouse secondary palate. *Development,* 100**,** 637-40.

BRONNER-FRASER, M. 1994. Neural crest cell formation and migration in the developing embryo. *Faseb j,* 8**,** 699-706.

BROUGHTON, G., 2ND, JANIS, J. E. & ATTINGER, C. E. 2006. The basic science of wound healing. *Plast Reconstr Surg,* 117**,** 12s-34s.

BROUSSARD, J. A., WEBB, D. J. & KAVERINA, I. 2008. Asymmetric focal adhesion disassembly in motile cells. *Curr Opin Cell Biol,* 20**,** 85-90.

BROWN, D. C. & GATTER, K. C. 2002. Ki67 protein: the immaculate deception? *Histopathology,* 40**,** 2-11.
CABALLERO, D., VOITURIEZ, R. & RIVELINE, D. 2015. The cell ratchet: interplay between efficient protrusions and adhesion determines cell motion. *Cell adhesion & migration,* 9**,** 327-334.
CALZOLARI, E., BIANCHI, F., RUBINI, M., RITVANEN, A. & NEVILLE, A. J. 2004. Epidemiology of cleft palate in Europe: implications for genetic research. *Cleft Palate Craniofac J,* 41**,** 244-9.
CAMELLITI, P., BORG, T. K. & KOHL, P. 2005. Structural and functional characterisation of cardiac fibroblasts. *Cardiovascular Research,* 65**,** 40-51.
CARRINO, D. A., SORRELL, J. M. & CAPLAN, A. I. 2000. Age-related changes in the proteoglycans of human skin. *Arch Biochem Biophys,* 373**,** 91-101.
CASTILLA, E. E., LOPEZ-CAMELO, J. S. & CAMPANA, H. 1999. Altitude as a risk factor for congenital anomalies. *Am J Med Genet,* 86**,** 9-14.
CHA, J., KWAK, T., BUTMARC, J., KIM, T.-A., YUFIT, T., CARSON, P., KIM, S.-J. & FALANGA, V. 2008. Fibroblasts from non-healing human chronic wounds show decreased expression of βig-h3, a TGF-β inducible protein. *Journal of Dermatological Science,* 50**,** 15-23.
CHAI, Y. & MAXSON, R. E., JR. 2006. Recent advances in craniofacial morphogenesis. *Dev Dyn,* 235**,** 2353-75.
CHANG, H. Y., CHI, J. T., DUDOIT, S., BONDRE, C., VAN DE RIJN, M., BOTSTEIN, D. & BROWN, P. O. 2002. Diversity, topographic differentiation, and positional memory in human fibroblasts. *Proc Natl Acad Sci U S A,* 99**,** 12877-82.
CHEN, B. R., CHENG, H. H., LIN, W. C., WANG, K. H., LIOU, J. Y., CHEN, P. F. & WU, K. K. 2012. Quiescent fibroblasts are more active in mounting robust inflammatory responses than proliferative fibroblasts. *PLoS One,* 7**,** e49232.
CHEN, L., LI, M., LI, Q., WANG, C. J. & XIE, S. Q. 2013. DKK1 promotes hepatocellular carcinoma cell migration and invasion through beta-catenin/MMP7 signaling pathway. *Mol Cancer,* 12**,** 157.
CHENG W, Y.-H. R., FANG-GANG N, GUO-AN Z 2011. The content and ratio of type I and III collagen in skin differ with age and injury. *African Journal of Biotechnology,* 10.
CHIQUET, M., KATSAROS, C. & KLETSAS, D. 2015. Multiple functions of gingival and mucoperiosteal fibroblasts in oral wound healing and repair. *Periodontol 2000,* 68**,** 21-40.
CHITAYAT, D., MATSUI, D., AMITAI, Y., KENNEDY, D., VOHRA, S., RIEDER, M. & KOREN, G. 2016. Folic acid supplementation for pregnant women and those planning pregnancy: 2015 update. *Journal of clinical pharmacology,* 56**,** 170-175.
CHITTURI, R. T., BALASUBRAMANIAM, A. M., PARAMESWAR, R. A., KESAVAN, G., HARIS, K. T. M. & MOHIDEEN, K. 2015. The role of myofibroblasts in wound healing, contraction and its clinical implications in cleft palate repair. *Journal of international oral health: JIOH,* 7**,** 75-80.
CHOU, Y., LIN, H.-C., CHEN, K.-C., CHANG, C.-C., LEE, W.-S. & JUAN, S.-H. 2013. Molecular mechanisms underlying the anti-proliferative and anti-migratory effects of folate on homocysteine-challenged rat aortic smooth muscle cells. *British journal of pharmacology,* 169**,** 1447-1460.
CHOW, I., PURNELL, C. A., HANWRIGHT, P. J. & GOSAIN, A. K. 2016. Evaluating the Rule of 10s in Cleft Lip Repair: Do Data Support Dogma? *Plast Reconstr Surg,* 138**,** 670-9.
COBOURNE, M. T. 2004. The complex genetics of cleft lip and palate. *Eur J Orthod,* 26**,** 7-

16.
CONWAY, J. C., TAUB, P. J., KLING, R., OBEROI, K., DOUCETTE, J. & JABS, E. W. 2015. Ten-year experience of more than 35,000 orofacial clefts in Africa. *BMC pediatrics,* 15**,** 8-8.
CORR, B. R., FINLAY-SCHULTZ, J., ROSEN, R. B., QAMAR, L., POST, M. D., BEHBAKHT, K., SPILLMAN, M. A. & SARTORIUS, C. A. 2015. Cytokeratin 5-Positive Cells Represent a Therapy Resistant subpopulation in Epithelial Ovarian Cancer. *Int J Gynecol Cancer,* 25**,** 1565-73.
CORR, D. T., GALLANT-BEHM, C. L., SHRIVE, N. G. & HART, D. A. 2009. Biomechanical behavior of scar tissue and uninjured skin in a porcine model. *Wound Repair Regen,* 17**,** 250-9.
CORRE, J., HEBRAUD, B. & BOURIN, P. 2013. Concise review: growth differentiation factor 15 in pathology: a clinical role? *Stem Cells Transl Med,* 2**,** 946-52.
COUCHMAN, J. R. & PATAKI, C. A. 2012. An introduction to proteoglycans and their localization. *The journal of histochemistry and cytochemistry: official journal of the Histochemistry Society,* 60**,** 885-897.
CRANE. (2018). *Results of the audit in England, Wales and Northern Ireland for children born between January 2000 and December 2017*. Available at: https://www.crane-database.org.uk. (Last accessed 15th June 2019).
DARBY, I. A. & HEWITSON, T. D. 2007. Fibroblast differentiation in wound healing and fibrosis. *Int Rev Cytol,* 257**,** 143-79.
DE PASCALIS, C. & ETIENNE-MANNEVILLE, S. 2017. Single and collective cell migration: the mechanics of adhesions. *Mol Biol Cell,* 28**,** 1833-1846.
DENG, J., SHI, Y., GAO, Z., ZHANG, W., WU, X., CAO, W. & LIU, W. 2018. Inhibition of Pathological Phenotype of Hypertrophic Scar Fibroblasts Via Coculture with Adipose-Derived Stem Cells. *Tissue Eng Part A,* 24**,** 382-393.
DESAI, S. N. 1990. Cleft lip repair in newborn babies. *Annals of the Royal College of Surgeons of England,* 72**,** 101-103.
DESMOULIERE, A., GEINOZ, A., GABBIANI, F. & GABBIANI, G. 1993. Transforming growth factor-beta 1 induces alpha-smooth muscle actin expression in granulation tissue myofibroblasts and in quiescent and growing cultured fibroblasts. *J Cell Biol,* 122**,** 103-11.
DESMOULIÈRE, A., REDARD, M., DARBY, I. & GABBIANI, G. 1995. Apoptosis mediates the decrease in cellularity during the transition between granulation tissue and scar. *The American journal of pathology,* 146**,** 56-66.
DIAH, E., LO, L. J., YUN, C., WANG, R., WAHYUNI, L. K. & CHEN, Y. R. 2007. Cleft oronasal fistula: a review of treatment results and a surgical management algorithm proposal. *Chang Gung Med J,* 30**,** 529-37.
DIETRICH M, G. U. H., KRAMER B, WALCH H 2011. RealTime ready RT-qPCR Assay Development and Qualification
DIEWERT, V. M. & WANG, K. Y. 1992. Recent advances in primary palate and midface morphogenesis research. *Crit Rev Oral Biol Med,* 4**,** 111-30.
DIXON, M. J., MARAZITA, M. L., BEATY, T. H. & MURRAY, J. C. 2011. Cleft lip and palate: understanding genetic and environmental influences. *Nat Rev Genet,* 12**,** 167-78.
DOMOSLAWSKA, A., JURCZAK, A. & JANOWSKI, T. 2013. Oral folic acid supplementation decreases palate and/or lip cleft occurrence in Pug and Chihuahua puppies and elevates folic acid blood levels in pregnant bitches. *Pol J Vet Sci,* 16**,** 33-7.
DUDAS, M., KIM, J., LI, W. Y., NAGY, A., LARSSON, J., KARLSSON, S., CHAI, Y. & KAARTINEN, V. 2006. Epithelial and ectomesenchymal role of the type I TGF-beta

receptor ALK5 during facial morphogenesis and palatal fusion. *Dev Biol,* 296**,** 298-314.
DURAIYAN, J., GOVINDARAJAN, R., KALIYAPPAN, K. & PALANISAMY, M. 2012. Applications of immunohistochemistry. *Journal of pharmacy & bioallied sciences,* 4**,** S307-S309.
EBISAWA, K., KATO, R., OKADA, M., SUGIMURA, T., LATIF, M. A., HORI, Y., NARITA, Y., UEDA, M., HONDA, H. & KAGAMI, H. 2011. Gingival and dermal fibroblasts: their similarities and differences revealed from gene expression. *J Biosci Bioeng,* 111**,** 255-8.
ECKES, B., MAUCH, C., HUPPE, G. & KRIEG, T. 1993. Downregulation of collagen synthesis in fibroblasts within three-dimensional collagen lattices involves transcriptional and posttranscriptional mechanisms. *FEBS Lett,* 318**,** 129-33.
EDISON, R. J. & MUENKE, M. 2004. Central nervous system and limb anomalies in case reports of first-trimester statin exposure. *N Engl J Med,* 350**,** 1579-82.
ELWOOD, J. M. & COLQUHOUN, T. A. 1997. Observations on the prevention of cleft palate in dogs by folic acid and potential relevance to humans. *N Z Vet J,* 45**,** 254-6.
EMORY, R. E., JR., CLAY, R. P., BITE, U. & JACKSON, I. T. 1997. Fistula formation and repair after palatal closure: an institutional perspective. *Plast Reconstr Surg,* 99**,** 1535-8.
EVANS, K. N., SIE, K. C., HOPPER, R. A., GLASS, R. P., HING, A. V. & CUNNINGHAM, M. L. 2011. Robin sequence: from diagnosis to development of an effective management plan. *Pediatrics,* 127**,** 936-48.
EVANS, R. A., TIAN, Y. C., STEADMAN, R. & PHILLIPS, A. O. 2003. TGF-beta1-mediated fibroblast-myofibroblast terminal differentiation-the role of Smad proteins. *Exp Cell Res,* 282**,** 90-100.
EZRATTY, E. J., PARTRIDGE, M. A. & GUNDERSEN, G. G. 2005. Microtubule-induced focal adhesion disassembly is mediated by dynamin and focal adhesion kinase. *Nat Cell Biol,* 7**,** 581-90.
FARRONATO, G., KAIRYTE, L., GIANNINI, L., GALBIATI, G. & MASPERO, C. 2014. How various surgical protocols of the unilateral cleft lip and palate influence the facial growth and possible orthodontic problems? Which is the best timing of lip, palate and alveolus repair? literature review. *Stomatologija,* 16**,** 53-60.
FERGUSON, M. W. 1978a. Palatal shelf elevation in the Wistar rat fetus. *J Anat,* 125**,** 555-77.
FERGUSON, M. W. 1978b. The teratogenic effects of 5-fluoro-2-desoxyuridine (F.U.D.R.) on the Wistar rat fetus with particular reference to cleft palate. *J Anat,* 126**,** 37-49.
FERGUSON, M. W. 1988. Palate development. *Development,* 103 Suppl**,** 41-60.

FIEGUTH, A., FELDBRUGGE, H., GERICH, T., KLEEMANN, W. J. & TROGER, H. D. 2003. The time-dependent expression of fibronectin, MRP8, MRP14 and defensin in surgically treated human skin wounds. *Forensic Sci Int,* 131**,** 156-61.
FIGUEIREDO, J. C., GRAU, M. V., HAILE, R. W., SANDLER, R. S., SUMMERS, R. W., BRESALIER, R. S., BURKE, C. A., MCKEOWN-EYSSEN, G. E. & BARON, J. A. 2009. Folic acid and risk of prostate cancer: results from a randomized clinical trial. *J Natl Cancer Inst,* 101**,** 432-5.
FIGUEROA, A. A., GLUPKER, T. J., FITZ, M. G. & BEGOLE, E. A. 1991. Mandible, tongue, and airway in Pierre Robin sequence: a longitudinal cephalometric study. *Cleft Palate Craniofac J,* 28**,** 425-34.
FILLIES, T., HOMANN, C., MEYER, U., REICH, A., JOOS, U. & WERKMEISTER, R. 2007. Perioperative complications in infant cleft repair. *Head & face medicine,* 3**,** 9-9.

FIRTH, S. M. & BAXTER, R. C. 2002. Cellular actions of the insulin-like growth factor binding proteins. *Endocr Rev,* 23**,** 824-54.

FISCHER, F., ACHTERBERG, V., MARZ, A., PUSCHMANN, S., RAHN, C. D., LUTZ, V., KRUGER, A., SCHWENGLER, H., JASPERS, S., KOOP, U., BLATT, T., WENCK, H. & GALLINAT, S. 2011. Folic acid and creatine improve the firmness of human skin in vivo. *J Cosmet Dermatol,* 10**,** 15-23.

FISHER, D. M. & SOMMERLAD, B. C. 2011. Cleft lip, cleft palate, and velopharyngeal insufficiency. *Plast Reconstr Surg,* 128**,** 342e-360e.

FITZPATRICK, D. R., DENHEZ, F., KONDAIAH, P. & AKHURST, R. J. 1990. Differential expression of TGF beta isoforms in murine palatogenesis. *Development,* 109**,** 585-95.

FOREMAN, D. M., SHARPE, P. M. & FERGUSON, M. W. J. 1991. Comparative biochemistry of mouse and chick secondary-palate development in vivo and in vitro with particular emphasis on extracellular matrix molecules and the effects of growth factors on their synthesis. *Archives of Oral Biology,* 36**,** 457-471.

FOXALL, E., PIPILI, A., JONES, G. E. & WELLS, C. M. 2016. Significance of kinase activity in the dynamic invadosome. *Eur J Cell Biol,* 95**,** 483-492.

FRANÇOIS, C., POLI-MEROL, M. L., TOURNOIS, C., CORNILLET-LEFEBVRE, P., GUILLARD, T., DJERADA, Z., DOCO FENZY, M. & NGUYEN, P. 2017. New in vivo model to analyse the expression of angiogenic genes in the borders of a cleft lip. *British Journal of Oral and Maxillofacial Surgery,* 55**,** 488-495.

FRAZIER, S. B., ROODHOUSE, K. A., HOURCADE, D. E. & ZHANG, L. 2008. The Quantification of Glycosaminoglycans: A Comparison of HPLC, Carbazole, and Alcian Blue Methods. *Open glycoscience,* 1**,** 31-39.

FRIES, M. H., KULLER, J. A., NORTON, M. E., YANKOWITZ, J., KOBORI, J., GOOD, W. V., FERRIERO, D., COX, V., DONLIN, S. S. & GOLABI, M. 1993. Facial features of infants exposed prenatally to cocaine. *Teratology,* 48**,** 413-20.

FUDALEJ, P., KATSAROS, C., DUDKIEWICZ, Z., OFFERT, B., PIWOWAR, W., KUIJPERS, M. & KUIJPERS-JAGTMAN, A. M. 2012. Dental arch relationships following palatoplasty for cleft lip and palate repair. *J Dent Res,* 91**,** 47-51.

FUNATO, N. & NAKAMURA, M. 2017. Identification of shared and unique gene families associated with oral clefts. *Int J Oral Sci,* 9**,** 104-109.

GABBIANI, G. 2003. The myofibroblast in wound healing and fibrocontractive diseases. *J Pathol,* 200**,** 500-3.

GALLAGHER, S. 2001. Quantitation of nucleic acids with absorption spectroscopy. *Curr Protoc Protein Sci,* Appendix 4**,** Appendix 4K.

GALLOWAY, J. L., JONES, S. J., MOSSEY, P. A. & ELLIS, I. R. 2013. The control and importance of hyaluronan synthase expression in palatogenesis. *Frontiers in physiology,* 4**,** 10-10.

GANGULY, A., YANG, H., SHARMA, R., PATEL, K. D. & CABRAL, F. 2012. The role of microtubules and their dynamics in cell migration. *J Biol Chem,* 287**,** 43359-69.

GARZÓN, I., CARRIEL, V., MARÍN-FERNÁNDEZ, A. B., OLIVEIRA, A. C., GARRIDO-GÓMEZ, J., CAMPOS, A., SÁNCHEZ-QUEVEDO, M. D. C. & ALAMINOS, M. 2012. A combined approach for the assessment of cell viability and cell functionality of human fibrochondrocytes for use in tissue engineering. *PloS one,* 7**,** e51961-e51961.

GARZON, I., PEREZ-KOHLER, B., GARRIDO-GOMEZ, J., CARRIEL, V., NIETO-AGUILAR, R., MARTIN-PIEDRA, M. A., GARCIA-HONDUVILLA, N., BUJAN, J., CAMPOS, A. & ALAMINOS, M. 2012. Evaluation of the cell viability of human Wharton's jelly stem cells for use in cell therapy. *Tissue Eng Part C Methods,* 18**,** 408-19.

GAUGLITZ, G. G., KORTING, H. C., PAVICIC, T., RUZICKA, T. & JESCHKE, M. G. 2011. Hypertrophic scarring and keloids: pathomechanisms and current and emerging treatment strategies. *Molecular medicine (Cambridge, Mass.),* 17**,** 113-125.

GE, X. Q., JACKSON, D. A. & BLOW, J. J. 2007. Dormant origins licensed by excess Mcm2-7 are required for human cells to survive replicative stress. *Genes & development,* 21**,** 3331-3341.

GONZALEZ, A. C., COSTA, T. F., ANDRADE, Z. A. & MEDRADO, A. R. 2016. Wound healing - A literature review. *An Bras Dermatol,* 91**,** 614-620.

GOODACRE, T. & SWAN, M. C. 2008. Cleft lip and palate: current management. *Paediatrics and Child Health,* 18**,** 283-292.

GREEN, M. R. & PASTEWKA, J. V. 1974. Simultaneous differential staining by a cationic carbocyanine dye of nucleic acids, proteins and conjugated proteins. I. Phosphoproteins. *J Histochem Cytochem,* 22**,** 767-81.

GREENBERG, J. A., BELL, S. J., GUAN, Y. & YU, Y.-H. 2011. Folic acid supplementation and pregnancy: more than just neural tube defect prevention. *Reviews in Obstetrics and Gynecology,* 4**,** 52.

GREENHALGH, D. G. 1998. The role of apoptosis in wound healing. *Int J Biochem Cell Biol,* 30**,** 1019-30.

GREILING, D. & CLARK, R. A. 1997. Fibronectin provides a conduit for fibroblast transmigration from collagenous stroma into fibrin clot provisional matrix. *Journal of Cell Science,* 110**,** 861.

GRIEB, G., STEFFENS, G., PALLUA, N., BERNHAGEN, J. & BUCALA, R. 2011. Chapter one - Circulating Fibrocytes—Biology and Mechanisms in Wound Healing and Scar Formation. *In:* JEON, K. W. (ed.) *International Review of Cell and Molecular Biology.* Academic Press.

GROSEN, D., CHEVRIER, C., SKYTTHE, A., BILLE, C., MØLSTED, K., SIVERTSEN, A., MURRAY, J. C. & CHRISTENSEN, K. 2010. A cohort study of recurrence patterns among more than 54,000 relatives of oral cleft cases in Denmark: support for the multifactorial threshold model of inheritance. *Journal of medical genetics,* 47**,** 162-168.

GUO, S. & DIPIETRO, L. A. 2010. Factors affecting wound healing. *J Dent Res,* 89**,** 219-29.

GUVAKOVA, M. A. 2007. Insulin-like growth factors control cell migration in health and disease. *The International Journal of Biochemistry & Cell Biology,* 39**,** 890-909.

HABIB, Z. 1978. Genetic counselling and genetics of cleft lip and cleft palate. *Obstet Gynecol Surv,* 33**,** 441-7.

HALDIN, C. E. & LABONNE, C. 2010. SoxE factors as multifunctional neural crest regulatory factors. *Int J Biochem Cell Biol,* 42**,** 441-4.

HALL, B. K. 2008. *The neural crest and neural crest cells in vertebrate development and evolution*, Springer Science & Business Media.

HARDWICKE, J. T., LANDINI, G. & RICHARD, B. M. 2014. Fistula incidence after primary cleft palate repair: a systematic review of the literature. *Plast Reconstr Surg,* 134**,** 618e-27e.

HARVILLE, E. W., WILCOX, A. J., LIE, R. T., VINDENES, H. & ABYHOLM, F. 2005. Cleft lip and palate versus cleft lip only: are they distinct defects? *Am J Epidemiol,* 162**,** 448-53.

HAWIGER, J. 1987. Formation and regulation of platelet and fibrin hemostatic plug. *Hum Pathol,* 18**,** 111-22.

HAY, E. D. 2005. The mesenchymal cell, its role in the embryo, and the remarkable signaling mechanisms that create it. *Dev Dyn,* 233**,** 706-20.

HENDERSON, D. J. & COPP, A. J. 1997. Role of the extracellular matrix in neural crest cell

migration. *J Anat,* 191 (Pt 4)**,** 507-15.
HERNANDEZ-VASQUEZ, M. N., ADAME-GARCIA, S. R., HAMOUD, N., CHIDIAC, R., REYES-CRUZ, G., GRATTON, J. P., COTE, J. F. & VAZQUEZ-PRADO, J. 2017. Cell adhesion controlled by adhesion G protein-coupled receptor GPR124/ADGRA2 is mediated by a protein complex comprising intersectins and Elmo-Dock. *J Biol Chem,* 292**,** 12178-12191.
HINZ, B. & GABBIANI, G. 2003. Mechanisms of force generation and transmission by myofibroblasts. *Curr Opin Biotechnol,* 14**,** 538-46.
HINZ, B., MASTRANGELO, D., ISELIN, C. E., CHAPONNIER, C. & GABBIANI, G. 2001. Mechanical tension controls granulation tissue contractile activity and myofibroblast differentiation. *The American journal of pathology,* 159**,** 1009-1020.
HINZ, B., PHAN, S. H., THANNICKAL, V. J., GALLI, A., BOCHATON-PIALLAT, M.-L. & GABBIANI, G. 2007. The myofibroblast: one function, multiple origins. *The American journal of pathology,* 170**,** 1807-1816.
HODGKINSON, P. D., BROWN, S., DUNCAN, D., GRANT, C., MCNAUGHTON, A. M. Y., THOMAS, P. & MATTICK, C. R. 2005. MANAGEMENT OF CHILDREN WITH CLEFT LIP AND PALATE: A REVIEW DESCRIBING THE APPLICATION OF MULTIDISCIPLINARY TEAM WORKING IN THIS CONDITION BASED UPON THE EXPERIENCES OF A REGIONAL CLEFT LIP AND PALATE CENTRE IN THE UNITED KINGDOM. *Fetal and Maternal Medicine Review,* 16**,** 1-27.
HOFFMAN W.Y. 2011. Cleft Lip & Palate. In: *CURRENT Diagnosis & Treatment in Otolaryngology - Head and Neck Surgery*. 3rd ed. New York: McGraw-Hill Education.
HONRADO, C. P., BRADLEY, D. T. & LARRABEE, W. F. 2018. Chapter 1 - Facial Embryology. *In:* AZIZZADEH, B., MURPHY, M. R., JOHNSON, C. M., MASSRY, G. G. & FITZGERALD, R. (eds.) *Master Techniques in Facial Rejuvenation (Second Edition).* Elsevier.
HOOVER, R. L. 1977. The effect of folic acid on glycosyl transferase activity and cell adhesion. *Experimental Cell Research,* 106**,** 185-189.
HOSOKAWA, R., NONAKA, K., MORIFUJI, M., SHUM, L. & OHISHI, M. 2003. TGF-beta 3 decreases type I collagen and scarring after labioplasty. *J Dent Res,* 82**,** 558-64.
HOU, L. T., LIU, C. M. & WONG, M. Y. 1995. Expression of matrix proteins in cloned fibroblasts derived from periodontal tissue under different cell growth densities. *Proc Natl Sci Counc Repub China B,* 19**,** 176-84.
HU, X., GAO, J., LIAO, Y., TANG, S. & LU, F. 2013. Retinoic acid alters the proliferation and survival of the epithelium and mesenchyme and suppresses Wnt/β-catenin signaling in developing cleft palate. *Cell death & disease,* 4**,** e898-e898.
HUANG, X. & SAINT-JEANNET, J.-P. 2004. Induction of the neural crest and the opportunities of life on the edge. *Developmental Biology,* 275**,** 1-11.
HUANG, X., YANG, N., FIORE, V. F., BARKER, T. H., SUN, Y., MORRIS, S. W., DING, Q., THANNICKAL, V. J. & ZHOU, Y. 2012. Matrix stiffness-induced myofibroblast differentiation is mediated by intrinsic mechanotransduction. *Am J Respir Cell Mol Biol,* 47**,** 340-8.
HUGHES, P., MARSHALL, D., REID, Y., PARKES, H. & GELBER, C. 2007. The costs of using unauthenticated, over-passaged cell lines: how much more data do we need? *Biotechniques,* 43**,** 575, 577-8, 581-2 passim.
HWANG, S. Y., KANG, Y. J., SUNG, B., JANG, J. Y., HWANG, N. L., OH, H. J., AHN, Y. R., KIM, H. J., SHIN, J. H. & YOO, M. A. 2018. Folic acid is necessary for proliferation and differentiation of C2C12 myoblasts. *Journal of cellular physiology,* 233**,** 736-747.
IAMAROON, A., TAIT, B. & DIEWERT, V. 1996. Cell proliferation and expression of EGF,

TGF-α, and EGF receptor in the developing primary palate. *Journal of dental research,* 75**,** 1534-1539.

IBITOYE, R. M., ROBERTS, J., GOODACRE, T. & KINI, U. 2015. 17p13.3 microduplication, a potential novel genetic locus for nonsyndromic bilateral cleft lip and palate. *Cleft Palate Craniofac J,* 52**,** 359-62.

ICHI, S., COSTA, F. F., BISCHOF, J. M., NAKAZAKI, H., SHEN, Y. W., BOSHNJAKU, V., SHARMA, S., MANIA-FARNELL, B., MCLONE, D. G., TOMITA, T., SOARES, M. B. & MAYANIL, C. S. 2010. Folic acid remodels chromatin on Hes1 and Neurog2 promoters during caudal neural tube development. *J Biol Chem,* 285**,** 36922-32.

IMBARD, A., BENOIST, J.-F. & BLOM, H. J. 2013. Neural tube defects, folic acid and methylation. *International journal of environmental research and public health,* 10**,** 4352-4389.

IPDTOC 2011. Prevalence at birth of cleft lip with or without cleft palate: data from the International Perinatal Database of Typical Oral Clefts (IPDTOC). *Cleft Palate Craniofac J,* 48**,** 66-81.

ISHISE, H., LARSON, B., HIRATA, Y., FUJIWARA, T., NISHIMOTO, S., KUBO, T., MATSUDA, K., KANAZAWA, S., SOTSUKA, Y., FUJITA, K., KAKIBUCHI, M. & KAWAI, K. 2015. Hypertrophic scar contracture is mediated by the TRPC3 mechanical force transducer via NFkB activation. *Sci Rep,* 5**,** 11620.

ITO, Y., YEO, J. Y., CHYTIL, A., HAN, J., BRINGAS, P., JR., NAKAJIMA, A., SHULER, C. F., MOSES, H. L. & CHAI, Y. 2003. Conditional inactivation of Tgfbr2 in cranial neural crest causes cleft palate and calvaria defects. *Development,* 130**,** 5269-80.

IULIANO, D. J., SAAVEDRA, S. S. & TRUSKEY, G. A. 1993. Effect of the conformation and orientation of adsorbed fibronectin on endothelial cell spreading and the strength of adhesion. *J Biomed Mater Res,* 27**,** 1103-13.

IVEY, M. J. & TALLQUIST, M. D. 2016. Defining the Cardiac Fibroblast. *Circulation journal: official journal of the Japanese Circulation Society,* 80**,** 2269-2276.

JAGOMAGI, T., SOOTS, M. & SAAG, M. 2010. Epidemiologic factors causing cleft lip and palate and their regularities of occurrence in Estonia. *Stomatologija,* 12**,** 105-8.

JAHANBIN, A., SHADKAM, E., MIRI, H. H., SHIRAZI, A. S. & ABTAHI, M. 2018. Maternal Folic Acid Supplementation and the Risk of Oral Clefts in Offspring. *J Craniofac Surg,* 29**,** e534-e541.

JIA, S., ZHOU, J., FANELLI, C., WEE, Y., BONDS, J., SCHNEIDER, P., MUES, G. & D'SOUZA, R. N. 2017. Small-molecule Wnt agonists correct cleft palates in Pax9 mutant mice in utero. *Development***,** dev. 157750.

JIANG, R., BUSH, J. O. & LIDRAL, A. C. 2006. Development of the upper lip: morphogenetic and molecular mechanisms. *Developmental dynamics: an official publication of the American Association of Anatomists,* 235**,** 1152-1166.

JUGESSUR, A., SHI, M., GJESSING, H. K., LIE, R. T., WILCOX, A. J., WEINBERG, C. R., CHRISTENSEN, K., BOYLES, A. L., DAACK-HIRSCH, S., TRUNG, T. N., BILLE, C., LIDRAL, A. C. & MURRAY, J. C. 2009. Genetic determinants of facial clefting: analysis of 357 candidate genes using two national cleft studies from Scandinavia. *PLoS One,* 4**,** e5385.

JUNQUEIRA, L. C., BIGNOLAS, G. & BRENTANI, R. R. 1979. Picrosirius staining plus polarization microscopy, a specific method for collagen detection in tissue sections. *Histochem J,* 11**,** 447-55.

KAARTINEN, V., CUI, X. M., HEISTERKAMP, N., GROFFEN, J. & SHULER, C. F. 1997. Transforming growth factor-beta3 regulates transdifferentiation of medial edge epithelium during palatal fusion and associated degradation of the basement membrane.

Dev Dyn, 209**,** 255-60.
KALDERÉN, C., STADLER, C., FORSGREN, M., KVASTAD, L., JOHANSSON, E., SYDOW-BÄCKMAN, M. & SVENSSON GELIUS, S. 2014. CCL2 mediates anti-fibrotic effects in human fibroblasts independently of CCR2. *International Immunopharmacology,* 20**,** 66-73.
KATULA, K. S., HEINLOTH, A. N. & PAULES, R. S. 2007. Folate deficiency in normal human fibroblasts leads to altered expression of genes primarily linked to cell signaling, the cytoskeleton and extracellular matrix. *The Journal of Nutritional Biochemistry,* 18**,** 541-552.
KAVERINA, I., KRYLYSHKINA, O. & SMALL, J. V. 1999. Microtubule targeting of substrate contacts promotes their relaxation and dissociation. *J Cell Biol,* 146**,** 1033-44.
KAWAI, M., BREGGIA, A. C., DEMAMBRO, V. E., SHEN, X., CANALIS, E., BOUXSEIN, M. L., BEAMER, W. G., CLEMMONS, D. R. & ROSEN, C. J. 2011. The heparin-binding domain of IGFBP-2 has IGF binding-independent biologic activity in the growing skeleton. *Journal of Biological Chemistry***,** jbc. M110. 193334.
KE, C. Y., XIAO, W. L., CHEN, C. M., LO, L. J. & WONG, F. H. 2015. IRF6 is the mediator of TGFbeta3 during regulation of the epithelial mesenchymal transition and palatal fusion. *Sci Rep,* 5**,** 12791.
KEARSEY, S. E. & LABIB, K. 1998. MCM proteins: evolution, properties, and role in DNA replication. *Biochim Biophys Acta,* 1398**,** 113-36.
KELLY, D., O'DOWD, T. & REULBACH, U. 2012. Use of folic acid supplements and risk of cleft lip and palate in infants: a population-based cohort study. *Br J Gen Pract,* 62**,** e466-72.
KHANNA, R., TIKKU, T. & WADHWA, J. 2012. Nasomaxillary complex in size, position and orientation in surgically treated and untreated individuals with cleft lip and palate: A cephalometric overview. *Indian journal of plastic surgery: official publication of the Association of Plastic Surgeons of India,* 45**,** 68-75.
KIELTY C.M., GRANT, M.E. (2002). The Collagen Family: Structure, Assembly, and Organization in the Extracellular Matrix. In: *Connective Tissue and Its Heritable Disorders: Molecular, Genetic, and Medical Aspects*. 2nd ed. New York: Wiley-Liss. p159-204.
KIM, B. C., KIM, H. T., PARK, S. H., CHA, J. S., YUFIT, T., KIM, S. J. & FALANGA, V. 2003. Fibroblasts from chronic wounds show altered TGF-beta-signaling and decreased TGF-beta Type II receptor expression. *J Cell Physiol,* 195**,** 331-6.
KIM, E. K., KHANG, S. K., LEE, T. J. & KIM, T. G. 2010. Clinical features of the microform cleft lip and the ultrastructural characteristics of the orbicularis oris muscle. *Cleft Palate Craniofac J,* 47**,** 297-302.
KISCHER, C. W. & HENDRIX, M. J. 1983. Fibronectin (FN) in hypertrophic scars and keloids. *Cell Tissue Res,* 231**,** 29-37.
KOHLI, S. S. & KOHLI, V. S. 2012. A comprehensive review of the genetic basis of cleft lip and palate. *Journal of oral and maxillofacial pathology: JOMFP,* 16**,** 64-72.
KONDO, S., SCHUTTE, B. C., RICHARDSON, R. J., BJORK, B. C., KNIGHT, A. S., WATANABE, Y., HOWARD, E., DE LIMA, R. L., DAACK-HIRSCH, S., SANDER, A., MCDONALD-MCGINN, D. M., ZACKAI, E. H., LAMMER, E. J., AYLSWORTH, A. S., ARDINGER, H. H., LIDRAL, A. C., POBER, B. R., MORENO, L., ARCOS-BURGOS, M., VALENCIA, C., HOUDAYER, C., BAHUAU, M., MORETTI-FERREIRA, D., RICHIERI-COSTA, A., DIXON, M. J. & MURRAY, J. C. 2002. Mutations in IRF6 cause Van der Woude and popliteal pterygium syndromes. *Nat Genet,* 32**,** 285-9.

KOYANAGI, M., KAWAKABE, S. & ARIMURA, Y. 2016. A comparative study of colorimetric cell proliferation assays in immune cells. *Cytotechnology,* 68**,** 1489-1498.
KRIENS, O. 1989. LAHSHAL: a concise documentation system for cleft lip, alveolus, and palate diagnoses. *What is a cleft lip and palate***,** 32-3.
KRISTENSEN, J. H. & KARSDAL, M. A. 2016. Chapter 30 - Elastin. *In:* KARSDAL, M. A. (ed.) *Biochemistry of Collagens, Laminins and Elastin.* Academic Press.
KUHN, K. 1995. Basement membrane (type IV) collagen. *Matrix Biol,* 14**,** 439-45.
KULKARNI, K. R., PATIL, M. R., SHIRKE, A. M. & JADHAV, S. B. 2013. Perioperative respiratory complications in cleft lip and palate repairs: An audit of 1000 cases under 'Smile Train Project'. *Indian journal of anaesthesia,* 57**,** 562-568.
KUMARI, P., ALI, A., SUKLA, K. K., SINGH, S. K. & RAMAN, R. 2013. Lower incidence of nonsyndromic cleft lip with or without cleft palate in females: is homocysteine a factor? *J Biosci,* 38**,** 21-6.
KURISU, K., OHSAKI, Y., NAGATA, K., KUKITA, T., YOSHIKAWA, H. & INAI, T. 1987. Immunocytochemical demonstration of simultaneous synthesis of types I, III and V collagen and fibronectin in mouse embryonic palatal mesenchymal cells in vitro. *Coll Relat Res,* 7**,** 333-40.
KURISU, S. & TAKENAWA, T. 2009. The WASP and WAVE family proteins. *Genome Biol,* 10**,** 226.
KUROKAWA, K. & MATSUDA, M. 2005. Localized RhoA activation as a requirement for the induction of membrane ruffling. *Molecular biology of the cell,* 16**,** 4294-4303.
LABERGE, L. C. 2007. Unilateral cleft lip and palate: Simultaneous early repair of the nose, anterior palate and lip. *The Canadian journal of plastic surgery = Journal canadien de chirurgie plastique,* 15**,** 13-18.
LAMMER, E. J., CHEN, D. T., HOAR, R. M., AGNISH, N. D., BENKE, P. J., BRAUN, J. T., CURRY, C. J., FERNHOFF, P. M., GRIX, A. W., JR., LOTT, I. T. & ET AL. 1985. Retinoic acid embryopathy. *N Engl J Med,* 313**,** 837-41.
LAN, Y., XU, J. & JIANG, R. 2015. Cellular and Molecular Mechanisms of Palatogenesis. *Current topics in developmental biology,* 115**,** 59-84.
LATTOUF, R., YOUNES, R., LUTOMSKI, D., NAAMAN, N., GODEAU, G., SENNI, K. & CHANGOTADE, S. 2014. Picrosirius red staining: a useful tool to appraise collagen networks in normal and pathological tissues. *J Histochem Cytochem,* 62**,** 751-8.
LAWRENCE, W. T. 1998. Physiology of the acute wound. *Clin Plast Surg,* 25**,** 321-40.
LAWSON, C. D. & RIDLEY, A. J. 2018. Rho GTPase signaling complexes in cell migration and invasion. *The Journal of Cell Biology,* 217**,** 447-457.
LEE, D. H., YANG, Y., LEE, S. J., KIM, K. Y., KOO, T. H., SHIN, S. M., SONG, K. S., LEE, Y. H., KIM, Y. J., LEE, J. J., CHOI, I. & LEE, J. H. 2003. Macrophage inhibitory cytokine-1 induces the invasiveness of gastric cancer cells by up-regulating the urokinase-type plasminogen activator system. *Cancer Res,* 63**,** 4648-55.
LEE, H.-G. & EUN, H. C. 1999. Differences between fibroblasts cultured from oral mucosa and normal skin: implication to wound healing. *Journal of Dermatological Science,* 21**,** 176-182.
LEE, Y.-H. & SAINT-JEANNET, J.-P. 2011. Sox9 function in craniofacial development and disease. *Genesis (New York, N.Y.: 2000),* 49**,** 200-208.
LEES, M. M., WINTER, R. M., MALCOLM, S., SAAL, H. M. & CHITTY, L. 1999. Popliteal pterygium syndrome: a clinical study of three families and report of linkage to the Van der Woude syndrome locus on 1q32. *J Med Genet,* 36**,** 888-92.
LEGESSE-MILLER, A., RAITMAN, I., HALEY, E. M., LIAO, A., SUN, L. L., WANG, D. J., KRISHNAN, N., LEMONS, J. M. S., SUH, E. J., JOHNSON, E. L., LUND, B. A.

& COLLER, H. A. 2012. Quiescent fibroblasts are protected from proteasome inhibition-mediated toxicity. *Molecular biology of the cell,* 23**,** 3566-3581.
LESLIE, E. J. & MARAZITA, M. L. 2013. Genetics of cleft lip and cleft palate. *American journal of medical genetics. Part C, Seminars in medical genetics,* 163C**,** 246-258.
LETRA, A., FAKHOURI, W., FONSECA, R. F., MENEZES, R., KEMPA, I., PRASAD, J. L., MCHENRY, T. G., LIDRAL, A. C., MORENO, L., MURRAY, J. C., DAACK-HIRSCH, S., MARAZITA, M. L., CASTILLA, E. E., LACE, B., ORIOLI, I. M., GRANJEIRO, J. M., SCHUTTE, B. C. & VIEIRA, A. R. 2012. Interaction between IRF6 and TGFA genes contribute to the risk of nonsyndromic cleft lip/palate. *PLoS One,* 7**,** e45441.
LEVINSON, H. 2013. A Paradigm of Fibroblast Activation and Dermal Wound Contraction to Guide the Development of Therapies for Chronic Wounds and Pathologic Scars. *Advances in wound care,* 2**,** 149-159.
LEWIS, C. M., SMITH, A. K. & KAMEN, B. A. 1998. Receptor-mediated folate uptake is positively regulated by disruption of the actin cytoskeleton. *Cancer Res,* 58**,** 2952-6.
LEWIS, P. M., DUNN, M. P., MCMAHON, J. A., LOGAN, M., MARTIN, J. F., ST-JACQUES, B. & MCMAHON, A. P. 2001. Cholesterol modification of sonic hedgehog is required for long-range signaling activity and effective modulation of signaling by Ptc1. *Cell,* 105**,** 599-612.
LI, B. & WANG, J. H. 2011. Fibroblasts and myofibroblasts in wound healing: force generation and measurement. *J Tissue Viability,* 20**,** 108-20.
LI, L. T., JIANG, G., CHEN, Q. & ZHENG, J. N. 2015. Ki67 is a promising molecular target in the diagnosis of cancer (review). *Mol Med Rep,* 11**,** 1566-72.
LI, W.-Y., DUDAS, M. & KAARTINEN, V. 2008. Signaling through Tgf-β type I receptor Alk5 is required for upper lip fusion. *Mechanisms of Development,* 125**,** 874-882.
LI, X., QIAN, H., ONO, F., TSUCHISAKA, A., KROL, R. P., OHARA, K., HAYAKAWA, T., MATSUEDA, S., SASADA, T., OHATA, C., FURUMURA, M., HAMADA, T. & HASHIMOTO, T. 2014. Human dermal fibroblast migration induced by fibronectin in autocrine and paracrine manners. *Exp Dermatol,* 23**,** 682-4.
LIANG, C. C., PARK, A. Y. & GUAN, J. L. 2007. In vitro scratch assay: a convenient and inexpensive method for analysis of cell migration in vitro. *Nat Protoc,* 2**,** 329-33.
LIDRAL, A. C., MURRAY, J. C., BUETOW, K. H., BASART, A. M., SCHEARER, H., SHIANG, R., NAVAL, A., LAYDA, E., MAGEE, K. & MAGEE, W. 1997. Studies of the candidate genes TGFB2, MSX1, TGFA, and TGFB3 in the etiology of cleft lip and palate in the Philippines. *Cleft Palate Craniofac J,* 34**,** 1-6.
LITTLE, J., CARDY, A. & MUNGER, R. G. 2004. Tobacco smoking and oral clefts: a meta-analysis. *Bull World Health Organ,* 82**,** 213-8.
LITTLE, J., GILMOUR, M., MOSSEY, P., FITZPATRICK, D., CARDY, A., CLAYTON-SMITH, J., HILL, A., DUTHIE, S., FRYER, A. & MOLLOY, A. 2008. Folate and clefts of the lip and palate—a UK-based case-control study: part II: Biochemical and genetic analysis. *The Cleft Palate-Craniofacial Journal,* 45**,** 428-438.
LIU, W., SUN, X., BRAUT, A., MISHINA, Y., BEHRINGER, R. R., MINA, M. & MARTIN, J. F. 2005. Distinct functions for Bmp signaling in lip and palate fusion in mice. *Development,* 132**,** 1453.
LIU, Y., LI, Y., LI, N., TENG, W., WANG, M., ZHANG, Y. & XIAO, Z. 2016. TGF-beta1 promotes scar fibroblasts proliferation and transdifferentiation via up-regulating MicroRNA-21. *Sci Rep,* 6**,** 32231.
LO, C. M., WANG, H. B., DEMBO, M. & WANG, Y. L. 2000. Cell movement is guided by the rigidity of the substrate. *Biophys J,* 79**,** 144-52.

LOMBARD, J. 2014. Once upon a time the cell membranes: 175 years of cell boundary research. *Biology direct,* 9**,** 32-32.

LORENTE, C., CORDIER, S., GOUJARD, J., AYMÉ, S., BIANCHI, F., CALZOLARI, E., DE WALLE, H. E. & KNILL-JONES, R. 2000. Tobacco and alcohol use during pregnancy and risk of oral clefts. Occupational Exposure and Congenital Malformation Working Group. *American journal of public health,* 90**,** 415-419.

LU, X.-C., YU, W., TAO, Y., ZHAO, P.-L., LI, K., TANG, L.-J., ZHENG, J.-Y. & LI, L.-X. 2014. Contribution of Transforming Growth Factor α Polymorphisms to Nonsyndromic Orofacial Clefts: A HuGE Review and Meta-Analysis. *American Journal of Epidemiology,* 179**,** 267-281.

LULEVICH, V., SHIH, Y.-P., LO, S. H. & LIU, G.-Y. 2009. Cell tracing dyes significantly change single cell mechanics. *The journal of physical chemistry. B,* 113**,** 6511-6519.

MACHACEK, M., HODGSON, L., WELCH, C., ELLIOTT, H., PERTZ, O., NALBANT, P., ABELL, A., JOHNSON, G. L., HAHN, K. M. & DANUSER, G. 2009. Coordination of Rho GTPase activities during cell protrusion. *Nature,* 461**,** 99-103.

MADINE, M. A., SWIETLIK, M., PELIZON, C., ROMANOWSKI, P., MILLS, A. D. & LASKEY, R. A. 2000. The roles of the MCM, ORC, and Cdc6 proteins in determining the replication competence of chromatin in quiescent cells. *J Struct Biol,* 129**,** 198-210.

MAH, W., JIANG, G., OLVER, D., CHEUNG, G., KIM, B., LARJAVA, H. & HÄKKINEN, L. 2014. Human gingival fibroblasts display a non-fibrotic phenotype distinct from skin fibroblasts in three-dimensional cultures. *PloS one,* 9**,** e90715-e90715.

MANN, G. B., FOWLER, K. J., GABRIEL, A., NICE, E. C., WILLIAMS, R. L. & DUNN, A. R. 1993. Mice with a null mutation of the TGF alpha gene have abnormal skin architecture, wavy hair, and curly whiskers and often develop corneal inflammation. *Cell,* 73**,** 249-61.

MARAZITA, M. L. 2012. The evolution of human genetic studies of cleft lip and cleft palate. *Annual review of genomics and human genetics,* 13**,** 263-283.

MARINKOVIC, A., MIH, J. D., PARK, J. A., LIU, F. & TSCHUMPERLIN, D. J. 2012. Improved throughput traction microscopy reveals pivotal role for matrix stiffness in fibroblast contractility and TGF-beta responsiveness. *Am J Physiol Lung Cell Mol Physiol,* 303**,** L169-80.

MARINUCCI, L., BALLONI, S., BODO, M., CARINCI, F., PEZZETTI, F., STABELLINI, G., CARMELA, C. & LUMARE, E. 2009. Patterns of some extracellular matrix gene expression are similar in cells from cleft lip-palate patients and in human palatal fibroblasts exposed to diazepam in culture. *Toxicology,* 257**,** 10-16.

MATEU, R., ŽIVICOVÁ, V., KREJČÍ, E. D., GRIM, M., STRNAD, H., VLČEK, Č., KOLÁŘ, M., LACINA, L., GÁL, P., BORSKÝ, J., SMETANA, K., JR. & DVOŘÁNKOVÁ, B. 2016. Functional differences between neonatal and adult fibroblasts and keratinocytes: Donor age affects epithelial-mesenchymal crosstalk in vitro. *International journal of molecular medicine,* 38**,** 1063-1074.

MATIC, D. B. & POWER, S. M. 2011. Correction of the cleft lip lateral bulge deformity using anatomic muscle repair. *J Craniofac Surg,* 22**,** 514-9.

MAYOR, R. & ETIENNE-MANNEVILLE, S. 2016. The front and rear of collective cell migration. *Nat Rev Mol Cell Biol,* 17**,** 97-109.

MAZIERES, J., ANTONIA, T., DASTE, G., MURO-CACHO, C., BERCHERY, D., TILLEMENT, V., PRADINES, A., SEBTI, S. & FAVRE, G. 2004. Loss of RhoB expression in human lung cancer progression. *Clin Cancer Res,* 10**,** 2742-50.

MCCALL, M. N., MCMURRAY, H. R., LAND, H. & ALMUDEVAR, A. 2014. On non-detects in qPCR data. *Bioinformatics (Oxford, England),* 30**,** 2310-2316.

MCCLOY, R. A., ROGERS, S., CALDON, C. E., LORCA, T., CASTRO, A. & BURGESS, A. 2014. Partial inhibition of Cdk1 in G 2 phase overrides the SAC and decouples mitotic events. *Cell Cycle,* 13**,** 1400-12.

MCDOUGALL, S., DALLON, J., SHERRATT, J. & MAINI, P. 2006. Fibroblast migration and collagen deposition during dermal wound healing: mathematical modelling and clinical implications. *Philos Trans A Math Phys Eng Sci,* 364**,** 1385-405.

MCNULTY, H. & PENTIEVA, K. 2004. Folate bioavailability. *Proc Nutr Soc,* 63**,** 529-36.

MENÉNDEZ-MENÉNDEZ, Y., OTERO-HERNÁNDEZ, J., VEGA, J. A., PÉREZ-BASTERRECHEA, M., PÉREZ-LÓPEZ, S., ÁLVAREZ-VIEJO, M. & FERRERO-GUTIÉRREZ, A. 2017. The role of bone marrow mononuclear cell-conditioned medium in the proliferation and migration of human dermal fibroblasts. *Cellular & molecular biology letters,* 22**,** 29-29.

MENG, L., BIAN, Z., TORENSMA, R. & VON DEN HOFF, J. W. 2009. Biological mechanisms in palatogenesis and cleft palate. *J Dent Res,* 88**,** 22-33.

MEYER, K. A., WERLER, M. M., HAYES, C. & MITCHELL, A. A. 2003. Low maternal alcohol consumption during pregnancy and oral clefts in offspring: the Slone Birth Defects Study. *Birth Defects Res A Clin Mol Teratol,* 67**,** 509-14.

MITCHELL, L. E., MURRAY, J. C., O'BRIEN, S. & CHRISTENSEN, K. 2003. Retinoic acid receptor alpha gene variants, multivitamin use, and liver intake as risk factors for oral clefts: a population-based case-control study in Denmark, 1991-1994. *Am J Epidemiol,* 158**,** 69-76.

MOEPHULI, S. R., KLEIN, N. W., BALDWIN, M. T. & KRIDER, H. M. 1997. Effects of methionine on the cytoplasmic distribution of actin and tubulin during neural tube closure in rat embryos. *Proceedings of the National Academy of Sciences of the United States of America,* 94**,** 543-548.

MOGILNER, A. & OSTER, G. 1996. Cell motility driven by actin polymerization. *Biophysical journal,* 71**,** 3030-3045.

MOREIRA, I., SURI, S., ROSS, B., TOMPSON, B., FISHER, D. & LOU, W. 2014. Soft-tissue profile growth in patients with repaired complete unilateral cleft lip and palate: A cephalometric comparison with normal controls at ages 7, 11, and 18 years. *Am J Orthod Dentofacial Orthop,* 145**,** 341-58.

MORRIS-WIMAN, J. & BRINKLEY, L. 1992. An extracellular matrix infrastructure provides support for murine secondary palatal shelf remodelling. *Anat Rec,* 234**,** 575-86.

MORRIS-WIMAN, J. & BRINKLEY, L. 1993. Rapid changes in the extracellular matrix accompany in vitro palatal shelf remodelling. *Anat Embryol (Berl),* 188**,** 75-85.

MORTON, L. M. & PHILLIPS, T. J. 2016. Wound healing and treating wounds: Differential diagnosis and evaluation of chronic wounds. *J Am Acad Dermatol,* 74**,** 589-605; quiz 605-6.

MOSLEM, M., EGGENSCHWILER, R., WICHMANN, C., BUHMANN, R., CANTZ, T. & HENSCHLER, R. 2017. Kindlin-2 Modulates the Survival, Differentiation, and Migration of Induced Pluripotent Cell-Derived Mesenchymal Stromal Cells. *Stem cells international,* 2017**,** 7316354-7316354.

MOSSEY, P. A. 2002. Epidemiology of oral clefts: an international perspective. *Cleft lip & palate: from origin to treatment*.

MOSSEY, P. A., DAVIES, J. A. & LITTLE, J. 2007. Prevention of orofacial clefts: does pregnancy planning have a role? *Cleft Palate Craniofac J,* 44**,** 244-50.

MOSSEY, P. A., LITTLE, J., MUNGER, R. G., DIXON, M. J. & SHAW, W. C. 2009. Cleft lip and palate. *Lancet,* 374**,** 1773-85.

MOSSEY, P. A. & MODELL, B. 2012. Epidemiology of oral clefts 2012: an international

perspective. *Front Oral Biol,* 16**,** 1-18.
MOXHAM, B. 2003. The development of the palate - A brief review. *Eur. J. Anat.,* 7**,** 53-74.
MUIR, I. F. 1990. On the nature of keloid and hypertrophic scars. *Br J Plast Surg,* 43**,** 61-9.
MULLINS, R. D., HEUSER, J. A. & POLLARD, T. D. 1998. The interaction of Arp2/3 complex with actin: nucleation, high affinity pointed end capping, and formation of branching networks of filaments. *Proceedings of the National Academy of Sciences,* 95**,** 6181-6186.
MUNGER, R. G., TAMURA, T., JOHNSTON, K. E., FELDKAMP, M. L., PFISTER, R. & CAREY, J. C. 2009. Plasma zinc concentrations of mothers and the risk of oral clefts in their children in Utah. *Birth Defects Res A Clin Mol Teratol,* 85**,** 151-5.
MURRAY, J. C. & SCHUTTE, B. C. 2004. Cleft palate: players, pathways, and pursuits. *J Clin Invest,* 113**,** 1676-8.
MURTHY, J. 2011. Descriptive study of management of palatal fistula in one hundred and ninety-four cleft individuals. *Indian J Plast Surg,* 44**,** 41-6.
NAGASE, Y., NATSUME, N., KATO, T. & HAYAKAWA, T. 2010. Epidemiological Analysis of Cleft Lip and/or Palate by Cleft Pattern. *Journal of maxillofacial and oral surgery,* 9**,** 389-395.
NAGY, K. & MOMMAERTS, M. Y. 2009. Lip adhesion revisited: A technical note with review of literature. *Indian J Plast Surg,* 42**,** 204-12.
NAHAI, F. R., WILLIAMS, J. K., BURSTEIN, F. D., MARTIN, J. & THOMAS, J. 2005. The Management of Cleft Lip and Palate: Pathways for Treatment and Longitudinal Assessment. *Seminars in Plastic Surgery,* 19**,** 275-285.
NAWSHAD, A., LAGAMBA, D. & HAY, E. D. 2004. Transforming growth factor beta (TGFbeta) signalling in palatal growth, apoptosis and epithelial mesenchymal transformation (EMT). *Arch Oral Biol,* 49**,** 675-89.
NEGMADJANOV, U., GODIC, Z., RIZVI, F., EMELYANOVA, L., ROSS, G., RICHARDS, J., HOLMUHAMEDOV, E. L. & JAHANGIR, A. 2015. TGF-β1-mediated differentiation of fibroblasts is associated with increased mitochondrial content and cellular respiration. *PloS one,* 10**,** e0123046-e0123046.
NEWGREEN, D. & THIERY, J. P. 1980. Fibronectin in early avian embryos: synthesis and distribution along the migration pathways of neural crest cells. *Cell Tissue Res,* 211**,** 269-91.
NIE, X. 2005. Dkk1,-2, and-3 expression in mouse craniofacial development. *Journal of molecular histology,* 36**,** 367-372.
NIESSEN, F. B., SPAUWEN, P. H., SCHALKWIJK, J. & KON, M. 1999. On the nature of hypertrophic scars and keloids: a review. *Plast Reconstr Surg,* 104**,** 1435-58.
NIK, A. M., JOHANSSON, J. A., GHIAMI, M., REYAHI, A. & CARLSSON, P. 2016. Foxf2 is required for secondary palate development and Tgfβ signaling in palatal shelf mesenchyme. *Developmental Biology,* 415**,** 14-23.
NOBES, C. D. & HALL, A. 1995. Rho, rac, and cdc42 GTPases regulate the assembly of multimolecular focal complexes associated with actin stress fibers, lamellipodia, and filopodia. *Cell,* 81**,** 53-62.
NUGENT, P., SUCOV, H. M., PISANO, M. M. & GREENE, R. M. 1999. The role of RXR-alpha in retinoic acid-induced cleft palate as assessed with the RXR-alpha knockout mouse. *Int J Dev Biol,* 43**,** 567-70.
OJI, T., SAKAMOTO, Y., OGATA, H., TAMADA, I. & KISHI, K. 2013. A 25-year review of cases with submucous cleft palate. *Int J Pediatr Otorhinolaryngol,* 77**,** 1183-5.
OKA, K., HONDA, M. J., TSURUGA, E., HATAKEYAMA, Y., ISOKAWA, K. & SAWA,

Y. 2012. Roles of collagen and periostin expression by cranial neural crest cells during soft palate development. *The journal of histochemistry and cytochemistry : official journal of the Histochemistry Society,* 60**,** 57-68.

OLIVEIRA, G. V., HAWKINS, H. K., CHINKES, D., BURKE, A., TAVARES, A. L. P., RAMOS-E-SILVA, M., ALBRECHT, T. B., KITTEN, G. T. & HERNDON, D. N. 2009. Hypertrophic versus non hypertrophic scars compared by immunohistochemistry and laser confocal microscopy: type I and III collagens. *International wound journal,* 6**,** 445-452.

WHO. 2004. Global strategies to reduce the health care burden of craniofacial anomalies: report of WHO meetings on international collaborative research on craniofacial anomalies. *Cleft Palate Craniofac J,* 41**,** 238-43.

WHO. 2005. Vitamin and mineral requirements in human nutrition.

PALIOTO, D. B., DELLA COLETTA, R., MARTELLI JUNIOR, H., JOLY, J. C., GRANER, E. & DE LIMA, A. F. 2002. [Comparison between gingival and periodontal ligament fibroblasts from the same subject]. *Pesqui Odontol Bras,* 16**,** 319-25.

PANG, H., MA, N., JIAO, M., SHEN, W., XIN, B., WANG, T., ZHANG, F., LIU, L. & ZHANG, H. 2017. The Biological Effects of Dickkopf1 on Small Cell Lung Cancer Cells and Bone Metastasis. *Oncol Res,* 25**,** 35-42.

PANKOV, R. & YAMADA, K. M. 2002. Fibronectin at a glance. *J Cell Sci,* 115**,** 3861-3.

PARK, J. W., MCINTOSH, I., HETMANSKI, J. B., JABS, E. W., VANDER KOLK, C. A., WU-CHOU, Y.-H., CHEN, P. K., CHONG, S. S., YEOW, V., JEE, S. H., PARK, B. Y., FALLIN, M. D., INGERSOLL, R., SCOTT, A. F. & BEATY, T. H. 2007. Association between IRF6 and nonsyndromic cleft lip with or without cleft palate in four populations. *Genetics in medicine: official journal of the American College of Medical Genetics,* 9**,** 219-227.

PARSONS, J. T., HORWITZ, A. R. & SCHWARTZ, M. A. 2010. Cell adhesion: integrating cytoskeletal dynamics and cellular tension. *Nat Rev Mol Cell Biol,* 11**,** 633-43.

PARWAZ, M. A., SHARMA, R. K., PARASHAR, A., NANDA, V., BISWAS, G. & MAKKAR, S. 2009. Width of cleft palate and postoperative palatal fistula--do they correlate? *J Plast Reconstr Aesthet Surg,* 62**,** 1559-63.

PASTAR, I., STOJADINOVIC, O., YIN, N. C., RAMIREZ, H., NUSBAUM, A. G., SAWAYA, A., PATEL, S. B., KHALID, L., ISSEROFF, R. R. & TOMIC-CANIC, M. 2014. Epithelialization in Wound Healing: A Comprehensive Review. *Advances in wound care,* 3**,** 445-464.

PELTON, R. W., HOGAN, B. L., MILLER, D. A. & MOSES, H. L. 1990. Differential expression of genes encoding TGFs beta 1, beta 2, and beta 3 during murine palate formation. *Dev Biol,* 141**,** 456-60.

PENN, J. W., GROBBELAAR, A. O. & ROLFE, K. J. 2012. The role of the TGF-beta family in wound healing, burns and scarring: a review. *Int J Burns Trauma,* 2**,** 18-28.

PERRIS, R. 1997. The extracellular matrix in neural crest-cell migration. *Trends in Neurosciences,* 20**,** 23-31.

PERRIS, R., BRANDENBERGER, R. & CHIQUET, M. 1996. Differential neural crest cell attachment and migration on avian laminin isoforms. *Int J Dev Neurosci,* 14**,** 297-314.

PETROV, V. V., FAGARD, R. H. & LIJNEN, P. J. 2002. Stimulation of collagen production by transforming growth factor-beta1 during differentiation of cardiac fibroblasts to myofibroblasts. *Hypertension,* 39**,** 258-63.

PFAFFL, M. W. 2001. A new mathematical model for relative quantification in real-time RT-PCR. *Nucleic Acids Res,* 29**,** e45.

PISANO, M. M., BHATTACHERJEE, V., WONG, L., FINNELL, R. H. & GREENE, R. M.

2010. Novel folate binding protein-1 interactions in embryonic orofacial tissue. *Life Sci,* 86**,** 275-80.

POLLARD, T. D. & BELTZNER, C. C. 2002. Structure and function of the Arp2/3 complex. *Curr Opin Struct Biol,* 12**,** 768-74.

POOL, R. 1995. Tissue mobilization with preoperative lip taping. *Operative Techniques in Plastic and Reconstructive Surgery,* 2**,** 155-158.

PORTER, F. D. 2006. Cholesterol precursors and facial clefting. *J Clin Invest,* 116**,** 2322-5.

POUJADE, M., GRASLAND-MONGRAIN, E., HERTZOG, A., JOUANNEAU, J., CHAVRIER, P., LADOUX, B., BUGUIN, A. & SILBERZAN, P. 2007. Collective migration of an epithelial monolayer in response to a model wound. *Proceedings of the National Academy of Sciences of the United States of America,* 104**,** 15988-15993.

POWELL, D. W., MIFFLIN, R. C., VALENTICH, J. D., CROWE, S. E., SAADA, J. I. & WEST, A. B. 1999. Myofibroblasts. I. Paracrine cells important in health and disease. *Am J Physiol,* 277**,** C1-9.

PRADAT, P., ROBERT-GNANSIA, E., DI TANNA, G. L., ROSANO, A., LISI, A. & MASTROIACOVO, P. 2003. First trimester exposure to corticosteroids and oral clefts. *Birth Defects Res A Clin Mol Teratol,* 67**,** 968-70.

PRAHL, C., PRAHL-ANDERSEN, B., VAN 'T HOF, M. A. & KUIJPERS-JAGTMAN, A. M. 2006. Infant orthopedics and facial appearance: a randomized clinical trial (Dutchcleft). *Cleft Palate Craniofac J,* 43**,** 659-64.

PROETZEL, G., PAWLOWSKI, S. A., WILES, M. V., YIN, M., BOIVIN, G. P., HOWLES, P. N., DING, J., FERGUSON, M. W. & DOETSCHMAN, T. 1995. Transforming growth factor-beta 3 is required for secondary palate fusion. *Nat Genet,* 11**,** 409-14.

RAAB, M. & DISCHER, D. E. 2017. Matrix rigidity regulates microtubule network polarization in migration. *Cytoskeleton (Hoboken),* 74**,** 114-124.

RABELLO, F. B., SOUZA, C. D. & FARINA JÚNIOR, J. A. 2014. Update on hypertrophic scar treatment. *Clinics (Sao Paulo),* 69**,** 565-73.

RABENSTEIN, D. L. 2002. Heparin and heparan sulfate: structure and function. *Nat Prod Rep,* 19**,** 312-31.

RAHIMOV, F., MARAZITA, M. L., VISEL, A., COOPER, M. E., HITCHLER, M. J., RUBINI, M., DOMANN, F. E., GOVIL, M., CHRISTENSEN, K., BILLE, C., MELBYE, M., JUGESSUR, A., LIE, R. T., WILCOX, A. J., FITZPATRICK, D. R., GREEN, E. D., MOSSEY, P. A., LITTLE, J., STEEGERS-THEUNISSEN, R. P., PENNACCHIO, L. A., SCHUTTE, B. C. & MURRAY, J. C. 2008. Disruption of an AP-2alpha binding site in an IRF6 enhancer is associated with cleft lip. *Nat Genet,* 40**,** 1341-7.

REYNOLDS, E. 2002. Folic acid, ageing, depression, and dementia. *BMJ: British Medical Journal,* 324**,** 1512.

RIAHI, R., YANG, Y., ZHANG, D. D. & WONG, P. K. 2012. Advances in wound-healing assays for probing collective cell migration. *J Lab Autom,* 17**,** 59-65.

RICARD-BLUM, S. The collagen family. *Cold Spring Harbor perspectives in biology,* 3**,** a004978-a004978.

RICH, L. & WHITTAKER, P. 2005. *Collagen and Picrosirius Red Staining: A polarized light assessment of fibrillar hue and spatial distribution.*

RICHARD, B., RUSSELL, J., MCMAHON, S. & PIGOTT, R. 2006. Results of randomized controlled trial of soft palate first versus hard palate first repair in unilateral complete cleft lip and palate. *Cleft Palate Craniofac J,* 43**,** 329-38.

RICHARD, B. M., QIU, C. X. & FERGUSON, M. W. 2000. Neonatal palatal cysts and their morphology in cleft lip and palate. *Br J Plast Surg,* 53**,** 555-8.

RIDLEY, A. J. & HALL, A. 1992. The small GTP-binding protein rho regulates the assembly of focal adhesions and actin stress fibers in response to growth factors. *Cell,* 70**,** 389-99.

RIMOIN DL, C. J., PYERITZ RE, KORF BR 2006. Clefting, Dental, and Craniofacial Syndromes. *Principles and Practice of Medical Genetics.* London: Churchill Livingstone.

RIVELINE, D., ZAMIR, E., BALABAN, N. Q., SCHWARZ, U. S., ISHIZAKI, T., NARUMIYA, S., KAM, Z., GEIGER, B. & BERSHADSKY, A. D. 2001. Focal contacts as mechanosensors: externally applied local mechanical force induces growth of focal contacts by an mDia1-dependent and ROCK-independent mechanism. *J Cell Biol,* 153**,** 1175-86.

ROBSON, M. C., STEED, D. L. & FRANZ, M. G. 2001. Wound healing: biologic features and approaches to maximize healing trajectories. *Curr Probl Surg,* 38**,** 72-140.

ROGERS, C. D., JAYASENA, C. S., NIE, S. & BRONNER, M. E. 2012. Neural crest specification: tissues, signals, and transcription factors. *Wiley Interdiscip Rev Dev Biol,* 1**,** 52-68.

ROZARIO, T. & DESIMONE, D. W. 2010. The extracellular matrix in development and morphogenesis: a dynamic view. *Dev Biol,* 341**,** 126-40.

RYDHOLM, S., ROGERS, R. A. & BRISMAR, H. 2005. Parafilm Dependent Cell Patterning. *Microscopy and Microanalysis,* 11**,** 1174-1175.

SADHU, P. 2009. Oronasal fistula in cleft palate surgery. *Indian journal of plastic surgery: official publication of the Association of Plastic Surgeons of India,* 42 Suppl**,** S123-S128.

SADLER, T. W., GREENBERG, D., COUGHLIN, P. & LESSARD, J. L. 1982. Actin distribution patterns in the mouse neural tube during neurulation. *Science,* 215**,** 172-4.

SAKAGUCHI, K., NAGATA, J., NAGAYAMA, K., SUGIHARA, K. & MIYAWAKI, S. 2008. Orthodontic treatment using maxillary distraction osteogenesis on a patient with cleft soft palate, maxillary hypoplasia, total crossbite and mental retardation. *Orthodontic Waves,* 67**,** 65-71.

SAKAI, T., LARSEN, M. & YAMADA, K. M. 2003. Fibronectin requirement in branching morphogenesis. *Nature,* 423**,** 876-81.

SANDHU, S. V., GUPTA, S., BANSAL, H. & SINGLA, K. 2012. *Collagen in Health and Disease*.

SANFORD, L. P., ORMSBY, I., GITTENBERGER-DE GROOT, A. C., SARIOLA, H., FRIEDMAN, R., BOIVIN, G. P., CARDELL, E. L. & DOETSCHMAN, T. 1997. TGFbeta2 knockout mice have multiple developmental defects that are non-overlapping with other TGFbeta knockout phenotypes. *Developmental Dynamics : An Official Publication of the American Association of Anatomists,* 210**,** 415-27.

SASAKI, Y., TANAKA, S., HAMACHI, T. & TAYA, Y. 2004. Deficient cell proliferation in palatal shelf mesenchyme of CL/Fr mouse embryos. *J Dent Res,* 83**,** 797-801.

SCHAMBONY A, W. D. 2013. Wnt Signaling and Cell Migration. *Madame Curie Bioscience Database [Internet]*. Austin (TX): Landes Bioscience.

SCHINDELIN, J., ARGANDA-CARRERAS, I., FRISE, E., KAYNIG, V., LONGAIR, M., PIETZSCH, T., PREIBISCH, S., RUEDEN, C., SAALFELD, S., SCHMID, B., TINEVEZ, J. Y., WHITE, D. J., HARTENSTEIN, V., ELICEIRI, K., TOMANCAK, P. & CARDONA, A. 2012. Fiji: an open-source platform for biological-image analysis. *Nat Methods,* 9**,** 676-82.

SCHMITT-GRAFF, A., DESMOULIERE, A. & GABBIANI, G. 1994. Heterogeneity of myofibroblast phenotypic features: an example of fibroblastic cell plasticity. *Virchows*

Arch, 425**,** 3-24.
SCHOENWOLF, G., BLEYL, S., BRAUER, P., FRANCIS-WEST, P.H. 2015. Larsen's Human Embryology. 5th ed. Philadelphia: Churchill Livingstone. p431-466.
SCHWARZBAUER, J. E. & DESIMONE, D. W. 2011. Fibronectins, their fibrillogenesis, and in vivo functions. *Cold Spring Harb Perspect Biol,* 3.
SELHUB, J. 1999. Homocysteine metabolism. *Annu Rev Nutr,* 19**,** 217-46.
SENAPATI, S., RACHAGANI, S., CHAUDHARY, K., JOHANSSON, S. L., SINGH, R. K. & BATRA, S. K. 2010. Overexpression of macrophage inhibitory cytokine-1 induces metastasis of human prostate cancer cells through the FAK-RhoA signaling pathway. *Oncogene,* 29**,** 1293-302.
SENDERS, C. W., PETERSON, E. C., HENDRICKX, A. G. & CUKIERSKI, M. A. 2003. Development of the upper lip. *Arch Facial Plast Surg,* 5**,** 16-25.
SETO-SALVIA, N. & STANIER, P. 2014. Genetics of cleft lip and/or cleft palate: association with other common anomalies. *Eur J Med Genet,* 57**,** 381-93.
SHAFI, T., KHAN, M. R. & ATIQ, M. 2003. Congenital heart disease and associated malformations in children with cleft lip and palate in Pakistan. *Br J Plast Surg,* 56**,** 106-9.
SHANNON, D. B., MCKEOWN, S. T., LUNDY, F. T. & IRWIN, C. R. 2006. Phenotypic differences between oral and skin fibroblasts in wound contraction and growth factor expression. *Wound Repair Regen,* 14**,** 172-8.
SHAW, G. M., CARMICHAEL, S. L., LAURENT, C. & RASMUSSEN, S. A. 2006. Maternal nutrient intakes and risk of orofacial clefts. *Epidemiology,* 17**,** 285-91.
SHAW, G. M., LAMMER, E. J., WASSERMAN, C. R., O'MALLEY, C. D. & TOLAROVA, M. M. 1995. Risks of orofacial clefts in children born to women using multivitamins containing folic acid periconceptionally. *Lancet,* 346**,** 393-6.
SHAW, W. C., SEMB, G., NELSON, P., BRATTSTROM, V., MOLSTED, K., PRAHL-ANDERSEN, B. & GUNDLACH, K. K. 2001. The Eurocleft project 1996-2000: overview. *J Craniomaxillofac Surg,* 29**,** 131-40; discussion 141-2.
SHAWE-TAYLOR, M., KUMAR, J. D., HOLDEN, W., DODD, S., VARGA, A., GIGER, O., VARRO, A. & DOCKRAY, G. J. 2017. Glucagon-like petide-2 acts on colon cancer myofibroblasts to stimulate proliferation, migration and invasion of both myofibroblasts and cancer cells via the IGF pathway. *Peptides,* 91**,** 49-57.
SHETTY, A., LODDO, M., FANSHAWE, T., PREVOST, A. T., SAINSBURY, R., WILLIAMS, G. H. & STOEBER, K. 2005. DNA replication licensing and cell cycle kinetics of normal and neoplastic breast. *Br J Cancer,* 93**,** 1295-300.
SHETYE, P. R. 2004. Facial growth of adults with unoperated clefts. *Clin Plast Surg,* 31**,** 361-71.
SHIANG, R., LIDRAL, A. C., ARDINGER, H. H., BUETOW, K. H., ROMITTI, P. A., MUNGER, R. G. & MURRAY, J. C. 1993. Association of transforming growth-factor alpha gene polymorphisms with nonsyndromic cleft palate only (CPO). *American journal of human genetics,* 53**,** 836-843.
SHIN, D. & MINN, K. W. 2004. The effect of myofibroblast on contracture of hypertrophic scar. *Plast Reconstr Surg,* 113**,** 633-40.
SHKOUKANI, M. A., CHEN, M. & VONG, A. 2013. Cleft lip - a comprehensive review. *Frontiers in pediatrics,* 1**,** 53-53.
SHOULDERS, M. D. & RAINES, R. T. 2009. Collagen structure and stability. *Annu Rev Biochem,* 78**,** 929-58.
SHPRINTZEN, R. J. 1992. The implications of the diagnosis of Robin sequence. *Cleft Palate Craniofac J,* 29**,** 205-9.

SINGH, A. K. & NANDINI, R. 2009. Bilateral cleft lip nasal deformity. *Indian journal of plastic surgery: official publication of the Association of Plastic Surgeons of India,* 42**,** 235-241.

SINGH, G. D., MOXHAM, B. J., LANGLEY, M. S. & EMBERY, G. 1997. Glycosaminoglycan biosynthesis during 5-fluoro-2-deoxyuridine-induced palatal clefts in the rat. *Archives of Oral Biology,* 42**,** 355-363.

SINGH, G. D., MOXHAM, B. J., LANGLEY, M. S., WADDINGTON, R. J. & EMBERY, G. 1994. Changes in the composition of glycosaminoglycans during normal palatogenesis in the rat. *Arch Oral Biol,* 39**,** 401-7.

SINNO, H. & PRAKASH, S. 2013. Complements and the wound healing cascade: an updated review. *Plastic surgery international,* 2013**,** 146764-146764.

SITZMAN, T. J., HOSSAIN, M., CARLE, A. C., HEATON, P. C. & BRITTO, M. T. 2017. Variation among cleft centres in the use of secondary surgery for children with cleft palate: a retrospective cohort study. *BMJ Paediatrics Open,* 1.

SMITH, A. W., KHOO, A. K. & JACKSON, I. T. 1998. A modification of the Kernahan "Y" classification in cleft lip and palate deformities. *Plast Reconstr Surg,* 102**,** 1842-7.

SMITH, D., ABDULLAH, S. E., MOORES, A. & WYNNE, D. M. 2013. Post-operative respiratory distress following primary cleft palate repair. *J Laryngol Otol,* 127**,** 65-6.

SMITH, D. M., VECCHIONE, L., JIANG, S., FORD, M., DELEYIANNIS, F. W., HARALAM, M. A., NARAN, S., WORRALL, C. I., DUDAS, J. R., AFIFI, A. M., MARAZITA, M. L. & LOSEE, J. E. 2007. The Pittsburgh Fistula Classification System: a standardized scheme for the description of palatal fistulas. *Cleft Palate Craniofac J,* 44**,** 590-4.

SMITH, L. T., HOLBROOK, K. A. & MADRI, J. A. 1986. Collagen types I, III, and V in human embryonic and fetal skin. *Am J Anat,* 175**,** 507-21.

SNIDER, T. N. & MISHINA, Y. 2014. Cranial neural crest cell contribution to craniofacial formation, pathology, and future directions in tissue engineering. *Birth defects research. Part C, Embryo today: reviews,* 102**,** 324-332.

SOLTANI, A. M., FRANCIS, C. S., MOTAMED, A., KARATSONYI, A. L., HAMMOUDEH, J. A., SANCHEZ-LARA, P. A., REINISCH, J. F. & URATA, M. M. 2012. Hypertrophic scarring in cleft lip repair: a comparison of incidence among ethnic groups. *Clin Epidemiol,* 4**,** 187-91.

SOMERVILLE, N. & FENLON, S. 2005. Anaesthesia for cleft lip and palate surgery. *Continuing Education in Anaesthesia Critical Care & Pain,* 5**,** 76-79.

SQUIER, C. A. & KREMER, M. J. 2001. Biology of oral mucosa and esophagus. *J Natl Cancer Inst Monogr***,** 7-15.

STADELMANN, W. K., DIGENIS, A. G. & TOBIN, G. R. 1998. Physiology and healing dynamics of chronic cutaneous wounds. *Am J Surg,* 176**,** 26s-38s.

STEFFEN, A., LADWEIN, M., DIMCHEV, G. A., HEIN, A., SCHWENKMEZGER, L., ARENS, S., LADWEIN, K. I., MARGIT HOLLEBOOM, J., SCHUR, F., VICTOR SMALL, J., SCHWARZ, J., GERHARD, R., FAIX, J., STRADAL, T. E., BRAKEBUSCH, C. & ROTTNER, K. 2013. Rac function is crucial for cell migration but is not required for spreading and focal adhesion formation. *J Cell Sci,* 126**,** 4572-88.

STEPHENS, P., DAVIES, K. J., AL-KHATEEB, T., SHEPHERD, J. P. & THOMAS, D. W. 1996. A comparison of the ability of intra-oral and extra-oral fibroblasts to stimulate extracellular matrix reorganization in a model of wound contraction. *J Dent Res,* 75**,** 1358-64.

STERNBERG, J. & KIMBER, S. J. 1986. Distribution of fibronectin, laminin and entactin in

the environment of migrating neural crest cells in early mouse embryos. *J Embryol Exp Morphol,* 91**,** 267-82.
STOVER, P. J. & FIELD, M. S. 2011. Trafficking of intracellular folates. *Adv Nutr,* 2**,** 325-31.
STRACHAN, L. R. & CONDIC, M. L. 2008. Neural crest motility on fibronectin is regulated by integrin activation. *Exp Cell Res,* 314**,** 441-52.
STROBL-MAZZULLA, P. H. & BRONNER, M. E. 2012. Epithelial to mesenchymal transition: new and old insights from the classical neural crest model. *Semin Cancer Biol,* 22**,** 411-6.
SULL, J. W., LIANG, K. Y., HETMANSKI, J. B., WU, T., FALLIN, M. D., INGERSOLL, R. G., PARK, J. W., WU-CHOU, Y. H., CHEN, P. K., CHONG, S. S., CHEAH, F., YEOW, V., PARK, B. Y., JEE, S. H., JABS, E. W., REDETT, R., SCOTT, A. F. & BEATY, T. H. 2009. Evidence that TGFA influences risk to cleft lip with/without cleft palate through unconventional genetic mechanisms. *Hum Genet,* 126**,** 385-94.
SUN, D., BAUR, S. & HAY, E. D. 2000. Epithelial-mesenchymal transformation is the mechanism for fusion of the craniofacial primordia involved in morphogenesis of the chicken lip. *Dev Biol,* 228**,** 337-49.
SYED, F. & BAYAT, A. 2012. Notch signaling pathway in keloid disease: enhanced fibroblast activity in a Jagged-1 peptide-dependent manner in lesional vs. extralesional fibroblasts. *Wound Repair Regen,* 20**,** 688-706.
SYMONS, M., DERRY, J. M., KARLAK, B., JIANG, S., LEMAHIEU, V., MCCORMICK, F., FRANCKE, U. & ABO, A. 1996. Wiskott-Aldrich syndrome protein, a novel effector for the GTPase CDC42Hs, is implicated in actin polymerization. *Cell,* 84**,** 723-34.
TAIPALE, J. & KESKI-OJA, J. 1997. Growth factors in the extracellular matrix. *Faseb j,* 11**,** 51-9.
TANAKA, S. A., MAHABIR, R. C., JUPITER, D. C. & MENEZES, J. M. 2013. Updating the epidemiology of isolated cleft palate. *Plast Reconstr Surg,* 131**,** 650e-2e.
TANG, Q., LI, L., JIN, C., LEE, J. M. & JUNG, H. S. 2015. Role of region-distinctive expression of Rac1 in regulating fibronectin arrangement during palatal shelf elevation. *Cell Tissue Res,* 361**,** 857-68.
TANG, Q., LI, L., LEE, M. J., GE, Q., LEE, J. M. & JUNG, H. S. 2016. Novel insights into a retinoic-acid-induced cleft palate based on Rac1 regulation of the fibronectin arrangement. *Cell Tissue Res,* 363**,** 713-22.
TAPARIA, S., GELINEAU-VAN WAES, J., ROSENQUIST, T. H. & FINNELL, R. H. 2007. Importance of folate-homocysteine homeostasis during early embryonic development. *Clin Chem Lab Med,* 45**,** 1717-27.
TAPON, N. & HALL, A. 1997. Rho, Rac and Cdc42 GTPases regulate the organization of the actin cytoskeleton. *Curr Opin Cell Biol,* 9**,** 86-92.
TAYA, Y., O'KANE, S. & FERGUSON, M. W. 1999. Pathogenesis of cleft palate in TGF-beta3 knockout mice. *Development,* 126**,** 3869-79.
THANNICKAL, V. J., LEE, D. Y., WHITE, E. S., CUI, Z., LARIOS, J. M., CHACON, R., HOROWITZ, J. C., DAY, R. M. & THOMAS, P. E. 2003. Myofibroblast differentiation by transforming growth factor-β1 is dependent on cell adhesion and integrin signaling via focal adhesion kinase. *Journal of Biological Chemistry,* 278**,** 12384-12389.
THEVENEAU, E. & MAYOR, R. 2011. Collective cell migration of the cephalic neural crest: the art of integrating information. *genesis,* 49**,** 164-176.
THOMAS, P. S., KIM, J., NUNEZ, S., GLOGAUER, M. & KAARTINEN, V. 2010. Neural crest cell-specific deletion of Rac1 results in defective cell-matrix interactions and severe craniofacial and cardiovascular malformations. *Developmental biology,* 340**,**

613-625.
TING, P. C., LEE, W. R., HUO, Y. N., HSU, S. P. & LEE, W. S. 2019. Folic acid inhibits colorectal cancer cell migration. *J Nutr Biochem,* 63**,** 157-164.
TOMASEK, J. J., GABBIANI, G., HINZ, B., CHAPONNIER, C. & BROWN, R. A. 2002. Myofibroblasts and mechano-regulation of connective tissue remodelling. *Nat Rev Mol Cell Biol,* 3**,** 349-63.
TONNESEN, M. G., FENG, X. & CLARK, R. A. 2000. Angiogenesis in wound healing. *J Investig Dermatol Symp Proc,* 5**,** 40-6.
TORRES-RENDON, A., ROY, S., CRAIG, G. T. & SPEIGHT, P. M. 2009. Expression of Mcm2, geminin and Ki67 in normal oral mucosa, oral epithelial dysplasias and their corresponding squamous-cell carcinomas. *British Journal Of Cancer,* 100**,** 1128.
TRACY, L. E., MINASIAN, R. A. & CATERSON, E. J. 2016. Extracellular Matrix and Dermal Fibroblast Function in the Healing Wound. *Adv Wound Care (New Rochelle),* 5**,** 119-136.
TREMEL, A., CAI, A., TIRTAATMADJA, N., HUGHES, B. D., STEVENS, G. W., LANDMAN, K. A. & O'CONNOR, A. J. 2009. Cell migration and proliferation during monolayer formation and wound healing. *Chemical Engineering Science,* 64**,** 247-253.
TULLBERG-REINERT, H. & JUNDT, G. 1999. In situ measurement of collagen synthesis by human bone cells with a sirius red-based colorimetric microassay: effects of transforming growth factor beta2 and ascorbic acid 2-phosphate. *Histochem Cell Biol,* 112**,** 271-6.
VALLEE, B. L. & FALCHUK, K. H. 1993. The biochemical basis of zinc physiology. *Physiol Rev,* 73**,** 79-118.
VAN DE WATER, L., VARNEY, S. & TOMASEK, J. J. 2013. Mechanoregulation of the Myofibroblast in Wound Contraction, Scarring, and Fibrosis: Opportunities for New Therapeutic Intervention. *Adv Wound Care (New Rochelle),* 2**,** 122-141.
VAN HORSSEN, R., GALJART, N., RENS, J. A., EGGERMONT, A. M. & TEN HAGEN, T. L. 2006. Differential effects of matrix and growth factors on endothelial and fibroblast motility: application of a modified cell migration assay. *J Cell Biochem,* 99**,** 1536-52.
VAN ROOIJ, I. A., OCKE, M. C., STRAATMAN, H., ZIELHUIS, G. A., MERKUS, H. M. & STEEGERS-THEUNISSEN, R. P. 2004. Periconceptional folate intake by supplement and food reduces the risk of nonsyndromic cleft lip with or without cleft palate. *Prev Med,* 39**,** 689-94.
VAN ROOIJ, I. A., SWINKELS, D. W., BLOM, H. J., MERKUS, H. M. & STEEGERS-THEUNISSEN, R. P. 2003. Vitamin and homocysteine status of mothers and infants and the risk of nonsyndromic orofacial clefts. *Am J Obstet Gynecol,* 189**,** 1155-60.
VANDERAS, A. P. 1987. Incidence of cleft lip, cleft palate, and cleft lip and palate among races: a review. *Cleft Palate J,* 24**,** 216-25.
VAUGHAN, M. B., HOWARD, E. W. & TOMASEK, J. J. 2000. Transforming growth factor-beta1 promotes the morphological and functional differentiation of the myofibroblast. *Exp Cell Res,* 257**,** 180-9.
VEGA, F. M. & RIDLEY, A. J. 2018. The RhoB small GTPase in physiology and disease. *Small GTPases,* 9**,** 384-393.
VELNAR, T., BAILEY, T. & SMRKOLJ, V. 2009. The wound healing process: an overview of the cellular and molecular mechanisms. *J Int Med Res,* 37**,** 1528-42.
VIEIRA, A. R. 2006. Association between the Transforming Growth Factor Alpha Gene and Nonsyndromic Oral Clefts: A HuGE Review. *American Journal of Epidemiology,* 163**,** 790-810.

VIEIRA, A. R. & DATTILO, S. 2018. Oxygen, Left/Right Asymmetry, and Cleft Lip and Palate. *J Craniofac Surg,* 29**,** 396-399.

WADDINGTON, S. N., CROSSLEY, R., SHEARD, V., HOWE, S. J., BUCKLEY, S. M. K., COUGHLAN, L., GILHAM, D. E., HAWKINS, R. E. & MCKAY, T. R. 2010. Gene delivery of a mutant TGFβ3 reduces markers of scar tissue formation after cutaneous wounding. *Molecular therapy: the journal of the American Society of Gene Therapy,* 18**,** 2104-2111.

WAHL, S. E., KENNEDY, A. E., WYATT, B. H., MOORE, A. D., PRIDGEN, D. E., CHERRY, A. M., MAVILA, C. B. & DICKINSON, A. J. G. 2015. The role of folate metabolism in orofacial development and clefting. *Developmental Biology,* 405**,** 108-122.

WALD, N. 1991. Prevention of neural tube defects: Results of the Medical Research Council Vitamin Study. *The Lancet,* 338**,** 131-137.

WANG, R., GHAHARY, A., SHEN, Q., SCOTT, P. G., ROY, K. & TREDGET, E. E. 2000. Hypertrophic scar tissues and fibroblasts produce more transforming growth factor-beta1 mRNA and protein than normal skin and cells. *Wound Repair Regen,* 8**,** 128-37.

WANG X, L. Y., HOU Z 2017. Insulin-like growth factor binding protein 2 regulates cell proliferation and migration in the adjuvant arthritis synovial cells through ERK signaling pathway. *Int J Clin Exp Pathol* 10**,** 3219-2336.

WATSON, S. L., MARCAL, H., SARRIS, M., DI GIROLAMO, N., CORONEO, M. T. C. & WAKEFIELD, D. 2010. The effect of mesenchymal stem cell conditioned media on corneal stromal fibroblast wound healing activities. *British Journal of Ophthalmology,* 94**,** 1067.

WEBSTER, W. S. & ABELA, D. 2007. The effect of hypoxia in development. *Birth Defects Res C Embryo Today,* 81**,** 215-28.

WEHBY, G. L., FÉLIX, T. M., GOCO, N., RICHIERI-COSTA, A., CHAKRABORTY, H., SOUZA, J., PEREIRA, R., PADOVANI, C., MORETTI-FERREIRA, D. & MURRAY, J. C. 2013. High dosage folic acid supplementation, oral cleft recurrence and fetal growth. *International journal of environmental research and public health,* 10**,** 590-605.

WEHLAND, J., OSBORN, M. & WEBER, K. 1977. Phalloidin-induced actin polymerization in the cytoplasm of cultured cells interferes with cell locomotion and growth. *Proceedings of the National Academy of Sciences of the United States of America,* 74**,** 5613-5617.

WEINZWEIG, J., PANTER, K. E., SEKI, J., PANTALONI, M., SPANGENBERGER, A. & HARPER, J. S. 2006. The fetal cleft palate: IV. Midfacial growth and bony palatal development following in utero and neonatal repair of the congenital caprine model. *Plast Reconstr Surg,* 118**,** 81-93.

WERNER, S. & GROSE, R. 2003. Regulation of wound healing by growth factors and cytokines. *Physiol Rev,* 83**,** 835-70.

WIELAND, T. 1977. Interaction of phallotoxins with actin. *Advances in Enzyme Regulation,* 15**,** 285-299.

WIERZBICKA-PATYNOWSKI, I. & SCHWARZBAUER, J. E. 2003. The ins and outs of fibronectin matrix assembly. *J Cell Sci,* 116**,** 3269-76.

WILCOX, A. J., LIE, R. T., SOLVOLL, K., TAYLOR, J., MCCONNAUGHEY, D. R., ABYHOLM, F., VINDENES, H., VOLLSET, S. E. & DREVON, C. A. 2007. Folic acid supplements and risk of facial clefts: national population based case-control study. *Bmj,* 334**,** 464.

WILLIAMS, A. C., BEARN, D., MILDINHALL, S., MURPHY, T., SELL, D., SHAW, W. C.,

MURRAY, J. J. & SANDY, J. R. 2001. Cleft lip and palate care in the United Kingdom--the Clinical Standards Advisory Group (CSAG) Study. Part 2: dentofacial outcomes and patient satisfaction. *Cleft Palate Craniofac J,* 38**,** 24-9.

WONG, W. Y., ESKES, T. K., KUIJPERS-JAGTMAN, A. M., SPAUWEN, P. H., STEEGERS, E. A., THOMAS, C. M., HAMEL, B. C., BLOM, H. J. & STEEGERS-THEUNISSEN, R. P. 1999. Nonsyndromic orofacial clefts: association with maternal hyperhomocysteinemia. *Teratology,* 60**,** 253-7.

WU, C., ASOKAN, S. B., BERGINSKI, M. E., HAYNES, E. M., SHARPLESS, N. E., GRIFFITH, J. D., GOMEZ, S. M. & BEAR, J. E. 2012. Arp2/3 complex is critical for lamellipodia and organization of cell-matrix adhesion but dispensable for fibroblast chemotaxis. *Cell,* 148**,** 973.

WU, M. Y. & HILL, C. S. 2009. Tgf-beta superfamily signaling in embryonic development and homeostasis. *Dev Cell,* 16**,** 329-43.

WYSZYNSKI, D. F., BEATY, T. H. & MAESTRI, N. E. 1996. Genetics of nonsyndromic oral clefts revisited. *Cleft Palate Craniofac J,* 33**,** 406-17.

YAZDY, M. M., HONEIN, M. A. & XING, J. 2007. Reduction in orofacial clefts following folic acid fortification of the U.S. grain supply. *Birth Defects Res A Clin Mol Teratol,* 79**,** 16-23.

YOSHIMURA, T. & LEONARD, E. J. 1990. Secretion by human fibroblasts of monocyte chemoattractant protein-1, the product of gene JE. *J Immunol,* 144**,** 2377-83.

YOUNG, A. & MCNAUGHT, C.-E. 2011. The physiology of wound healing. *Surgery (Oxford),* 29**,** 475-479.

YU, W., SERRANO, M., MIGUEL, S. S., RUEST, L. B. & SVOBODA, K. K. 2009. Cleft lip and palate genetics and application in early embryological development. *Indian J Plast Surg,* 42 Suppl**,** S35-50.

YU, X. M., LI, C. W., CHAO, S. S., LI, Y. Y., YAN, Y., ZHAO, X. N., YU, F. G., LIU, J., SHEN, L., PAN, X. L., SHI, L. & WANG, D. Y. 2014. Reduced growth and proliferation dynamics of nasal epithelial stem/progenitor cells in nasal polyps in vitro. *Scientific Reports,* 4**,** 4619.

YUE, B. 2014. Biology of the extracellular matrix: an overview. *Journal of glaucoma,* 23**,** S20-S23.

ZETTER, B. R. & BRIGHTMAN, S. E. 1990. Cell motility and the extracellular matrix. *Current Opinion in Cell Biology,* 2**,** 850-856.

ZHANG, K., GARNER, W., COHEN, L., RODRIGUEZ, J. & PHAN, S. 1995. Increased types I and III collagen and transforming growth factor-beta 1 mRNA and protein in hypertrophic burn scar. *J Invest Dermatol,* 104**,** 750-4.

ZHANG, L. Q., LAATO, M., MUONA, P., PENTTINEN, R., OIKARINEN, A. & PELTONEN, J. 1995. A fibroblast cell line cultured from a hypertrophic scar displays selective downregulation of collagen gene expression: barely detectable messenger RNA levels of the pro alpha 1(III) chain of type III collagen. *Arch Dermatol Res,* 287**,** 534-8.

ZHANG, Z., STEIN, M., MERCER, N. & MALIC, C. 2017. Post-operative outcomes after cleft palate repair in syndromic and non-syndromic children: a systematic review protocol. *Systematic reviews,* 6**,** 52-52.

ZHAO, H., HO, P.-C., LO, Y.-H., ESPEJO, A., BEDFORD, M. T., HUNG, M.-C. & WANG, S.-C. 2012. Interaction of proliferation cell nuclear antigen (PCNA) with c-Abl in cell proliferation and response to DNA damages in breast cancer. *PloS one,* 7**,** e29416-e29416.

ZHAO, M., ZHOU, J., CHEN, Y. H., YUAN, L., YUAN, M. M., ZHANG, X. Q., HU, Y. &

YU, H. 2018. Folic Acid Promotes Wound Healing in Diabetic Mice by Suppression of Oxidative Stress. *J Nutr Sci Vitaminol (Tokyo)*, 64**,** 26-33.

ZHAO, Z. S. & MANSER, E. 2005. PAK and other Rho-associated kinases--effectors with surprisingly diverse mechanisms of regulation. *Biochem J,* 386**,** 201-14.

ZIMERMAN, B., VOLBERG, T. & GEIGER, B. 2004. Early molecular events in the assembly of the focal adhesion-stress fiber complex during fibroblast spreading. *Cell Motil Cytoskeleton,* 58**,** 143-59.

ŽIVICOVÁ, V., LACINA, L., MATEU, R., SMETANA, K., JR., KAVKOVÁ, R., DROBNÁ KREJČÍ, E., GRIM, M., KVASILOVÁ, A., BORSKÝ, J., STRNAD, H., HRADILOVÁ, M., ŠÁCHOVÁ, J., KOLÁŘ, M. & DVOŘÁNKOVÁ, B. 2017. Analysis of dermal fibroblasts isolated from neonatal and child cleft lip and adult skin: Developmental implications on reconstructive surgery. *International journal of molecular medicine,* 40**,** 1323-1334.

ZUCCHERO, T. M., COOPER, M. E., MAHER, B. S., DAACK-HIRSCH, S., NEPOMUCENO, B., RIBEIRO, L., CAPRAU, D., CHRISTENSEN, K., SUZUKI, Y., MACHIDA, J., NATSUME, N., YOSHIURA, K., VIEIRA, A. R., ORIOLI, I. M., CASTILLA, E. E., MORENO, L., ARCOS-BURGOS, M., LIDRAL, A. C., FIELD, L. L., LIU, Y. E., RAY, A., GOLDSTEIN, T. H., SCHULTZ, R. E., SHI, M., JOHNSON, M. K., KONDO, S., SCHUTTE, B. C., MARAZITA, M. L. & MURRAY, J. C. 2004. Interferon regulatory factor 6 (IRF6) gene variants and the risk of isolated cleft lip or palate. *N Engl J Med,* 351**,** 769-80.